The effect of NCX1.1 inhibition in primary cardiac myofibroblast cellular motility, contraction, and proliferation

By

Joshua E. Raizman

A Thesis submitted to the Faculty of Graduate Studies of

The University of Manitoba

in partial fulfilment of the requirements of the degree of

MASTER OF SCIENCE

Department of Physiology

University of Manitoba

Winnipeg

ABSTRACT

Cardiac myofibroblasts participate in post-myocardial infarct (MI) wound healing, infarct scar formation, and remodeling of the ventricle remote to the site of infarction. The role of intracellular calcium handling in cardiac myofibroblasts as a modulator of cellular motility, contractile responses, and proliferation is largely unexplored. We have investigated the role of sodium calcium exchange (Na Ca exchange or NCX1.1) and non-selective cation channels (NSCCs) in regulation of myofibroblast function using a pharmacological inhibitor approach *in vitro*. Primary myofibroblasts were stimulated with PDGF-BB and cellular chemotaxis, contraction and proliferative responses were characterized using standard bioassays (Costar Transwell apparatuses, pre-formed collagen type I gel deformation assays, and ^{3}H-thymidine incorporation). Stimulated cellular responses were compared to those in the presence of AG1296 (PDGFβR inhibitor), KB-R7943 (NCX inhibitor), gadolinium, nifedipine or ML-7. Immunofluorescence was used to determine localized expression of αSMA, SMemb, NCX1.1, and $Ca_v1.2a$ in cultured myofibroblasts. Motility of myofibroblasts in the presence of 50 ng/ml PDGF-BB was blocked with AG1296 treatment (2, 5, 10 and 20 μM). Chelation of extracellular calcium with EGTA (2, 3, and 4 mM) resulted in decreased motility, contractility, and proliferation in the presence of 50 ng/ml PDGF-BB. Reintroduction of 2, 5, and 10 mM $CaCl_2$ to chelated media resulted in reversal of the EGTA-mediated response, and this was attended by a morphological reversion of cells with a rounded appearance in the presence of EGTA, to a normal cellular appearance as characterized by reformation of lamellipodia and filopodia. No change in cellular motility was observed in ionomycin-treated (18, 56, and 166 nM) myofibroblasts in the presence of either 50 ng/ml PDGF-BB, or 20 ng/ml LoFGF-2. Immunoblotting and immunocytochemical studies revealed expression of NCX1.1 in fibroblasts and myofibroblasts. Motility (in the presence of either 50 ng/ml PDGF-BB, or 10 ng/ml CT-1), contraction (in the presence of either 10 ng/ml PDGF-BB or 10 ng/ml TGFβ1), and proliferation (in the presence of 10 ng/ml PDGF-BB) were sensitive to KB-R7943 treatment of cells (7.5 and 10 μM for motility, 5 and 10 μM for contractility, and 10 μM for proliferation). Proliferation (in the presence of PDGF-BB), and contractility (in the presence of either PDGF-BB or TGFβ) but not motility (in the presence of PDGF-BB) are sensitive to 10 μM nifedipine treatment, while 10 and 20 μM gadolinium treatment was associated only with decreased motility of cells (in the presence of either PDGF-BB, CT-1, or 20 ng/ml LoFGF-2). We found that ML-7 treatment

inhibited cellular chemotaxis (10 and 20 μM), and contraction (20 μM). Thus cellular chemotaxis, contractile, and proliferation responses were sensitive to different pharmacologic treatment.

Regulation of transplasmalemmal calcium movements may be important in cytokine and growth factor receptor-mediated cardiac myofibroblast motility, contractility, and proliferation. Furthermore, our results support the hypothesis that activation of specific calcium transport proteins is an important determinant of physiologic responses.

ACKNOWLEDGEMENTS

Albert Einstein once said, *"The most beautiful thing we can experience is the mysterious. It is the source of all true art and science. He to whom this emotion is a stranger, who can no longer pause to wonder and stand rapt in awe, is as good as dead: his eyes are closed."* In order to become immersed in the mysterious, it is perhaps most important to be capable of asking a good question. My first gratitude goes to my mentor and supervisor, Dr. Ian Dixon. I thank him for teaching me that science isn't just about answering questions but rather knowing how to ask the one's which are most relevant. Thank you for instilling in me all of the artillery necessary to become the best possible scientist: intellectual prowess, technical proficiency, and most importantly the art of question making. His wisdom, leadership, and professional resolve has been instrumental in helping to keep the flame of excitement for science burning strongly in me, while his down to earth personality has helped me to keep things in perspective. His genuine friendship, relentless guidance, and unwavering encouragement have inspired me to achieve high merits in pursuit of this degree and future endeavors. To the members of my committee - Drs Newman Stephens, Michael Czubryt, and Nasrin Mesaeli - for being a constant source of support and technical expertise. Thank you for providing me with important insights, useful critiques, and helping me to think outside the box. I could always rely on your honest scientific advice during the course of my studies. To the current and former members of the lab – Mr. Ryan Cunnington, Ms. Aran Dangerfield, Mr. Sunil Rattan, Ms. Kristen Bedosky, Ms. Rose Chang, Ms. Cicie Deng, Ms. Vanja Drobic, Mr. Stephen Jones, Mr. Amer Omar, Ms. Jelena Komljenovic, Mr. Vinit Elimban, Ms. Tanja Angelovska, Dr. Baiqui Wang, and Dr. Darren Freed – for your comradely, your laughs, your patience, and your eagerness to help me through both the good and tough times. Thank you for your everlasting friendships, your brilliant ideas, scientific and personal conversations, and making the lab environment the most colorful and pleasurable place to work in the entire research centre. A special thanks to Dr. Mark Hnatowich for digging deep within his vast technical knowledge base from which he gave me extensive insight into experimental design and advice. Another special thanks to Jacqui Fox for her tireless encouragement, support, devotion, and for being a driving source of inspiration. She taught me that to be a good scientist one must also be a balanced human being. To my entire family. Dad, Mom, and Alisa, if it wasn't for your unconditional love, unyielding support, and unremitting commitment this degree would have no start nor end. I am in forever appreciation for providing

me with the foundations to become all that I aspire to be, for helping me realize my potential, and most importantly for showing me how to become a *mench*. Without your love my eyes would be permanently closed, my ears deaf to the world. Lastly, my gratitude is extended to the St. Boniface Hospital Research Foundation for generously providing me with financial support during the course of my studies.

To my family

TABLE OF CONTENTS

LIST OF FIGURES

LIST OF ABBREVIATIONS

αSMA	α-smooth muscle actin
ACE	angiotensin converting enzyme
aFGF	acidic fibroblast growth factor
AngII	angiotensin II
ARB	receptor blockers for angiotensin
ATP	adenosine triphosphate
BCA	bicinchoninic acid
BSA	bovine serum albumin
bFGF	basic fibroblast growth factor
Ca^{2+}	calcium
$[Ca^{2+}]$	calcium concentration
$[Ca^{2+}]_i$	intracellular calcium concentration
$[Ca^{2+}]_o$	extracellular calcium concentration
CAD	coronary artery disease
CaM	calmodulin
CHF	congestive heart failure
cAMP	cyclic adenosine monophosphate
CT-1	cardiotrophin-1
CVD	cardiovascular disease
Cx	connexin
DAG	diacylglycerol
DDW	double distilled water
DMEM	Dulbecco's Modified Eagle Medium
DMSO	dimethyl sulfoxide
ECM	extracellular matrix
EDTA	ethylenediaminetetraacetic acid
EGTA	ethylenebis glycol tetraacetic acid
ER	endoplasmic reticulum
ERK	extracellular signal regulated kinase
F-actin	fibrillar actin
FA	focal adhesion
FAK	focal adhesion kinase
FBS	fetal bovine serum
FGF	fibroblast growth factor
FGFR	fibroblast growth factor receptor
Frz	frizzled gene
G-actin	globular actin
Gd^{3+}	gadolinium
Gp130	granulation protein-130
GTPase	guanosine triphosphatase
^{3}H-thymidine	tritiated thymidine
HSPG	heparin sulfate proteoglycans
HiFGF-2	high molecular weight fibroblast growth factor-2
IL	interleukin

IP_3	inositol 1,4,5-triphosphate
JAK	janus kinase
JNK	c-jun N-terminal kinases
KBR	KB-R7943
LoFGF-2	low molecular weight fibroblast growth factor-2
LDH	lactate dehydrogenase
LIF	leukemia inhibitory factor
LV	left ventricle
MAP	mitogen activated protein
MAPK	mitogen activated protein kinase
MI	myocardial infarction
MIP	mechanically induced potential
MLC	myosin light chain
MLCK	myosin light chain kinase
rMLC	regulatory myosin light chain
MMP	matrix metalloproteinase
mRNA	messenger ribonucleic acid
MSC	mechanically sensitive channel
NCX	NCX1.1, sodium calcium exchanger, Na Ca exchanger
NSCC	non-selective cation channels
P0/P1/P2	passage 0/1/2
PBS	phosphate buffered saline
PDGF	platelet derived growth factor-BB
PDGFR	platelet derived growth factor receptor
PI3K	phosphatidylinositol 3'-kinase
PIP_2	phosphatidylinositol-3,4 bisphosphate
PIP_3	phosphatidylinositol-3,4,5 triphosphate
PKC	protein kinase C
PLC	phospholipase C
RNA	ribonucleic acid
ROCK	rho kinase
ROS	reactive oxygen species
SAC	stretch activated channel
SCF	stem cell factor
SDS	sodium dodecyl sulfate
SE	standard error
SEA	SEA0400
SH	src homology domain
SIC	stretch inactivated channel
SMEM	simple minimum essential medium
SMemb	embryonic isoform of smooth muscle myosin heavy chain (myosin IIa)
SMC	smooth muscle cell
SOC	store operated channels
SOCE	store operated calcium entry
SOCS	suppressor of cytokine signaling

SR	sarcoplasmic reticulum
STAT	signal transducer and activator of transcription
TBS	tris-buffered saline
TBST	tris-buffered saline with tween
TCA	trichloroacetic acid
TGFβ	transforming growth factor-β
TIMP	tissue inhibitors of matrix metaloproteinase
TNF-α	transforming growth factor-α
TRP	transient receptor potential
Tyr	tyrosine
VDCC	voltage dependent calcium channel
VEGF	vascular endothelial growth factor

LIST OF COPYRIGHTED MATERIAL FOR WHICH PERMISSION WAS OBTAINED

Figure 1. Schematic diagram of the basic steps required for cell motility - Page 42
Adapted from Figure 16-85 on page 972 from The Molecular Biology of the Cell, 4th Edition, Alberts *et al.* 2002. Permission obtained from Elsevier Ltd.

Figure 2. Proposed model for calcium entry in non-excitable cells - Page 58
Adapted from Figure 2 on page 614 from CELL CALCIUM, 11:611-624, Putney: "Capacitative calcium entry revisited", 1990. Permission obtained from Garland Science, Taylor and Francis Group.

I INTRODUCTION

Heart disease has reached epidemic proportions in Canada and worldwide. Estimates in 2002 predicted that cardiovascular disease accounted for 30% of all global deaths, while in Canada of this same year, 20% of all deaths were ascribed to coronary heart disease. In recent decades, improvements in the treatment of acute myocardial infarction (MI) have led to declining rates in mortality and morbidity in recovering post-MI patients (1). However, concomitant with improved patient outcome, greater numbers of patients survive the acute phases of MI and undergo the processes associated with myocardial tissue healing, resulting in abnormal expansion of myocardial extracellular matrix (ECM) interstitium with many ultimately succumbing to ventricular dysfunction and, depending on the size of the initial infarct, development of congestive heart failure (CHF) (2). Cardiac wound healing post-MI may be acompanied by excessive remodeling of the ECM (3). In response to time-dependent changes in the humoral milieu of the myocardium, gross ventricular changes ensue and give rise to altered patterns of myocardial cell gene expression (4). Initially, wound healing of the infarct zone in the ventricular wall works to repopulate the metabolically active infarct scar with non-myocytes (5, 6). Changes in ventricular architecture, characterized by excessive collagen accumulation, occur not only at the site of the infarct (acute process), but also in remote regions (chronic process) unaffected by the ischemic insult. The onset of chronic MI following fibrosis is detrimental to cardiac function due to physical stiffening of the myocardium and disruption of electrical connectivity between cardiomyocytes (7). Despite ongoing work to elucidate the sequelae of events that transpire in the course of cardiac remodeling in post-MI hearts, we do not fully understand the nature of this process. Cardiomyocyte necrosis and apoptosis is recognized as the primary basis for loss of ventricular function following ischemic injury (8). However, the non-myocyte cell population is now recognized as a major regulator of normal and pathological ventricular performance (9, 10).

Interstitial cardiac fibroblasts and their differentiated derivatives, i.e. myofibroblasts, play a major role in modulating the abnormal expansion of collagen content during cardiac fibrosis. Although cardiac fibrosis contributes to the development of heart failure, the mechanisms by which these cells congregate at the site of injury during the inflammatory response to manifest the infarct scar remains poorly understood. In the early stage or acute post-MI, the cellularity of the infarct zone is restored by migrating interstitial fibroblasts that move from the adjacent

infarct border zone and non-infarcted myocardium (11). Differentiation of fibroblasts to specialized contractile myofibroblasts occurs in response to altered expression of transforming growth factor (TGF)-β1 in the infarct scar (12, 13). Myofibroblasts are present in the infarct site soon after infiltration of inflammatory cells (14). These cells exhibit smooth muscle cell-like features characterized by the expression of embryonic smooth muscle myosin heavy chain (SMemb) (10, 15), α-smooth muscle actin (αSMA) (16-20) and fibrillar collagen types I and III (21). As such, myofibroblasts are well suited to confer mechanical tension to the developing scar by contracting (22). Wound contraction brings together the denuded edges of the wound, which reduces overall scar area. Myofibroblast contractile responses together with the deposition of collagen provide tensile strength to the wound and functions to prevent scar rupture.

The availability of multiple pro-fibrotic factors in the infarcted region regulates myofibroblast cell function, and therefore contributes to the progression of cardiac wound healing *in vivo*. Cardiotrophin-1 (CT-1) is a member of the interleukin-6 (IL-6) family of cytokines. Protein levels of this cytokine are found to be elevated in serum of patients with various types of heart conditions (23, 24), and has cardioprotective properties (25). Results from our lab implicate CT-1 in the cardiac wound healing process as it is expressed at elevated levels in the post-MI heart, exerts chemotactic and mitogenic effects in cultured cardiac myofibroblasts, and functions to down regulate collagen production in these cells *in vitro* (10). Local monocytes and leukocytes release platelet derived growth factor (PDGF) secondary to angiotensin II (AngII) release (26) in the infarct region where it plays a major role in angiogenesis (27). PDGF is elevated in plasma of post-MI patients (28), and is implicated in progression of cardiac fibrosis (29), inducing powerful chemotactic, mitogenic, and contractile effects in a variety of cell types including dermal fibroblasts, vascular smooth muscle, and endothelial cells (30). Fibroblast growth factor (FGF)-2 exists as multiple isoforms and plays a role in cardiomyocyte hypertrophy and apoptosis (31). The low molecular weight AUG initiation codon isoform, low (Lo)-FGF-2, modulates a variety of cell behaviors including proliferation, migration, differentiation and apoptosis. LoFGF-2 is recognized as a stimulator of migration of fibroblasts and vascular smooth muscle cells and functions as a major angiogenic factor for new capillary development (32).

Enhanced cellularity of the infarct scar improves ventricular performance irrespective of cell type (33, 34). Myofibroblast cell function, i.e. motility, proliferation and contractile responses, is poorly understood in the context of cardiac wound restoration. Unlike dermal

myofibroblasts (35), cardiac myofibroblasts resist apoptosis and persist in the infarct scar for many decades in human post-MI hearts (18). Myofibroblast turnover also plays a role in contributing to excessive accumulation of collagen content in the heart. Thus, in response to altered expression of multiple cytokines and growth factor *in vivo*, time dependent activation of myofibroblast function is involved in coordinating net collagen deposition in the chronic phases of the post-MI heart.

Cell motility involves spatial and temporal control of a multitude of cellular processes that work in unison to coordinate forward directed cell movement (36). The cyclical process of cell locomotion requires activation of surface receptors located on membrane protrusions (lamellipodia, filopodia or pseudopodia) in a chemotactic gradient. Actin polymerization at the leading cell edge drives membrane protrusion in the direction of the chemotactic stimuli (37), while integrin receptor dependent adhesions to the ECM at the level of cytoskeletal associated focal adhesions (FA) exert tractional forces to the ECM and provide sufficient adherence to anchor the cell to the substratum (38). At the same time, myosin motors, through phospho-myosin light chain (MLC) activation by myosin light chain kinase (MLCK), generate actin cross-bridge cycling leading to contractile forces in the cell cortex, which pull the cell body forward over recently established cell-ECM contacts, and help physically disrupt old contacts at the trailing edge (uropod) (39, 40). The rate of cell motility is directly related to the phosphorylation state of focal adhesion kinases (FAK), which regulate the assembly of FA complexes in turn, regulating the degree of cell adhesion (41). The mechanisms of FA assembly and function are not limited to cell motility but rather modulate other cellular functions such as cell division and contractility (42). Proliferation involves chromosome disjunction, and cytokinesis (43) – processes that involve the participation of FA stabilizing complexes (44).

The subcellular processes involved in contractility are similar to motility in that myosin motors direct cell body contraction with the exception of no forward movement, probably due in part to reduction of FA turnover. In smooth muscle, the activity of myosin motors is regulated by the phosphorylation of regulatory myosin light chain (rMLC), which in turn is regulated by MLCK and phosphatase (45). Phosphorylation of rMLC governs activation of the myosin ATPase by actin, with subsequent cross-bridge cycling and contractile activity leading to generation of tractional forces exerted at the level of FA mediated cell-ECM contacts. Though MLCK can be activated by Src kinases (46, 47) and rho-kinase (ROCK) (48), MLCK is

classically activated by elevated intracellular calcium $[Ca^{2+}]_i$ which binds to calmodulin, in turn binding to and activating MLCK (45, 49).

Ca^{2+} is a ubiquitous second messenger in all cell types. Cytoplasmic free Ca^{2+} relays intracellular signals that modulate many cellular processes including motility, contractility and cell division, with roles in regulating phosphorylation of MLC, myosin II cross-bridge cycling, actin assembly, FAK turnover, chromosome disjunction, and gene transcription (50). The extracellular space and intracellular stores (i.e. the endoplasmic reticulum, ER) control cytoplasmic Ca^{2+} content. Traditionally, non-excitable cells lack voltage dependent Ca^{2+} channels (51, 52). Therefore, unlike electrically excitable cardiomyocytes, $[Ca^{2+}]_i$ content in cardiac fibroblasts and myofibroblasts may be regulated by tightly controlled mechanisms of transplasmalemmal Ca^{2+} movement from the extracellular space independent of membrane activation. The ligand dependent modes of Ca^{2+} entry in myofibroblasts as regulators of motility, contractility and proliferation are largely unexplored. Rat atrial fibroblasts generate mechanically induced potentials (MIPs) by allowing influx of Ca^{2+} through activation of gadolinium sensitive non-selective cation conductance (53, 54). In human valvular myofibroblasts, activation of a Ca^{2+}-signaling pathway involves inositol triphosphate (IP_3) mediated mobilization from ER stores and activation of a capacitative Ca^{2+} entry mechanism through NSCC (55). Treatment with KB-R7943, an NCX inhibitor, of Madin-Darby canine kidney cells resulted in a marked diminution in cell migration under control conditions suggesting the involvement of the Na^+/Ca^{2+} exchange (NCX) (56). Recently, it was demonstrated that TGF-β1-mediated fibrogenesis is dependent on NCX reverse mode operation and was accompanied by a KB-R7943-sensitive increase in $[Ca^{2+}]_i$ (57).

Cytokine and growth factor receptor based Ca^{2+} signaling may be important in fibroblast and myofibroblast-mediated wound repair by augmenting cellular function through the mechanisms of capacitative Ca^{2+} entry or NCX1.1. However, very little work to investigate this possibility has been carried out. We have undertaken studies using blockade (KB-R7943) of plasmalemmal NCX1.1 to gain insight into the function of this protein in myofibroblast chemotaxis, contraction, and proliferation. We found that motility, contraction, and proliferation of PDGF-BB stimulated cells are sensitive to KB-R7943 treatment when compared to vehicle-treated control cells. We conclude that NCX1.1 is an important protein in mediating Ca^{2+} entry to the myofibroblast and that it may be important for multiple functions of these cells. Parallel

experiments were carried out to compare the effects of gadolinium blockade of NSCCs, and these studies revealed that only cellular motility was affected. The current results contribute to an understanding of myofibroblast physiology and Ca^{2+} homeostasis, specifically via KB-R7943- and gadolinium- dependent mechanisms which provide a link between myofibroblast Ca^{2+} handling vis-a-vis NCX1.1 and NSCC function.

II STATEMENT OF HYPOTHESIS

Molecular mechanisms of intracellular calcium (Ca^{2+}) signaling are well studied in cardiomyocyte function; however Ca^{2+} handling in cardiac nonmyocytes and especially myofibroblasts is poorly understood. Cultured cardiac myofibroblasts are motile, contractile and proliferative in response to various ligands including CT-1 and PDGF-BB. The current investigation is designed to address these functions with a focus on myofibroblast migration and their response to PDGF-BB, a relatively strong chemotactic agent for these cells.

WORKING HYPOTHESIS

Sodium-calcium exchange (Na^{+}/Ca^{2+} exchange) e.g., NCX1.1 is present in myofibroblast plasma membrane and may contribute to altered intracellular Ca^{2+} changes in response to PDGF-BB ligand binding and receptor activation; as a result, pharmacologic inhibition of plasmalemmal NCX1.1 may inhibit PDGF-BB mediated chemotaxis.

To a lesser extent we have pursued the following corollaries of the main hypothesis:

Corollary 1 – Inhibition of NCX1.1 may also affect PDGF-BB mediated myofibroblast contraction as assessed by collagen I gel deformation assays.

Corollary 2 - Inhibition of NCX1.1 may also affect PDGF-BB mediated myofibroblast proliferation.

Corollary 3 – In addition to NCX1.1, PDGF-BB mediated responses (see above) of myofibroblast requires non-selective cation channels (NSCC).

Corollary 4 – Conversion of fibroblasts to myofibroblasts is associated with blunted chemotaxis of these cells. In other words, freshly isolated rat cardiac fibroblasts (P0 cells) are more motile compared to cultures of myofibroblasts of increasing passage (P1 and P2).

Corollary 5 – PDGF-BB induced myofibroblast chemotaxis and contraction are dependent on phosphorylation of MLC, as determined by inhibition of MLCK with ML-7.

III. LITERATURE REVIEW

1.0 Cardiovascular disease

1. 1 Epidemiology and impact on Canadian society

Cardiovascular disease (CVD) is the leading cause of morbidity and mortality not only in Canada but also worldwide, and represents a major global socio-economic burden. According to the World Health Organization (WHO) in 2002, 16.7 million people died (30% of all global deaths) from CVD with coronary heart disease afflicting 7.2 million people – the largest proportion of CVD deaths (58). In Canada, over one third of all deaths were due to CVD in 1999. In this same year, coronary heart disease accounted for the greatest percentage of total deaths (20%) of which half were attributable to acute MI (59, 60). While genetic factors play a contributing factor in the development of CVD, 8 out of 10 Canadians are estimated to have at least one of the following major risk factors influenced by lifestyle choices: tobacco use, alcohol use, obesity, high blood pressure, high cholesterol, and diabetes; 1 in 10 have at least three or more (60). Despite overall declining mortality rates throughout the country (1, 60) due to development of better therapeutic interventions that improve patient outcome and prolong lifespan (2), CVD continues to have a significant economic impact in Canada. Health Canada estimated that in 1998 the total cost of CVD on the health sector of the Canadian economy was $18.5 billion in expenditures or 11.6% of the total cost of all illnesses (60). Direct costs of CVD – hospitalization, therapeutic interventions, and research – amounted to approximately $6.8 billion while indirect cost – loss of individual contributions to the economy due to premature death or disabilities – were $11.7 billion (60). Health Canada estimated that for the fiscal year 2000-2001, 18% of all hospitalizations were due to complications of CVD (60).

This societal burden of CVD warrants the need for enhanced understanding of cellular mechanisms relevant to the progression of cardiac dysfunction and heart failure. The development of efficacious therapeutic interventions to reverse or attenuate development of this disease is of primary importance.

1.2 Heart Failure: definition and etiology

Classically, heart failure is defined as a pathological state in which the heart is unable to supply blood to the systemic circulation at a rate commensurate with the metabolic demands of

bodily tissues (61). Aside from gradual deterioration in cardiac function due to cardiomyocyte death associated with the natural aging process (62), and despite the many etiologies, progression of heart failure generally involves common mechanisms. In response to myocardial injury or insult, the myocardium initially acts to compensate for loss of contractile function but over time these adaptive changes become maladaptive. Decompensation is associated with irreversible damage to the myocardium and thereby contributes to the onset of overt heart failure and patient death (61). Loss of cardiac pumping function may occur in the setting of causally diverse and multifactorial pathological settings (63). These pathological settings will be discussed as 3 broad categories: coronary artery disease (CAD), cardiomyopathies, and other forms.

1.2.1 Coronary artery disease

CAD is the most common cause of death in the world (64, 65). The hallmark of this disease is an accumulation of cholesterol in walls of the coronary arteries and development of atherosclerotic lesions or plaques (2). This condition is called atherosclerosis and often leads to ischemic heart disease. Lifestyle choices largely influence development, disruption and subsequent progression of plaques, although hereditary factors also play a role. Increased plasma low density lipoprotein (LDL), decreased high density lipoprotein (HDL), smoking, high blood pressure, alcohol, diet, obesity, inactivity, and diabetes all contribute to CAD (2, 66).

Atherosclerotic plaques obstruct coronary blood flow by physically occluding coronary arteries or suddenly rupture initiating a coagulation cascade causing hemorrhage (65) and intraluminal thrombosis (2, 66). Delivery of vital nutrients and oxygen to myocardial tissue becomes blocked. Known as ischemia, this conditions impairs energy metabolism in cardiac cells (14). The imbalance between myocardial oxygen supply and demand often manifests in clinical symptoms of a squeezing chest pain known as unstable angina (67). Short time periods of obstructed coronary blood flow followed by reperfusion are known to “stun” the myocardium (14). Termed preconditioning, transient functional abnormalities such as these are not lethal but help the heart to resist the damaging effects of future ischemic insults (14). If ischemia persists longer than 30 minutes, however, myocardial tissue endures irreversible damage, a condition called MI (2). Due to muscle injury, an inflammatory response is initiated at the site of the injury and aids in the reparative process involving formation of a myocardial infarct scar. The events

proceeding MI involve altered patterns of neurohormonal signaling cascades that primarily include Ang II, noradrenaline, endothelin-1, tumor necrotic factor (TNF-α), and TGFβ.

Hypoxia occurs as a consequence of ischemic insult. Under hypoxic conditions necrosis and apoptosis of cardiomyocytes ensue in the focal infarct and in the hypoperfused border zone, respectively (62). As cardiomyocytes are generally known to be terminally differentiated cells (it should be noted that this concept has recently become somewhat controversial), cardiomyocyte drop out results in substantial loss of contractile tissue. Structural changes in the left ventricle (LV) accompany functional changes enabling the heart to sustain cardiac performance in the face of increased hemodynamic load as seen in hypertension (5). These structural changes include: increased ratio of heart to body weight due to enhancement of sarcomeric protein expression in cardiomyocytes (hypertrophy) (68); breakdown of collagen tissue which holds individual myocytes together ("myocyte slippage") (63); breakdown of elatin resulting in loss of tissue strength, extensibility, resilience, and myocardium architecture (63); angiogenesis in the infarcted region; and disproportionate accumulation of interstitial collagen type I and III (5). Development of LV hypertrophy is initially compensatory as it acts to functionally augment loss of contractile units (68). Over time, structural changes to the myocardium overwhelm its ability to maintain appropriate function. Dysfunction occurs when the compensatory response transitions into a maladaptive or decompensated response. Alteration of ventricular shape from ellipsoid to a more spherical chamber contributes to LV dysfunction (69). Furthermore, ongoing wound healing of the infarct scar, which serves to replace non-functional tissue in this region, results in progressive accumulation of collagen into the non-infarcted myocardium. This process may continue indefinitely (69) and lead to the condition of cardiac fibrosis and end stage heart failure.

Cardiac fibrosis adversely affects the mechanical and electrical properties in the heart by increasing cardiac stiffness resulting in both systolic and diastolic dysfunction (5) and disrupting electrical continuity between myocytes which culminates in arrhythmogenesis (63). Pathological LV hypertrophy and fibrosis also contribute to CHF whereby fluid accumulation in lungs is indicative of this condition.

1.2.2. Cardiomyopathies

Cardiomyopathies are mostly genetic disorders (70). Dilated and hypertrophic cardiomyopathies are most common and are caused by genetic mutations (70). Dilated cardiomyopathy is due to a diverse array of mutations in proteins involved in force generation and force transmission. These mutations disrupt linkages between the cytoskeleton, sarcolemma and sarcomere (70). Dilated cardiomyopathy causes left ventricular chamber dilation and progressive wall thinning (9). Hypertrophic cardiomyopathy is idiopathic and is thought to occur as a result of genetic mutations in the sarcomere structure (70). This disorder is associated with a thickened intraventricular septum and LV walls. Hypertrophic cardiomyopathy results in obstruction of blood flow from the LV to aorta thereby leading to inefficient pumping action and ultimately diastolic dysfunction (9, 70). Heart failure resulting from both types of cardiomyopathies may arise from development of LV hypertrophy, LV MI, fibrosis, arrhythmias, and sudden cardiac death (9, 70, 71).

Toxic cardiomyopathies are generally induced by cancer therapies such as Adriamycin treatment (62). The toxic effects of Adriamycin are associated with global cardiomyocyte apoptosis and conditions arising from severe LV hypertrophy (62).

1.2.3 Other forms

Patients with diabetes have a high risk of developing heart failure (72). Termed diabetic cardiomyopathy, it is becoming more widely accepted that this disease directly damages myocardial structure and function independent from traditional risk factors ascribed to CAD such as high blood pressure, obesity, and age (72, 73). Hearts of patients with diabetes show a host of abnormal structural changes including LV hypertrophy, microvascular constriction, interstitial fibrosis (72), endothelial dysfunction, inflammation and vascular remodeling (73). These changes are exacerbated in patients with hypertension (72). Valvular heart disease is a condition resulting in aortic or mitral stenosis in which cardiac valves become narrowed (74). Regurgitation of blood back into the LV or atria due to valve dysfunction, causes LV volume and pressure overload and leads to progressive LV hypertrophy, remodeling and fibrosis (74). Although the cardioprotective effects of moderate alcohol consumption is subject to much debate, chronic alcohol consumption is linked to alcoholic cardiomyopathy. Adverse effects on the heart include LV hypertrophy, sudden cardiac death and arrhythmia (75). Myocarditis is an

inflammatory disease of the myocardium caused by a viral, bacterial or parasitic infection which weakens the heart and may lead to heart failure (76).

2.0. Pathophysiology of cardiac wound healing after myocardial infarction

The scar derived at the site of infarction post-MI has long been considered an inert and acellular tissue comprised mainly of interwoven collagen fibers (6). The infarct scar was generally regarded as dead tissue whose function was to restore structural support to the infarct region, thus preventing scar rupture by resisting tissue deformation and providing tensile strength (6). This notion was radically debunked as a growing body of evidence showed that collagen accumulation continued well after establishment of the healed infarct scar (77-79). Furthermore, evidence for scar vascularization led researchers to believe that the infarct scar was far more dynamic than previously thought (6). Current thinking reflects the hypothesis that the infarct scar is a living tissue populated with fibroblasts, myofibroblasts, and inflammatory cells. The infarct scar is thus metabolically active and is believed to provide both structural and paracrine function in part to the infarcted myocardium: neovascularization nourishes hypersynthetically active myofibroblasts, which in response to various peptides found upregulated in the infarct scar, confer contractile behavior, persist, and synthesize connective tissues (5). Ongoing wound healing coupled to its metabolic activity provides the impetus for ventricular remodeling and accumulation of fibrous tissue in the non-infarcted myocardium (5). The various phases of infarct wound healing, scar formation and the pathophysiology underlying ventricular remodeling leading to cardiac fibrosis will be discussed below.

2.1 The infarct scar is a metabolically active tissue

Obstruction of blood supply to myocardial tissue induces myocardial ischemia (80). Although the myocardium may recover from short-lived ischemic insults, deprivation of vital oxygen and nutrients for significant duration invariably leads to the development of an infarction and triggers an inflammatory response (14). The infarct zone is essentially a hypoxic tissue where a build up of lactic acid results in Ca^{2+} overload in cardiomyocytes and reactive oxygen species (ROS) formation (81). Toxic effects of intracellular calcium overload are a major determinant of myocardial cell damage and cardiac dysfunction by causing altered gene expression and damage to myofibril function during excitation-contraction coupling (81).

Reperfusion of the infarct zone in the early stages is beneficial in preventing cardiac damage but may also exacerbate myocardial injury, a condition called ischemia-reperfusion injury (80). ROS are formed from an excessive burst of oxygen which occurs during reperfusion (80). ROS such as superoxide, hydroxyl radicals, and hydrogen peroxide (80, 82) augment the damaging effects of Ca^{2+} overload and help to initiate the early inflammatory response (14, 80, 82).

Irreversible loss of cardiac tissue is characterized as death of cardiomyocytes via necrotic or apoptotic pathways (5, 83). Deficiencies in cellular energy metabolism through depletion of adenosine triphosphate (ATP) are known to cause necrosis 6-25 hours post-MI (62). The distinguishing feature of necrosis involves membrane rupture and is mostly localized in the region of the infarct zone (84) Apoptosis, on the other hand, is manifested within 6-8 hours (5, 62), and although found in the central infarcted region (62) it is thought to be predominantely localized in the border zone between the focal infarct and uncompromised myocardial tissue (84). Apoptosis of myocytes arises from the effects of elevated levels of Ang II, mechanical factors (84), and also exposure to ROS (85). Remnant cellular debris formed by apoptotic bodies are engulfed by macrophages and monocytes (84). Lysosomal enzymes, which are liberated into the extracellular space during necrosis, further enhance the appearance of phagocytotic cells into the infarct zone. These events invoke the early phase of the inflammatory response (5).

In the early phase of the inflammatory response (between 12 hrs and 4 days post-MI), blood platelets aggregate in the infarct zone (5, 35). They release granules that contain a number of bioactive molecules including PDGF and TGFβ. PDGF is chemotactic for blood neutrophils, monocytes, and fibroblasts and thus aids in initiating an inflammatory cascade (86). Neutrophils migrate into the infarct zone within 6-8 hr post-MI (5). They function to clear contaminating bacteria and degrade surrounding ECM by releasing matrix metaloproteinases (MMPs) (35). In addition, elevated levels of the cytokine, TNF-α, is found in the infarcted myocardium and plays a crucial role in triggering an inflammatory cascade (14). TNF-α is a known contributor to LV dysfunction due to its ability to induce intracellular calcium overload (87), myocyte apoptosis (88, 89), matrix and collagen degradation by inducing increases in MMP activity, and upregulation of AngII type I receptors (AT1) thereby favoring AngII mediated ECM deposition in the non-infarcted myocardium (88). Other cytokines found upregulated post-MI include: interleukin (IL)-6 (90), IL-8, IL-1, monocyte chemoattractant protein-1 (MCP)-1(91), basic fibroblast growth factor (bFGF), vascular endothelial growth factor (VEGF), (14), and

endothelin-1 (92). These cytokines also provide the chemotactic impetus for recruitment of mast cells, monocytes, and lymphocytes (14).

Once they have taken up residence in the infarct zone monocytes differentiate into macrophages (14) and function to scavenge tissue debris including dead myocytes (5, 35). Macrophages and mast cells further augment the inflammatory response by releasing a cocktail of cytokines, growth factors and ECM proteins which facilitates recruitment of additional cells like cardiac fibroblasts and endothelial cells into the infarct zone (14, 35).

The next phase of the wound healing process involves development of the infarct scar and is characterized by formation of granulation tissue. Under the influence of various cytokines including bFGF, PDGF, TGFβ, and VEGF, fibroblasts and endothelial cells migrate into the wound where they are stimulated to proliferate and metabolize ECM components (14). Mechanical stretch and elevated levels of TGFβ are factors involved in differentiation of normally quiescent synthetic fibroblasts into hypersynthetic contractile smooth muscle cell-like cells called myofibroblasts (6). Myofibroblasts play a key role in the pathophysiology of infarct wound healing as they synthesize and deposit collagen type I and III (21) through TGFβ (93) and Ang II dependent signaling mechanisms (94). The initial role of ECM deposition in the infarct zone is beneficial as it acts to replace dead myocytes and provides structural integrity to the infarct scar.

Building or remodeling of the infarct zone requires time dependent events and involves regulation of collagen turnover (95) as well as scar contraction (6). Within the first week post-MI the balance between collagen synthesis and degradation initially shifts in favor of the latter by myofibroblast dependent production and activation of specific MMPs (5), which function to degrade interstitial collagens (5). For instance, remodeling of the infarct scar in a rat model of left coronary artery ligation is associated with increased expression of MMP-1, 4-5 days post-MI (96). MMP-1 activity initially predominates and serves to degrade fibrillar collagen at the site of infarction (96). Myofibroblast contraction contributes to scar tonicity but prolonged collagenolytic activity and contractility results in myocardial wall rupture due to wall thinning, dilatation, and loss of tissue architecture (5, 6). After the end of the first week, expression of tissue inhibitors of MMPs (TIMPs) are elevated in the infarct zone, and function to suppress the activity of MMPs (94).

Formation of granulation tissue is also marked by newly forming neuronal innervations and vasculature. Vasculature is derived from endothelial cells spouting from neighboring capillaries (angiogenesis), transdifferentiation of bone marrow progenitor cells into endothelial cells (vasculogenesis), and enlargement of neighboring collateral vessels (arteriogenesis) (6). Neovasculature nourishes myofibroblasts and provides sustenance for the newly forming metabolically active scar (6). After 2-3 weeks, granulation tissue is replaced by type I mature cross-linked interstitial collagens. The organized assembly of collagen fibers continue to accumulate and mature for many weeks thereafter (94).

As residents in the infarct scar, myofibroblasts align themselves in a highly organized array. Orientation parallel to the epi- and endocardium is required for organization of the wound healing process. Although the mechanism that control myofibroblast alignment are largely unknown, there is evidence that migrating cardiac myofibroblasts express a homologue of *Drosophila* tissue polarity genes namely, *frizzled 2 (fz2)* (97) and *Dishevelled-1* (98). Upregulation of *fz2* gene expression and Dishevelled mRNA is found early after MI with a maximal peak occurring between day 4 and 7 (97, 98). The above findings suggest that once myofibroblasts are localized in granulation tissue of the infarcted region these genes may be involved in spatial control of wound healing (i.e. migration and proliferation) since mutations in the *fz2* gene impaired myofibroblast alignment (97).

Although macrophages begin to disappear in the granulation tissue via apoptosis, myofibroblasts continue to proliferate and contract - a hallmark of cardiac wound healing. In contrast to dermal wound healing (5, 35), cardiac myofibroblasts resist apoptosis and persist in the infarct scar continually depositing collagen (5, 6, 94) for prolonged period of time (18) Concomitant with inactivation of collagen degradation through activity of TIMP and myofibroblast presence in the infarct scar, the collagen remodeling balance shifts in favor of collagen deposition. Progressive collagen accumulation and myofibroblast contraction results in inappropriate or pathological wound healing and leads to hypertrophic scar formation, setting the stage for remodeling of the remnant or non-infarcted myocardium.

2.2 Remodeling of the non-infarcted myocardium

Changes in myocardial structure following an ischemic insult are collectively called myocardial remodeling (9). As the heart must adapt to altered hemodynamic load the remodeling

process is initially compensatory. Over time these changes overwhelm the functional capabilities of the heart. The factors that play a role in the pathophysiology of the scar post-MI are not limited to the scar itself, but rather provide the mechanisms for the development of inappropriate wound healing. Over time, cardiac wound healing culminates in the condition of cardiac fibrosis which is characterized by disproportionate accumulation of interstitial collagen in sites remote to the site of infarction (9). Although the extent of remodeling is dependent on size of the infarct (99), the infarct zone also serves to perpetuate remodeling of the non-infarcted (viable or remnant) myocardium.

As cardiomyocytes are terminally differentiated cells (62) their necrosis and apoptosis in both the infarct and non-infarcted myocardium results in a loss of contractile tissue which imposes extra strain in the non-infarcted myocardium (5, 62). Furthermore, repopulation of the infarct scar with myofibroblasts and their deposition of fibrillar collagen to replace dead tissue disrupt electrical impulses, which are normally conducted between closely coupled myocytes. Therefore, in response to loss of function, the myocardium undergoes remote time-dependent architectural and biochemical changes (100). To compensate for loss of contractile cells the myocardium dramatically increases in muscle mass via myocyte hypertrophy (101). Remnant myocytes also alter their phenotype to that of a fetal state which helps conserve energy expenditure by working at a lower oxygen consumption level (5)

The persistent nature of cardiac myofibroblasts triggers a positively reinforced cycle originating in the infarct scar which influences the remodeling process of the non-infarcted myocardium. TGFβ acts in an autocrine and paracrine fashion to influence myofibroblast phenotype transdifferentiation and collagen production. Since cardiac myofibroblasts synthesize and secrete TGFβ and resist apoptosis, a posivitely-reinforced cycle develops. The resultant pool of TGFβ and collagen accumulation produces a situation of inappropriate wound healing, infarct expansion (102) and subsequent hypertrophic scar formation. Elevated levels of AngII have also been implicated in the remodeling process by promoting TGFβ synthesis and by regulating collagen degradation via attenuation of MMP-1 activity while enhancing TIMP-1 production – further promoting collagen accumulation (94, 103, 104). Proliferation of fibroblasts and differentiation into myofibroblasts in the non-infarcted myocardium (105) is accompanied by increased transcription of fibrillar collagens type I and III within the first week post-MI (21, 94, 105). Furthermore, studies showed that the interplay between ECM organization, cytomechanical

stress and growth factor signals may also regulate the transition from fibroblasts to myofibroblasts (106). For instance, regulation of MMP activity plays a role in integrin formation (107), which are found at FA sites in the cell membrane and normally function to mediate interactions between the cytoskeleton and ECM (68, 107). Increased cell stretching in the setting of hypertrophy also enhances production of myofibroblast mediated pro-collagen type II mRNA synthesis (16).

2.3 Extracellular matrix and cardiac fibrosis

Normal myocardial ECM is comprised of an intimately organized network of collagen (108), fibronectin, laminin, elastin and chondroitin sulfate. These ECM proteins provide structural scaffolding thereby physically stabilizing, integrating, and transmitting myocyte-generated contractile forces throughout the myocardium (100, 107, 109). Fibrillar collagen is not only the most abundant ECM component but is also considered the most prevalent protein in mammals accounting for 25% of total bodily protein mass (100). In the myocardium, fibrillar collagen types I and III comprise 90% of the total collagen content (109). Collagen is deposited in interstitial spaces between parenchymal cells of the respective organ. It is produced by fibroblasts and regulated genetically by TGFβ mediated Smad signaling (see 103, 110-112 for extensive reviews on TGFβ signaling and the fibrotic response), and posttranscriptionaly by prolyl-4-hydroxylase (9). Collagen provides a scaffold that stabilizes the physical structure of tissue. In the myocardium it maintains ventricular geometry and myocyte alignment by forming struts or molecular tethers between cells (109). Moreover, collagen and other ECM components provide a medium for various cell processes (i.e. cell growth, migration and proliferation) and serve as storage sites for bioactive signaling molecules involved in these processes (100). Integrin receptors provide direct communication between cells and the ECM (109). Therefore, the matrix plays an important role in regulation of cell development and differentiation, migration, proliferation, shape and function (100).

Increased interstitial collagen is found in the non-infarcted region of the human myocardium post-MI (113) and this phenomenon is the principle determinant of alterations in cardiac structure. Thus fibrosis is a connective tissue disorder defined as the disproportionate expansion of fibrous connective tissue as a consequence of chronic inflammation or healing. Fibrosis functions to replace lost parenchymal tissue in the respective organ (106). Limited

wound healing in the post-MI heart may first be reparative. The regions of myocyte death are replaced with a structural scar but the progressive nature of the disease leads to reactive fibrosis involving dispersed accumulation of ECM deposition in regions unrelated to the focal insult (9). Clinical consequences of increased collagen content result in enhanced mechanical stiffness or decreased compliance which contributes first to diastolic (7, 9, 114) and later to systolic dysfunction (9). As well, increased collagen disrupts electrical continuity between myocytes which enhances the risk for reentrant arrhythmogenesis (9). Lastly, the appearance of *de novo* accumulation of collagen interferes with intracoronary arterioles (perivascular fibrosis) impairing myocyte oxygen availability. The effects of fibrosis on the myocardium further exacerbates the initial ishemic injury and depending on its severity may ultimately lead to heart failure (9, 114).

Other forms of fibrosis are studied in many organs including kidney, lung, and liver and represents a common pathway to organ failure (104). All fibrotic diseases have similar mechanisms with the defining characteristic being TGFβ mediated activation of myofibroblasts, their persistent nature, and *de novo* accumulation of interstitial collagen (104). Cardiac fibrosis, for example, reflects a common nexus in progression of heart failure etiologies despite substantial genetic and environmental factors that influence disease outcomes in individual patients (9). Thus, myofibroblasts are considered disease modifiers (9) and this, in turn, reflects a growing body of research directed at finding therapies to counteract or attenuate the pathological functions of these cells.

Therapeutic strategies are aimed to block excessive neuroendocrine activation post-MI. Angiotensin converting enzyme (ACE) inhibitors are enzymatic inhibitors of the angiotensin converting enzyme and function to reduce AngII production. Angiotensin receptor blockers (ARB) (4, 26, 115), aldosterone (9, 116), and endothelin-1 (92) all have proven beneficial in dampening the effects of cardiac fibrosis. Losartan, an ARB, is a common therapy with collagen attenuating benefits in a number of post-MI animal models (116-120). Other therapies target cytokine availability such as anti-TNF (9) and -TGFβ (103) while MMP inhibitors help attenuate ECM remodeling (9).

3.0 The non-myocytes

In normal myocardium, parenchymal tissue composed mainly of myocytes account for approximately three quarters of total volume whereas the other quarter is attributed to connective

tissue elements composed of mostly non-myocytes (102). Non-myocytes include fibroblasts, vascular smooth muscle cells, endothelial cells, mast cells and macrophages (121). In contrast to volume, non-myocytes account for three-quarters of total myocardial cell number, the majority of which are quiescent synthetic fibroblasts (102, 122). Cell cardiology literature is inundated with studies primarily focused on understanding the biology of the cardiac myocyte in physiological and pathological settings. In the last couple of decades, however, a growing body of knowledge has incited an increasing appreciation for the important contribution of the non-myocyte cell population – namely, cardiac fibroblast and myofibroblasts - in the functioning of the normal and failing heart, respectively (9).

3.1 Fibroblasts

Fibroblast cells populate all organs of the body (9). They are responsible for homeostatic maintenance of connective tissue components such as elastin, proteoglycans, and collagen with the latter being the principle manufactured protein (9, 123). In the healthy heart, cardiac fibroblasts function to produce and regulate a homeostatic balance of interstitial ECM components. Although each organ, such as kidney, lung, and skin, is thought to be comprised of fibroblasts with specific functional portfolios (9) all fibroblasts regardless of residence display similar morphological and cytological characteristics (123). They have a smooth contoured nucleus as well as numerous cisternae of rough ER and mitochondria (123). Fibroblasts express vimentin, desmin (123), procollagen type I and III, β- and γ-cytoplasmic actins (22), myosin isoforms IIa and IIb, tropomyosin, α-actinin, filamin, and tubulin (123). Our lab showed that fibroblasts express small but basal levels of αSMA (unpublished observations). They have migratory capabilities and as such must adhere to a substrate (123). Focal contacts containing integrin receptors provide direct communication between the actin cytoskeleton and ECM components (123). Cardiac fibroblasts are organized in a three dimensional network connected to each other as well as to myocytes via connexin-40 (124) and -43 and -45 (125), respectively. These attachments implicate electrical and biosignaling continuity between different cell types (124-126). Disruption of cell and electrical syncytium between fibroblasts and myocytes post-MI has adverse effects on the functionality of the myocardium. These adverse effects are attributable to the presence of myofibroblasts.

3.2 Myofibroblasts

Myofibroblast cells are important in the growth, development, and repair of diseased tissues affecting many different organs (127). The appearances of myofibroblasts are observed primarily during pathological processes such as during tissue injury and inflammation (20). An exception to this rule is in the normal myocardium where myofibroblasts are found only in valve leaflets (6, 94). Myofibroblast motility, proliferation, and isometric contraction contribute to net matrix deposition in the pathogenesis of cardiac fibrosis (5).

3.2.1 Structural properties

Myofibroblasts are differentiated hypersynthetic fibroblasts that display prominent cytoplasmic actin microfilaments (stress fibers), and produce elevated amounts of collagen type I and III, glycosaminoglycans, tenascin, and fibronectin (127). They have a highly developed rough ER and bundles of smooth muscle myofilaments with focal densities (128). Gap, adheren and fibronexus junctions attach to the ECM via focal contacts (3, 20, 127, 128). As is found in smooth muscle cells, a marker of myofibroblasts is the appearance of a contractile apparatus that includes expression of αSMA (20, 128, 129). A recent study showed that cardiac myofibroblasts express SMemb; this protein is a non-muscle-type myosin heavy chain abundantly expressed in embryonic and dedifferentiated smooth muscle cells (15). Both αSMA and SMemb expression are elevated in the infarct scar following coronary artery ligation (15, 18). The presence of myofibroblasts in the infarct scar implicates that they play an important role in mediating wound contraction during cardiac repair (15, 18, 129). Myofibroblast contraction is thought to reduce the denuded surface area of wounded tissue (127). In the latter phases of wound healing, contraction contributes both to infarct thinning leading to ventricular rupture (94), and to scar contracture, in turn leading to hypertrophic scar formation (130).

3.2.2 Influences of humoral factors on transdifferentiation

Myofibroblasts are thought to appear in the developing infarct scar 3-4 days post-MI. (94). Unlike dermal myofibroblasts which apoptose during the transition from granulation tissue to scar (35, 131), cardiac myofibroblasts persist in the infarct scar for many years. Although recruitment of myofibroblasts may be derived from resident fibroblasts there is evidence to suggest more than one recruitment route exists. They are thought to arise from either interstitial

fibroblasts, adventitial fibroblasts, pericytes, fibrocytes or circulating monocytes, or bone marrow-derived progenitor cells that transdifferentiate at the infarct site (6, 9, 127, 131).

TGFβ is considered an important player responsible for upregulation of αSMA expression and therefore maintenance of fibroblast-myofibroblast differentiation (9, 22, 94, 127, 131-134). Furthermore, fibroblasts embedded in granulation tissue of dermal wounds express high levels of TGFβ1 type I and II receptors (135). Excessive scarring is associated with a failure to eliminate TGFβ1 receptor expressing fibroblasts which resulted in overproduction of matrix proteins and subsequent fibrosis (135). In contrast, PDGF, TNF-α, and IL-1 do not stimulate myofibroblast formation (134).

Cytokines and growth factors that act to modulate fibroblast differentiation are released by cells involved in the inflammatory response (i.e. platelets, macrophages and neutrophils) or by myofibroblasts themselves and act in an autocrine fashion (127, 131). As they infiltrate the infarct and later the non-infarcted myocardium, cardiac myofibroblasts produce and secrete a plethora of chemokines, cytokines, growth factors, adhesion and matrix molecules such as: IL-8, IL-1, IL-6, TNF-α, IL-10, TGFβ, AngII, α1β1 integrins, endothelin-1, PDGF-BB, bFGF, and SCF (127). Acting in a persistent autocrine, paracrine, and positive feedback loop these factors help in the restoration of the wound and exacerbate ventricular remodeling.

3.2.3 Myofibroblast differentiation depends on mechanical tension

In addition to cytokine modulation, studies on primary cultures of rat cardiac myofibroblasts showed that differentiation occurs when fibroblasts are plated at low cell density (13). Furthermore, when cardiac fibroblasts were cultured in low serum conditions they were found to secrete increased concentrations of matrix proteins (136). Mechanical tension has also been suggested to play a role in transdifferentiation.

Gabbianni's research has set the foundations for the notion of mechanoregulation as an impetus for phenotypic modulation (22, 123, 134, 137). Cardiac fibroblasts "sense", integrate, and respond to changes in mechanical stimuli in the injured myocardium by altering patterns of gene expression (106, 138). For example, in ventricular remodeling and hypertrophy, α1β1 integrin receptors play a key role in transmitting the mechanical signals caused by altered myocardial stretch to cytoskeletal proteins, in turn, mediating activation of intracellular signal transduction pathways. Activation of these pathways is linked to upregulation of αSMA,

secretion of a number of profibrotic factors (TNF-α, AngII and TGFβ) and increased production of collagen fibers (138, 139). The concept of mechanosensation also occurs *in vivo:* granulation tissue subjected to increases in mechanical tension resulted in stress fiber formation and early upregulation of αSMA (140). Under the influence of tensile forces *in vitro*, cardiac fibroblasts differentiate into αSMA expressing myofibroblasts and the degree of αSMA expression in these cells is further modulated by the degree of force application (141). Although tractional forces generated by fibroblast motility may be sufficient to initiate wound closure, the above observations indicate that the appearance of resistance in the surrounding tissue as a consequence of ECM remodeling, would subsequently induce fibroblast-myofibroblast differentiation (106). Through αSMA-mediated contraction, myofibroblasts exert isometric tension on the surrounding ECM. This tension is further exerted at the level of FA and is dependent on both TGFβ and integrin function (142, 143).

The mechanical properties of the ECM have an important influence on myofibroblast morphology and function. All connective tissue is under mild mechanical tension (106) but fibroblasts are protected from the external tensile stress by their surrounding ECM. Furthermore, since fibroblasts have immature FA contacts they lack fully developed cell-matrix interactions. This "shielding" effect prevents uncontrolled myofibroblast activation and allows the meshwork of collagen fibers in the dermis and especially the myocardium to become subjected to large deformations without being transmitted to interstitial fibroblasts (106). Stress fibers do not develop and fibroblast quiescence is maintained (106). Alternatively, after injury as is the case post-MI, fibroblasts migrate from neighboring viable tissue. During formation of granulation tissue, the increasing number of motile cells enhances matrix rigidity by application of tractional forces exerted at the level of FA contacts. Elevation of mechanical tension is sensed by more fibroblasts and this induces additional reinforcement of fibroblast-matrix adhesions and development of intracellular contractile stress fibers. Finally, differentiation of fibroblasts into proto-myofibroblasts is thought to occur (144).

3.2.4 The proto-myofibroblast

Recently, Tomasek *et al.* described the wound healing process as playing host to two types of myofibroblast-like cells in that phenotypic transition from fibroblasts to fully differentiated myofibroblasts is proposed to require more than one step (106). For instance,

granulation tissue of lung alveolar septa comprise a heterogeneous composition of cytoskeletal proteins such that these cells show morphological characteristics of myofibroblasts (i.e. stress fibers) but are devoid of αSMA *in vivo* (145). A similar cell type appeared when fibroblasts were cultured on plastic and in the presence of serum (106). These cells are referred to as proto-myofibroblasts. Since they do not express αSMA, they are partly differentiated myofibroblasts whereas those cells that express this protein are considered fully differentiated myofibroblasts (106). Therefore, unlike myofibroblasts, proto-myofibroblasts are characterized by formation of stress fibers expressing only β and γ cytoplasmic actins (22). Once migrated into the wound, fibroblasts orient themselves parallel to the wound along expected lines of stress. Mechanical tension in the surrounding ECM is one of the principle factors that induce proto-myofibroblast phenotype (132); these cells acquire stress fibres, FAs and extracellular fibronectin fibrils (146).

During the wound healing process fibroblasts express an embryonic form of the fibronectin mRNA transcript, ED-A. Fibronectin exists in multiple forms and arises from a single mRNA transcript that can be alternatively spliced in three regions: EIIA (ED-A), EIIIB, and V (147). The ED-A splice variant, which is only present in wound healing situations, is regulated by TGFβ and plays an important role in promoting myofibroblast differentiation (106, 132). TGFβ also induces formation of mature and supermature FA (142, 148). Immature FAs are unique to proto-myofibroblasts whereas mature and supermature FAs are native to differentiated myofibroblasts. Mature and supermature FA have *de novo* appearance of tensin and FAK and express vinculin and paxillin (142).

The proposed existence of proto-myofibroblasts and differentiated myofibroblasts reflects the dynamic nature of the scar. Proto-myofibroblasts may function as an independent cell type having the ability to transition to αSMA expressing differentiated myofibroblasts, or revert back to a quiescently synthetic fibroblast-like phenotype in response to putative factors that occur in fibrocontractive diseases (106).

3.2.5 The myofibroblast as a target for therapeutic intervention

Phenotypic modulation of cells is crucial for wound formation. It provides the healing myocardium with a large population of hypersynthetic and contractile myofibroblasts that have a high proliferative potential and phenotypic plasticity (9). Understanding the characteristics and

functional properties of myofibroblasts during healing of myocardial infarcts is critical in the designing of therapeutic interventions aimed at improving cardiac recovery after MI (9).

4.0 Platelet-derived growth factor

Platelet-derived growth factor (PDGF) was identified in 1974 during a search for serum factors that stimulate proliferation of arterial smooth muscle cells originating from atherosclerotic plaques (149). PDGF was subsequently purified from α granules of blood platelets (86, 150, 151), which aggregate at the site of the wound during the inflammatory response. Since its discovery, PDGF has been extensively studied in culture-based assays of connective tissue cells where it's produced in different cell types and provides the intracellular signals that mediate a diverse range of cellular responses (150, 152). PDGF is a potent stimulator of cell motility, proliferation, growth and ECM protein synthesis and is a regulator of intracellular Ca^{2+} handling. Pathologically, PDGF plays an important role in wound healing and ECM remodeling in different organs (29, 30, 86, 150-153).

4.1 Structural diversity and cellular responses of PDGF isoforms

The PDGF molecule consists of two different but structurally similar polypeptide chains (154), termed A and B (30, 150). Recently, C and D chains were identified as novel members of the PDGF family (150). A pair of polypeptide chains form the active PDGF molecule by linking to each other via disulfide bridges (154) and forming combinations of either homo- or heterodimers. Genes for A- and B- chains are located on chromosomes 7 and 22, respectively (30). Protein expression is regulated at the transcriptional and post-translational levels (155). Isoforms are synthesized as precursor molecules and secreted into the extracellular space where they interact with collagen or heparin sulfate and become stored in the matrix (30). Proteolysis of matrix-stored PDGF may regulate its bioavailability (30). PDGF binding proteins such as α_2-macroglobulin (156) and PDGF-associated protein (PAP) (157) enhance PDGF activity by regulating its availability for interaction with cell receptors (30).

Synthesis of different isoforms takes place in a plethora of cell types, each isoform exerting a diverse range of cellular responses (30). For example, both A- and B- chains are produced in fibroblasts, vascular smooth muscle cells, vascular endothelial cells, and macrophages, whereas only PDGF-AA is synthesized in skeletal myoblasts, astrocytes, and

oocytes (30). In one study, exposure of rat embryonic hearts to PDGF-BB resulted in a substantial increase in protein synthesis and myofibrillar differentiation suggesting that PDGF may play a role in myocardial development (158). *In vitro*, PDGF-BB upregulates collagen synthesis in cultures of fetal rat calvaria, proteoglycan synthesis in arterial smooth muscle cells (159), induction of fibronectin mRNA in a mouse embryo cell line (160), and stimulation of hyaluronan synthesis in human cultured fibroblasts (161).

The PDGF-BB isoform is considered the most potent mitogen, but PDGF-AA is also a moderate stimulant of DNA synthesis in primary rat cardiac fibroblasts (162, 163) and smooth muscle cells (164). Whereas PDGF-AA inhibits chemotaxis, PDGF-BB induces potent stimulation of motility in a variety of cell types (151). Furthermore, PDGF of an unspecified isoform is implicated in the formation of proto-myofibroblasts *in vitro* and *in vivo*. PDGF does not induce αSMA expression and, therefore, is not associated with formation of fully differentiated myofibroblasts (165, 166).

4.2 PDGF receptors and signaling targets

Since PDGF isoforms are dimeric molecules, they exert cellular actions on responsive cells by simultaneously binding to two structurally homologous α- and β PDGF receptors (PDGFR). Binding forms a bridge between the receptors (29, 30, 86, 150-153). PDGFRα binds A, B, and C chains while PDGFRβ binds only B and D chains (150). Different signaling receptor complexes are formed based on which receptor types the target cell expresses and the particular PDGF isoform present (151). PDGF-AA, -AB, -BB, and –CC induces αα receptor homodimers, PDGF-AB and –BB αβ receptor heterodimers, and PDGF-BB and DD ββ receptor homomeric receptor complexes (150). The extracellular region of each receptor contains a ligand binding domain consisting of 5 immunoglobulin-like domains while the intracellular region consists of a tyrosine kinase domain (30, 153).

Upon ligand binding, receptors dimerize causing cross-phosphorylation leading to kinase activation, autophosphorylation of key tyrosine residues in the receptors and, in turn, phosphorylation of downstream intracellular effectors (30, 151, 153). Conserved tyrosine residues (Tyr857 in β –receptors and Tyr849 in α –receptors), located in the activation loop of the tyrosine kinase domain function to increase kinase activity while other autophosporylated tyrosine residues located outside the kinase domain provide docking sites for a class of signal

transduction molecules containing Src homology 2 (SH2) domains (167). A large number of SH2 domain proteins bind PDGFRβ and PDGFRα. Each SH2 domain molecules that binds to PDGFR either directly initiates or connects the receptor with the activation of downstream signal transduction pathways thereby driving different cellular responses (30). Enzymes involved in catalyzing downstream signaling cascades include: phosphatidylinositol 3'-kinase (PI 3-kinase), phospholipase C-γ (PLC), Src family of tyrosine kinases, tyrosine phosphatase SHP-2, and the family of small guanosine triphosphatase (GTPase) activating proteins (GAP) for Ras (30). Other molecules are devoid of enzymatic activity but function as adaptor proteins to link the receptor with downstream catalytic molecules. Adaptor proteins include: Grb2 which forms a complex with the nucleotide exchange molecule Sos1 that activates the family of small GTPase Ras, Grb7, Nck, Shc, and Crk (30, 150). Furthermore, members of the signal transducer and activator (STAT) family also bind to PDGFR, become phosphorylated themselves and translocate into the nucleus where they act as transcription factors (30).

PDGF receptor combinations transduce similar but sometimes mutually exclusive cellular signals and the response is dependent on which of the two receptor types the cell expresses. Fibroblasts and smooth muscle cells are considered the classical target cell for PDGF; these cells express high levels of β-receptors (30). While cells like human platelets and rat endothelial cells only express α-receptors, others such as mouse capillary endothelial cells only express β-receptors (30). In vascular smooth muscle cells, stimulation with bFGF selectively increased expression of α-receptors (164). In another experiment, IL1 and TNF-α were found to induce upregulation of α-receptors in osteoblast cultures (168). On the other hand, TGFβ stimulation of lung fibroblasts (169) and human neonatal fibroblasts (170) led to α-receptor downregulation (169) suggesting that TGFβ inhibits the mitogenic activity of PDGF. It is generally accepted, however, that α and β receptors mediate potent mitogenic signals independent of cell type. As described above, while activation of β receptors stimulates chemotaxis and formation of actin structures, activation of α receptors inhibits chemotaxis in certain cell types such as fibroblasts and smooth muscle cells but still stimulates chemotaxis in other types (151, 171). In smooth muscle cells, both receptors mediate mobilization of Ca^{2+} transients from extracellular stores via membrane channels (172) and intracellular stores (173).

4.3 Physiological and Pathophysiological role of PDGF

PDGF is important for orchestrating the wound healing process (30, 150). To that end, PDGF stimulates proliferation and chemotaxis of fibroblasts and smooth muscle cells as well as chemotaxis of neutrophils and macrophages; induces fibroblasts to synthesize ECM, i.e. collagen; stimulates contraction of collagen gels *in vitro* (30); and modulates proliferation of endothelial cells thereby enhancing angiogenesis (27). In contrast to non-healing tissue, granulation tissue of healing wounds contain elevated expression of PDGF isoforms (174). In addition, application of topical recombinant human PDGF to open dermal wounds augments healing by increasing the rate of myofibroblast contraction. Also, rapid formation of granulation tissue occurred due to enhanced mitogenic and chemotactic actions on fibroblasts, smooth muscle cells, neutrophils and macrophages (30). PDGF also regulates tonus in blood vessels, aggregation of platelets, and tissue homeostasis through its ability to stimulate interactions between connective tissue cells and molecules of the ECM (30).

In vivo studies utilizing gene knockout and gain-of-function transgenic tools, show that PDGF drives distinct cellular responses during successive stages of embryogenesis in mice (152). PDGF plays an important role in driving migration, differentiation and function of specialized mesenchymal and progenitor cell types during embryonic development of the kidney, blood vessels, lungs, central nervous system and various connective tissue compartments (150, 152). In many cases, PDGFR gene knockouts have proven embryonic lethal (153).

There is a clear association between PDGF and the pathogenesis of certain disease states (86). Since the sis oncogene encodes the B-chain, PDGF may also be involved in viral transformation (30). Furthermore, human malignant mesodermal cells express PDGF receptors *in vitro* and *in vitro* (175). These findings provide evidence that over-activity of PDGF may be involved in stimulation of growth and metastasis of human tumors (30, 175). In contrast to healthy arteries, PDGF expression is increased in atherosclerotic lesions (30, 86). Moreover, elevated levels of plasma PDGF are present in post-MI and stable angina patients (28). Taken together these findings provide direct evidence that progression of the inflammatory response that characterizes CAD is augmented with elevated expression of PDGF (30, 86). The link between PDGF as a potent mitogen and chemokine is evident during conditions of restenosis following balloon angioplasty (176). Migration of arterial smooth muscle cells through injured vessel endothelium, and their subsequent proliferation in the intimal layer, results in generation

of neointema and may lead to vessel occlusion (176). Since activation of PDGFRβ plays a prominent role in the cell processes associated with atherosclerotic lesions, selective inhibition of receptor kinases at the site of balloon angioplasty might be of significant therapeutic benefit (176). PDGF is further implicated during ECM remodeling and fibrosis of a variety of organs such as heart, liver, skin and kidney (29, 30). Myofibroblast migration, proliferation, survival and collagen synthesis is enhanced by PDGF (153).

Based on its cellular functions PDGF and its receptors are, therefore, considered pro-inflammatory and –fibrotic, the effects of which are exacerbated due to its autocrine and paracrine signaling actions.

5.0 Cardiotrophin-1

Screening from a cDNA library of embryonic stem cell clones which induced hypertrophy in cultured cardiomyocytes led to the identification and cloning of a novel cardiac growth factor, CT-1 (177). Isolated in 1995 with a molecular weight of 21.5 kDa (177), CT-1 is classified among the interleukin (IL)-6 family of cytokines (177, 178). Aside from CT-1, members of the IL6 family include IL-6, IL-11, oncostatin M, and ciliary neutrophic factor. Members share sequence similarities, a common four α-helix bundle topology (178), activation of a common receptor subunit granulation protein (GP)-130, and intracellular signaling via activation of Janus kinases (JAKs) and transcription factors of the STAT family (178, 179). Like PDGF, the IL-6 family of cytokines shares functional redundancy: different types of cytokines invoke the same biological activities in a specific cell or tissue. They play an important role in regulation of complex cellular processes such as gene activation, proliferation and differentiation. Recent studies show that CT-1 regulates cardiac myofibroblast function implicating the involvement of this cytokine in cardiac wound healing post-MI.

5.1 Signal Transduction Cascade

Ligand binding of CT-1 dimerizes a receptor complex consisting of gp130 and leukemia inhibitory factor receptor (LIFR) (178, 180). Hetero-dimerization of receptors leads to activation and auto/trans-phosphorylation of gp130-associated JAK1, JAK2, or Tyk2 proteins (181, 182). Activation of JAKs phosphorylate gp130 at cytoplasmic tyrosine residues thereby creating matching docking sites for SH2 domains of inactive STAT1 and STAT3 (183). Recruitment of

STATs through interactions with gp130 and JAKs and their subsequent tyrosine phosphorylation leads to formation of STAT homo or heterodimers (183). Once activated, STATs act as transcription factors by translocating into the nucleus and binding to specific promoter regions to stimulate or repress transcription of target genes (178, 183). Some target genes associated with STAT are TIMP-1, interstitial collagenase, heat shock protein (hsp)-90, lipopolysaccharide-binding protein, and suppressor of cytokine signaling (SOCS) (178, 179). Aside from activation of STATs, JAKs also activate a variety of other signaling pathways responsible for mediating cardiac hypertrophy and other cellular responses. Some of the signaling pathways include activation of extracellular signal regulated kinases (ERK), mitogen activated protein (MAP) kinases, PI3-kinase, AKT, and the Src pathway (178, 179).

SOCS are an endogenous family of molecules that act as negative feedback regulators for the IL-6 family of cytokines. The SOCS family is thought to contain a SH2 domain that interacts directly with the kinase domain of JAKs (184). SOCS inhibit the tyrosine phosphorylation activity of JAKs, gp130, STAT1 and STAT3 (184, 185). Upregulation of SOCS3 via forced gene transfer and mechanical stretch suppresses CT-1 mediated cardiomyocyte hypertrophy (186) while AngII treatment enhances the expression of SOCS3 mRNA in rat hearts and cardiomyocytes (187).

5.2 Physiological role of CT-1

CT-1 is a pleiotrophic cytokine based on its ability to exert a variety of cellular activities *in vitro*. Some biological functions of CT-1 include: inhibition of mouse myeloid leukemic cell growth, modulation of sympathetic neuron transmitter phenotype, promotion of dopaminergic neuron and spinal neuron survival, inhibition of embryonic stem cell differentiation and increase of protein expression in hepatocytes (178). Basal levels of CT-1 mRNA are expressed in heart, kidney, skeletal muscle and liver (177), and expression of gp130 and LIF receptors are found in most tissues of rodents and humans (178). Activation of the gp130/LIF receptor regulates growth and differentiation in a variety of cells including hematopoietic and lymphoid cells, neuronal cells, hepatocytes and osteoclasts (178). CT-1 treatment in cultures of mouse bone osteoclasts resulted in osteroclast differentiation and activation suggesting that CT-1 has an important role in bone remodeling during osteoporosis (188, 189). CT-1 is abundantly expressed in both cardiomyocytes and non-myocytes (190). Fluorescent *in situ* hybridization analysis has

demonstrated that, unlike other IL-6 members, the mouse CT-1 gene is located on chromosome 7F3 and contains a variety of transcription factor binding motifs which are known to be important in cardiomyocyte growth and differentiation: CREB, MyoD, NF-IL6, Nkx2.5, and GATA (191). Norepinephrine (NE) may regulate transcription of CT-1 based on evidence that: i) expression of CT-1 mRNA in cardiac myocytes is augmented in the presence of NE *in vitro* and *in vivo*; and ii) the discovery that the NE responsive elements is located in the promoter region of the gene (191). Embryonic knockout mice homozygous for gp130 have severely under developed heart tube formation and are non viable (178). Furthermore, CT-1 is expressed during the early phases of heart tube formation (178). These studies provide evidence for the importance of the gp130 signal transduction pathways, particularly CT-1, in development of the ventricular chamber (178). While most studies have focused on the functional properties of CT-1 in cardiomyocytes, little is known about the effects of CT-1 on cardiac fibroblast function (10). CT-1 induces phosphorylation and subsequent activation of the JAK/STAT pathway in cultures of rat cardiac myofibroblasts (178, 192). Furthermore, cardiac canine fibroblasts express gp130, and LIF receptors and treatment with CT-1 *in vitro* resulted in proliferation of these cells (178, 193) as well as rat cardiac myofibroblasts (178, 192). CT-1 is also a chemokine, albeit a weak one, for rat cardiac myofibroblasts (192) and stimulates enhanced collagen secretion/synthesis, but when cell number is normalized, CT-1 appears to downregulate collagen synthesis in these cells (10)

5.3 CT-1 in the pathogenesis of the myocardium

While endogenous expression of CT-1 in healthy tissues is maintained at a balanced equilibrium, elevated levels are well documented in contributing to the pathogenesis of the myocardium.

Immunoluminometric analyses revealed elevated levels of CT-1 in samples of plasma extracted from patients diagnosed with heart failure and unstable angina (23), left ventricular systolic dysfunction (LVSD) due to MI (23, 24) and aortic stenosis (24). Moreover, levels of CT-1 mRNA are increased in ventricles of 4 week old genetically induced spontaneous hypertensive rats but expression did not correlate with severity of LV hypertrophy (194). Induction of pressure overload in rats by ligation of the abdominal aorta also resulted in enhanced CT-1 mRNA expression and was concomitant with time-dependent activation of CT-1 mediated JAK/STAT

pathway (194). In another study, increases in CT-1, gp130 mRNA and protein levels were observed up to 56 days post-MI; immunohistochemistry revealed that these proteins are expressed in cardiomyocytes and fibroblast-like cells with intensity of staining peaking at 7 days post-MI (195). In another rat model of acute MI, CT-1 protein expression was found elevated in the infarct zone as early as 24 hour post-MI and persisted through 2, 4 and 8 weeks, compared to sham-operated animals (196). In this same study, at 8 weeks a trend toward increased expression of CT-1 in the non-infarcted myocardium is consistent with progress of LV hypertrophy post-MI (196).

Chronic administration of CT-1 causes dose-dependent increases in ratios of heart rate and ventricular weight to body weight with no changes in number of cardiac cells, indicating that myocardial hypertrophy is developed in animals treated with CT- 1 (197). This finding is consistent with the observation that treatment with CT-1 *in vitro* induces cardiac myocyte hypertrophy by adding sarcomeres in series which leads to increased cardiac myocyte size due to increases in cell length with little changes in width (198). Sarcomeric assembly in series results in eccentric hypertrophy and chamber dilatation (199). CT-1 mRNA expression was augmented in mice cardiomyocytes subjected to hypoxic conditions along with increased activation of STAT3 (200). Activation of the JAK/STAT pathway in cardiomyocytes is induced by mechanical stretch and partially dependent on AngII-mediated activation of protein kinase C (PKC) and a rise in intracellular calcium (201). Furthermore, AngII-stimulated conditioned medium from cultures of cardiac rat fibroblasts contained elevated levels of CT-1 protein. Hypertrophy resulted upon exposure of this medium to cultures of rat myocytes (202). These results suggest CT-1 may be secreted from cardiac fibroblasts further suggesting a cross-talk phenomenon between cardiomyocytes and fibroblasts subsequent to AngII-induced cardiomyocyte hypertrophy (202). These data provide both *in vivo* and *in vitro* evidence for the role of CT-1 in cardiomyocyte hypertrophy and ventricular remodeling following acute MI.

5.4 CT-1 promotes cell survival

Research into the cytoprotective role of cytokine signaling through gp130 is burgeoning. Signaling through gp130 by CT-1 administration delayed the onset of motor neuron degeneration in a mouse model of amyotrophic lateral sclerosis (203) and promotes survival of embryonic and neonatal rat cardiomyocytes *in vitro* (25). The latter provides evidence that in the presence of

CT-1, myocardial cells may resist the effects of apoptosis in the post-MI myocardium. Anti-apoptotic effects are mediated through activation of STAT3 in conjunction with MAP kinase (25), and PI3K/Akt pathways (204). Promotion of cardiomyocyte survival through STAT3 signaling is, therefore, contradictory since STAT3 is also known to induce hypertrophy in cultures of cardiomyocytes. This suggests that gp130 mediated cardiomyocyte hypertrophy may be independent from MAPK and PI3K signaling indicating that these biological responses occur through divergent signaling pathways (178). CT-1 promotes cardiac cell survival *in vivo* and *in vitro* when treatment commences prior to or after hypoxic/ishemic conditions (205), and protects cardiomyocytes *in vitro* against re-oxygenation injury (206, 207). Activation of gp130 *in vivo* by intravenous injection of LIF in mice at 2 weeks post-MI induced myocardial regeneration by protecting myocytes from death and enhancing neovascularization (208). Injection of CT-1 in this same model resulted in reduction in mean arterial pressure and increases in heart rate without changing cardiac output (209).

In the compensatory phase of the post-MI myocardium, elevated levels of CT-1 may provide dual effects. CT-1 may be cardioprotective by promoting cardiac hypertrophy thereby compensating for loss of myocytes and protecting myocytes from death. Secondly, CT-1 helps in the repopulation and hence increases the cellularity of the infarct scar by providing chemotactic and mitogenic signals for cardiac myofibroblasts. The putative role of CT-1 in cardiac remodeling may initially act to downregulate collagen synthesis on a per cell basis *in vitro* (10) and in this way may oppose TGFβ pro-fibrotic effects.

6.0 Fibroblast growth factor-2

In 1974 a polypeptide purified from brain and pituitary gland stimulated DNA synthesis in quiescent 3T3 fibroblasts (210). The protein was found to have two isoelectic points residing at pHs of 9.6 and 5.6 resulting in the terms basic (b)FGF and acid (a)FGF, respectively (211). Despite its name, subsequent studies showed that FGF is produced and exerts mitogenic and survival signals in and for a wide variety of cultured mesoderm-derived cells found in epithelia, muscle, connective and nervous tissues (212, 213). In 1991 aFGF and bFGF were renamed and classified into subfamilies of FGF-1 and -2, respectively (214). Currently, 23 structurally related polypeptides of the FGF family (i.e. FGF-1 through -23) are identified in human and other vertebrates (211, 215). Like CT-1 and PDGF, FGF-2 is well characterized as a pleiotrophic

cytokine that exerts multiple effects on a variety of cell types (216). FGF plays a crucial role in embryonic development, maintenance of tissues, angiogenesis, and wound healing and repair (217). Similar to vascular endothelial growth factor (VEGF) and heparin-binding epidermal growth factor-like growth factors, FGF-2 binds with high affinity to heparin and is further classified as a member of the heparin binding growth factor family (32). FGF-2 is also thought to be cardioprotective and is implicated in a number of myocardial pathological conditions such as cardiac hypertrophy, atherosclerosis and wound healing post-MI.

6.2 Structure of FGF-2: high and low molecular weight isoforms

Within the last decade a new classification strategy was developed to describe the FGF family. FGF-2 exists as a high (Hi) or low (Lo) molecular weight species consisting of 21-24 and 18kDa, respectively (31). Hi and LoFGF-2 are derived from alternative translation initiation sites of different promoter regions on the same FGF-2 DNA sequence (31) and is regulated by internal ribosomal entry sites on the FGF-2 mRNA (218). Translation initiation on the conventional methionine (AUG) start site produces the 18kda form (LoFGF) (211, 219), while translation on upstream leucine (CUG) sites produce the larger FGF-2 isoforms (HiFGF) (31, 219). Studies on localization of FGF-2 show that HiFGF-2 localizes exclusively to the nucleus where it acts as a transcription factor (219-222). Nuclear localization comes from evidence that the N-terminal region of the protein contains a nuclear localization signal and has the ability to guide fusion proteins to the nucleus (220, 223, 224). Whereas HiFGF-2 is predominantly targeted to the nucleus, LoFGF-2 is largely thought to have cytoplasmic distribution. It is secreted into the extracellular environment where it functions as an autocrine and paracrine cytokine by binding to membrane receptors (31, 225). LoFGF2 exerts its effects as a mitogen and chemokine (226). LoFGF-2 is devoid of a secretory sequence. Consequently, the mechanism of exocytosis utilizes an alternative pathway independent of the ER-Golgi complex (227) but is energy dependent (228). Most studies focus on LoFGF-2 since its biological effects are easier to study.

6.3 Mechanisms of action: extra- and intracellular signaling

FGF-2 exerts its biological activities both as an extracellular and intracellular factor. As a ligand, FGF2 exerts paracrine and autocrine actions by binding to high affinity FGF receptors (FGFRs). FGFRs are divided into four distinct types, FGFR1-4, and each are encoded by a

separate gene (217, 229). These receptors share common features including a cytoplasmic conserved intrinsic tyrosine kinase domain and an extracellular binding domain. A lower affinity class of binding sites for FGF2 has also been identified as heparin sulfate proteoglycans (HSPGs) and are located either in the plasma membrane and/or ECM (230). HSPGs may regulate the action of FGF-2 by enhancing FGF-FGFR interaction (229) via increasing its affinity for its receptor while protecting them from protease degradation and thermal denaturation (215). Further studies have revealed that heparin-like molecules help modulate binding of FGF-2 to its receptor by increasing the concentration of the ligand available for receptor binding (231).

Binding of FGF-2 results in the dimerization of FGFR and leads to autophosphorylation of tyrosine kinases in the cytoplasmic domain of the receptor. Phosphorylation of tyrosine residues activates SH2 binding sites and leads to activation of intracellular signaling pathways such as MAPK (via Ras activation), PKC, and Src-associated pathways (31, 217). FGF2 also activates extracellular signal regulated kinases (ERKs), p38 and c-jun N-terminal kinases (JNKs) in different cell types (31, 232). After binding to high affinity FGFRs, FGF and FGFR are internalized by a clathrin-mediated mechanism where they enter endosomes or lysosomes causing their desensitization and degradation (215).

As HiFGF-2 is known to contain a nuclear localization signal, it functions as an intracrine factor by targeting the nucleus. Under various conditions such as hypertrophy, FGFR1 is released from the Golgi and forms an intracellular complex with HiFGF-2 followed by nuclear transport via importin β (31). The FGFR1-HiFGF-2 complex associates with nuclear structures such as polymerase II (31). In the nucleus, FGFR1 activates promoters of various genes including that of FGF-2 (31). LoFGF-2 also interacts with other proteins involved in intracellular trafficking including translokin (233), FGF-2 interacting factor (FIF) and casein kinase (CK)2 (215, 234). FGF-2 dependent CK2 activation, for example, leads to activation of rRNA synthesis (31, 215, 234).

6.4 Biological and pathological roles of FGF-2

FGF-2 regulates cell survival, apoptosis, proliferation, differentiation, ECM deposition, chemotaxis, cell adhesion, migration, and growth (235). Furthermore, FGF-2 plays a role in vertebrate limb formation during embryogenesis, vasculogenesis, wound healing, tumorigenesis, angiogenesis and blood vessel remodeling (235). Immunostaining has revealed expression of

FGF-2 in a wide variety of normal human tissues including basement membranes and smooth muscle cells of blood vessels, basement membranes and endothelial cells of capillaries of brain, lung, skin and lymph nodes, and cardiac muscle fibers, vascular, gastrointestinal, and uterine smooth muscle cells (216). Ubiquitous expression of FGF-2, therefore, provides evidence for its role in development and function of numerous organ systems.

In the myocardium, FGF-2 isoforms are expressed in several cells such as myocytes (236), vascular endothelial cells (212), fibroblasts, macrophages and mast cells (237). FGF-2 acts on FGFR1 and expression of this receptor is required for normal cardiac development (238). FGF-2 is found in the extracellular milieu surrounding cardiac myocytes (229) and its release from myocytes via exocytosis is associated with the activity of the Na^+/K^+ ATPase pump (32). FGF-2 secretion may also occur from a passive process involving cell lysis during tissue injury and cell death (31). In the postnatal heart, FGF-2 release occurs on a beat-to-beat basis (32, 239). FGF-2 is upregulated after cardiac injury (240) and during coronary collateralization (241), and exerts cardioprotective effects both *in vivo* and *in vitro* (32). LoFGF-2 enhanced survival rates of cultures of neonatal rat cardiac myocytes treated with hydrogen peroxide to simulate ischemic-reperfusion injury (32). *In vivo*, LoFGF-2 confers cardioprotective effects in rat hearts subjected to ischemia with or without reperfusion (242), and in spontaneously hypertensive rats (243). LoFGF-2 mediated improved myocardial function post-MI by reducing infarct size (244) and protected against arrhythmias (245). Intramyocardial FGF-2 administration after onset of ischemia-reperfusion injury protected acute and chronic cardiac dysfunction and damage. Cardioprotection occurs through activation of FGFR1 and triggering of PKC. PKC stimulates phosphorylation of Cx43 (246), which depresses metabolic coupling via this gap junction (247). Myocyte uncoupling is cytoprotective by prevention of hypercontracture as well as spreading of harmful oxygen species caused by reperfusion injury (247). Increased myocardial expression of endogenous FGF-2 by transgenic overexpression was also associated with increases in myocyte viability following a model of ishemic-reperfusion injury (248) while mice deficient in FGF-2 expression developed no compensatory response to cardiac hypetrophy in an AngII-dependent hypertensive mouse model (249). FGF-2 enhanced myocardial capillary collateral development in dogs with coronary occlusions (250).

The role of FGF-2 in cardiac hypertrophy and cardiac remodeling is not well defined. Nevertheless, implications of FGF-2 in the hypertrophic response is supported by studies in

which lack of a pressure-induced hypertrophic response was observed in transgenic mice deficient in FGF-2 (251). Furthermore, FGF-2 enhanced fibroblasts, myofibroblasts and vascular smooth muscle proliferation and motility *in vitro* (252), abrogated the formation of type I collagen fibers in ECM of cultured human vascular smooth muscle cells, decreased pro-chains of type I and III collagen mRNA, and augmented expression of MMP-1 (253). FGF-2 treatment of cultured cardiac fibroblasts increased intercellular electrical coupling between fibroblasts via upregulation of Cx43 mRNA and protein (246). Subcutaneous treatment of FGF-2 to dermal wounds in mice resulted in an anti-scarring-like effect by inhibiting fibroblast-myofibroblast phenotypic differentiation and improving collagen crosslinking in the chronic phase of the wound healing process (254).

In addition to its proposed role for maintenance of the healthy myocardium, presence of FGF-2 at various stages of injury may affect, positively or negatively, the disease process (32). Taken together these results support the notion that FGF-2 may be of therapeutic potential during cardiac injury. FGF-2 may preserve the functionality of the myocardium and the infarct scar in the early phases of wound healing post-MI by enhancing cardiomyocyte survival and stimulating cardiac hypertrophy, angiogenesis, and overall repopulation of the infarct scar. Increases in fibroblast-fibroblast and fibroblast-myocyte connectivity through Cx43 accumulation may compensate for interruption of electrical conduction by providing alternative means for electrical communication, and in this way help prevent arrhythmogenesis, which is prevalent during the onset of cardiac fibrosis (32).

7.0 Cellular motility

Cell motility (also referred to as chemotaxis, migration, or locomotion) is crucial for the survival of multi and single celled organisms. In prokaryotes motility is equally as important for moving toward sustenance as moving away from harmful substances (255). In eukaryotic organisms, cell motility is involved in maintaining overall health and is implicated in physiological and pathological conditions. Cell migration orchestrates morphogenesis throughout embryonic development (36, 256). Examples of this are during gastrulation whereby groups of progenitor cells migrate from various epithelial layers to target specific locations and differentiate to form tissues or organs (256) such as the development of the nervous system (36) and heart tube. Renewal of skin and the intestinal epithelium involves migration of new

epithelial cells from the basal layer and crypts, respectively (256). The inflammatory response is mediated by migrating leukocytes that infiltrate areas of injury where they perform phagocytic and immune functions by destroying invading microorganisms, getting rid of infected cells, and clearing debris (36, 256). Wound healing involves a wave of migrating fibroblasts and vascular endothelial cells (36) which work in concert to generate a scar and new blood vessels (257). In metastasis, tumor cells migrate from the focal tumor mass into the circulatory system, travel throughout the body and later invade tissues forming new tumor growths (36). Other pathological processes that occur as a result of cell migration are vascular disease (atherosclerosis), osteoporosis, rheumatoid arthritis, multiple sclerosis, mental retardation and chronic inflammatory diseases (256). With respect to the latter, infiltration of the developing infarct scar by interstitial cardiac fibroblasts from the viable myocardium and border zone of the infarct not only aids in reparative fibrosis (258) by increasing the cellularity of the scar, but also contributes to activation of myofibroblasts and ultimately development of a hypertrophic scar leading to reactive cardiac fibrosis.

7.1 Migrating back in time: the scientific history of cell motility

The discovery of cell motility is a classic example of how science only progresses as far as the availability of technology will allow for those discoveries. In other words, discovery of motility and the associated molecular mechanisms has intimately paralleled the technological innovations used to observe single celled organisms. With a history spanning hundreds of years, cell migration is one of the oldest fields in cell biology (257). Invention of the compound microscope by Dutch biologists Hans and Zacharias Jansen in 1590, and later refined by Robert Hooke in 1665 was accomplished to observe living cells (259). The modern theory of cell migration was established in the early 1970s when Michael Abercrombie used video and electron microscopy to study how cells crawl on solid surfaces (257). Abercrombie suggested cell motility is guided by extending membrane protrusions while forming new cell contacts with the substratum which are followed by contractile forces to pull the cell body toward the newly formed adhesions (257). Today, invention of computer based models and electronic microscopes with real-time image processing has allowed for the observation of single microtubules in living cells. Laser-scanning confocal microscopy has allowed for examination of specific fluorescently

labeled proteins in clearly resolved pictures, such as the polymerization of the actin cytoskeleton (259).

These technological innovations have revealed that cell motility is a physically integrated molecular process involving multiple components of spatially and temporally coordinated structures (Figure 1) (36). Through significant advancements in the last two decades, a more unified picture of cell migration now exists (257). Powerful new scientific tools allow for a better understanding of signal transduction mechanisms, cell structures, regulation of the dynamic process of actin and microtubule polymerization (256), and membrane-matrix interactions. In 2001, the National Institute of General Medical Sciences launched the *Cell Migration Consortium*, a multidisciplinary multisite (257). The website is "designed to facilitate navigation through the complex world of cell migration research" (see http://www.cellmigration.org).

7.2 Morphological polarization

To transform intracellularly generated forces into net forward cell body movement, cells must first achieve spatial asymmetry of the cell body (36). That is, a clear morphological distinction must exist between the front and rear (36). This polarization allows the cell to enhance movement toward a specific source in a persistent and coordinated manner (255). Establishment of cell polarity occurs during the time cells spend moving in a spatial gradient of chemoattractants and is enhanced proportional to the magnitude of the gradient present in the extracellular environment (255). Cell movement is guided by membrane receptors that probe and seek out extracellular signals.

The type of extracellular signal processed is a reflection of the different forms of cell motility that exist. Haptokinesis and haptotaxis for example, are induced by adhesion-related signals such that control of movement occurs from less adherent to more adherent surfaces (260). The attractant is not diffusible but rather bound to the ECM. Mechanotaxis is controlled by stretch of the cell membrane conferred through introduction of a mechanical stimulus or sensed through the migrating cell itself. Chemotaxis is another type of cell motility controlled by exposure to soluble chemicals. These diffusible factors trigger signals via cell surface receptors independent from cell-substratum adhesion molecules (260). These soluble factors are referred to as chemokines, and exist as growth factors, cytokines, or hormones. Chemotaxis is the result of directed cell locomotion towards a chemical gradient like PDGF, CT-1 or LFGF-2 and occurs

during such processes as the inflammatory response and wound healing (261). Since all forms of cell motility are dependent on cell-substratum adhesion forces, chemotaxis is also superimposed upon haptokinetic locomotion (260).

To coordinate movement, fibroblasts use spatial and temporal aspects of the chemoattractant gradient (255). Prokaryotic cells, for instance, are too small to process spatial information but rather undergo "random walking" with no directed movement (255). It is only when they encounter an increase in chemoattractant concentration that the frequency of random motion declines and movement in the direction of the source is prolonged (255). Eukaryotic cells, like fibroblasts, are larger (10-20μm in diameter) and more highly developed allowing them to process information in both a spatial and temporal manner. They can respond to small chemoattractant concentration differences that exist between the front and back of the cell (255).

During chemotaxis, extension of active membrane processes occurs in the direction of the chemoattractant gradient (36), whereas uropods at the trailing rear edge of the cell retract in response to myosin mediated contraction (255). These outgrowths are referred to as pseudopods and are temporary extensions of the membrane formed by actin polymerization. Lamellipodia are broad, flat, sheet-like and have a branching "dendritic" network, while filopodia are thin, cylindrical, needle-like and organized into long parallel bundles (36, 256). Changing position of the chemoattractant source led to formation of new pseudopods on lateral sides of the cell body marking the new front of the cell. These experiments provide evidence for the function of pseudopods as sensors of cell motility. Retraction of those on the old front of the cell (now the new uropod) gave the appearance that cells made U-turns toward the new chemoattractant sources (255).

To generate a cellular response, small differences in signaling between the front and rear need to be amplified into steeper intracellular signaling gradients (256). Members of the Rho protein family of small GTPases, Rho, Cdc-42 and Rac as well as the phosphoinositides, phosphatidylinositol-3,4,5 triphosphate (PIP_3) and -3,4 bisphosphate (PIP_2), are active in the front and back of migrating cells (262, 263) where they influence organization of actin networks, and protrusion of filopodia and lamellipodia (41, 256, 262, 263). Exposure to chemoattractants involves localized accumulation and activation of PI3K at the front of the cell and subsequent generation of PIP_3/PIP_2 and G-protein activated cAMP (255, 256). One of the downstream targets of PI3K is Rac (256). Rac signals in a positive feedback cycle and maintains directional

membrane protrusion by positively enhancing recruitment of PI3K and cdc42 at the plasma membrane, stabilizing microtubule and actin polymerization, and activating integrins at the edge of lamellipodia (256, 262, 263). The actions of Rho and Rac are mutually antagonistic: active Rac at the leading edge suppresses Rho activity, whereas Rho is more active at the sides and rear of the cell and suppress Rac activity (256, 262, 263). This would prevent Rac-mediated protrusions at sites other than the leading edge thereby keeping the cell body streamlined and in pursuit of the chemokine (256, 262, 263). A cytosolic gradient of Ca^{2+} is also established, with the lowest concentration at the cell front and the highest concentration at the rear (264).

7.3 Membrane extension

Membrane extensions in the form of lamellopodia or filopodia occur as a result of net actin growth (see Figure 1). Polymerization involves assembly of monomeric, globular (G)-actin monomers to growing fibrous (F)-actin sites at a rate that exceeds actin turnover due to depolymerization (36, 37). Actin filaments are organized with their fast growing plus (barbed) ends oriented in the direction of protrusion (37). Although the mechanism providing new actin polymerization sites for membrane extension remains unclear, polymerization is thought to be generated in two ways: elongation of existing filaments by addition of actin monomers in series, or by a combination of nucleation of new filaments and the former (37, 265).

Nucleation sites on actin filaments regulate rate and direction of membrane extension. Capping proteins, which restrict polymerization of new filaments close to the membrane, function to terminate filament extension. Gelsolin functions to sever actin filaments and promote actin dissociation, while capping protein β2 stabilizes the newly formed nucleation site. Other proteins involved are cortactin (266-270), Arp 2/3, WASP and WAVE complexes (271, 272). Regulated by Cdc42 and Rac (41, 270-272), these proteins mediate actin polymerization by binding to sides or tips of pre-existing actin filaments, stabilizing them and inducing formation of a new daughter filament that branches off the mother filament (256, 271, 272). Addition of actin monomers may arise from uncapping of already-existing filaments, severing of filaments, or both, as well as *de novo* formation of new actin nucleation sites (36). Cytosolic concentrations of G-actin monomers exist in two forms: free G-actin and G-actin bound to a monomer binding proteins (36). Actin binding proteins regulate the rate and organization of actin polymerization by affecting the pool of available monomers and free ends (256). They include profilins, cilins,

and β-thymosins. Actin filament binding proteins such as fimbrin, α-actinin, and filamin serve to enhance actin filament cross-linking and help to increase rigidity of the actin polymer network against the load of membrane which, as filopods or lamellipods attempt to extend, resists deformation (36).

The process of actin assembly must generate a protrusive force sufficient to extend the plasma membrane against the compressive forces imposed on it by the inherent tension on the membrane and by the extracellular environment (273). Two models are proposed for generation of membrane protrusive forces: one involving the action of motor proteins, and the other in which actin polymerization itself produces protrusive force (37, 265). In the motor-based model, forward movement of the leading edge of the membrane is driven by ATP dependent motor proteins (myosin I or II) that move toward filament plus ends and push the actin cytoskeleton towards the cell cortex (37, 265). Polymerization of actin filaments fills in the resultant gap thereby extending the membrane forward (37). The second is called the thermal ratchet model or cortical expansion mechanism (36, 37). Gaps between filaments are created by thermally driven movements due to fluctuations in the position of the membrane, the length of the actin filament, or osmotically driven swelling of the membrane (36, 37). As in the first model, polymerization fills in the gap to prevent backward movement of the membrane (37).

7.4 Adhesion to the matrix

Studies show that if extended lamellipodia do not form attachments with the substratum (ECM components), the leading edge of the cell retracts and forward movement is prevented (260). Newly formed membrane protrusions must become stabilized by tethering to surrounding ECM molecules (256). Adhesion to the underlying substrate is mediated through discrete regions of the plasma membrane referred to as adhesion plaques, focal contacts or FAs (41, 274).

When the leading edge of the cell protrudes outwards in the direction of a chemoattractant gradient, FA complexes assemble there to form reversible interactions between the ECM and the cytoskeleton, remain fixed and are drawn rearwards thereby providing the necessary traction for the cell to translocate forward (see Figure 1) (36, 273). Control of translocation is further regulated by FA detachment at the trailing edge. Thus FA remodeling or turnover (rate of FA assembly and disassembly) regulates speed of locomotion. Slower moving cells generally display slower FA turnover (256).

Cell adhesion receptors are classified into six major groups: immunoglobulin gene superfamily, cadherin, selectins, mucins, CD44 family, and integrins (275). Integrins are the most extensively studied cell adhesion receptor. They form the major transmembrane component of FAs and their clustering and activation induces formation cell-ECM interactions (41, 275). Integrins comprise a large family of αβ heterodimeric membrane spanning glycoprotein receptors involved in various adhesion interactions with ECM components (via fibronectin, laminin, collagens and vitronectin) and cell-cell contacts (via vascular-cell adhesion molecule, VCAM; and intercellular adhesion molecule, ICAM) (42, 275, 276). Currently, eighteen α subunits and eight β subunits have been identified and combine to form 24 known adhesion receptors (42). Structurally, the N-terminal domains of α and β subunits associate to form the integrin headpiece, which contains ECM binding sites and serve as receptors for ECM binding. The C-terminal segment traverses the membrane and mediates direct or indirect interactions with the cytoskeleton network and with signaling molecules (42, 276). Specific integrin heterodimers bind to specific ECM components. β1 containing integrins bind collagen, αvβ5 integrin bind to vitronectin, and αvβ3 bind to a variety of ECM proteins containing the peptide sequence arginine-glycine-aspartate including collagen, fibronectin and vitronectin (276).

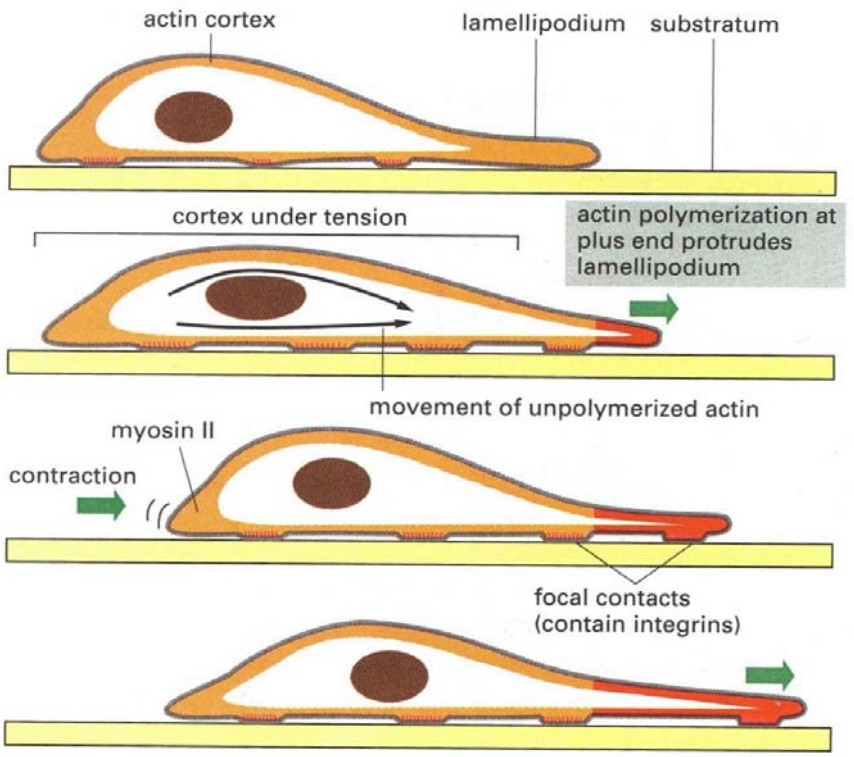

Figure 1. Schematic diagram of the basic steps required for cell motility. In response to increasing chemotactic gradients, receptors at the leading edge of the cell become activated. Cellular extensions in the form of lamellipodia or filopodia project outwards as a result of actin-polymerization-dependent protrusion and gain firm FA mediated attachments with the substratum. Isometric tension develops in the cell cortex which is transmitted to the underlying substratum at the level of FA complexes. Myosin II favored contraction at the rear of the cell breaks rearward adhesions and propels the body of the cell forward. Relaxation of cortical tension creates tractional forces that reorganizes the matrix. New FA are established in the leading edge and old ones are disassembled as the rear as the cell translocates forward. The same cycle is repeated in a tightly coordinated manner, moving the cell forward smoothly. Newly polymerized actin is shown in red. Figure reprinted from, Molecular Biology of the Cell, 4th Edition, *Alberts et al*, Figure 16-85, pg 972, copyright (2002) with permission from Garland Science.

Integrins are associated with other transmembrane proteins which provide a supporting role during migration and include the transmembrane 4 superfamily (TMF4SF), integrin-associated protein (IAP), CD98, and syndecan-4 (42). Direct or indirect associations with proteins at the cytoplasmic domain regulate integrin affinity and cytoskeletal interaction. Chaperone proteins are calreticulin and calnexin; the adaptor protein, paxillin; structural proteins such as talin, α-actinin, filamin, vinculin, tensin; and regulatory enzymes including FAK, src, MAPK, integrin linked-kinase, receptor activated protein kinase C (RacK1), PKC, gelsolin, Crk-associated substrate (p130Cas), PI3K and calpain (42). Many of these cytoskeleton associated proteins have SH2 and SH3 binding domains and it is through these multiple binding domains that molecular interconnections can be enhanced, modified, and linked to intracellular signaling pathways (36, 275).

Engagement of integrins with the ECM triggers a complex signaling cascade resulting in changes in intracellular pH (277), elevated levels of cytoplasmic Ca^{2+} (278), activation of PI3K, and stimulation of both serine/threonine and protein tyrosine kinases (279). Integrins, however, lack intrinsic tyrosine kinase activity (275).

Identified in 1992 (38) and expressed in most tissues and cell types FAK is an important tyrosine kinase implicated in integrin-regulated signaling and thus regulation of FA complexes (38, 41, 275, 279). FAK is required for sensing of mechanical forces at the level of the ECM (141, 280) and spatial organization of the leading edge in migrating cells (281). Activation of FAK through a plethora of interactions with other signaling molecules results in assembly of a multicomponent signaling complex that is involved in a variety of important signal transduction pathways (38, 275). For instance, clustering of integrins in the presence of ECM molecules combined with activation of growth factor receptors (38) leads to the rapid recruitment of FAK to the FA complex via the Focal Adhesion Targeting (FAT) region. Subsequently, autophosphorylation at tyrosines 397/576/577 leads to its catalytic activity (38, 41, 275, 282). An indirect association of FAK with integrins occurs through binding and phosphorylation of integrin and actin-associated proteins such as paxillin, α-actinin and talin (38, 283). FAK does not contain SH3 or SH3 domains but upon phosphorylation, high affinity binding sites are created in proline-rich regions (275, 283). These binding sites are recognized by SH2 domains of src-related family of tyrosine kinase members including fyn, csk, and src, and other SH2-containing proteins including PI3K, PLCγ, Rho, p130Cas, SOCs, and adaptor protein Grb7 (38,

41, 283). Resultant activation of Ras, ERK2, MAPK, and JNK pathways ensue (38, 283)). The ERK and MAPK pathways are linked to migration-promoting signals like increased activation of actin-myosin cell contractility which is required to create tractional forces for forward movement (283). Activation of Rac and Cdc42 coupled to inhibition of Rho activity is important in promoting the dynamic regulation of actin polymerization during membrane protrusion (38, 275, 283).

7.5 Cell traction and contractile forces

Once adhesion is established, a contractile force, dependent on cytoskeletal associated active myosin-based motors within the anterior and posterior region of the cell, is required to pull the cortex (body) forward (see Figure 1) (36). This force is expressed as traction on the ECM at the level of integrin receptors (273). Traction helps overcome the opposing forces of frictional drag imposed on the cell by the inherent nature of the ECM, fluid in the environment, as well as the rearward pull due to adhesive interactions. Measurement of traction during fibroblast migration has revealed that these cells generate an estimated 1-5 $nN/\mu m^2$ on the substrata – the equivalent of the force of 1000 myosin molecules working synchronously (284). Maximal migration speeds are reported at ~1 μm/min (285).

The interplay between generation of forces in the cell front and rear are such that frontal attachments remain fixed while rearward attachments are released (36). Thus, migration speed is a biphasic function since migrating cells must be able to detach from the ECM in synchrony with development of traction (256). Traction is directly related to intracellularly generated contractile force but is not identical since traction may be altered at any moment due to disruption of cell-substratum attachments (36). In other words, the substratum exerts equal but opposite forces on the cell, the magnitude of which is reliant on density of attachments and susceptibility of these attachments to disruption (36, 256). Therefore, the extent of cell-generated contractile forces does not by itself determine cell migration speed. Rather it is the combination or ratio of contractile force to cell-substratum adhesion strength that contributes to the rate (36).

Unlike the loose meshwork of short, randomly organized cortical actin filaments originating in lamellipodia, actin in the cortex is oriented in highly organized bundles. Here it is referred to as stress fibres (37). Stress fibers are similar to muscle sarcomeres in terms of

organization: having short actin filaments arranged in bundles of alternating polarity and associated with bipolar myosin II filaments (37).

Myosins are actin-dependent molecular motors that use the energy of ATP hydrolysis to move along actin filaments (39). Myosin heavy chains consist of three distinct regions: an amino-terminal motor or head domain responsible for actin binding and ATP hydrolysis, a neck region containing motifs that bind light chains e.g essential or regulatory myosin light chains, and a carboxyl-terminal tail responsible for cargo binding and/or dimerization of heavy chains such as calmodulin and calmodulin associated proteins (39). The myosin superfamily is divided into 20 known classes based on sequence comparison of myosin head domains. Myosin II is a double-headed, long rod-like molecule capable of polymerizing into bipolar filaments whereas myosin I is a single-headed molecule with a short tail (36, 39). Expressed predominantly in muscle cells, myosin II is implicated in the "sliding filament" theory of muscle contraction but also present in non-muscle cells where it plays a role in regulation of cell migration and control of cell shape (40). Myosin II is abundant in the cell cortex. Its bipolar filaments can pull two actin filaments past one another. Myosin I, on the other hand, functions to traffic membrane-associated proteins (vesicles) along actin filaments (36).

Myosin motors display functional diversity in their ability to perform specific intracellular functions. Duty ratio for example, is the proportion of the ATPase cycle a motor spends strongly attached to its actin-associated tracks (39). Myosin IIa and myosin IIb are both represented by low-duty ratios. Furthermore, both may be expressed in the same cell but perform different functions: IIa may be responsible for rapid contractile movements whereas IIb may be associated with maintenance of cortical tension (39). The major function of myosin II-based contraction, however, may be to aid in the breaking of adhesive interaction by direct application of physical stress (36). Myosin II contraction pulls on actin filaments which are connected to integrin adhesion receptors associated with the ECM and, in turn, accelerates bond disruption either at the extracellular receptor-ligand site or at an intracellular receptor-cytoskeleton site (36, 260). In combination with myosin II mediated contraction at the rear to reduce restrictive cell-substratum traction, myosin II or I also generates contractile force behind the leading lamella by pulling the cell body forward (36, 37, 260). Myosin II is also important for directional motility by preventing formation of unwanted lateral pseudopods, and involved in establishment, maintenance and recycling of integrin molecules (39).

The activity of myosin II motors are regulated by a tightly controlled feedback cycle and involves phosphorylation of regulatory myosin light chain (rMLC) in the neck region of the molecule (286). Phosphorylation of rMLC activates myosin ATPase situated in the globular head domain, which is further associated with actin filaments. ATPase activation results in cross-bridge cycling and contractile force. The sequence of molecular events leading to cross-bridge cycling is as follows: rapid increases in Ca^{2+} due to influx of extracellular calcium and release from ER results in binding of Ca^{2+} to calmodulin (287), which further binds to and activates MLCK leading to phosphorylation of rMLC residues (45). Phosphorylation of rMLC allows myosin ATPase to be activated by actin thereby initiating contraction of the cell cortex (45). In addition to being regulated by MLCK, rMLC is positively regulated by Rho kinase (ROCK) and negatively regulated by MLC phosphatase (45, 48, 288). ROCK phosphorylates MLC phosphatase rendering it inactive. Therefore, ROCK positively regulates MLCK by preventing its dephosphorylation by MLC phosphatase (45, 48, 288). Whereas MLCK is regulated by intracellular calcium concentration and ROCK, ROCK is regulated by binding Rho-GTP activators (guanosine exchange factors, GEF) (45).

7.6 Moving forward: rear release of attachments

The release of cell-ECM attachments at the rear marks the end of a full cycle of motion. Once rear release occurs the cell translocates forward (see Figure 1). Studies that track integrins on migrating fibroblasts reveal that cell "footprints" are left on the substrata in the wake of forward cell movement (289, 290). Other studies show that fractions of integrins remain intact during forward translocation, are collected into vesicles for intracellular trafficking and recycled back to the leading edge of the cell (289). This ripping of adhesions may occur from myosin II mediated contraction as discussed above, and through activation of rho and tyrosine kinases activity (291). Ca^{2+}- dependent proteases and phosphatases such as calpain and calcineurin, respectively, play a role in FA turnover by cleaving and inactivating the many structural components associated with integrin adhesion such as talin and FAK (36, 291). The catalytic activity of FAK is also a key regulator of FA turnover (292). Positively regulated by Rho, Rac has also been implicated in detachment at the rear (256).

8.0 Wound contraction

Moderate levels of mechanical tension exist in all connective tissue and serve as an important regulator of tissue function in lung alveoli, kidney capsule, uterine involution, and cardiomyocyte contraction (106). An elevation in tension, however, is known to occur in pathological situations, most particularly during contraction of granulation tissue of open wounds and burn-scar contracture (106). In the process of wound healing, normal contraction plays a beneficial role by facilitating earlier wound closure. This occurs by reducing the surface area of the original wound (106, 130) when the amount of tissue loss would otherwise have precluded adequate healing (293). Myofibroblasts appear during the wound-healing process and are the key players in generating contractile force. Since these cells are able to form cell-matrix adhesions and cell-cell interactions between the fibrillar collagen network of the scar, they generate contractile forces in the wound by pulling both edges of the wound together (6, 130). Although more is known about dermal than cardiac myofibroblast contraction, similar mechanisms are at play during both types of wound healing.

8.1 Contraction and fibrotic disease

Activation of myofibroblasts 2-3 days after infarction and their persistence in the infarct scar contributes to remodeling of the myocardium and development of cardiac fibrosis. Fibrosis occurs as a result of synergistic effects of myofibroblast function: *de novo* synthesis and deposition of collagen types I and III and continual myofibroblast contraction (5, 94). Initially, myofibroblast contraction augments the wound healing process by increasing the tensile strength of granulation tissue to prevent infarct scar rupture (5). Over time there is a progressive increase in matrix stiffness while under tension.

Combined with unregulated MMP expression and TGFβ signaling, the remodeling process involves a positively reinforced cycle. Myofibroblast contraction deforms the collagen network and induces deposition of new collagen fibrils to stabilize this newly deformed network (106). Degradation of old collagen and subsequent deposition of new fibers reorganizes the fibrillar matrix in such a way that mechanical tension induced by a single myofibroblast influences surrounding myofibroblasts to undergo the same process (106). Therefore, the process of mechano-remodeling is continuously repeated. Called contracture, this process involves incremental and anatomical shortening of the ECM matrix (106). The full extent of cardiac

fibrosis is marked when shortening or compaction of the collagen network ceases to depend on cell-generated forces as initially seen during myofibroblast contraction during closure of the wound, but instead relies on the physical stiffness of tension generated by the collagen network itself (106).

8.2 Myofibroblast contraction theory vs. fibroblast traction theory

Two schools of thought exist for the way dermal fibroblasts and myofibroblasts facilitate wound contraction: cell contraction theory and cell traction theory (294, 295). Cell contraction or myofibroblast theory proclaims wound closure is the result of myofibroblast contraction (294, 296). Through integrin mediated FA interactions with collagen fibrils, myofibroblast contraction pulls the ECM toward the cell body, essentially pulling the wound edges together (294). Expression of αSMA combined with gap junction cell-cell interactions also allows myofibroblasts to pull on each other during contraction.

Contraction of dermal wounds is initiated 4 to 5 days following injury. It is thought to proceed 12-15 days at an average closure rate of 0.6-0.75 mm/day depending on tissue type and wound shape (294). Traditionally, the notion of wound contraction was rooted in the theory that the mechanism of contraction was mainly due to collagen shortening (106). However, Gabbiani dismissed this theory in 1972. The landmark paper showed that contractile behavior of dermal scar tissue is dependent on granulation-tissue cells for force generation (297). It is now widely accepted that modified fibroblasts with smooth muscle-like features (myofibroblasts) regulate and thus play a key role in production of contractile forces involved in this process. In the dermal wound, myofibroblasts appear on the third day after wound healing (294). Subsequent studies showed that dermal myofibroblasts express αSMA in granulation tissue of healing wounds (298, 299). Correlations between the levels of αSMA expression in lung fibroblasts and degree of contraction indicates that this contractile protein directly contributes to regulation of contractile activity (129). Other studies showed that TGFβ treatment in normally quiescent fibroblasts and myofibroblasts resulted in upregulation of αSMA and actin-associated proteins involved in the functioning of the contractile apparatus (12, 19, 300). Furthermore, formation and stability of supermature FA is dependent on TGFβ signaling and αSMA-mediated contractile activity (148). Supermature FA are hyperphosphorylated due to increased activity of FAK (142). Therefore the presence of supermature FA complexes in myofibroblasts suggests that these cells are less

motile. Less motility may be an adaptation, which allows myofibroblasts in the developing infarct scar to remain static and contractile while diverting cellular energy to synthesis and deposition of matrix components in addition to focusing energies on cell proliferation. Although fibroblast proliferation is an important process required to enhance cellularity of the infarct scar, this process will not be discussed in this review. The underlying molecular mechanisms involved in cell division are well characterized and discussed in comprehensive review articles (see 43, 301-305).

In the myocardium αSMA positive cells have been identified in human myocardial scars (18). αSMA (17) and SMemb (15) are expressed in myofibroblasts of right ventricles of pressure overloaded hearts and reperfused myocardial infarcts. Since TGFβ is also a known potent inducer of collagen I and III synthesis, these observations indicate that fully differentiated myofibroblasts contribute to force generation, ECM reorganization and wound contraction (106).

The second theory of contraction is cell traction theory and is thought to be the result of uncoordinated mechanical forces exerted by individual fibroblasts on the ECM by traction during cell motility or spreading (294, 296). Collagen fibers are reorganized and compacted by fibroblast locomotion (294) making the involvement of a specialized contractile cell unnecessary in this process (106). In an *in vitro* collagen gel model, traction exerted by migrating fibroblasts was sufficient enough to distort the gel surface to form patterns of a wrinkling appearance (306). As described previously, traction is exerted by fibroblasts as they migrate into the wound with traction occurring at the level of FA interactions with the substrata. Opponents of the cell contraction theory have argued that results from *in vitro* gel deformation models cannot be applied to physiological conditions *in vivo*, while proponents of the cell traction theory have challenged findings that fibroblasts are the most abundant cell type in granulation tissue (296). Moreover, it is possible that wound healing may result from a coordinated regulatory response from both cell types (296) and may include proto-myofibroblasts.

8.3 Regulation of myofibroblast contraction

Regulation of myofibroblast contraction parallels contraction of the cell cortex as seen in cell motility using mechanisms similar to those described for smooth muscle cells (144, 286). Stress fibres represent the cytoplasmic units of actin-myosin-mediated contractile activity in these cells (307). In response to elevated levels of intracellular Ca^{2+} due to agonist stimulation or

mechanical tension (ie. pharmacomechanical coupling), phosphorylation of MLC on serine 19 and threonine 18 by MLCK leads to cross-bridge cycling of myosin II motor heads and results in isometric force exerted on the surrounding ECM (45). Increasing intracellular Ca^{2+} levels with a Ca^{2+} permeable ionophore, however, did not augment contractilility *in vitro* or *in vivo* indicating that activation of Ca^{2+} dependent MLCK alone is not sufficient to promote contractile behavior (308). Another means to regulate and sustain isometric tension occurs through activation of Rho/Rho-kinase (ROCK) (309). ROCK promotes and sustains MLC phosphorylation and in the absence of Ca^{2+} by both directly phosphorylating MLC, and by inhibiting myosin phosphatase by phosphorylating the myosin-binding subunit of this enzyme (106). Since myosin phosphatase negatively regulates MLCK activity, ROCK-mediated inhibition results in a prolonged state of MLC phosphorylation therefore increasing the time that myosin II is active which allows an increase in force transmission (309).

The combined action of MLCK and ROCK suggest that the mechanisms of force generation are tightly regulated involving two regulatory systems. Rapid contraction that is short in duration may reflect the Ca^{2+}-calmodulin –MLCK system, which can also be rapidly terminated by myosin phosphatase (309). The notion that Ca^{2+} release in cells is rapid, transient and localized supports the concept that contraction triggered by Ca^{2+} may also be rapid, short-lived and localized (309). The second type of contraction is more sustained. A more energetically favorable mechanism may be achieved by controlling the level of myosin phosphatase activity through Rho-kinase, since a Ca^{2+}-dependent system is difficult to fine tune and alone could not control prolonged contraction (309).

8.4 Gel deformation studies

Currently, 3D collagen gel lattices provide the best model for examining wound contraction *in vitro* and are more biologically relevant to living organisms than conventional 2D cell cultures (310). By culturing fibroblasts on or imbedded in these matrices, studies can explore the molecular mechanisms of contractile responses, cell-matrix interactions between cells and ECM, and how these influences may affect myofibroblast differentiation. Three common variations of the *in vitro* collagen matrix contraction model are floating matrix contraction, anchored matrix contraction, and stress relaxation (311).

Free floating collagen matrices are detached from the plastic culture dish and suspended in culture media. Fibroblast migration and spreading result in exertion of tractional force on the matrix (106, 312). Deformation of the matrix occurs by reduction in diameter (311). In this case, the fibroblast traction theory holds because fibroblasts do not acquire the proto-myofibroblast phenotype and do not undergo static contraction (106). Fibroblasts in free-floating lattices become quiescent after 24 hours due to downregulation of the ERK pathway which plays a role in regulation of contractile force (313). This model resembles mechanically relaxed or unloaded tissues which is representative of the healthy myocardium. Because all tissues are tethered in such a way that cell contraction induces mechanical loading and tension in the surrounding ECM, this model is poorly designed to study mechanically regulated processes (106, 311)

Collagen gels are anchored to the culture dish and seeded with fibroblasts in the anchored matrix contraction model. Since the collagen gel is tethered to the underlying culture dish, tension develops and the cells are said to be mechanically loaded which is more reflective of an *in vivo* situation (106, 312). Tractional forces are isometric resulting in reorganization of collagen fibers. Under isometric tension, the collagen lattice is compressed and deformed in height (311). Fibroblasts align along lines of tension, develop prominent stress fibers, acquire a proto-myofibroblast phenotype, and form adhesion complexes (106, 312). Treatment of mechanically loaded cells with TGFβ also resulted in their differentiation into myofibroblasts (314).

Lastly, the stress relaxation model is designed similar to the anchored model except the collagen lattice is detached from the underlying culture dish subsequent to plating of fibroblasts. Mechanical stress develops during the period when the matrix is anchored but this stress dissipates after it is released (311). This model resembles the transition from granulation tissue to scar formation because closure of the wound results in unloading of mechanical tension in the surrounding ECM. Therefore, when attached matrices are released, tension is released and is concomitant with regression of cell adhesions, and disappearance of stress fibers (146, 315). These changes result in cells that revert back to undifferentiated fibroblasts or proto-myofibroblasts.

9.0 Calcium signaling and modes of transplasmalemmal movements

The Ca^{2+} signaling literature consists of a major breadth of all studied signaling mechanisms. It is inundated with thousands of articles concerning Ca^{2+} signaling in a wide variety of cell types but particularly in excitable cells. Neurons and muscle cells are the most widely studied excitable cell types (255). These cells are considered excitable since action potentials modulate their excitability and depolarization drives Ca^{2+} influx. On the other hand, non-excitable cells have limited capacity to become depolarized or activated and generally lack voltage-dependent Ca^{2+} channels (VDCC). For instance, depolarization-induced Ca^{2+} influx is not observed in fibroblasts, endothelial cells, and cancer cells (316). Rather, hyperpolarization is known to drive Ca^{2+} influx in these cells (317, 318). Many non-excitable cells like fibroblasts do display some capacity to depolarize but in general these cells lack the ability to undergo clearly defined action potentials (319). In smooth muscle cells, pharmacomechanical coupling can also regulate contraction independently of membrane potential and involves release of Ca^{2+} from the SR by a chemical messenger, IP_3, through agonist-receptor interactions. In excitable cells, much is known about the way in which Ca^{2+} functions and how it is regulated. In cardiac muscle cells for instance, it is well established that a dedicated Ca^{2+} delivery system - T-tubules - functions to regulate Ca^{2+} influx. Upon depolarization of the plasma membrane, VDCC triggers the Ca^{2+} - induced- Ca^{2+} release mechanism (320). Through a tightly regulated Ca^{2+} extrusion and reuptake process, intracellular Ca^{2+} concentrations ($[Ca^{2+}]_i$) are controlled, which enables the cell to relax (320). This section will explore the Ca^{2+} signaling mechanisms thought to play a role in non-excitable cells, such as fibroblasts, with special attention made to modes of transplasmalemmal Ca^{2+} flux.

9.1 The beginning of a new scientific era

The Ca^{2+} signaling era began in 1883 when Sidney Ringer serendipitously discovered that when isolated rat hearts were bathed in London tap water spontaneous contractions became more prolonged and pronounced as compared to when bathed in distilled water (321). In addition, Ringer found that contraction could be maintained if Ca^{2+} salts were added to the suspension medium (321). He deduced that since London tap water is enriched with salts containing Ca^{2+}, then Ca^{2+} must carry a message or signal responsible for initiation of heart contraction (321). This discovery was completely novel at the time, since Ca^{2+} was previously

considered merely a structural element found in teeth and bone but not active in the normal functioning of tissues (50). Groundbreaking discoveries soon followed and provided strong experimental evidence for the importance of Ca^{2+} in cellular signaling pathways. Ca^{2+} is now widely accepted as an important divalent element with essential second messenger properties. These properties are regulated in a spatio-temporal manner and are required for the functioning of all cellular processes.

9.2 Spatio-temporal properties: sparks, waves and oscillations

As an intracellular messenger Ca^{2+} relays information within cells to regulate activity of different cell types (322). At a subcellular level, Ca^{2+} enters the cell from the extracellular environment via routing through membrane spanning channels or exchangers. Ca^{2+} can also become released from internal Ca^{2+} stores through channels in the ER or SR (50, 322). The basic building blocks for the development of a Ca^{2+} signaling cascade are represented by *elementary events* (322). These events are localized signals called Ca^{2+} sparks, which result from entry of extracellular Ca^{2+} across the plasma membrane or release/uptake from internal stores (50, 323). In addition, Ca^{2+} can enter the nucleus to regulate gene transcription. Localized concentrations of Ca^{2+} regulate the activation of cytoplasmic processes such as trafficking of cellular material, opening of potassium (K^+) channels and metabolism in the mitochondria (322). The net combination of these subcellular processes results in specific cellular events such as membrane excitability, smooth muscle relaxation, mitosis and synaptic plasticity (322). Global signals are created when elementary Ca^{2+} release signals become coordinated such that communication corroborates between individual channels (323). The result is a Ca^{2+} wave that spreads throughout the cell and based on the type of signal coordinates different cellular end points: cell motility, fertilization, liver metabolism, gene transcription, cell proliferation, and skeletal, smooth, and cardiac contraction (322, 324). Global Ca^{2+} waves spread to adjacent cells through gap junction complexes and become intercellular waves (323). These waves further regulate the physiological roles of cells in a specific tissue: wound healing, ciliary beating, glial cell function, and bile flow (322).

Ca^{2+} signaling is a paradox since it is required both for cell survival and cell death; high $[Ca^{2+}]_i$ can lead to cell death signals which mediate the process of necrosis or apoptosis (324). Therefore, cells regulate $[Ca^{2+}]_i$ by using low-amplitude Ca^{2+} signals or in other words by

delivering the signals as brief "transients" (322). Repetitive transients are called Ca^{2+} oscillations and it is the shape of the oscillation that determines the magnitude of the Ca^{2+} signal (50). For instance, muscle contraction, synaptic transmission, and cell motility require the rapid delivery of a spatially confined signal that is high in intensity but transient in nature (50). Cytosolic Ca^{2+} oscillations may regulate cell movement. In eosinophils for example, low Ca^{2+} concentration at the leading edge favors formation of actin networks by activating myosin I, inactivating actin-severing proteins, and reversing the inhibition of Ca^{2+}-regulated actin cross-linking proteins (264). The high Ca^{2+} concentration at the trailing edge may contribute to eosinophil detachment due to disassembly of actin networks and activation of gelsolin (264). Hence, an internal gradient of Ca^{2+} contributes to turnover of actin filaments in migrating cells.

9.3 Ca^{2+} -binding proteins and signal transduction pathways

Unlike other second messenger molecules Ca^{2+} is not metabolized, produced or destroyed. Therefore, cells must tightly regulate intracellular levels through Ca^{2+} binding proteins and specialized extrusion pumps (319, 324). A large Ca^{2+} concentration gradient exists between the extracellular and intracellular environment. *In vivo* where the extracellular fluid is plasma, $[Ca^{2+}]_i$ is approximately 100nM or 20 000-fold lower than the 2 mM concentration found extracellularly (324). *In vitro*, where a saline solution exists as is the buffer, $[Ca^{2+}]_o$ is generally 1.6 mM. Ca^{2+} binding proteins maintain normal Ca^{2+} levels by acting as a buffer as well as by triggering second-messenger pathways and in this way help regulate Ca^{2+} transients.

G protein- and tyrosine kinase-linked receptors stimulate intracellular increases in Ca^{2+} levels and are required for fibroblast motility, contraction, and proliferation. A rise of $[Ca^{2+}]_i$ occurs via phospholipase C (PLC) driven pathways through the binding of cytokines such as PDGF and FGF. Activation of G-protein-linked tyrosine kinase receptors activates PLC which hydrolyzes phosphatidylinositol bisphosphate (PIP_2) into inositol 1,4,5-triphosphate (IP_3) and diacylglycerol (DAG) (324, 325). Acting like a second messenger, IP_3 binds to specialized tetrameric IP_3 receptors that span the ER and trigger release of Ca^{2+} (324, 325). IP_3-mediated signal transduction pathways are potent and may increase $[Ca^{2+}{}_i]$ from 100 nM to 1 μM (324).

Ca^{2+} triggers activation of a multitude of proteins implicated in the cellular processes discussed in this review. Trigger proteins change their conformation upon binding Ca^{2+} to modulate effector molecules such as enzymes and ion channels while buffering proteins bind

Ca^{2+} as intracellular concentrations increase (324). Some common proteins triggered by Ca^{2+} include: caldesmon (regulator of muscle contraction by binding actin in a Ca^{2+}/calmodulin-dependent manner) (326), MLCK (regulator of myosin activation) (308, 327), calpain (protease that regulates FAK) (328, 329), gelsolin (actin severing protein) (330), calmodulin (modulator of protein kinases such as MLCK, CaM kinase II, adenylyl cyclase I), calretinin (activator of guanyly cyclase), calcineurin B (phosphatase), PLC (generator of IP_3 and DAG and producer of arachidonic acid), PKC (protein kinase), Ca^{2+}-activated K channels (effector of membrane potential), IP_3 receptors (effector of intracellular Ca^{2+} release), Na^+/Ca^{2+} exchanger (NCX), calreticulin (Ca^{2+} buffer), calsequestrin (Ca^{2+} buffer) (324), α-actinin, and fimbrin (actin cross-linking accessory proteins), and the troponin/tropomyosin system (regulates actinomyosin interactions).

9.4 Transient receptor superfamily of ion channels

Transient receptor potentials (TRP) were first discovered to play a role in phototransduction in photoreceptors of *Drosophila*. Normally, in response to continual light, long lasting depolarization of the eye occurs and results in activation of receptors leading to sustained receptor potentials that triggered influx of extracellular Ca^{2+} ($[Ca^{2+}]_o$) (331). However, in a mutant, the response to illumination was initially identical to that of wild type flies, but within a few seconds the potential became transient and returned to baseline levels despite continual stimulation by illumination (332). TRP was named accordingly and in 1989 the *trp* gene was cloned (333). This gene encodes a Ca^{2+} -permeable cation channel (334) with structural homologies to VDCC (335). Unlike most ion channels which are identified based on modes of activation or ion selectivity, TRP channels are identified based on homology alone and as such many channels have sequence and structural similarities to the originally discovered *Drosophila* TRP gene (336). In general, *trp* gene products encode NSCC. They have been cloned from flies, worms, and mammals and together form the TRP superfamily.

TRP channels are classified into 6 subfamilies: TRPC, -V, -M, -P, -L, and –N. Structurally, all subfamilies have six transmembrane segments and intracellularly localized tails of amino and carboxyl termini (331, 336). These tails are similar to topographies of voltage-gated K^+, Na^+ and Ca^{2+} channels; cyclic nucleotide-gated channels; and hyperpolarization-activated channels (336). It is interesting to note that the N-terminal in the cytoplasmic domain

contains 2-4 ankyrin-binding repeats, while the C-terminal domain in some subfamilies contain a conserved region of amino acids with a kinase or phosphatase domain (331, 336). Ankyrin is a cytoskeletal associated protein that mediates cytoskeleton-substrate anchoring or protein-protein interactions and suggests that these channels directly interact with the cytoskeleton to trigger signals important for cell motility and contraction. Other sequence domains in the C-terminus include: interactions with IP_3 receptors; calmodulin-binding sites; and ATP-binding motifs (331). Topographically, the fourth transmembrane polypeptide segment lacks a complete set of positively charged residues, which are necessary for voltage sensing, while the sixth polypeptide assembles as tetramers to form cation-permeable pores (336). The modes of activation and selectivity for TRP channels are diverse. Some are activated by ligands, by physical stimuli (i.e. heat or mechanical force), and others by unknown mechanisms (336). All TRP channels are selective in terms of the type of ion (i.e. only cations) but are non-selective in terms of the type of cation. Selectivity ratios for Ca^{2+} to Na^{2+} vary widely between subfamilies (336).

The functions of the TRP superfamily are diverse and are further complicated by the overlapping functions of individual subfamilies. Furthermore, the division of TRPs into subfamilies on the basis of amino acid sequence and structural similarity do not clearly provide functional classification for TRP proteins (336). Nevertheless, TRPs are known to posses six main functions: they play a role in PLC-dependent Ca^{2+} flux, mechanosensation, function as thermal and noxious receptors, mechanosensors, taste sensors, and play a role in cell growth and ion homeostasis (336).

In PLC-dependent Ca^{2+} influx, e.g. as activated by PDGF-BB, activation of G-protein and PLC-coupled membrane receptors leads to increases in $[Ca^{2+}]_i$. Ca^{2+} entry occurs via store-operated channels (SOCs) and functions mainly to replenish internal Ca^{2+} depleted stores (see Figure 2) (336). TRPC1 through TRPC7 are representative of SOCs and are the closest relatives of the *Drosophila* TRP (331). Mechanical stimuli in the form of cellular membrane deformation are another important mechanism of TRP activation. These TRP channels include TRPV, TRPP, and TRPM (336). Mechanosensation is the basis for hearing, osmolar sensing, stretch, touch, and flow sensing (336). The notion that TRPs play a role in thermal and noxious receptors came from the discovery that the TRPV subfamily of receptors binds to capsaicin. Capsaicin is the active ingredient in chili peppers known to produce a “hot”, spicy sensation; binding of capsaicin activates TRPV. Accordingly, TRPV is expressed in primary afferent sensory neurons of the

dorsal root ganglion and trigeminal ganglion (337). TRPV is activated by noxious heat, low pH, tissue injury (which is accompanied by acidosis) and hypotonicity-induced cell swelling (336). The ability of TRPV and TRPM channels to integrate physical and chemical stimuli suggests they play a role in perception of taste (336). Consistent with this notion, TRPMs are expressed in taste buds. TRPM5, for example, may be responsible for perception of bitter or sweet compounds (338). TRPV and TRPM channels are implicated in reabsorbtion of Ca^{2+} and Mg^{2+} ions in kidney and intestines and plays a role in cell proliferation (336). Concerning the latter, increases in $[Ca^{2+}]_i$ due to upregulation of TRPV6 or TRPM8 triggers malignant transformation of cells (336).

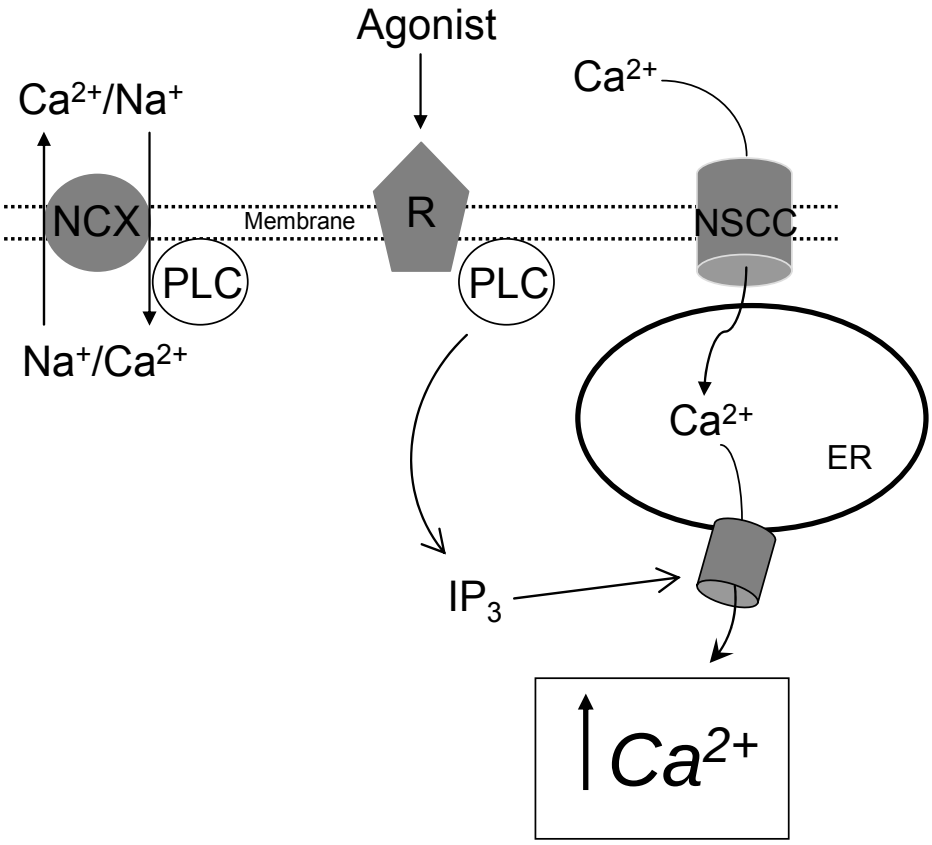

Figure 2. Proposed model for Ca^{2+} entry in non-excitable cells. In the capacitative Ca^{2+} conductance model, binding of an agonist (e.g. PDGF, FGF-2, or CT-1) to a membrane receptor (R) leads to activation of phosholipase C (PLC) and production of inositol 1,4,5, triphosphate (IP_3) which in turn triggers release of Ca^{2+} from internal stores (endoplasmic reticulum, ER). Although not fully understood, it is suggested that ER depletion in some manner triggers a pathway through NSCC for its direct refilling from the extracellular space. Continual receptor activation and production of IP_3 would result in net movement of Ca^{2+} from the extracellular space to the cytosol. NCX may be triggered by either intracellular messengers (e.g. PLC) or intracellular gradients of Ca^{2+} or Na^{+}. Activation of Ca^{2+} entry mode (reverse mode) or exit mode (forward mode) may be dependent on type of cell response. Intracellular Ca^{2+} modulates cell motility, contractility and proliferation by regulating contractile machinery, FA and cytoskeletal proteins associated with integrin complexes, and gene transcription. Figure adapted and reprinted from Cell Calcium, 11, Putney, J.W, Capacitative calcium entry revisited, 611-624, copyright (1991) with permission from Elsevier.

9.4.1 Store-operated Ca^{2+} entry

Eukaryotic cells increase $[Ca^{2+}]_i$ in one of two ways: either by releasing compartmentalized Ca^{2+} from intracellular stores (i.e. from the ER or SR) or by evoking Ca^{2+} influx from the extracellular environment (339). Release from intracellular stores is transient and deactivates quickly due to Ca^{2+} export from the cell by energy driven plasma membrane Ca^{2+} ATPase pumps (339). Since many cellular processes require a sustained wave of $Ca^{2+}{}_i$, influx from the extracellular environment plays a crucial role in maintaining these levels (339). It is now firmly established that in non-excitable cells store operated Ca^{2+} entry (SOCE) through store-operated channels (SOC) is one of the major mechanisms for Ca^{2+} entry (Figure 2) (336, 339). Candidate genes for this mode of Ca^{2+} entry include the Drosophila gene products *trp* and *trpl*; however, there is no definitive evidence that these genes encode TRP proteins responsible for the currents generated by SOCE. As well, a mammalian homologue has not yet been reported (324). TRPC channels are closely related in structure and function to the group of TRP channel proteins first identified in *Drosophila* that mediate PLC-dependent light-induced current in retinal cells (325). These channels have been implicated as important mediators of Ca^{2+} entry and evidence indicates that they function as SOC (325). For example, there is evidence that expression of TRPC6 mRNA exists in vascular smooth muscle cells (340). Impairment of TRPC4 in a knockout model of lung vascular endothelial cells resulted in a defect in Ca^{2+} influx and this was associated with lack of thrombin-induced actin-stress fiber formation and reduced endothelial cell retraction responses (341). SOCE is also implicated in regulation of gene expression in vascular smooth muscle cells (342).

The concept of SOCE is rooted in 1986 when Putney published a study using the fluorescent Ca^{2+} indicator, fura-2 (343). Putney showed that in parotoid acinar cells, a uniform $[Ca^{2+}]_i$ was maintained due to Ca^{2+} influx after stimulation with agonists of many receptors types such as muscarinic type 3 (343). $[Ca^{2+}]_i$ rose despite effective depletion of endoplasmic reticular stores from plasma membrane Ca^{2+} pumps and this rise in Ca^{2+} accompanied activation of Ca^{2+} entry across the plasma membrane (324). There are similar results for other cell types including arterial smooth muscle cells (344). Furthermore, treatment of cells with thapsigargan, an inhibitor of the ER Ca^{2+} ATPase pump, showed that depletion of stores alone was a sufficient stimulus to initiate Ca^{2+} entry (345, 346). Since both agonist and thapsigargin activated the same Ca^{2+} entry pathway, these studies demonstrated the existence of a Ca^{2+} mediated communication

pathway between Ca^{2+} stores and the extracellular environment. In addition, if Ca^{2+} pools emptied in the presence of IP_3, a pathway from the extracellular space to the pool opened; on the other hand, if the pool was replenished, the pathway from the extracellular space closed even in the presence of low extracellular Ca^{2+} or Ca^{2+} chelating agents (343). Thus, the emptying of Ca^{2+} stores automatically triggered Ca^{2+} influx and in this way, elevated $[Ca^{2+}]_i$ is likely maintained.

SOCE is now widely accepted to occur in various cell types including fibroblasts, mast cells, macrophages, epithelial cells embryonic kidney cells, platelets, smooth muscle cells and many others (339). A rise in $[Ca^{2+}]_i$ is accompanied by influx of Ca^{2+} from the extracellular space through SOC (325). Influx of Ca^{2+} is induced by a drop of Ca^{2+} content in IP_3 -sensitive Ca^{2+} stores and is maintained so long as the stores are not replenished (331). PLC dependent Ca^{2+} entry, however, is not exclusively limited to store depletion but may also be due to activation of surface Ca^{2+} channels by other second messengers such as DAG (336), IP_3, IP_4, cytosolic Ca^{2+} or arachidonic acid (331). Activation of protein kinase C (PKC) by DAG interacts and activates SOC (339). In these cases, Ca^{2+} entry is mediated by second messenger-operated channels (SMOC).

The mechanisms underlying how the filling state of intracellular stores is communicated to the cell membrane such that Ca^{2+} channels are activated are largely unknown. Alternative possibilities may be involved. A diffusible messenger in the cytosol called Ca^{2+} influx factor (CIF) is postulated to play an important role in SOCE (347, 348). An alternative mechanism is the proposal that Ca^{2+} stores and SOCs physically interact through protein-protein interactions. This situation is analogous to striated muscle cells where Ca^{2+} channels mediate Ca^{2+} release by physically coupling to the SR. Based on this analogy, levels of Ca^{2+} in the stores control gating of Ca^{2+} channels in the plasma membrane by altering the configuration of proteins within the store membrane which, in turn, directly interacts with the channels in the plasma membrane (331, 349). The “secretion-like coupling model” of SOCE suggests that pre-synthesized SOCs are transported in vesicles and fuse with the plasma membrane (331, 350). Lastly, non-excitable cells are known to produce membrane potentials whereby ligand induced mobilization of Ca^{2+} from intracellular stores activates Ca^{2+} activated K^+ channels and provokes a hyperpolarization effect on the membrane (318, 319, 351). The resultant K^+ hyperpolarization current is significantly larger than the current generated from Ca^{2+} influx, which, in turn, increases the electrochemical gradient for Ca^{2+} to flow into the cytosol leading to even more activation of

Ca^{2+}-activated K^+ hyperpolarization. Although unclear, PKC, which is itself regulated by Ca^{2+}, may negatively regulate K^+ channels (319). It is likely that NSCC provide the route of Ca^{2+} entry during this phenomenon. Functionally, K^+ driven hyperpolarization events are associated with cell motility (352-354). These channels can be regulated by phosphorylation (355, 356).

9.4.2 Stretch-activated Ca^{2+} entry

Mechanically sensitive channels (MSCs) are another type of NSCC and include stretch-activated channels (SACs) or stretch-inactivated channels (SICs) (357). Mechanosensitivity provides sensory inputs for hearing, touch, kinesthesis, proprioception, and regulation of bone and muscle (357). Activation and gating of SACs occur in response to tension conveyed to the channel either through the surrounding membrane lipids or membrane cytoskeletal elements (357). MSCs are coupled to the cytoskeleton and mechanochemical components such as actin and integrin. Since cell motility and contractility requires substrate-cytoskeleton mechanofeedback interactions, MSCs may modulate the mechanical forces involved in these processes. MSC are permeable to Ca^{2+}, Na^+, and sometimes K^+ (358). They are found in a variety of cell types including cardiac, smooth, and skeletal muscle cells, neurons, epithelial cells, oocytes and fibroblasts (358).

Although cardiac fibroblasts are involved in biochemical and structural changes during cardiac development and remodeling, the possible role of fibroblast electrophysiology remains unclear. Fibroblast membrane potential may be modulated by mechanical stretch which may contribute to intracardiac mechanoelectrical feedback during myocardial contraction (359). The changes that occur in fibroblast membrane potential during cardiac contraction have been called mechanically induced potentials (MIPs) (360). *In vivo*, MIPs are thought to be induced by myocyte contraction which physically squeeze and compress interstitial fibroblasts and lead to mechanical activation of NSCC (360, 361). Electrophysiological studies have clearly demonstrated that entry of Ca^{2+} to the cytosol occurs upon mechanical stimulation of the plasma membrane (362-364). A common characteristic of these channels is their sensitivity to the heavy metal blocker, gadolinium (Gd^{3+}) (358, 365).

9.5 Na^+/Ca^{2+} exchanger

The Na^+/Ca^{2+} (NCX) exchanger was first isolated in 1988 from cardiac sarcolemma (366) and then cloned in 1990 (367). In the ensuing decade a great deal of research has focused on its Ca^{2+} regulating properties and has revealed that NCX is an essential component of Ca^{2+} signaling pathways for the functioning of organs. The relative abundance of NCX expression in different types of tissue is representative of the importance of transplasmalemmal Ca^{2+} fluxes in the normal functioning of cells. NCX is expressed in most cell types but is more abundant in excitable cells. In some tissues for instance, the importance of the exchanger is low, such as the liver while in other tissues, NCX clearly plays a major role in regulating the physiological response to Ca^{2+}. These tissues include kidney, smooth muscle, brain, and heart (368).

NCX functions at the level of the plasma membrane and works as a bidirectional energy independent antiporter, transporting 3 Na^+ ions in exchange for 1 Ca^{2+} ion. The process of exchanging 3 Na^+ for 1 Ca^{2+} is electrogenic and implies the transport of one positive charge in the direction Na^+ is moved across the membrane. Therefore, NCX activity contributes to the electrical properties of cells. Recently, however, the 3:1 electrogenic stoichiometry became disputed when a study proposed a 4:1 stoichiometry (369), while another proposed a 3.2:1 ratio of ion movements (370). The concentration gradients for Na^+ and Ca^{2+}, and membrane potential provide the electrochemical driving forces that regulate the direction and magnitude of ion movement. Based on direction of Na^+ movement, forward mode produces an inward current and results in Ca^{2+} efflux whereas reverse mode produces an outward current and results in Ca^{2+} influx.

NCX is modeled to have 9 transmembrane segments forming a 938 amino acid long polypeptide chain (367). Two sets of hydrophobic domains, α-1 and α-2, are sequences that span transmembrane segments 2 and 3, and 7 and 8, respectively (372). These regions have an important role in ion transport (371, 372). The large intracellular loop contains the C-terminus of the protein. This segment is involved in regulation of NCX activity and contains the Exchanger Inhibitory Peptide (XIP) region, regulatory Ca^{2+} bindings sites and, the region of alternative splicing (373). The XIP region regulates the exchanger by deactivating it upon binding of a peptide with homologous sequence (373). Binding of Ca^{2+} to the regulatory binding sites of the intracellular loop causes conformational changes in the protein and its subsequent activation (374).

NCX proteins are members of the exchanger superfamily that fall into four different families (373). The first is the conventional NCX, Na^+-Ca^{2+} exchanger family. This family has sequence variability based on degree of expression and tissue distribution. In mammals, NCX is encoded in 3 different genes: NCX1 (367), NCX2 (375), and NCX3 (371). Different mRNA transcripts exist for each of the 3 genes and are further regulated by alternative promoters and alternative splicing. While NCX1 expression is generally considered ubiquitous, NCX2 and NCX3 are expressed mainly in brain and skeletal muscle (376). Based on the number and combinations of exons present in the RNA transcript for instance, 12 different isoforms of NCX1 have been identified and expressed in a tissue-specific manner (376, 377). NCX1.1 is found exclusively in the heart and skeletal muscle, while NCX1.3 is expressed in the kidney (378). The second family consists of 6 proteins similar to the Na^+-Ca^{2+} K^+ exchanger and is designated NCKX (373). NCKX proteins exchange four Na^+ for one Ca^{2+} plus one K^+ (379). The third family consists of bacterial proteins all of unknown function and lastly the fourth family consists of a Ca^{2+} H^+ exchanger (373).

In excitable cells like cardiomyocytes, NCX plays a critical role in excitation-contraction coupling (320). In the process of relaxation (diastole) the exchanger functions in forward mode by removing Ca^{2+} from the cytosol in exchange for extracellular Na^+ (320). However, NCX may also play a role in contractile activity by functioning in reverse mode insofar as transporting Ca^{2+} into the cytosol in exchange for intracellular Na^+ (Figure 2) (320). NCX dependent influx of Ca^{2+} is not sufficient to support contraction on its own, but rather induces the SR to release larger quantities of Ca^{2+} from its stores thereby helping to augment contraction on a beat to beat basis (e.g. Ca^{2+} induced Ca^{2+} release) (380). Intracellular Na^+ concentration is thought to be the key regulator of NCX function since high intracellular Na^+ concentrations and depolarized membrane potentials favor a Ca^{2+} influx mode (320). These conditions occur during the peak of cardiomyocyte action potentials and support the notion for a Ca^{2+} influx mode.

NCX has also been implicated in pathophysiological processes in the heart such as in cases of cardiomyopathies (381), MI (382), heart failure (383) and cardiac hypertrophy (384). In ischemic conditions, induction of an acidic environment stimulates the Na^+ H^+ exchanger to expel excess H^+ ions in exchange for Na^+. Efflux of Na^+ along with cessation of the Na^+ K^+ pump (due to ATP deficiency) activates the reverse mode of NCX to compensate for high

intracellular Na^+ concentrations. Enhanced influx of Ca^{2+} occurs and ultimately contributes to Ca^{2+} overload, cell damage and death (385, 386).

In cell types other than cardiomyocytes the role of NCX is less defined. Although studies have demonstrated that NCX is involved in regulating Ca^{2+} homeostasis in arterial myocytes (368, 387), and is expressed in vascular smooth muscle and endothelial cells (388-390), no information is known about the properties of NCX during cell migration, contractility or proliferation. However, phosphorylation of NCX by a Ca^{2+} -dependent kinase phenomenon and interactions with PLC, PKC, cAMP-dependent protein kinases, cAMP-dependent protein kinase-anchoring proteins, and phosphatases is demonstrated (Figure 2) (373, 391), and suggests possible roles of NCX in these cytokine mediated cell processes. Cytosolic Ca^{2+} signaling was impaired in a fibroblast cell line model of NCX over expression, by preventing increases of Ca^{2+} and leading to retardation of integrin-mediated adhesion (392).

A variety of NCX inhibitors exist and have different degrees of affinity and selectivity. Trivalent and divalent heavy metals are effective in blocking NCX in electrophysiological studies and have the following potency: $La^{3+} > Cd^{2+} > Ni^{2+} > Co^{2+} > Mn^{2+} > Mg^{2+}$ (393). Derivatives of amiloride such as benzamil, N^5-2,4,-dimethylbenzyl-amiloride (DBM), and 3,4-dichlorobenzamil (DCM) have poor selectivity and generally weak affinity for NCX (394, 395). Recently, benzyloxyphenyl derivatives such as KB-R7943, SEA0400, and SN-6 have been developed as selective NCX inhibitors and used as pharmacological tools to study the roles of the exchanger at the cellular and organ level (396). Both KB-R7943 and SEA0400 inhibit the reverse mode of NCX, though SEA0400 is approximately 10 times more potent for this mode of inhibition. Both have cardioprotective effects against ischemia-reperfusion injury (396-398).

IV MATERIALS AND METHODS

1.0 Materials and reagents

Culture media (Dulbecco's Modified Eagle Medium, DMEM/F12, and Minimum Essential Medium, SMEM), fetal bovine serum (FBS), antibiotics (penicillin and streptomycin) and trypsin-EDTA (0.05% v:v) were purchased from Gibco BRL (Grand Island, NY). Culture plates, flasks, and multi-well dishes were obtained from Fisher Scientific (Ottawa, Ontario, Canada). Collagenase type 2 was obtained from Worthington Biochemical Corporation (Lakewood, NJ). Recombinant human CT-1, PDGF-BB, TGFβ1, and TNF-α were acquired from R&D Systems (Minneapolis, MN). Recombinant wild type LoFGF2 (the 18 kDa, AUG-initiated isoform) was kindly provided by Dr. Elissavet Kardami (Department of Human Anatomy and Cell Sciences, University of Manitoba, Canada). FGF-2 was produced in *Escherichia coli* and purified to homogeneity according to standard protocols as published previously (399). Primary antibodies specific for SMemb were supplied by Abcam Inc. (Cambridge, MA), αSMA from Sigma-Aldrich Canada Ltd (Oakville, Ontario, Canada), NCX1.1 from Swant (Bellinzona, Switzerland), actin from Santa Cruz Biotechnology (Santa Cruz, CA) and $Ca_v1.2a$ from Alomone Labs (Jerusalem, Israel). Alexa Fluor-conjugated secondary antibodies were purchased from Molecular Probes (Eugene, OR) and anti-mouse Ig Texas Red-conjugated antibody was from Amersham Pharmacia Biotech (Arlington Heights, IL). Crystal Mount was obtained from Biomedia (Foster City, CA). Prestained low-molecular-weight markers and anti-mouse horseradish peroxidase (HRP) conjugated IgG antibodies were acquired from Bio-Rad Laboratories (Hercules, CA). Polyvinylidene difluoride (PVDF) blotting membranes were obtained from Roche Diagnostics (Laval, QC, Canada). The enhanced chemiluminescence (ECL Plus) and protein assay kits were supplied by Sigma-Aldrich. Costar Transwell apparatuses were obtained from Corning Inc. (Corning, NY). Collagen bovine solution was purchased from Stem Cell Technologies (Vancouver, BC, Canada). Surgical handle and blades were acquired from Becton-Dickinson Acute Care (Franklin Lakes, NJ). Whatman pH indicator paper was obtained from Whatman International Ltd (Middlesex, London). Lactate dehydrogenase assay (LDH) kit was purchased from Diagnostic Chemicals Limited (Charlottetown, PEI, Canada). ML-7, AG1296, and KB-R7943 were acquired from Calbiochem (San Diego, Ca). Ascorbate, $GdCl_3$, EGTA, dimethyl sulfoxide (DMSO), calcium chloride ($CaCl_2$), ouabain, bovine serum albumin

(BSA), ionomycin, nifedipine, cycloheximide, protease inhibitor cocktail, Hoechst 33342 stain and other laboratory grade reagents were purchased from Sigma-Aldrich Canada Ltd.

2.0 Use of cytokines, pharmacological inhibitors and blockers, and calculation of free [Ca^{2+}] using Softmax C

Working stocks of PDGF-BB, CT-1, TGFβ1, and TNF-α were stored in aliquots of 10 μg/ml in a carrier protein solution consisting of 0.1% BSA in PBS. For each separate experiment, stocks of 0.8 μg/μl LoFGF-2 were diluted to 10 μg/ml in 0.25% BSA in PBS. Working stocks of $CaCl_2$, $GdCl_3$, EGTA, and ouabain were kept at 400 mM in double distilled water (DDW), 5 mM in PBS, 100 mM in DDW, and 1 mM in DDW, respectively. Working stocks of ML-7, nifedipine, KB-R7943, and ionomycin were stored at 10, 10, 2, and 1 mM in DMSO, respectively. Working stocks of AG1296 were kept in 10 mg/ml in DMSO.

A computer based program called Softmax C (see http://www.stanford.edu/~cpatton/webmaxc/webmaxcS.htm) was used to calculate the appropriate concentration of EGTA to treat myofibroblasts in migration assays so that the effects of EGTA did not theoretically chelate free [Ca^{2+}] below damaging limits (i.e. under ~100 nM). Free [Ca^{2+}] was calculated by imputing increasing concentration of EGTA and creating a standard logarithmic curve. Extrapolation of specific concentration of free [Ca^{2+}] due to chelation effects enabled determination of the concentration of EGTA used in this study.

3.0 Isolation and culture of rat cardiac fibroblasts and myofibroblasts

Hearts from sacrificed male adult Sprague-Dawley rats of 150-200 grams were removed for preparation of cardiac fibroblasts as previously described with minor modifications (400, 401). Briefly, rats were anesthetized under 3% isoflurane gas at 2 L/min oxygen flow. Rat hearts were excised and subjected to Langendorff perfusion at a flow rate of ~5 ml/min at 37ºC with recirculating SMEM medium containing 0.1% collagenase type II for 20 min or until cardiac tissue was digested. Collagenase was neutralized by addition of an equal volume of DMEM/F12 medium. The slurry of liberated cells was collected by centrifugation at 2000 rpm for 5 min, and resuspended in feeding media consisting of DMEM/F12 supplemented with 10% FBS, 100 U/ml penicillin, 100 μg/ml streptomycin, and 1 μM ascorbic acid. Cells were seeded on 75 mm^2 non-coated culture flasks at 37ºC with 5% CO_2 for 2 hours. Non-adherent cells (i.e. myocytes) were

removed by aspirating the media, rinsing once with 1x phosphate buffered saline (PBS), then replaced and maintained in serum supplemented feeding media (10% FBS). Cells used in this study were of passage one (P1) unless otherwise noted. Different rats were used in each of the same experiment to achieve specified n values.

In order to obtain P1 cells, confluent P0 cells were passaged. Similarly, P1s were passaged to obtain P2s. Passaging of cells involved washing with PBS then application of trypsin for 3 min followed by gentle agitation of the flask or plate to dislodge adherent cells. Trypsinzed cells were neutralized with equal volumes of DMEM/F12 and centrifuged at 2000 rpms for 5 min. Depending on the experiment, cells were either counted in a hemocytometer or directly resuspended in media supplemented with serum.

4.0 Cellular migration assay: transwell apparatus system

Many techniques are available for studying chemotaxis including the wounded monolayer model, Boyden chamber, and Transwell system. The wounded monolayer model is simple, inexpensive and one of the earliest developed methods to study directed cell migration *in vitro* (402). Although two dimensional, this method mimics cell migration during wound healing *in vivo* because it involves creating a "wound" in a cell monolayer, capturing the images at time zero and during regular intervals as the wound is restored with cells (402). The Bodyen chamber (403) and Costar Transwell assay (404, 405) are set up with two chambers separated by a filter through which cells migrate. Chemotactic gradients are created by placing different concentrations of the putative chemoattractant in the lower chambers. The use of these systems requires that cells under test must move in three dimensions and squeeze through the pores of the particular filter (8 μm in this study). Results are reproducible and the chemokinetic chemotactic response easy to quantify. We preferred the Transwell method and found that cardiac myofibroblasts are motile in the presence of CT-1 compared to our previous study using Boyden chamber data (196). Limitations of the Costar Transwell system include the loss of chemotactic gradients over time due to diffusion of chemokines from the bottom chamber into the top. Nonetheless, our results confirm the efficacy of our experimental conditions.

Chemotaxis of rat cardiac fibroblasts (P0) and myofibroblasts (P1 or P2) were determined with a transmembrane, two-chamber system assay using Costar Transwell apparatuses. The procedure was performed as previously described with minor alterations (404, 405) (Figure 3). In lower chambers of 6 well Transwell plates, chemokines were diluted to specified concentrations

in 2.5 ml serum free DMEM/F12. Cells were plated into inserts, which were superimposed to (and separated from) the lower chamber by a polycarbonate membrane containing 8μm pores. For experiments using P1 and P2 myofibroblasts cells were passaged, counted with a hemocytometer, and 2 x 10^5 cells/well were plated directly into inserts. For experiments using P0 fibroblasts the pellet, obtained after cells were freshly liberated from rat hearts, was resuspended in serum free media then 2 ml was added into each insert. After 2 hours, inserts were gently washed twice with PBS to rid non-adherent cells followed by addition of 1.5 ml of serum free media. Inhibitors (AG1296, KB-R7943, and ML-7) or blockers (nifedipine and gadolinium) were added to insert at specified concentrations.

Transwell plates were incubated at 37ºC. After a 24 hour incubation period cells, which had migrated through the membrane toward the chemoattractant gradient, became adherent to the underlying membrane and at the bottom of the lower well. Media was carefully aspirated from both the inserts and wells and washed once with 1.5 ml PBS followed by addition of 1.5 ml of trypsin to the lower well. Plates were incubated for 5 minutes, gently agitated to detach adherent cells, and then neutralized with equal volumes of DMEM/F12. Inserts were removed and the cell suspension was diluted in filtered PBS, and counted with a Model ZM Coulter cell counter (Beckman Coulter, Fullerton, CA). The number of counted cells represents rate of migration. Each experimental group was performed in duplicate.

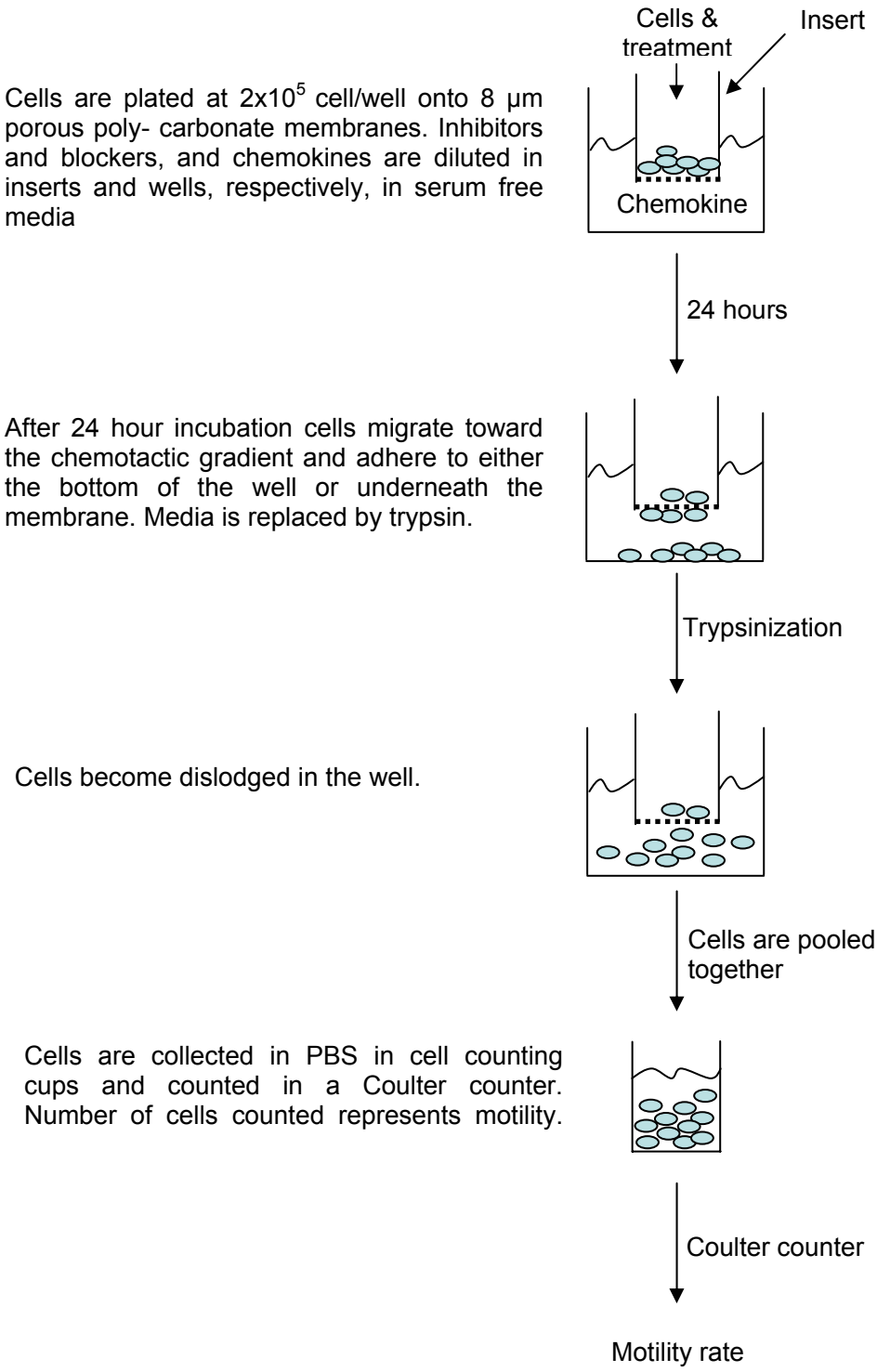

Figure 3. **Schematic diagram showing the steps involved in conducting Costar Transwell motility assays used in this study.**

4.1 Counting of cell number

In order to conduct experiments on cardiac fibroblasts we needed to develop a system that would allow for effective plating of these cells without phenotype being *lost* in culture. Cardiac fibroblasts are only found in freshly isolated rat hearts, which also contains an abundance of other cell types making it impossible to count fibroblasts. Counting of fibroblasts after resuspension of the isolated pellet was deemed technically impossible since the resuspension contained a heterogeneous population of unwanted cells and tissue debris. Therefore, cell counting was performed to determine the number of freshly isolated P0 fibroblasts present in one rat heart. In this way, a standard volume of resuspension media could be plated into the insert, which would contain a reasonable estimate of freshly isolated fibroblasts. It should be noted that we found this technique useful for estimation purposes only: it is not extremely accurate. We show that in average rat heart masses of ~170 grams there are ~400 000 - 500 000 fibroblasts or ~11% of total cell number, which likely includes cardiomyocytes, endothelial cells, vascular smooth muscle cells and mast cells. This percentage is surprisingly low, as fibroblasts account for the majority of the non-myocytes cell population and comprise three-quarters of total myocardial cell number (122). The low proportion of fibroblasts to total myocardial cells may account for the abundance of digested tissue debris found subsequent to the digestion phase of our Langendorff cell isolation procedure and/or the loss of cells during the isolation procedure (ie. necrosis due to oxygen deprivation). Despite this inconsistency, the actual number of fibroblasts is accurate as fibroblasts adhere to the culture plates in less than 2 hours, therefore allowing for their quantification. Using graphical equations generated by plotting fibroblast number, heart mass and body mass, we developed a formula that estimates the number of fibroblasts found in a rat heart at any given total body mass.

Briefly, after freshly isolated cells were incubated for 2 hours, feeding media was removed and cells were washed twice with PBS. Trypsinized cells were neutralized, pooled together, and then transferred to PBS. The number of fibroblasts was determined using a Coulter Counter and plotted against total body mass. Hearts were blotted onto paper towels to rid excess fluid then weighted. Total heart mass was also plotted against total body mass.

To correlate heart body mass with number of fibroblasts, whole rat mass data (with increments of 10 grams) from 150 to 200 grams were entered into equations of the aforementioned graphs. A linear relationship between rat body mass and fibroblast number was

also determined. The equation for the latter graph was determined and represents a standard theoretical relationship between these two variables:

$$\text{Fibroblast number} = 13584.02 \times \text{rat mass (g)} - 1.93 \times 10^6$$

5.0 Myofibroblast proliferation assay: ^{3}H - thymidine incorporation

Cells were passaged and plated with feeding media in 6-well dishes. They were allowed to grow until they reached 50-60% confluency, usually taking 1-2 days to achieve. Cells were then rendered quiescent (serum starved) by washing twice with PBS followed by addition of DMEM/F12 for 24 hours. Subsequently, cells were coincubated for another 24 hours with specified treatments (cytokines and blockers/inhibitors) in DMEM/F12 supplemented with 1% FBS. Following the latter step, cells were pulse labeled with (^{3}H) Thymidine (Amersham Pharmacia Biotech, Arlington Heights, IL) for 4 hours at 37 MBq/ml. Cold 20% trichloroacetic acid (TCA) was used to precipitate DNA from cell lysates, which were then filtered through GF/A filters (Fisher). Beta emissions from the dried filters were measured with 3 ml Cytoscint scintillation fluid (ICN Pharmaceuticals, Costa Mesa, CA) and a scintillation counter (LS6500, Beckman Coulter, Fullerton, CA). Each experimental group was performed with six trials.

6.0 Contractility assay: collagen type I gel deformation

Collagen gel deformation studies were performed to study the *in vitro* effects of myofibroblast contractile responses in a 3D environment. Briefly, collagen gels were prepared by mixing a 3.5:1:0.5 ratio of cold collagen type I solution (collagen concentration of 3 mg/ml), 5-times concentrated cold DMEM/F12, and DDW. Using Whatman pH indicator paper as a gauge, 1 M NaOH was added drop wise to adjust the pH to 7.4. Aliquots of 600 µl of the collagen type I gel cocktail were added into 24-well dishes, which produced a gel thickness of 3 mm. After gels were allowed to solidify for at least 2 hours, cells were passaged, counted in a hemocytometer, and plated overtop the gel at 1.0 x 10^5 cell/ml in feeding media. Cells were incubated and allowed to adhere and grow for 24 hours then rendered quiescent by serum starving for another 24 hours. Application of specified treatments and blockers/inhibitors was followed by detachment of the gel from the surrounding walls of the wells by using a surgical blade (Fisher Scientific). Detachment of gels marked initiation of the contraction phase. Wells were digitally

photographed at 0 and 24 hours. Gel surface area on a 2D digital image was used to assess the rate of contraction and determined using IDL based analysis Measure Gel custom made software. Each experimental group was performed in triplicate.

7.0 Lactate dehydrogenase (LDH) assay

An LDH assay kit was used to determine if the various treatments used in this study imposed any cytotoxic effects on cultured myofibroblasts. The assay is based on the principle that lactate dehydrogenase converts L-lactate and NAD to pyruvate and NADH. The rate of increase in absorbance of the reaction mixture at 340 nm due to the formation of NADH, is proportional to the LDH activity.

$$\text{L-lactate} + NAD^+ \xrightarrow{LDH} \text{Pyruvate} + NADH + H^+$$

Myofibroblasts were passaged, counted with a hemocytometer, and seeded in 6 well dishes at 2.0×10^5 cells/well. After adhering and growing for 24 hours, cells were serum starved for 24 hours, and then treated for 24 hours. Media was collected and stored at -20ºC for later use. LDH activity in cell media was assayed according to manufacturer's instructions. Absorbance readings were taken at 340 nm at 1 minute intervals until the change in absorbance remained constant. Activity was calculated using the following formula:

$$\text{LDH (U/ml)} = \Delta A/\text{min.} \times \text{assay volume (ml)} / 6.22 \times \text{light path (cm)} \times \text{sample volume (ml)}$$

Where ΔA/min is change in absorbance per minute, assay volume is the total reaction volume, 6.22 is the absorbance coefficient of NADH at 340 nm, and light path is the length of the light path (1.0 cm).

8.0 Determination of myofibroblast number and adhesion of cells in presence of EGTA

Myofibroblasts were passaged, counted with a hemocytometer and seeded on glass coverslips in 6 well dishes at 2.0×10^5 cells/well. After being allowed to adhere and grow for 24 hours, cells were serum starved for 24 hours. Cells were then treated with specified concentrations of EGTA for 24 hours, media was aspirated and cells were washed twice with

PBS to remove dislodged cells, and fixed in 4% paraformaldehyde for 15 minutes. Cells were rendered permeable with 0.1% Triton X-100 in PBS for 15 min, then incubated with Hoechst 33342 stain for 30 seconds. Coverslips were thoroughly dried and were mounted to slides with Crystal Mount then examined under a microscope (Nikon) equipped with epifluorescence optics. Digital pictures were photographed at 400x magnification using appropriate filters. Nuclei were counted within a digital grid using Adobe Photoshop CS. Relative image areas were calculated using Measure Gel custom made software. Cell density (number of cells/image area) was used to determine whether EGTA treatment had an effect on cell adhesion to culture substrata.

9.0 Protein extraction and assay

Cells were plated directly (P0) or passaged (P1 and P2) into 100 mm culture dishes in feeding media. To maintain fibroblast phenotype, P0 cells were allowed to adhere in feeding media for 2 hours, followed by a washing step to remove non-adherent cells (i.e. cardiomyoctyes), grown in fresh feeding media for another 2 hours, then serum starved for 24 hours. P1 and P2 were allowed to grow to ~90% confluence and then serum starved. Cells were then rinsed 3 times with cold PBS and lysed in 120 µl RIPA buffer with pH 8.0 (150 mM NaCl, 1% Triton X-100, 0.5% deoxycholate, 0.1% SDS, and 50 mM Tris) containing 1x commercially available protease inhibitor cocktail (Sigma-Aldrich Canada Ltd) and phosphatase inhibitors (10 mM NaF, 1 mM Na_3VO_4 and 1 mM EGTA). Cells were scraped and dislodged with a disposable cell scraper (Fisher Scientific, Ottawa, Canada) and allowed to lyse on ice for 45 minutes to 1 hour. Cells were then sonicated 3 times for 5 seconds. The insoluble membrane fraction was removed by centrifugation at 14 000 rpm for 15 minutes at 4°C. Supernatant was collected, aliquoted, and stored at -20°C for later use. Total protein concentrations of all samples were quantified using the bicinchoninic acid (BCA) method as previously described (406).

10.0 Western blot analysis

Laemmli loading buffer (125 mM Tris-HCL pH 6.8, 5% glycerol, 2.5% SDS, 5% 2-mercaptoethanol, and 0.125% bromophenol blue) was mixed with samples of cell lysates, and boiled for 5 minutes. Equal amounts of protein samples (30 µg) were loaded into and resolved with 10% SDS-polyacrylamide gel electrophoresis (PAGE) alongside 10 µl of a prestained low-molecular weight marker. Separated proteins were electrophoretically transferred to PVDF

membranes (Roche, Grenzacherstrasse, Switzerland) for 1 hour at 300 mA. PVDF membranes were blocked overnight at 4°C in Tris-buffered saline with 0.2% Tween 20 (TBS-T) containing 5% non-fat skim milk. They were then incubated for 24 hours with primary NCX1.1 antibodies diluted to 1:1000 in TBS-T containing 5% non-fat skim milk. Secondary antibodies included horseradish peroxidase (HRP)-labeled anti-mouse. It was diluted to 1:1000 in TBS-T containing 1% non-fat skim milk, and incubated for 1 hour at room temperature. Protein bands on Western blots were visualized by ECL Plus according to manufacturer's instructions, and developed on X-ray film. To determine equal protein loading (internal control), PVDF membranes were stripped with 0.2 M NaOH for 15 minutes, blocked with non-fat skim milk, then probed with anti-mouse actin at a 1:1000 dilution for 1.5 hours. Band intensity was quantified using a CCD camera imaging densitometer (GS670, Bio-Rad Laboratories, Mississauga, Ontario, Canada).

11.0 Immunoctyochemistry

Immunofluorescent staining with αSMA, SMemb, NCX1.1 and $Ca_v1.2a$ was performed to detect endogenous expression of these proteins in P0, P1, and P2 cells as well as expression in these cells treated in the presence of various cytokines and growth factors. Cells were seeded onto glass coverslips in 6 well dishes. P0 cells were plated directly from the Langendorff cell isolation process in feeding media as already described above and after 3-4 hours, were serum starved for 24 hours. P1 and P2 were allowed to grow for 24 hours in feeding media. Cells were then starved to arrest growth and to rinse away serum by washing twice with PBS followed by addition of serum free media. After 24 hours of serum starvation, cells were stimulated with specified treatments for 24 hours. At this point, cell confluency was consistently maintained at ~50-60%.

Immunofluorescent staining was performed as previously described (119). Briefly, cells were washed 3 times with cold PBS, fixed in 4% paraformaldehyde for 15 minutes, rendered permeable with 0.1% Triton X-100 in PBS for 15 min, then incubated with anti-mouse αSMA or anti-mouse SMemb for 90 minutes, and anti-rabbit NCX1.1 or anti-mouse $Ca_v1.2a$ primary antibodies overnight. After cells were washed 3 times with PBS they were incubated for 1.5 hours in the dark with anti-mouse or anti-rabbit conjugated Alexa Fluor secondary antibodies. All antibodies were diluted in 1xPBS containing 1% BSA with ratios of 1:200 for αSMA and SMemb, 1:75 for NCX1.1, 1:50 for $Ca_v1.2a$ and 1:700 for Alexa Fluor. Following another

washing cycle with PBS, cells were subjected to Hoechst 33342 (10ng/ml) for 30 seconds to stain nuclei and therefore visualize orientation of fluorescently labeled cells. An additional round of washing followed. After coverslips were thoroughly dried, they were mounted to slides with Crystal Mount then examined under a microscope (Nikon) equipped with epifluorescence optics. Digital pictures were photographed at 400 and 1000x magnification using appropriate filters.

12.0 Statistical analysis

All values were analyzed using Sigma Stat software (Point Richmond, CA) and are expressed as means ± standard error (SE). One-way analysis of variance (ANOVA) was used to determine if significant differences existed within all experimental groups. If significant differences were achieved, the Student-Newman-Keuls *post hoc* test was used to compare differences among multiple experimental groups. Significant differences among groups were defined as $P \leq 0.05$.

V RESULTS

1.0 Fibroblast/myofibroblast motility

1.01 Determination of fibroblast P0 cell number based on rat body mass

To standardize motility assays, a fixed number of cells are counted before seeding into Costar Transwell apparatuses. Cultures of P1 and P2 myofibroblasts are relatively pure insofar as they do not contain a heterogeneous population of cells and their phenotypes are generally stable in culture conditions. In contrast, P0 fibroblast phenotypes are less stable and in culture rapidly transdifferentiate into that of a myofibroblast phenotype when plated at low density and exposed to serum (13, 106, 136). To retain fibroblast phenotype and therefore study the migration properties of these cells in culture, we found that P0 cells must be plated directly into inserts in our Transwell system. P0 cells are technically impossible to count since they are located in the freshly digested heart, which consists of a mixture of a variety of different cell types, namely cardiomyocytes.

After collagenase digestion, cells were plated for 2 hours. Non-adherent cells were pooled and counted while the remaining adherent fibroblasts were trypsinized and also counted. We found ~4.13 x 10^5 number of fibroblasts in rat hearts averaging 172.67 ± 6.39 grams (Figure 4E), which comprises ~11% of the total rat cardiac cell population (i.e the ratio of average fibroblasts to total number of cells as indicated histologically in figure 4E). For our studies using fibroblasts our goal was to use cells within this 11% figure. To mathematically verify number of fibroblasts in rat hearts, counted fibroblasts were correlated with rat body mass (Figure 4A), and heart mass was correlated with rat mass (Figure 4B). All animals used in our study range from 150-200 grams. We inputed this range into the equations of the aforementioned relationships to mathematically correlate new relationships consisting of fibroblast number to heart mass (Figure 4C) and fibroblast number to rat mass (Figure 4D). A linear relationship exists between fibroblast numbers, heart mass and rat body mass indicating that young hearts provide proportionately the same numbers of fibroblasts. Extrapolation of 172.67 grams heart mass from Figure 4D reveals approximately the same number of fibroblast (~4.13 x 10^5) on the graph as determined using the basic counting method. Thus, the equation derived from figure 4D graph can be used to roughly estimate number of fibroblasts in rat hearts at any given body mass.

1.02 CT-1-induced motility profiles

We previously showed that CT-1 is a chemokine for rat cardiac myofibroblasts as tested in Boyden Chamber assays (196). Here**,** the Costar Transwell system was employed to test the ability of CT-1 to stimulate cell migration in both cardiac fibroblasts and myofibroblasts (Figure 5). After a 24 hour incubation period, cells which migrated to the lower chambers of Transwells were collected and counted. The number of cells counted represents rate of cell motility.

The dose dependent motility effects of CT-1 stimulation in evident in both P0 (Figure 5A) and P1 (Figure 5B) cells. CT-1 causes a biphasic motility effect. Motility increases in proportion to CT-1 concentration; 10 ng/ml CT-1 is most effective as a chemotactic stimulus. The second phase of the CT-1 dose response curve occurs at the highest concentration of CT-1 (50 ng/ml) and is characterized by diminution of the motile response. CT-1 causes no change in cell motility rate in P2 cells (Figure 5C). Figures 5A-C are superimposed in Figure D and indicates that P0 cells have greater motility potentials than those of P1 and P2 cells, while P1 cells have greater motility potentials than that of P2s. Furthermore, in P0 cells, 1 and 10 ng/ml CT-1 induced a significantly elevated rate of cell motility compared to that of P1 and P2 cells.

1.03 PDGF-induced motility profiles

Figure 6A and B show that PDGF-BB also induces a biphasic concentration dependent effect on P1 and P2 cells, respectively. PDGF-BB stimulates a significant number of P1 motile cells at 10 and 50 ng/ml compared to non treated controls, whereas only 10 ng/ml elicits significant motility rates in P2 cells. Superimposing P1 and P2 motility profiles reveals that P1 cells have greater motility potentials than P2 cells (Figure 6C). Furthermore, in P1 cells, optimal concentration of PDGF-BB occurs at 50 ng/ml. On the other hand, in P2 cells, the motility response declines at 50 ng/ml.

Coincubation of 2, 5, 10, and 20 μM AG1296 and 50 ng/ml PDGF-BB results in significant dose dependent decreases in cell motility compared to PDGF control values (Figure 7). This data suggest that motility stimulated by PDGF is dependent on PDGFβR activation.

1.04 LoFGF-2 and TNF-α motility profiles in P1 cells

Both LoFGF-2 and TNF-α (Figures 8A and B, respectively), stimulated a biphasic concentration dependent effect on P1 cell motility, with 20 ng/ml of either cytokine treatments eliciting the optimal migratory response.

1.05 Summary profiles of P1 migratory rates

Figure 9 illustrates a comparison between the individual optimal cytokine induced motility rates relative to non-stimulated control values. PDGF, LoFGF-2, CT-1, and TNF-α all stimulate significant increases in P1 myofibroblast migration at 62-, 6-, 4.5-, 1.5- fold relative to non treated control. Therefore, the ranking of chemotactic potency occurs in the following order: PDGF > LoFGF-2 > CT-1 > TNF-α. The optimal cytokine concentrations outlined for P1 cells in Figure 9 are used throughout the current investigation.

1.06 Characterization of cardiac fibroblast and myofibroblast phenotype

Expression of αSMA (129, 131, 298) and SMemb (15) are characteristic of myofibroblast phenotype. Expression of these proteins correlates to degree of myofibroblast contractile responses both *in vitro* and *in vivo* (129). The phenotypic differentiation from fibroblasts to myofibroblasts *in vivo* involves humoral and mechanical factors and contributes to infarct scar remodeling.

To determine whether the respective phenotypes of P0, P1, and P2 cells used in this study are preserved in culture, cells were incubated with or without the presence of different cytokine treatments. Using immunocytochemistry we qualitatively analyzed expression of αSMA and SMemb by immunostaining P0, P1, and P2 cells with these antibodies. As expected, unlike non-treated P0 cells (1 day after isolation), non-treated P1 cells (3-4 days after isolation) and non-treated P2 cells (5-7 days after isolation) had enhanced staining for endogenous expression of αSMA and SMemb (Figure 10A). This is consistent with the notion that increases in passage number induce the myofibroblast-like phenotype. Although smaller in cell size, P0 cell have relatively weaker expression of αSMA and SMemb and this suggests that preservation of a non-myofibroblast or fibroblast cell phenotype is achieved. TGFβ1 stimulation (Figure 10B) serves as the positive control for fibroblast/myofibroblast differentiation in this experiment. In contrast to PDGF (Figure 10C) and LoFGF-2 (Figure 10D) and compared to non-treated cells (Figure

10A), TGFβ1 stimulation was associated with increases in expression of αSMA and SMemb in P1 and P2 cells (Figure 10B). As expected, TGFβ1 also caused a slight increase in expression of these proteins in P0 cells (Figure 10B *vs.* Figure 10A) and this finding confirms that 24 hour TGFβ stimulation induces fibroblast to myofibroblast differentiation.

Compared to αSMA and SMemb expression in non-treated cells, treatment of P0, P1, and P2 cells with PDGF (Figure 10C *vs.* 10A) and LoFGF-2 (Figure 10D *vs.* 10A) for 24 hours preserves the expected phenotypes and results in no change in expression level between the same cell phenotype (i.e. expression in PDGF and LoFGF-2 stimulated cells remains uniform compared to non-treated control images).

1.07 Effect of extracellular Ca^{2+} chelation with EGTA treatment on motility

Ca^{2+} plays an important role in many cellular processes including motility, contraction, and proliferation. EGTA is a strong Ca^{2+} chelator (407). As Ca^{2+} is an important intracellular second messenger required for cell signaling processes, we found it necessary to determine the appropriate concentration of EGTA to add to the media so that $[Ca^{2+}]_o$ does not drop so low as to affect cellular function. Using the online software program, Softmax C, we used a range of 0 to 8 mM EGTA and applied these parameters into a prewritten algorithm. As shown in Figure 11A, theoretical application of 2, 3, and 4 mM EGTA into the media would result in 2.1 μM, 0.1 μM, and 66.1 nM free Ca^{2+} leftover in solution.

We used Costar Transwell apparatuses to test the effect of 24 hour EGTA Ca^{2+} chelation on P1 myofibroblast motility in the presence of PDGF. As seen in Figure 10B, EGTA treatment results in a concentration dependent decrease in cell migration with significant diminutions most evident at 3 and 4 mM. In the same experiment, cells were co-treated with 4 mM EGTA and increasing concentrations of $CaCl_2$. When free Ca^{2+} is added back into Ca^{2+} chelated media, the EGTA mediated inhibition of the migratory response is reversed in a dose-dependent manner. Thus, significant concentration-dependent changes in migration were observed.

To determine the effect of 24 hour EGTA treatment on cellular morphological changes, we plated P1 myofibroblasts with or without EGTA. Compared to non-treated cells, increasing concentrations of EGTA causes retraction of cellular extensions and invokes cells to become less asymmetrical and more rounded in shape (Figure 12A). Cells were then co-treated in the presence of 4 mM EGTA and increasing concentrations of $CaCl_2$. As shown in Figure 12B, re-

introduction of Ca^{2+} into chelated media reverts myofibroblast morphology back to that observed in non-treated cells. This indicates that in a concentration dependent manner, introduction of Ca^{2+} supercedes the chelation effects of EGTA, thereby reversing EGTA induced cellular retraction and returns cell shape back to a normal asymmetrical appearance. Changes in morphology as a result of EGTA treatment directly reflect the effects observed in migration.

Lamellipodia and filopodia extension and cellular attachments by integrin receptors require Ca^{2+} for normal function. To verify whether the drop in migration seen in Figure 11B, due to EGTA treatment, is the result of ablation of cell adherence to the substrata, we plated P1 myofibroblasts and treated them with or without EGTA. After 24 hours, cells were washed to remove non-adherent cells, fixed and then nuclei were stained with Hoechst 33342. Cell density was determined by counting nuclei in a standardized field (21 mm^2). As seen in Figure 12C, EGTA treatment did not affect cell density compared to non-treated controls, suggesting that EGTA does not interfere with cell adherence phenomena at the concentrations used in this study.

1.08 Effect of introduction of cytosolic Ca^{2+} to migrating cells

Ionomycin is a membrane soluble ionophore primarily selective for Ca^{2+} (408, 409). We treated P1 myofibroblasts with ionomycin for 24 hours to determine the effect of introduction of Ca^{2+} to the cytosol in the presence of ionomycin on Costar Transwell cell motility. Although not significant, ionomycin treatment maintained P1 PDGF (Figure 13A) and LoFGF-2 (Figure 13B) mediated motility and indicates that influx of Ca^{2+} to the cytosol is required to maintain the subcellular processes involved in cell motility.

Since cell phenotype may influence motility we sought to determine whether introduction of cytosolic Ca^{2+} has effects on myofibroblast phenotype. P0, P1, and P2 cells were plated in the presence of 166 nM ionomycin for 24 hours then immunostained with αSMA and SMemb antibodies. P1 and P2 cells stained positive for αSMA and SMemb (Figure 14). Low levels of staining for these proteins are exhibited in P0 cells. Comparing endogenous expression of these proteins without treatment (Figure 10A) to expression of cell treated in the presence of ionomycin (Figure 14), shows that ionomycin has no affect on cell phenotype.

1.09 The role of NCX1.1 in cell motility

As $[Ca^{2+}]_i$ plays a major role in cell motility, we sought to screen for the various modes of transplasmalemmal Ca^{2+} flux that contribute to the migratory response. One proposed mode of Ca^{2+} flux is through either forward or reverse mode NCX. We therefore used Costar Transwell apparatuses to determine the role of NCX1.1 function on P1 cell motility by inhibiting the exchanger using a selective NCX inhibitor, KB-R7943 (410, 411). KB-R7943 treatment results in a dose dependent decrease in both PDGF (Figure 15A) and CT-1 (Figure 15B) stimulated migration. A significant drop in migration for both treatment groups occurs at 7.5 and 10 μM KB-R7943.

NCX is regulated by intracellular Na^+ concentrations such that high intracellular Na^+ causes activation of the reverse mode of the exchanger, which in turn, induces the Ca^{2+} entry mode of the exchanger. To test whether our finding that KB-R7943-dependent decreases in migration are the result of reverse mode inhibition, we used ouabain to pharmacologically inhibit the Na^+/K^+ pump thereby driving up intracellular Na^+ concentrations. As seen in Figure 15C, coincubation of PDGF and ouabain at increasing doses results in no change in motility rates compared to PDGF control values.

1.10 Expression of NCX1.1 in cardiac fibroblasts and myofibroblasts

Isoforms of NCX1 are expressed in the myocardium (368). To verify endogenous protein expression of NCX1.1 in fibroblasts and myofibroblasts, we subjected cell lysates from P0, P1 and P2 cells to SDS-PAGE and Western blotting with specific NCX1.1 monoclonal antibodies. Quantitative NCX1.1 expression is calculated relative to actin expression. We found that NCX1.1 is expressed in P0, P1, and P2 cells but no change in expression is observed between cell passages (Figure 16A). To confirm this finding, we stimulated P0, P1, and P2 cells with or without cytokine treatments and subjected them to immunostaining with NCX1.1 antibodies. Immunostaining of NCX1.1 shows qualitatively that compared to non-treated P1 cells, P0 and P2 cells stain weakly for this protein (Figure 16B). Similar expression patterns of NCX1.1 between P0, P1, and P2 cells are seen in PDGF treatment (Figure 16C), LoFGF-2 treatment (Figure 16D), TGFβ1 treatment (Figure 16D), and CT-1 treatment (Figure 16E), suggesting that cytokine stimulation does not enhance NCX1.1 expression beyond that seen in non-treated control images.

1.11 The role of NSCCs in myofibroblast motility

NSCCs are membrane channels permeable to various cations including Ca^{2+}. To investigate the role of NSCC function in cell motility we treated P1 myofibroblasts with Gd^{3+}, a well known and selective blocker of NSCC (365). Using Costar Transwell apparatuses, we found that Gd^{3+} treatment results in a dose dependent decrease in CT-1 (Figure 17A), PDGF (Figure 17B), and LoFGF-2 (Figure 17C) stimulated cell migration. Gd^{3+} causes significant decreases in motility at concentrations of 10 and 20 μM. In particular, 20 μM Gd^{3+} treatments resulted in motility values dropping close to those seen in non-treated motile cells, suggesting that migrating cells require the functioning of NSCC to support motility.

1.12 The role of MLCK in cell motility

Activation of myosin motors by phosphorylation of rMLC at serin 19 and threonine 18 is a prerequisite for contraction of the cell cortex in order for migrating cells to translocate forward. Phosphorlyation of serine 2 and 3, and treonine 8 leads to rMLC inhibition. Phospho-MLC is modulated by the ATPase activity of MLC, which is further regulated by MLCK. MLCK is also dependent on a Ca^{2+}/calmodulin mechanism for its activation. To examine the role of MLCK on cell motility in P1 myofibroblasts we used Costar Transwell apparatuses and incubated cells for 24 hours in the presence of a MLCK inhibitor, ML-7 (412). ML-7 significantly decreases PDGF (Figure 18A) and LoFGF-2 (Figure 18B) induced migration in a dose dependent manner. Cell migration values dropped to or below non-treated control values, and indicates that PDGF and LoFGF-2 induced cell motility is dependent on phospho-MLC activation by MLCK.

1.13 The role of L-type Ca^{2+} channels in cell motility

L-type Ca^{2+} channels describe a broad category of voltage-dependent Ca^{2+} channels. Nifedipine, a general L-type Ca^{2+} channel blocker (413), was used to determine if P1 myofibroblast motility is dependent on these channels. Using Costar Transwell apparatuses, we found that after 24 hour treatment there is no overall change in PDGF induced cell motility between nifedipine treated cells and PDGF control values (Figure 19), indicating that either L-type Ca^{2+} channels are not expressed in P1 cardiac myofibroblasts or that these channels do not play a role in cell migration.

1.14 Expression of $Ca_v1.2a$

$Ca_v1.2a$ channels are members of the superfamily of voltage-dependent L-type Ca^{2+} channel, and known to be expressed in excitable cell types, namely cardiomyocytes and smooth muscle cells (414). P0, P1, and P2 cells were immunostained with $Ca_v1.2a$ antibodies to determine expression of this protein in cells of different cardiac fibroblast passage and stimulation with or without cytokines for 24 hours. Non-treated P0, P1, and P2 cells stained positive for $Ca_v1.2a$ and expression levels remained uniform between all three cell passages (Figure 20A). Compared to non-treated controls, expression followed similar patterns and is maintained but not elevated in the presence of PDGF (Figure 20B), LoFGF-2 (Figure 20C), TGFβ1 (Figure 20D), and CT-1 (Figure 20E). Expression throughout the cytosol is also evident.

1.15 Effect of DMSO in cell motility

DMSO is a solvent used to dissolve and store stock solutions of blockers and inhibitors. To rule out the possibility that DMSO does not interfere with transplasmalemmal Ca^{2+} flux thereby causing an epiphenomena, we determined that a solution containing 0.5% v:v or 70.4 mM DMSO does not change cell motility rates compared to non-treated controls. As seen in Figure 21, treatment of P1 myofibroblasts with 70.4 mM DMSO did not affect 24 hour PDGF stimulated motility compared to non-treated controls. The final concentrations of DMSO containing solutions used in this study do not exceed 70.4 mM DMSO (0.5% v:v in media).

2.0 Contractile responses of myofibroblasts to various stimuli: collagen I gel deformation assays

2.1 Modes of transplasmalemmal Ca^{2+} flux on myofibroblast gel deformation

P1 cells were plated on surfaces of pre-formed 3 mm thick collagen type I gels and rendered quiescent. For cells to mechanically load or confer tension to the underlying matrix, gel edges were released from the surrounding culture dish. Images of gel surfaces were obtained at the time of treatment and again after 24 hours. Gel surface area is analyzed with IDL custom made computer software (Measure Gel). We calculated the difference between the 24 hour gel surface area and 0 hour surface area to determine the rate of contractile response or gel deformation change.

Figure 22A shows the rate of myofibroblast mediated gel deformation change in the presence of various cytokine treatment groups. To ensure that our system works appropriately, our negative control consists of gels incubated without cells. As expected, compared to non-treated cells, gels without cells exhibited no gel deformation. We subjected P1 myofibroblast to various treatment groups. As shown in Figure 20A, TGFβ1, AngII and PDGF all significantly cause increases in rate of gel deformation change relative to non-treated cells, suggesting that these cytokines induce myofibroblast contractile responses. Furthermore, we found that PDGF induced contractile responses peak at 10 ng/ml and remain elevated up to 100 ng/ml. Although 10% FBS treatment stimulated significant myofibroblast contractile responses, the individual effects of TGFβ1, PDGF, and AngII showed a more potent effect on gel contraction.

To address the functions of transplasmalemmal movement of Ca^{2+} on P1 PDGF and TGFβ1 induced myofibroblast contractile responses we targeted overall Ca^{2+} chelation by EGTA, NCX inhibition using KB-R7943, MLCK inhibition using ML-7, L-type Ca^{2+} blockade using nifedipine, and NSCC blockade using Gd^{3+}. Compared to respective controls, PDGF (Figure 22B and C) and TGFβ1 (Figure 23A and B) induced contractile responses are significantly decreased in all treatment groups except for Gd^{3+} treatment. We found that Gd^{3+} did not cause any concentration dependent change between PDGF (Figure 22C) and TGFβ (Figure 23B) controls. This data suggests that although Ca^{2+} is involved in myofibroblast contractile responses, different mechanisms for modes of transplasmalemmal flux are at play.

3.0 Cellular proliferation

3.1 The functions of modes of transplasmalemmal Ca^{2+} flux on myofibroblast proliferation

Myofibroblast proliferation contributes to repopulation of the infarct scar and involves DNA synthesis. To assess cell proliferation rates or DNA synthesis in P1 cardiac myofibroblasts we measured incorporation of ^{3}H-thymidine into DNA. Quiescent cells were stimulated with or without co-incubation of 1% FBS together with PDGF and/or inhibitors/blockers. Since PDGF is a potent mitogen for various cells types, as expected, PDGF treatment stimulated significant concentration dependent increases in ^{3}H-thymidine incorporation (Figure 24A) compared to the 1% FBS control, suggesting that PDGF stimulates DNA synthesis and thus cell proliferation in these cells. The PDGF induced proliferation response is biphasic in that maximal proliferation rate is achieved at 5 and 10 ng/ml but rapidly declines at elevated PDGF concentrations.

To investigate the role of transplasmalemmal Ca^{2+} movement on P1 PDGF induced myofibroblast proliferation rates we subjected cells to the same experimental treatment groups used in gel deformation assays (Figure 24B). We found that in the presence of PDGF myofibroblasts proliferation is completely ablated at 3 and 4 mM EGTA compared to PDGF controls. Dose-dependent decreases in proliferation are also evident in KB-R7943 experimental groups, with 10 μM causing the most significant inhibition. While nifedipine also caused decreases in proliferation responses, although graded, we found no significant change in proliferation rate between PDGF controls and Gd^{3+} treated cells.

4.0 LDH as a measure of cytotoxicity

4.1 Cytotoxic effects of inhibitors and blockers

LDH is a cytosolic enzyme responsible for converting lactate to pyruvate. Thus, LDH plays a role in normal metabolism in cells. To test whether the various inhibitors or blockers used in this study have any cytotoxic affects on P1 myofibroblasts and rule out the possibility of artifact results, we assayed cell culture media for presence of LDH activity subsequent to 24 hour treatments. We used cycloheximide as a positive control for this experiment, since its major biological activity is translation inhibition in eukaryotic cells which results in inhibition of protein synthesis leading to cell growth arrest and death. As expected, we found that 24 hour cycloheximide treatment significantly causes increases in LDH activity in media compared to non treated control values in a dose-dependent manner (Figure 25A). In contrast, we found no change in LDH activity at increasing doses of EGTA (Figure 25B), KB-R7943 (Figure 25C), Gd^{3+} (Figure 25D), or ML-7 (Figure 25E) treatments compared to non-treated cells. This data verifies that these treatments do not cause cytotoxicity in myofibroblasts at the concentrations used in this study, indicating that the effects observed during application of these treatments in our bioassays is due to the bioactivity of the drug itself. As LDH resides in the cytosol, LDH activity found in the media as a result of cycloheximide treatment suggests that this drug is causing rupture of the cell membrane, likely via a necrotic pathway, thereby exposing cytosolic contents to the media.

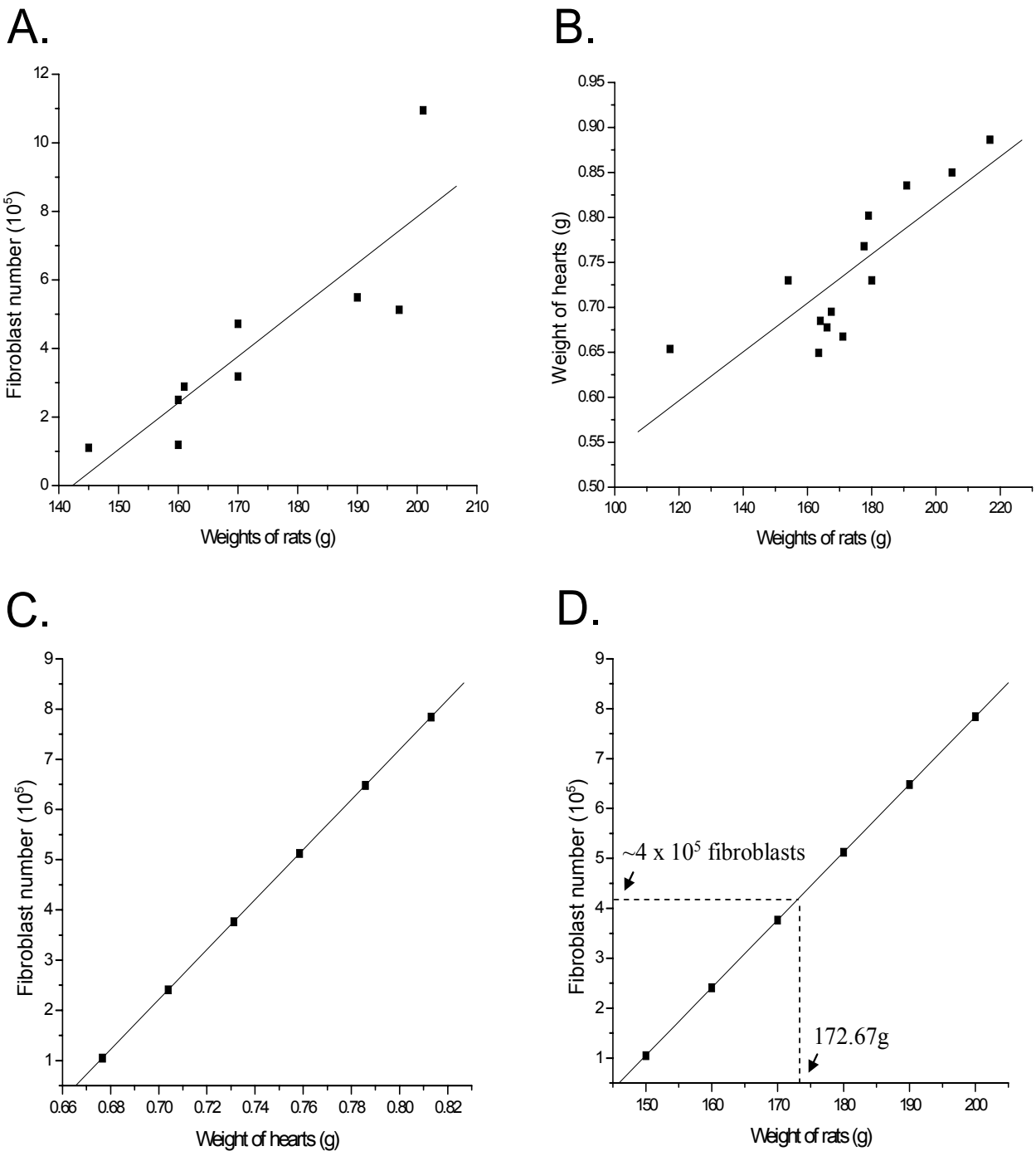

Figure 4. Fibroblast number in hearts of rats are directly proportional to total body mass and total heart mass. The equations from fibroblast number plotted against total rat mass (Panel A) and that from total heart mass plotted against total body mass (Panel B) were used to determine the relationship between fibroblast number and heart mass with respect to arbitrary rat mass (150-200 grams) (Panel C). Fibroblast count was then plotted against total rat mass (Panel D). The equation derived from Panel D represents a standardized formula to determine fibroblast number based on rat body mass. The proportion of total heart cells to average fibroblasts were also determined using a Coulter counter (Panel E).

E.

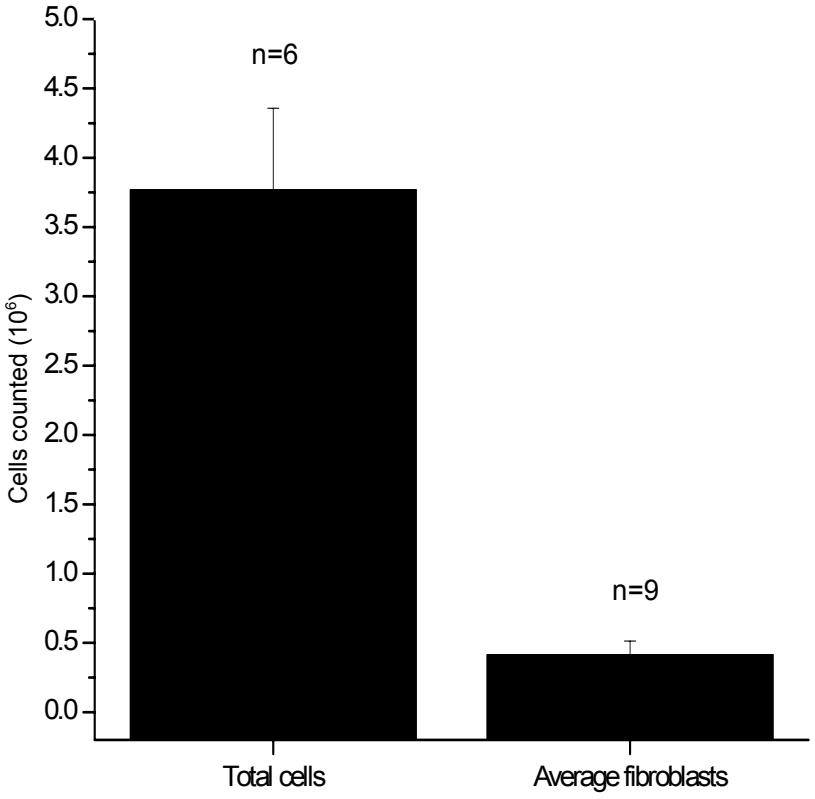

Average rat mass = 172.67g

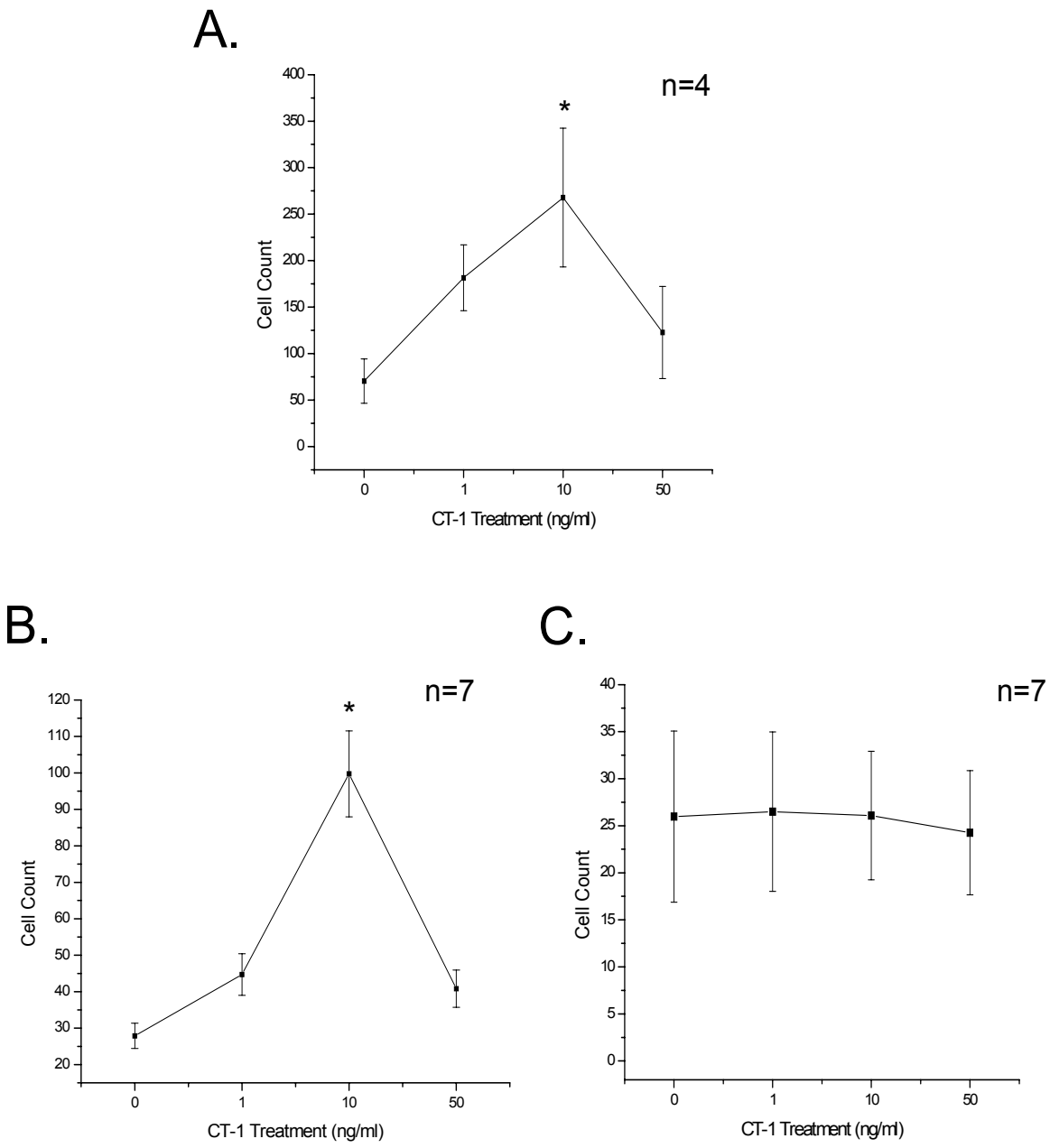

Figure 5. CT-1 induced motility profiles in cells of different passages. The concentration dependent effects of CT-1-induced-motility in P0 (Panel A), P1 (Panel B) and P2 (Panel C) cells were analyzed with Costar Transwell apparatuses. 0-50 ng/ml CT-1 in serum free media were loaded into lower wells while cardiac fibroblasts and myofibroblasts (2 x 10^5 cells/well) were loaded into inserts. Cells that migrated through the 8 μm pores after 24 hours were trypsinized and counted in a Coulter counter. Cell count is a measure of motility rate. Panels A, B and, C were combined to compare migratory rates between P0, P1, and P2 cells (Panel D). *p≤0.05 vs. non-treated control, #p≤0.05 vs. P1 cells, &p≤0.05 vs. P2 cells; all data expressed as mean ± SEM.

D.

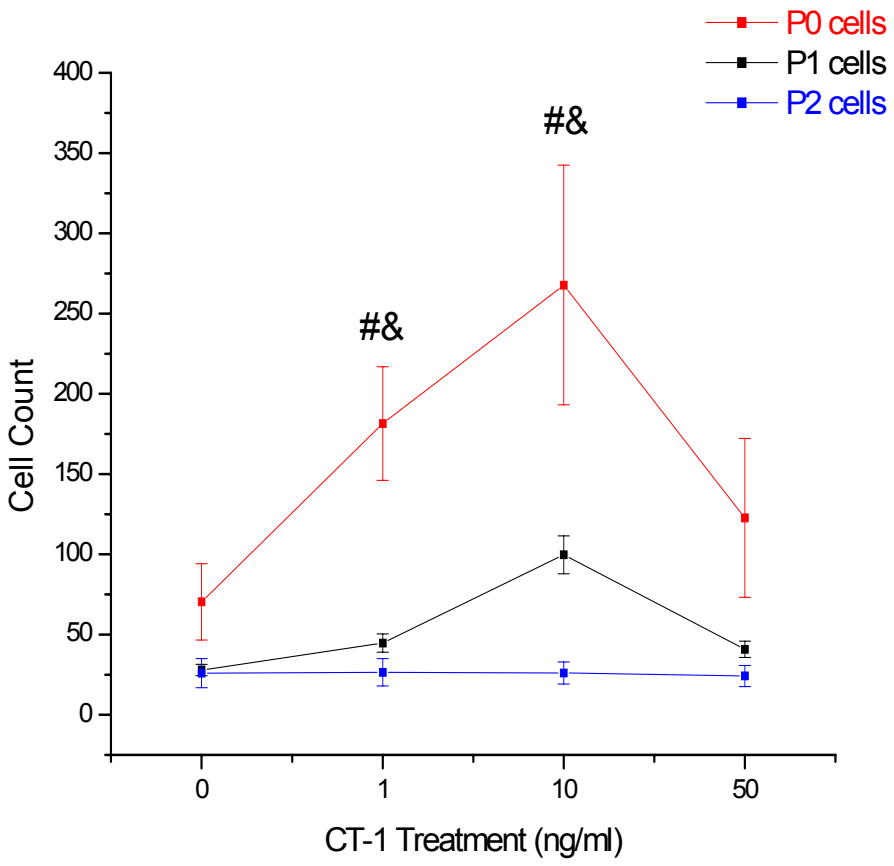
P0 cells
P1 cells
P2 cells
#&
#&
Cell Count
400
350
300
250
200
150
100
50
0
0
1
10
50
CT-1 Treatment (ng/ml)

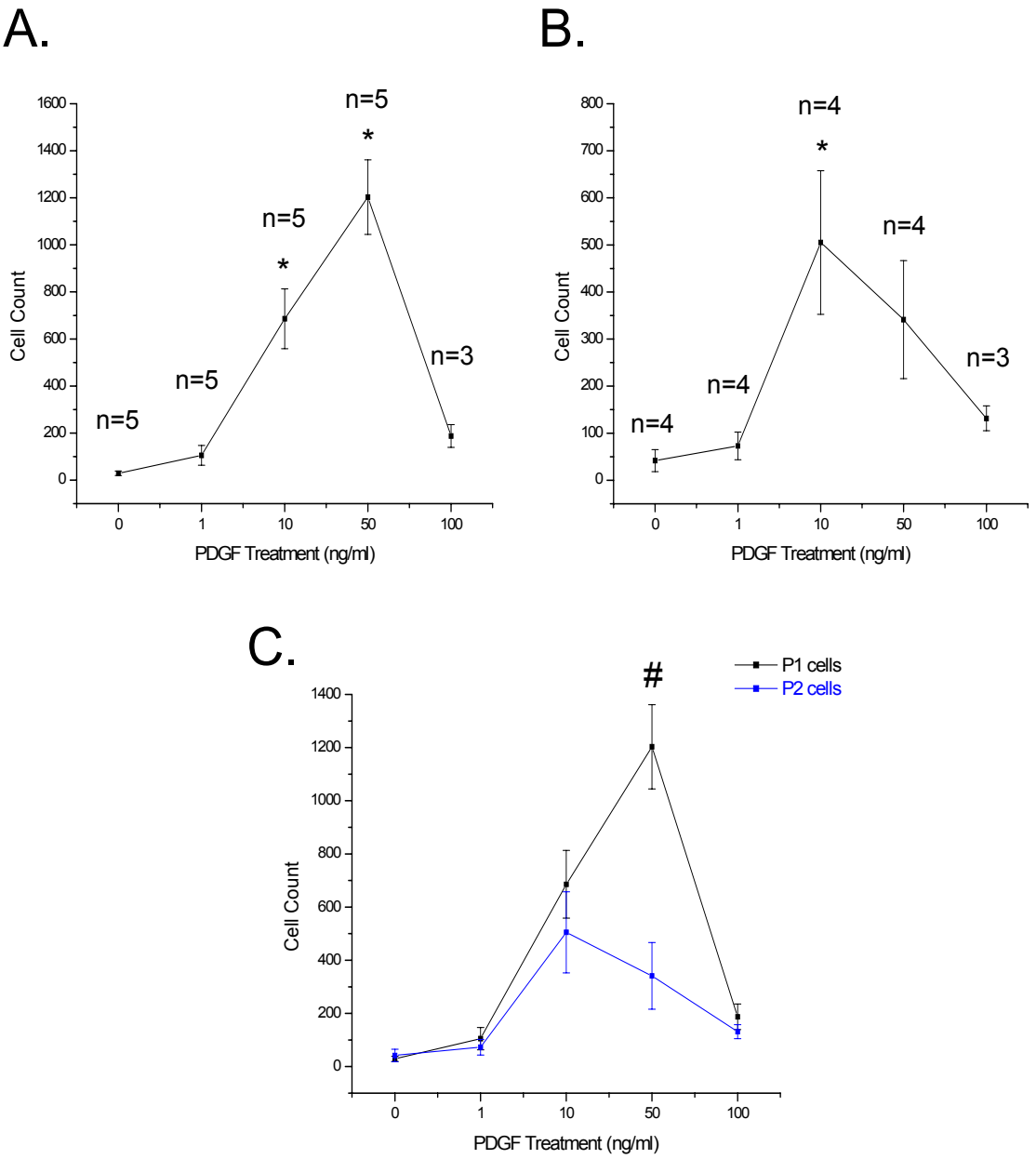

Figure 6. PDGF induced motility profiles in cells of different passages. The concentration dependent effects of CT-1-induced-motility in P1 (Panel A) and P2 (Panel B) cells were analyzed with Costar Transwell apparatuses. Indicated concentrations of PDGF in serum free media were loaded into lower wells while cardiac fibroblasts and myofibroblasts (2 x 10^5cells/well) were loaded into inserts. Cells that migrated through the 8 µm pores after 24 hours were trypsinized and counted in a Coulter counter. Cell count is a measure of motility rate. Panels A and B were combined to compare migratory rates between P1 and P2 cells (Panel C). *$p \leq 0.05$ vs. non-treated control, #$p \leq 0.05$ vs. P2 cells; all data expressed as mean ± SEM.

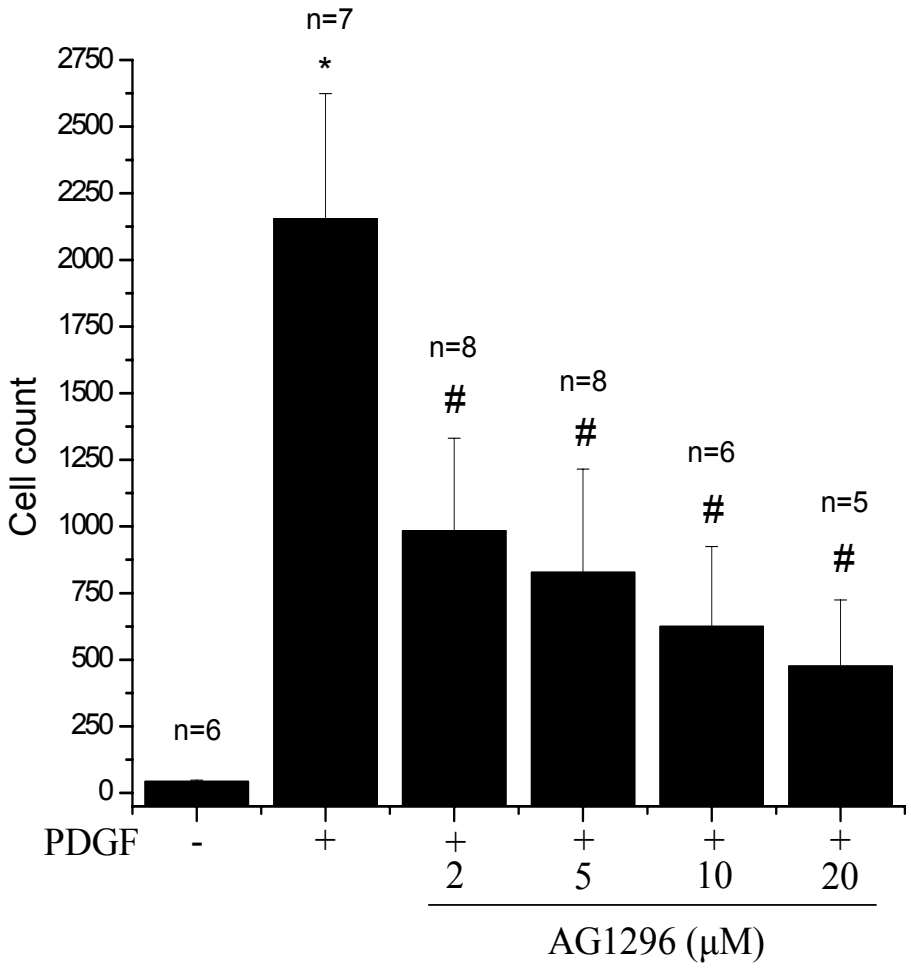

Figure 7. **PDGF stimulated motility is dependent on PDGFR activation.** PDGF-induced motility in P1 cells were analyzed with Costar Transwell apparatuses. 10 ng/ml PDGF in serum free media was loaded into lower wells while cardiac myofibroblasts (2 x 10^5 cells/well) and AG1296 were loaded into inserts. Cells that migrated through the 8 μm pores after 24 hours were trypsinized and counted in a Coulter counter. Cell count is a measure of motility rate. *$p \leq 0.05$ vs. non-treated control, #$p \leq 0.05$ vs. PDGF control; all data expressed as mean ± SEM.

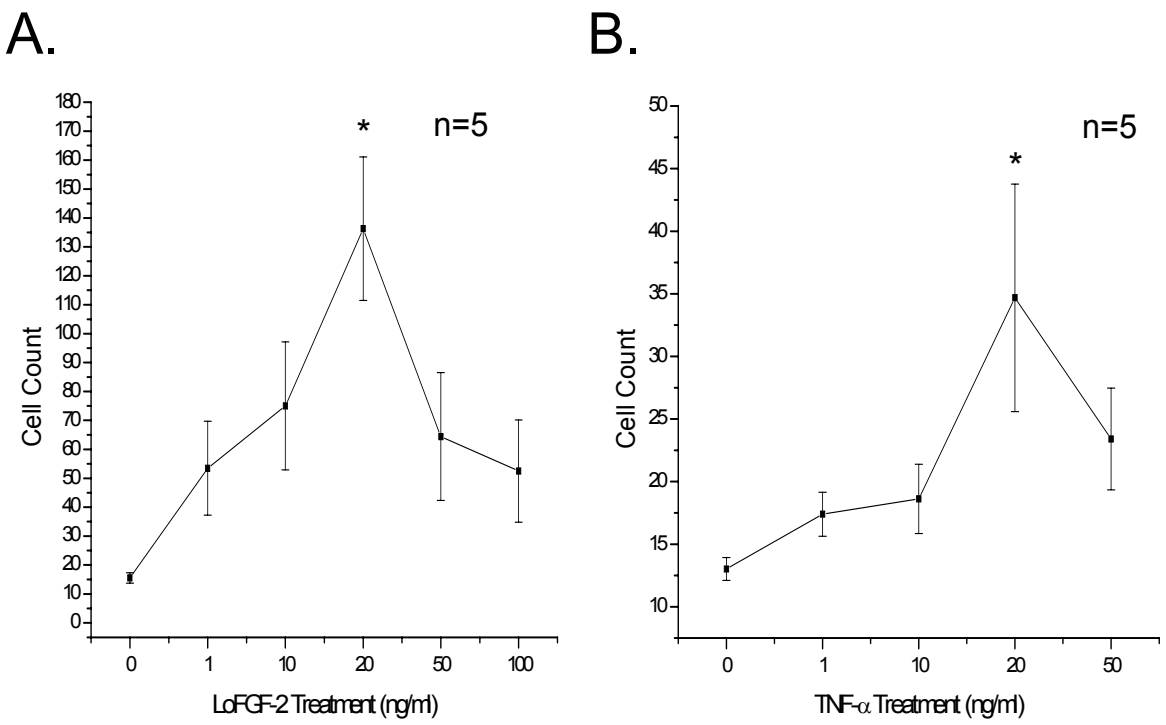

Figure 8. LoFGF-2 and TNF-α induced motility profiles in P1 cells. The concentration dependent effects of LoFGF-2 (Panel A)- and TNF-α (Panel B)-induced motility in P1 cells were analyzed with Costar Transwell apparatuses. Indicated concentrations of LoFGF-2 and TNF-α in serum free media were loaded into lower wells while cardiac myofibroblasts (2 x 10^5 cells/well) were loaded into inserts. Cells that migrated through the 8 μm pores after 24 hours were trypsinized and counted in a Coulter counter. Cell count is a measure of motility rate. *$p \leq 0.05$ vs. non-treated control; all data expressed as mean ± SEM.

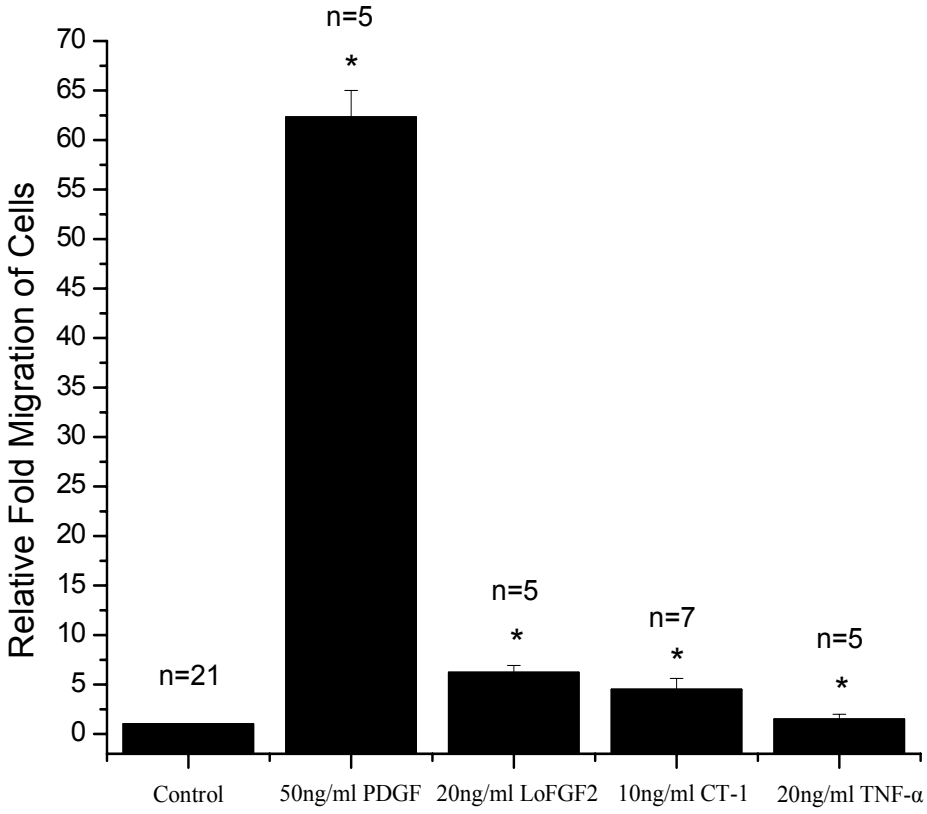

Figure 9. Summary profiles of optimal P1 motility rates between all cytokine groups. The optimal concentrations of 24 hour stimulated CT-1, PDGF, LoFGF-2, and TNF-α – induced motility rates in P1 myofibroblasts relative to non-treated controls. *$p \leq 0.05$ vs. non-treated control; all data expressed as mean ± SEM.

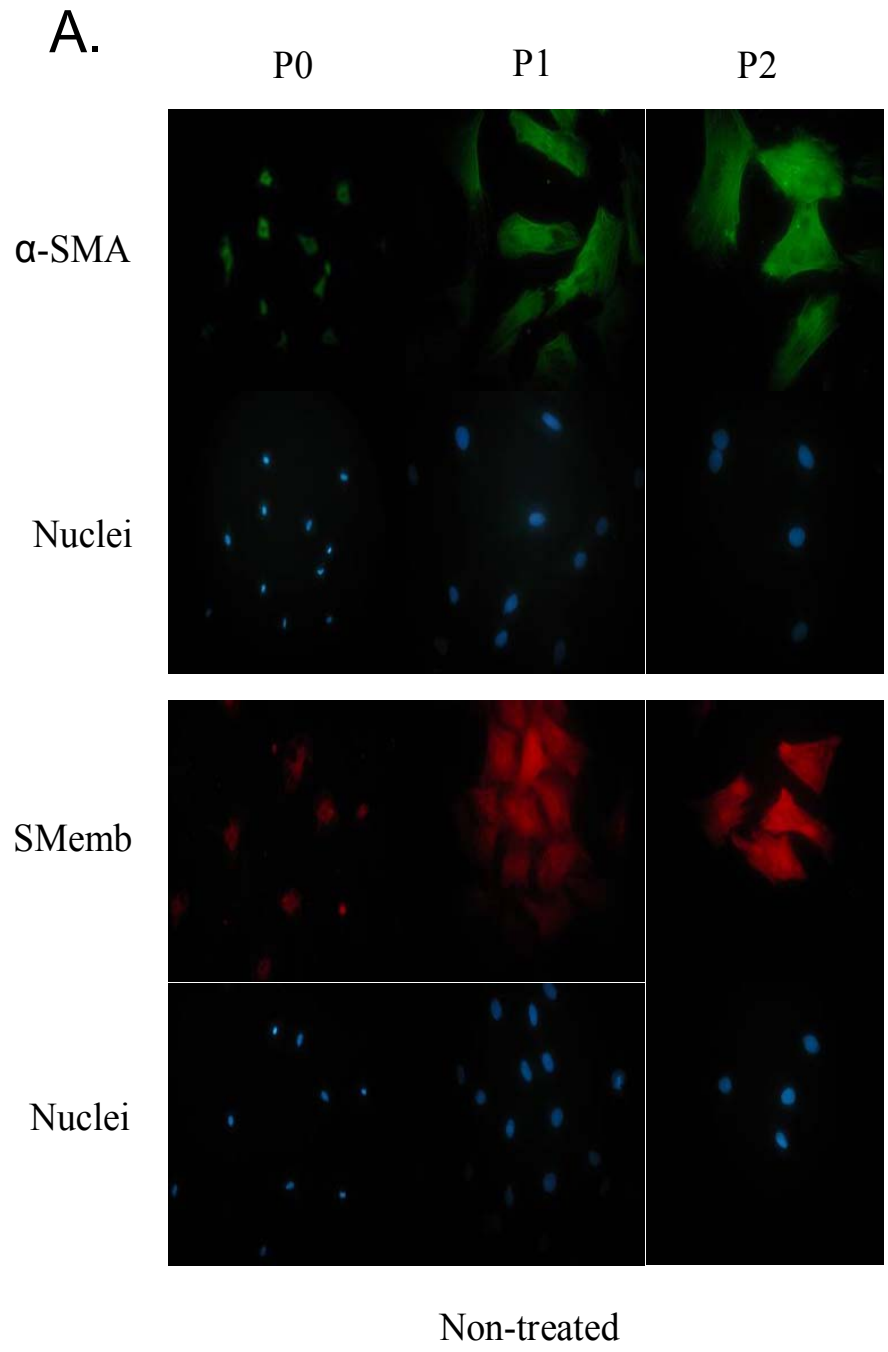

Figure 10. Effect of cytokine stimulation on expression of αSMA and SMemb in different cell phenotypes. Freshly isolated fibroblasts (P0) and cultured myofibroblasts (P1 and P2) were stimulated with 10 ng/ml TGFβ1 (Panel B), 50 ng/ml PDGF (Panel C), and 20 ng/ml LoFGF-2 (Panel D) for 24 hours and immunostained with anti-αSMA and SMemb. Endogenous expression of these proteins without cytokine treatment was also determined (Panel A). Nuclei were identified by staining with Hoechst. Representative images were taken at 400x magnification and are shown from 3 separate experiments.

B.

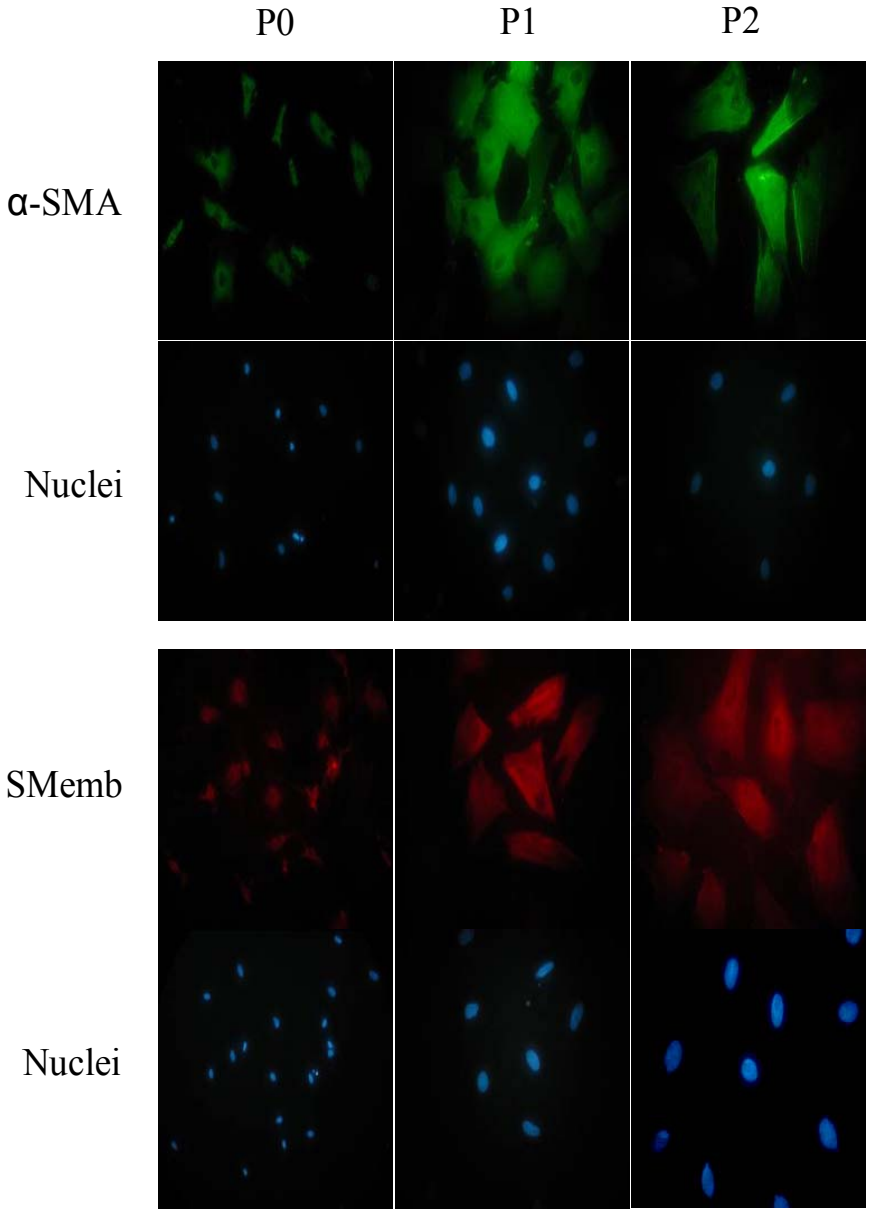

10 ng/ml TGFβ1 treatment

C.

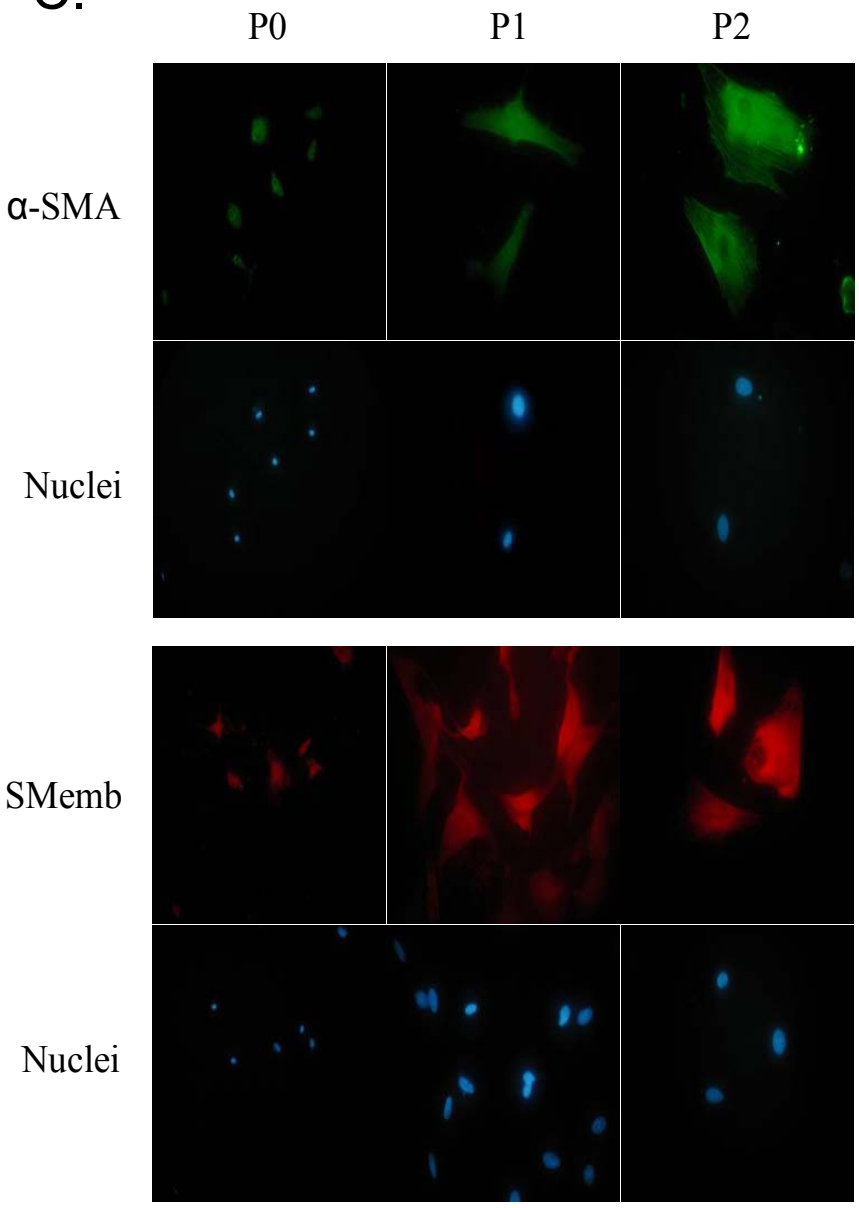

50 ng/ml PDGF treatment

D.

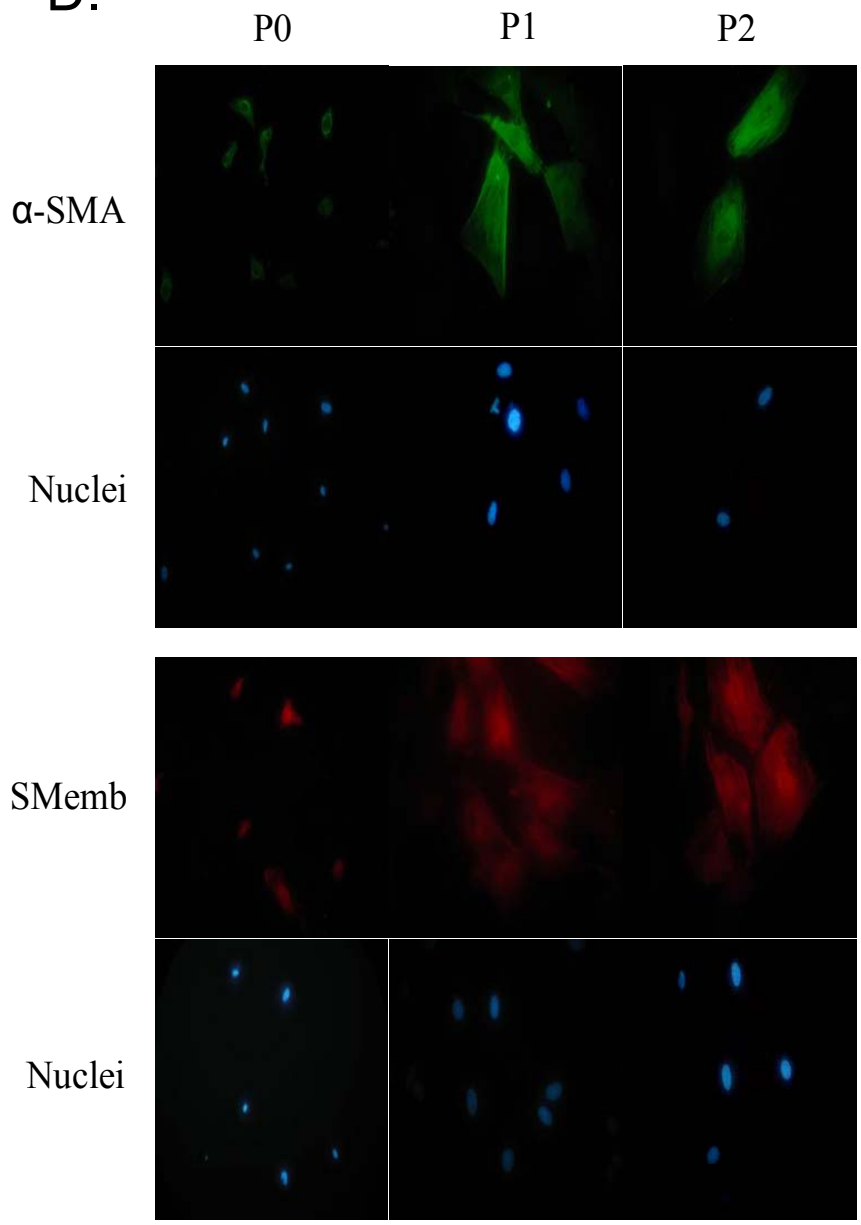

20 ng/ml LoFGF-2 treatment

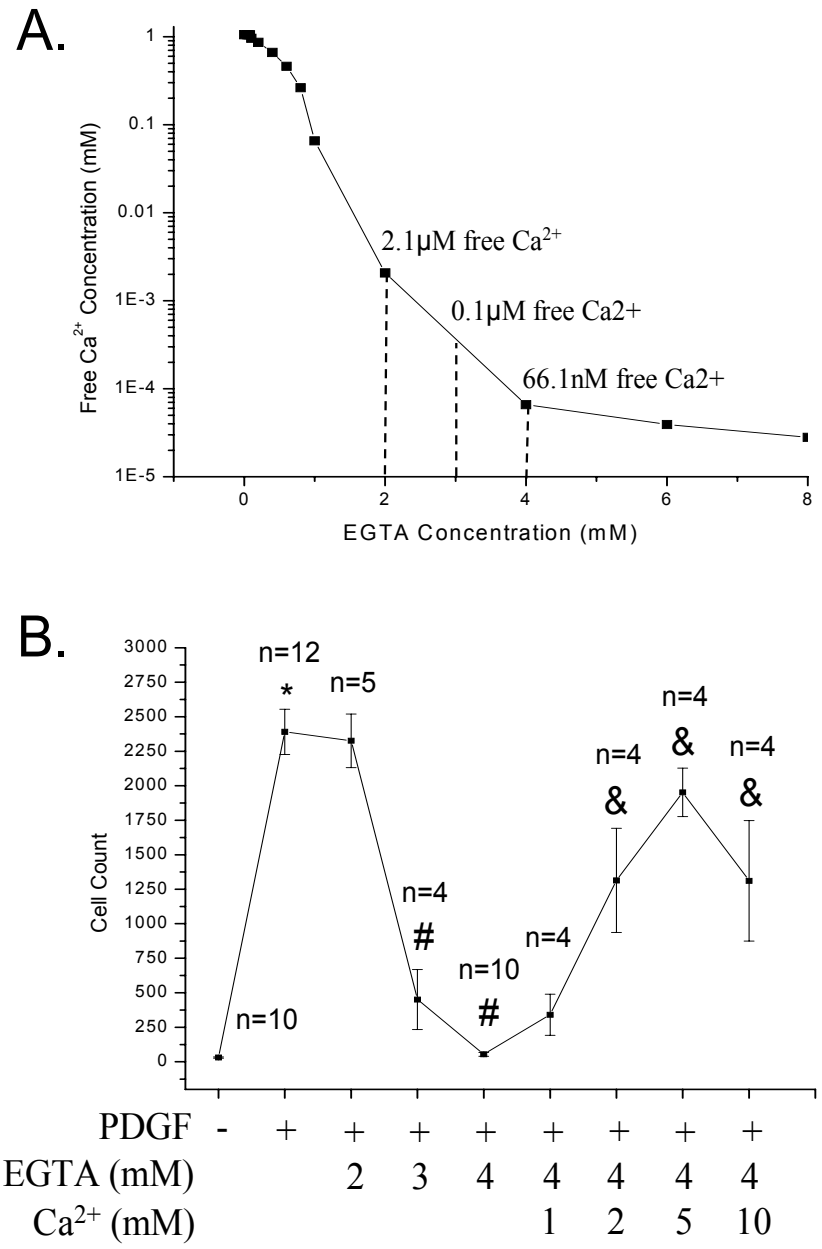

Figure 11. Effect of EGTA treatment on PDGF-induced motility. Based on the properties of EGTA, Softmax C was used to calculate the appropriate concentration of EGTA such that free Ca^{2+} in the media would not be totally chelated (Panel A). The concentration dependent effects of EGTA and the effect of re-introduction of Ca^{2+} into Ca^{2+} depleted medium (Panel B) in P1 cells were analyzed with Costar Transwell apparatuses. 50 ng/ml PDGF in serum free media was loaded into wells and indicated concentrations of EGTA and P1 myofibroblasts (2 x 10^5 cells/well) were loaded into inserts. Cell count is a measure of motility rate. *$p \leq 0.05$ vs. non-treated control, #$p \leq 0.05$ vs. PDGF control, &$p \leq 0.05$ vs. EGTA control; all data expressed as mean ± SEM.

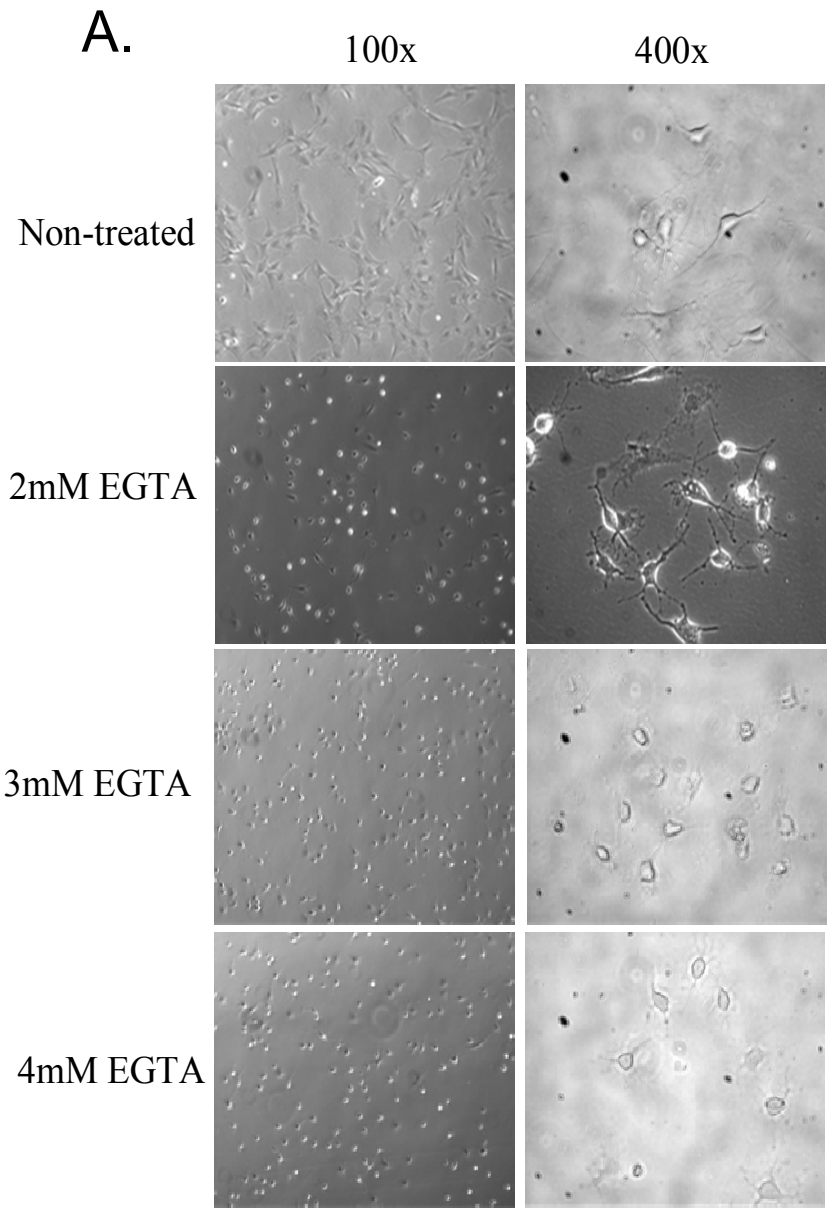

Figure 12. Morphological and cell adherence changes due to EGTA treatment. The effect of EGTA treatment (Panel A) and re-introduction of Ca^{2+} at indicated concentrations (Panel B) on P1 myofibroblasts for 24 hours were analyzed at 100 and 400x magnification. Representative images are from 3 separate experiments. Since motility is dependent on cell-substratum attachments and since EGTA may interfere with this adherence due to its Ca^{2+} chelation properties, the effect of EGTA treatment at specified concentrations on cell adherence was determine (Panel C). Using the same EGTA treatments, nuclei were stained with Hoechst and counted. The surface area of a 10x magnified optical field was determined to be 21 mm^2 and used to calculate cell density (counted cells/ mm^2). Representative images are from 4 separate experiments.

B.

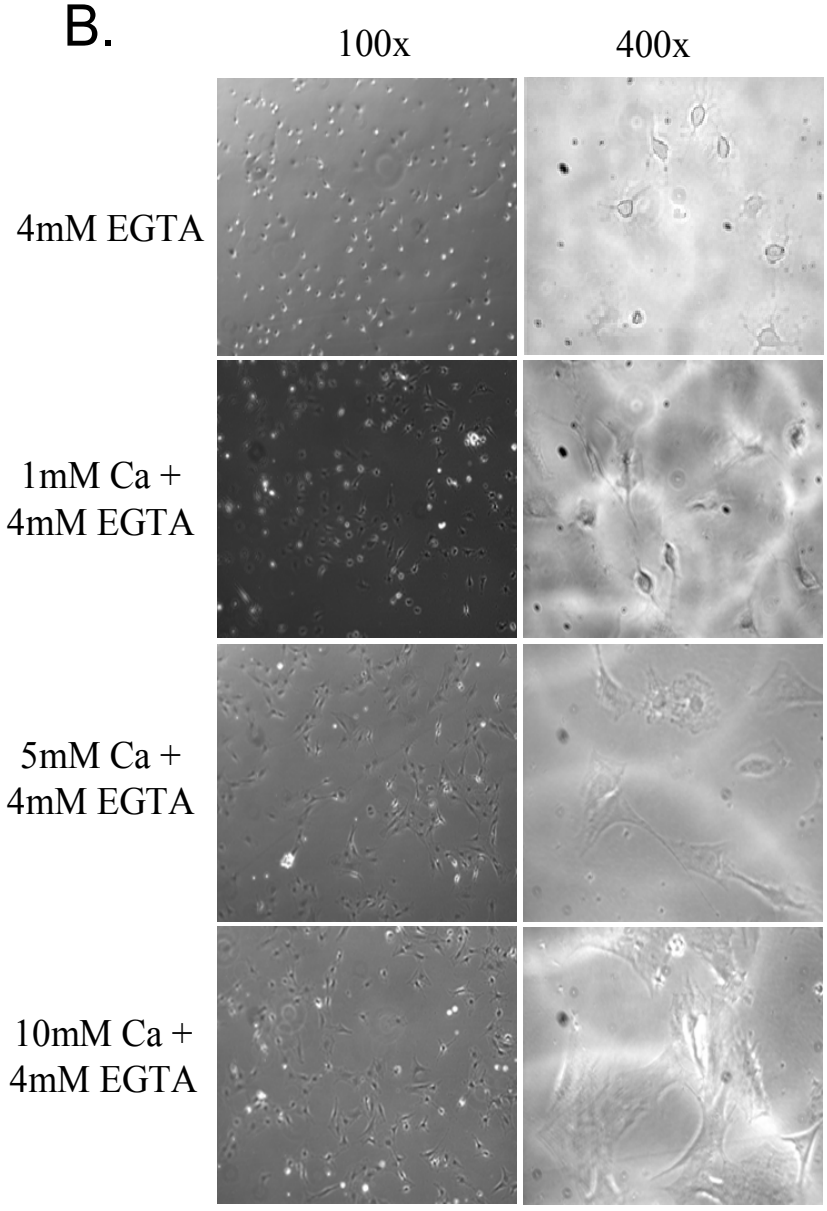
100x
400x
4mM EGTA
1mM Ca +
4mM EGTA
5mM Ca +
4mM EGTA
10mM Ca +
4mM EGTA

C.

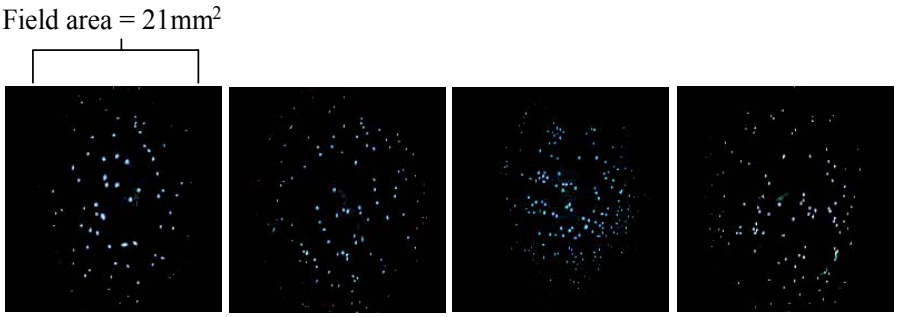

EGTA (mM) 0 2 3 4

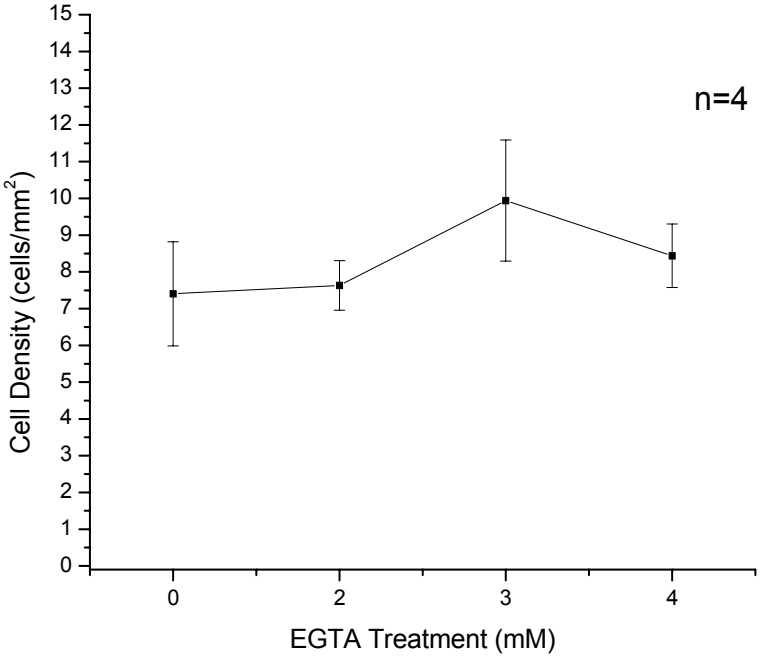

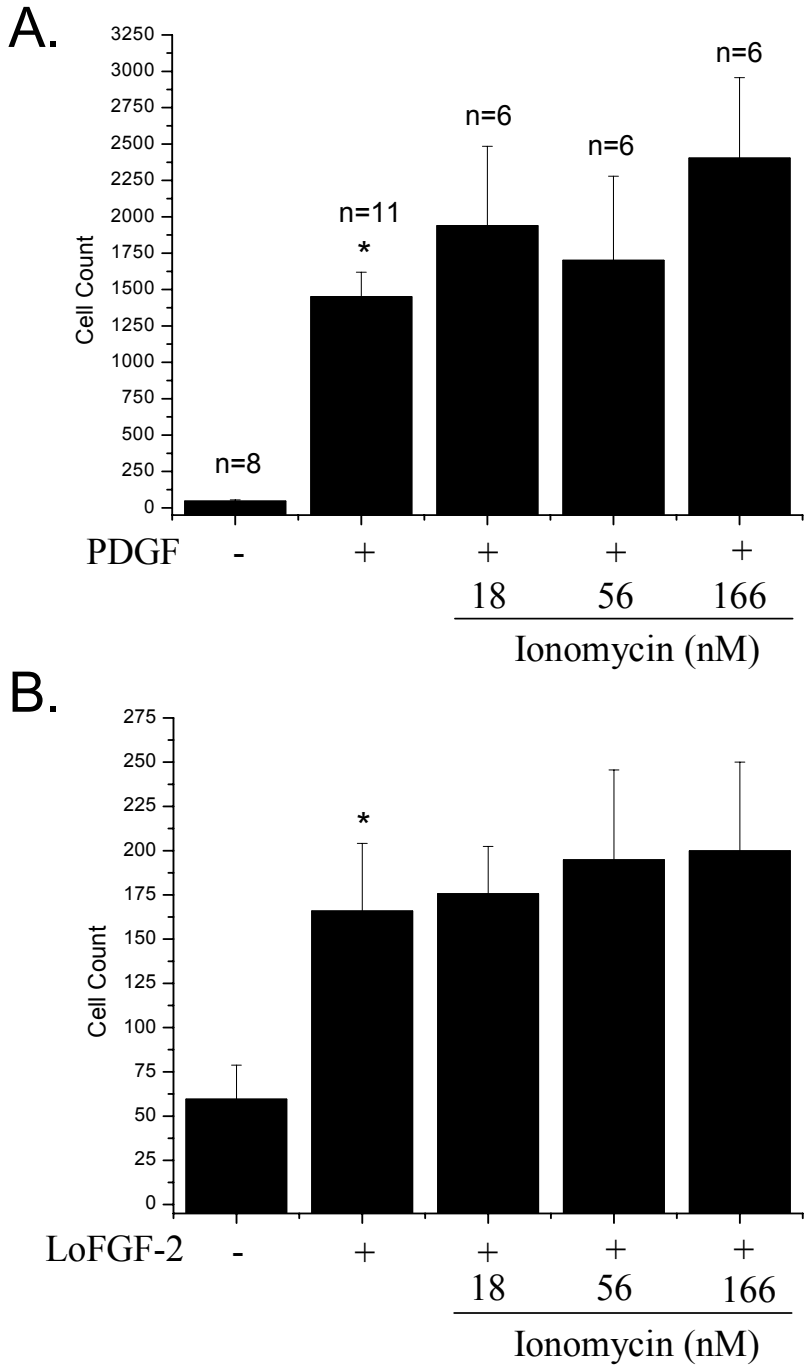

Figure 13. Effect of ionomycin treatment on motility. The effect of increasing cytosolic Ca^{2+} concentrations on cell migration with ionomycin treatment in P1 cells were analyzed with Costar Transwell apparatuses. 50 ng/ml PDGF (Panel A) or 20 ng/ml LoFGF-2 (Panel B) in serum free media was loaded into wells and specified concentrations of ionomycin and P1 myofibroblasts (2×10^5 cells/well) were loaded into inserts. Cell count is a measure of motility rate. *$p \leq 0.05$ vs. non-treated control; all data expressed as mean ± SEM.

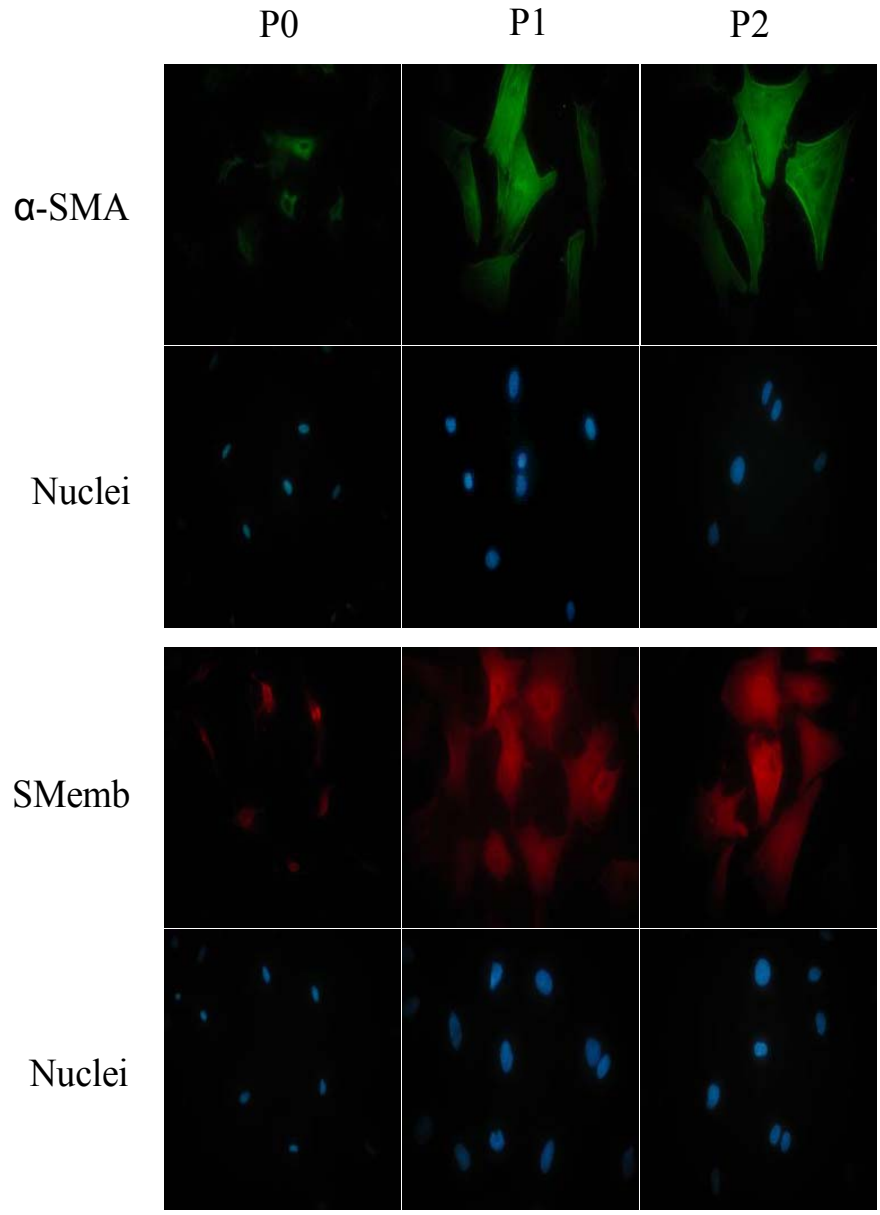

Figure 14. Effect of ionomycin stimulation on expression of αSMA and SMemb in different cell phenotypes. To determine whether increases in cytosolic Ca^{2+} concentration effect cell phenotype, freshly isolated fibroblasts (P0) and cultured myofibroblasts (P1 and P2) were stimulated with 166 nM ionomycin for 24 hours and immunostained with anti-αSMA and SMemb. Nuclei were identified by staining with Hoechst. Representative images were taken at 400x magnification and are shown from 3 separate experiments.

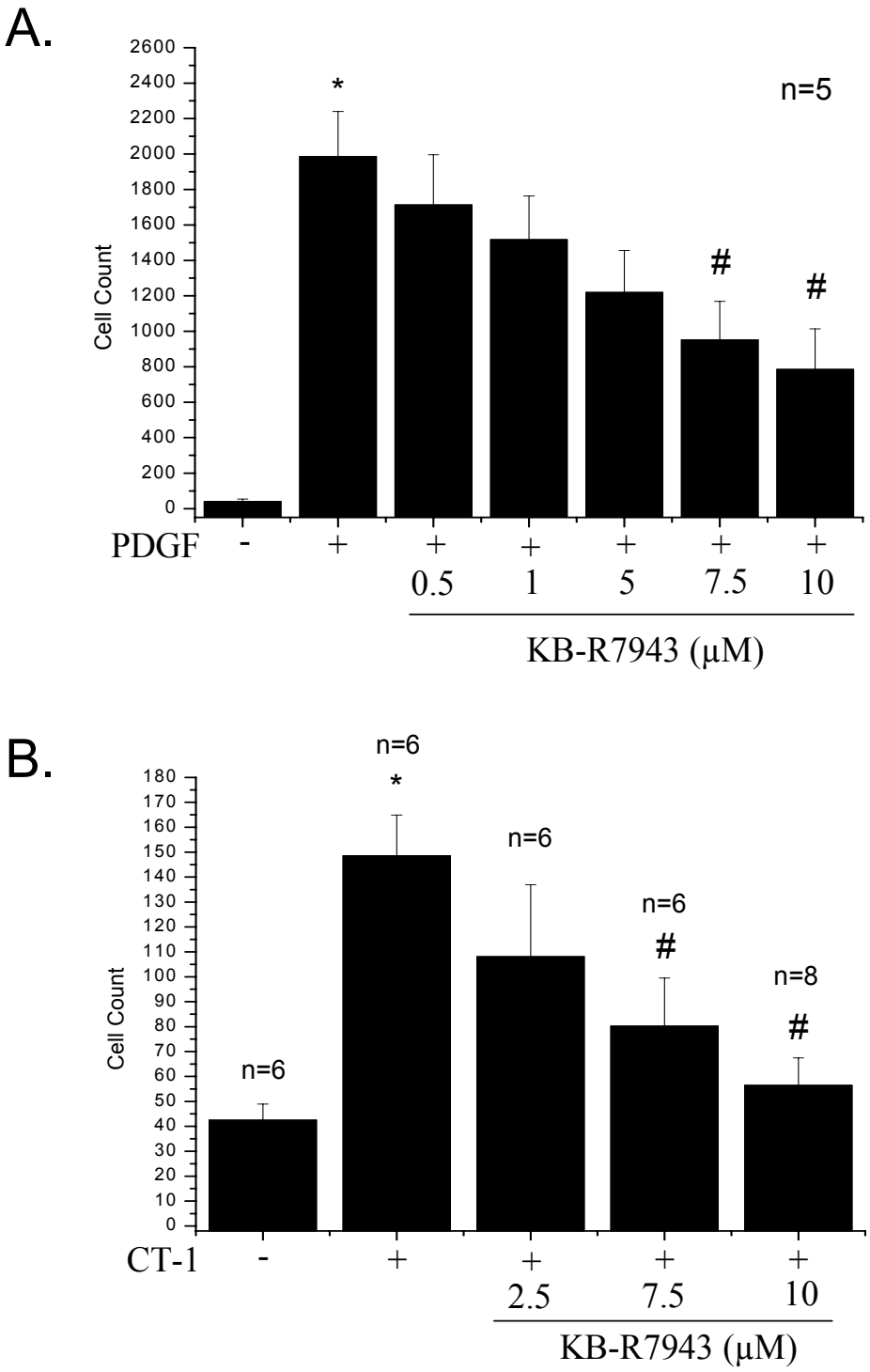

Figure 15. Motility is dependent on NCX function. The effect of NCX inhibition with KB-R7943 treatment on P1 myofibroblast motility was analyzed with Costar Transwell apparatuses. 50 ng/ml of PDGF (Panels A and C) and 10 ng/ml CT-1 (Panel B) in serum free media were loaded into lower wells while specified concentrations of KB-R7943 and ouabain (Panel C) and cardiac myofibroblasts (2 x 10^5 cells/well) were loaded into inserts. Cell count is a measure of motility rate; *$p \leq 0.05$ vs. non-treated control, #$p \leq 0.05$ vs. PDGF or CT-1 treatment; all data expressed as mean ± SEM.

C.

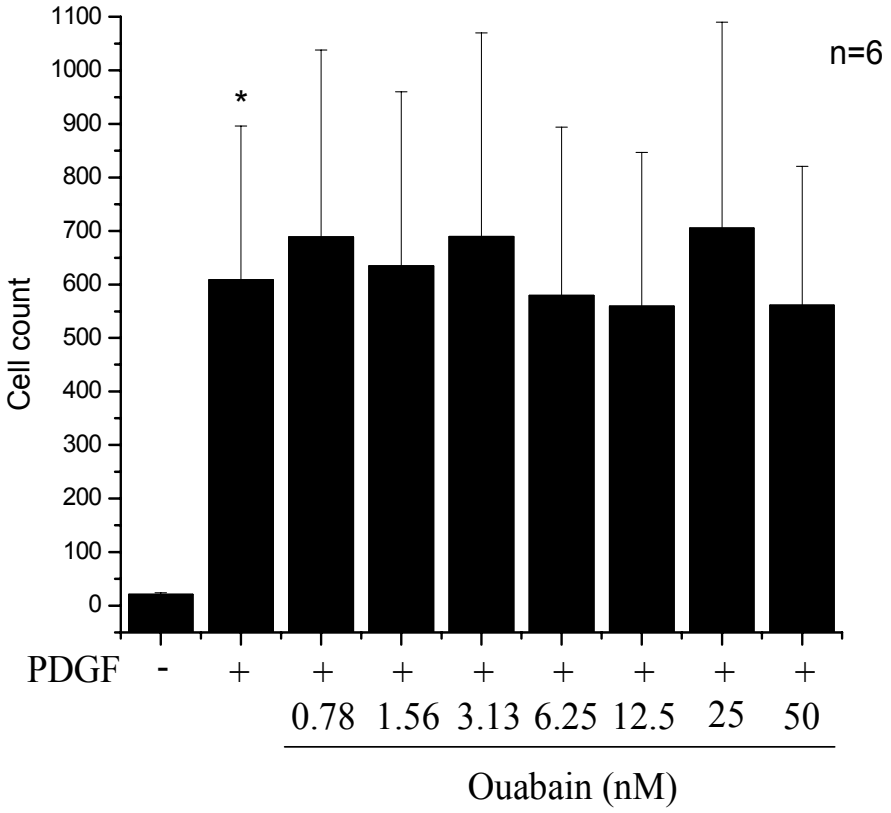
n=6
*
Cell count
1100
1000
900
800
700
600
500
400
300
200
100
0
PDGF - + + + + + + + +
0.78 1.56 3.13 6.25 12.5 25 50
Ouabain (nM)

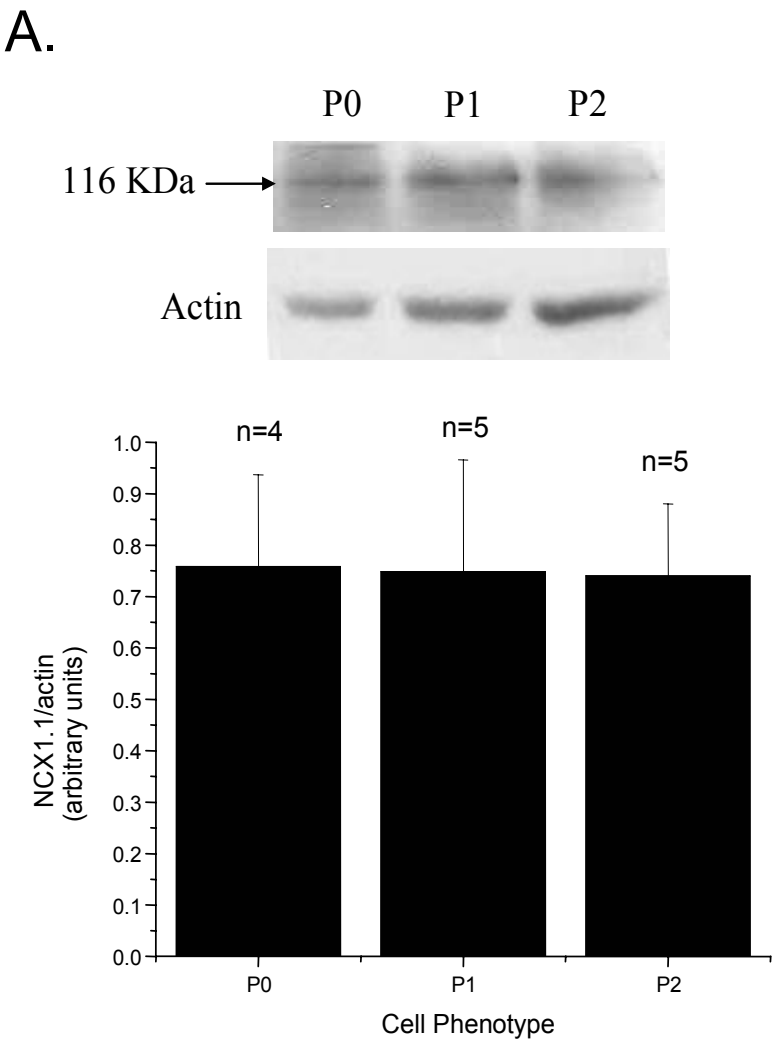

Figure 16. Effect of cytokine stimulation on expression of NCX in different cell phenotypes. NCX1.1 protein expression was analyzed by Western blot analysis and immunocytochemistry. Lysates (30 μg) from non-treated freshly isolated fibroblasts (P0) and cultured myofibroblasts (P1 and P2) were loaded into SDS-PAGE gels then immunoblotted with anti-NCX1.1 antibody (Panel A). The membrane was stripped then probed for actin. Samples from separate animals were quantified and band intensity is expressed relative to actin in arbitrary units (mean ± SEM). P0, P1, and P2 cells were stimulated with 50 ng/ml PDGF (Panel C), 20 ng/ml LoFGF-2 (Panel D), 10 ng/ml TGFβ1 (Panel E), and 10 ng/ml CT-1 (Panel F) for 24 hours and immunostained with anti-NCX1.1. Endogenous expression in non treated cells was also determined (Panel B). Nuclei were identified by staining with Hoechst. Representative images are shown from 3 separate experiments and were taken in oil immersion at 1000x magnification.

B.

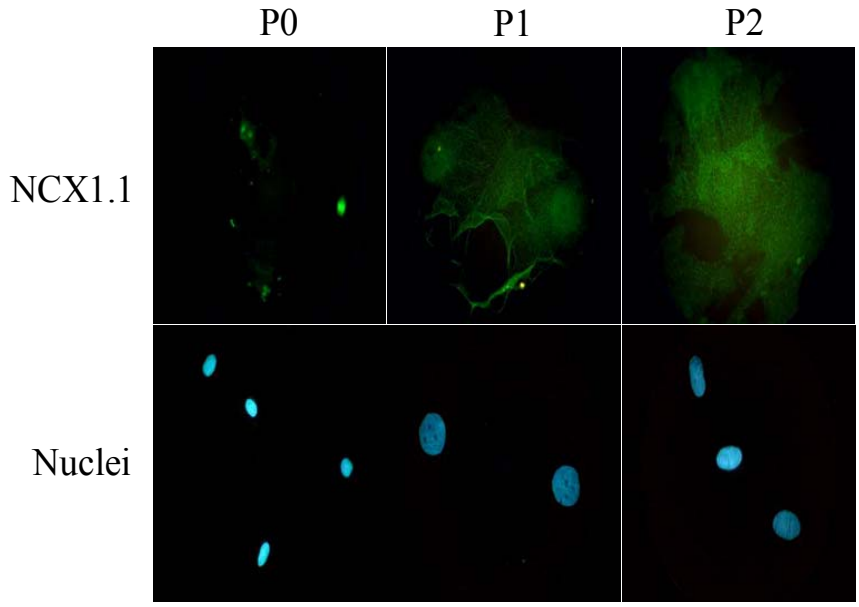

Non-treated

C.

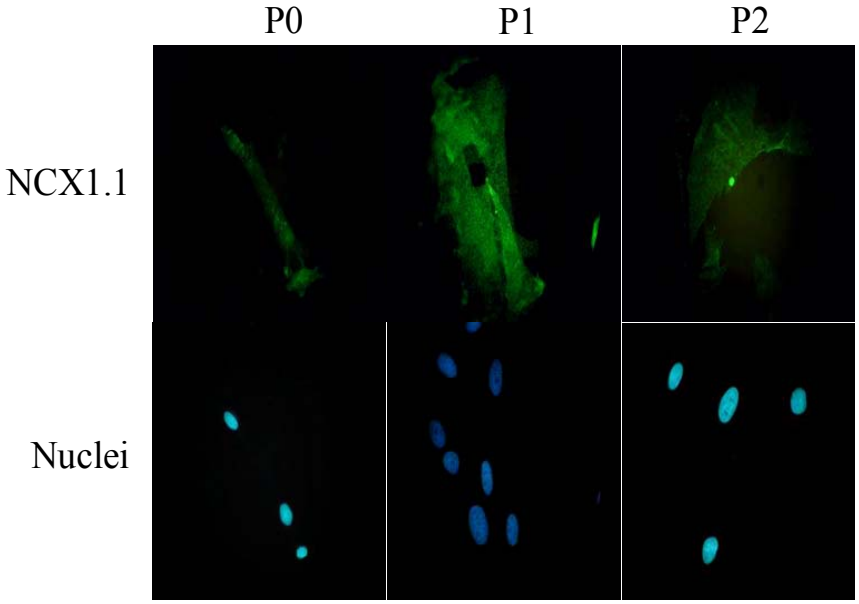

50 ng/ml PDGF treatment

D.

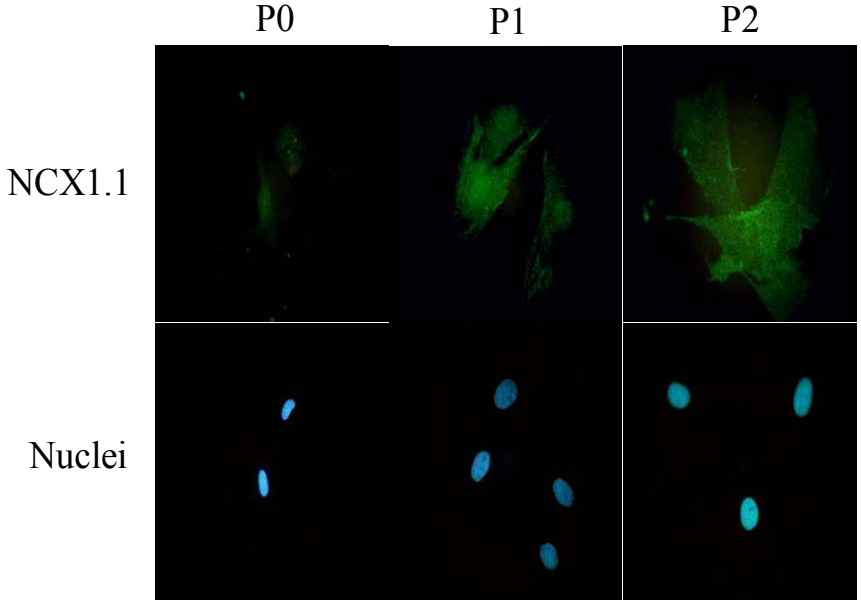

20 ng/ml LoFGF-2 treatment

E.

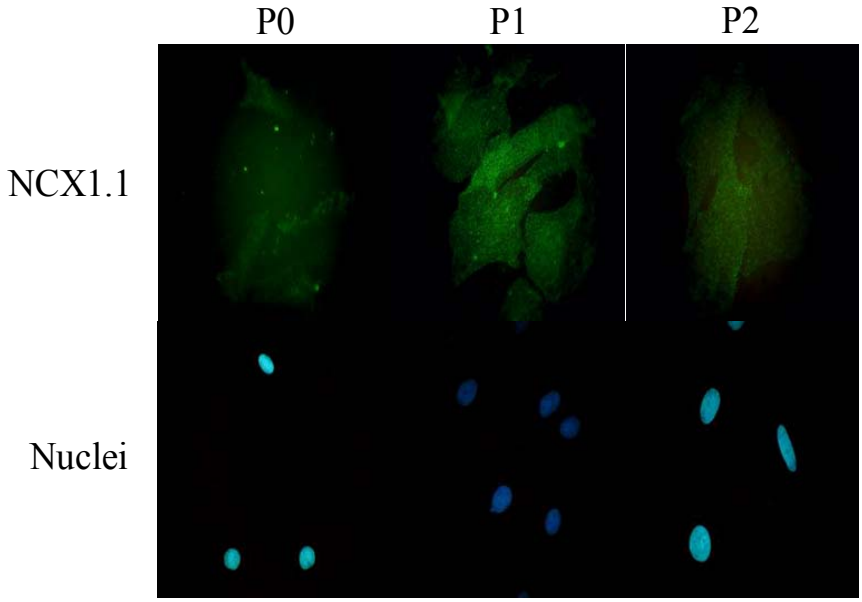

10 ng/ml TGFβ1 treatment

F.

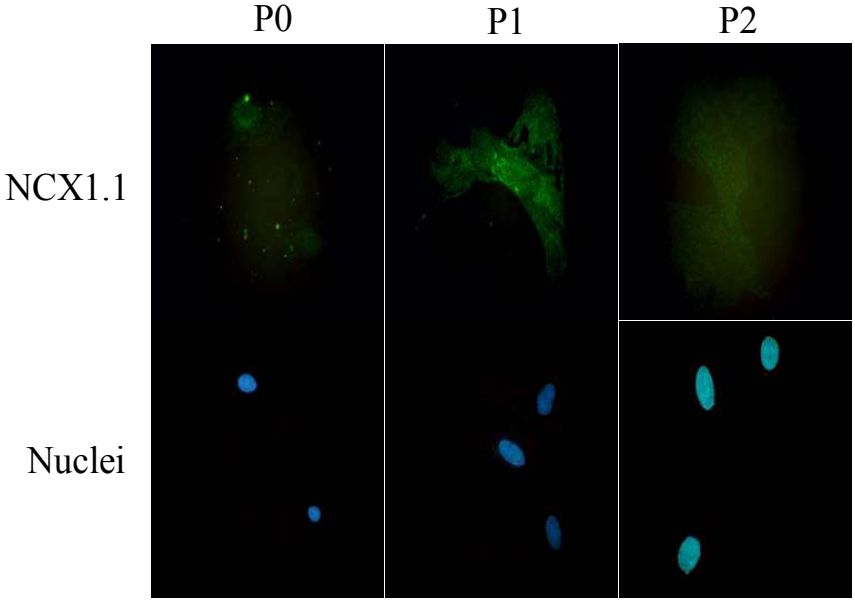

10 ng/ml CT-1 treatment

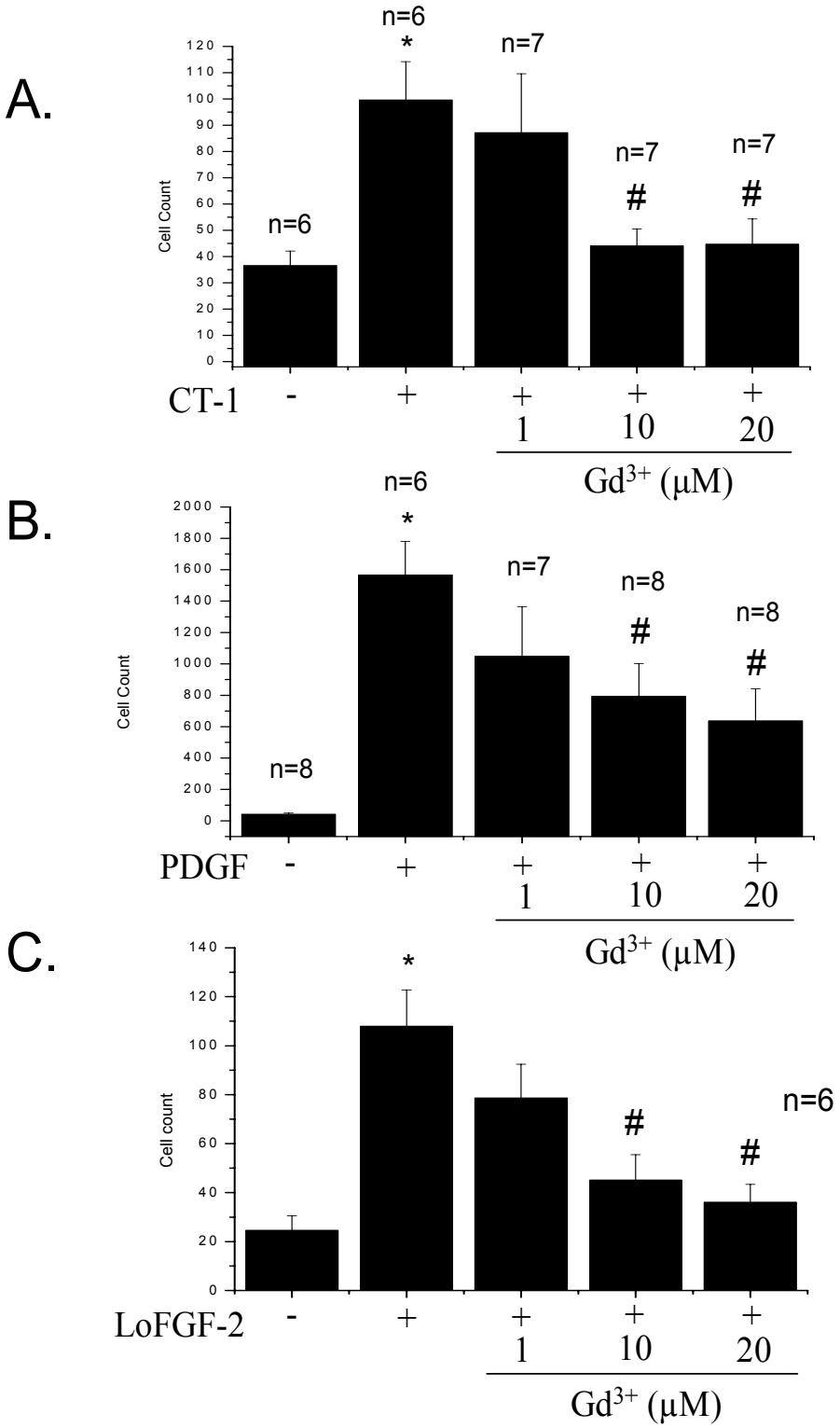

Figure 17. Motility is dependent on NSCC function. The effect of NSCC blockade with Gd^{3+} treatment on P1 myofibroblast motility was analyzed with Costar Transwell apparatuses. 10 ng/ml of CT-1 (Panel A), 50 ng/ml PDGF (Panel B), and 20 ng/ml LoFGF-2 in serum free media were loaded into lower wells while specified concentrations of Gd^{3+} and cardiac myofibroblasts (2 x 10^5 cells/well) were loaded into inserts. Cell count is a measure of motility rate; *p≤0.05 vs. non-treated control, #p≤0.05 vs. CT-1, PDGF or LoFGF-2 control; all data expressed as mean ± SEM.

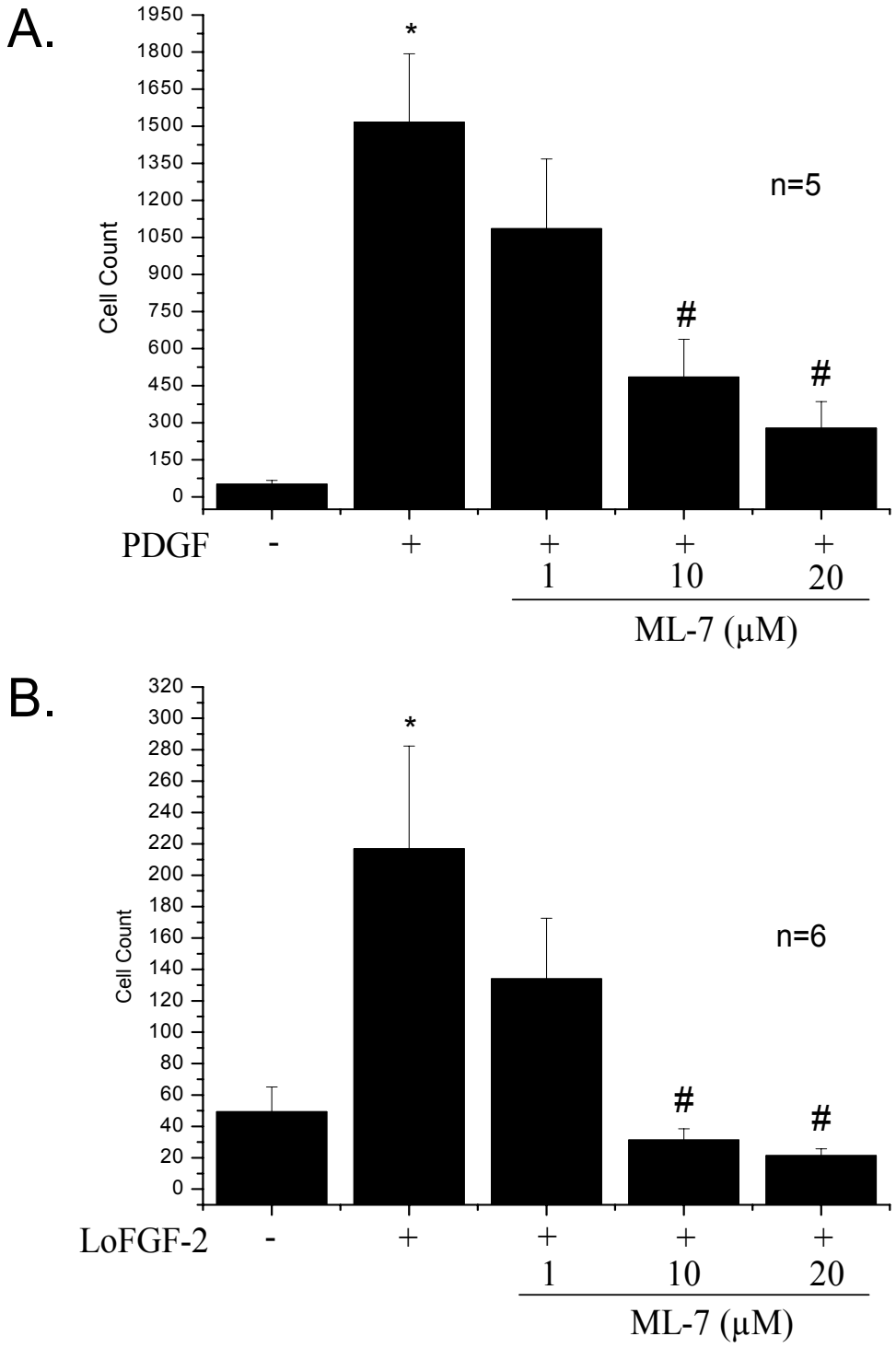

Figure 18. Motility is dependent on myosin light chain kinase activity. The effect of MLCK inhibition with ML-7 on P1 myofibroblast motility was analyzed with Costar Transwell apparatuses. 50 ng/ml PDGF (Panel A) or 20 ng/ml LoFGF-2 (Panel B) in serum free media was loaded into lower wells while specified concentrations of ML-7 and cardiac myofibroblasts (2 x 10^5 cells/well) were loaded into inserts. Cell count is a measure of motility rate; *p≤0.05 vs. non-treated control, #p≤0.05 vs. PDGF or LoFGF-2 control; all data expressed as mean ± SEM.

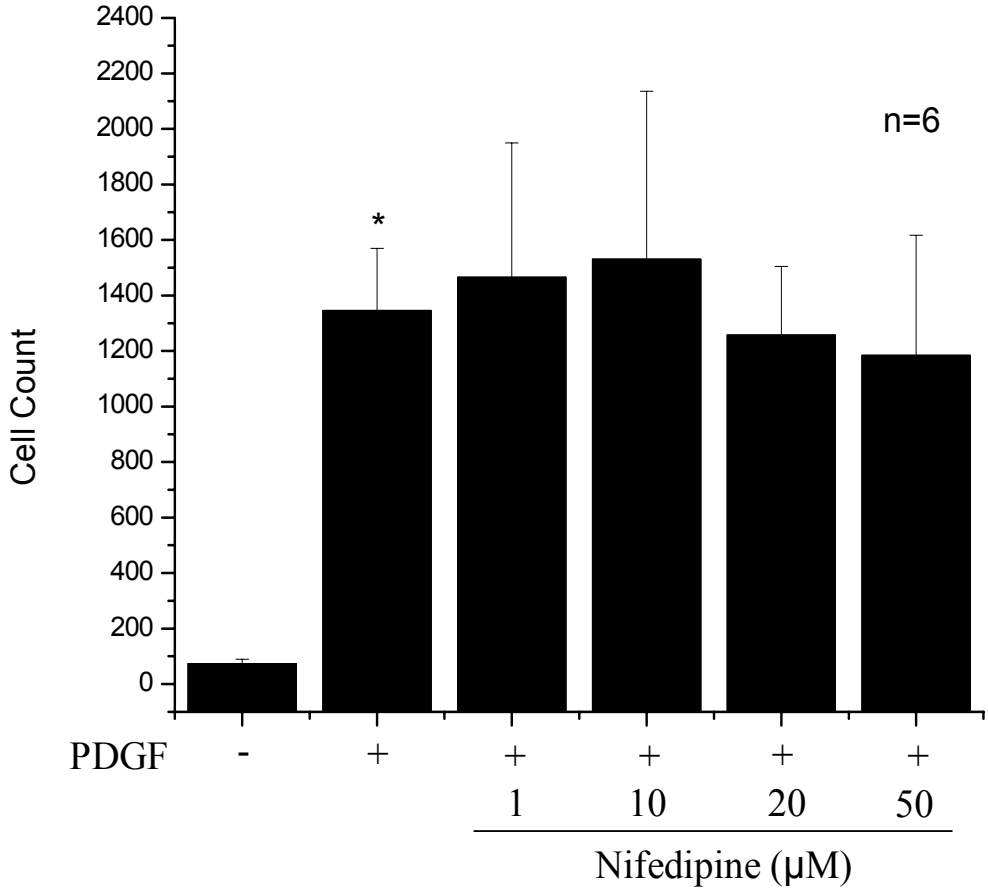

Figure 19. L-type Ca^{2+} channel blockade has no effect on cell motility. The effect of L-type Ca^{2+} channel blockade with nifedipine on P1 myofibroblast motility was analyzed with Costar Transwell apparatuses. 50 ng/ml of PDGF (Panel A) in serum free media was loaded into lower wells while specified concentrations of nifedipine and cardiac myofibroblasts (2 x 10^5 cells/well) were loaded into inserts. Cell count is a measure of motility rate; *p≤0.05 vs. non-treated control, #p≤0.05 vs. PDGF or LoFGF-2 control; all data expressed as mean ± SEM.

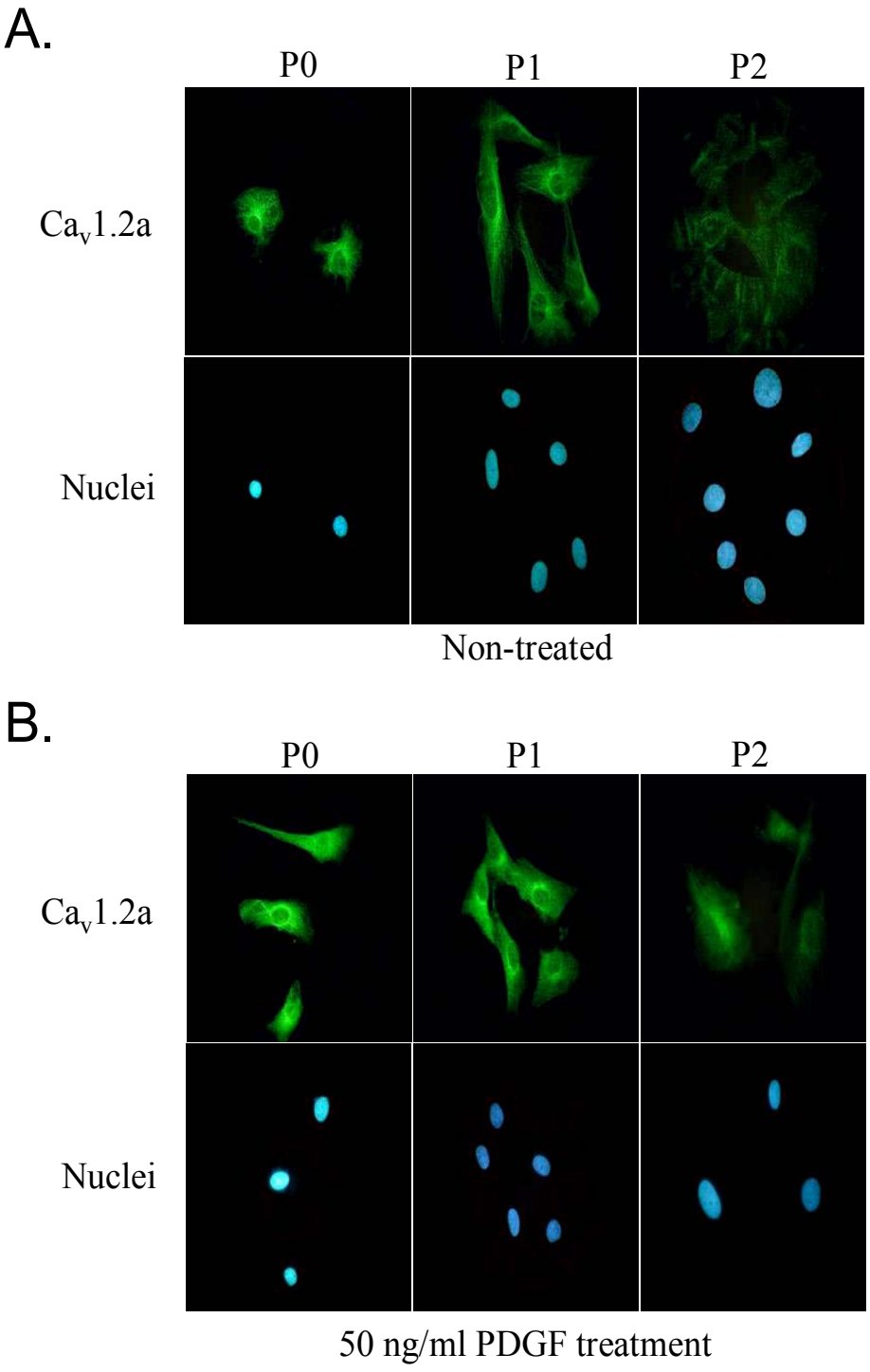

Figure 20. Effect of cytokine stimulation on expression of $Ca_v1.2a$ in different cell phenotypes. P0, P1, and P2 cells were stimulated with 50 ng/ml PDGF (Panel B), 20 ng/ml LoFGF-2 (Panel C), 10 ng/ml TGFβ1 (Panel D), or 10 ng/ml CT-1 (Panel E) for 24 hours and immunostained with anti- $Ca_v1.2a$. Endogenous expression in non-treated cells was also determined (Panel A). Nuclei were identified by staining with Hoechst. Representative images are shown from 3 separate experiments and were taken in oil immersion at 1000x magnification.

C.

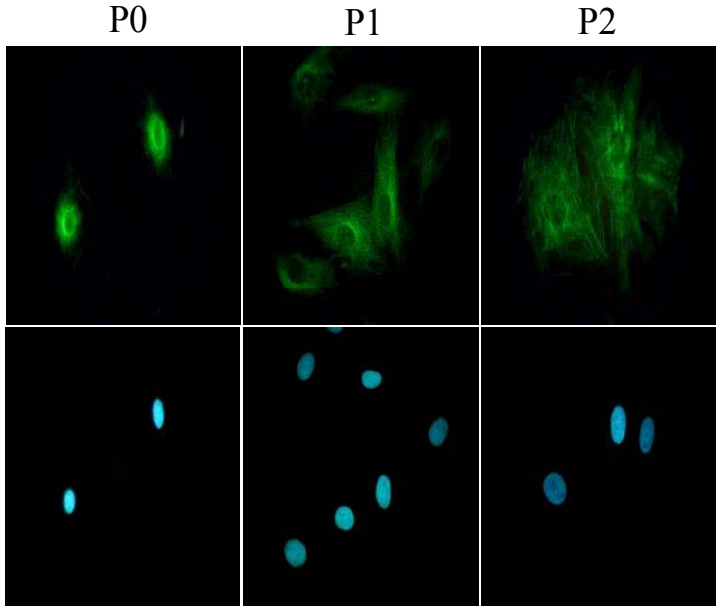

20 ng/ml LoFGF-2 treatment

D.

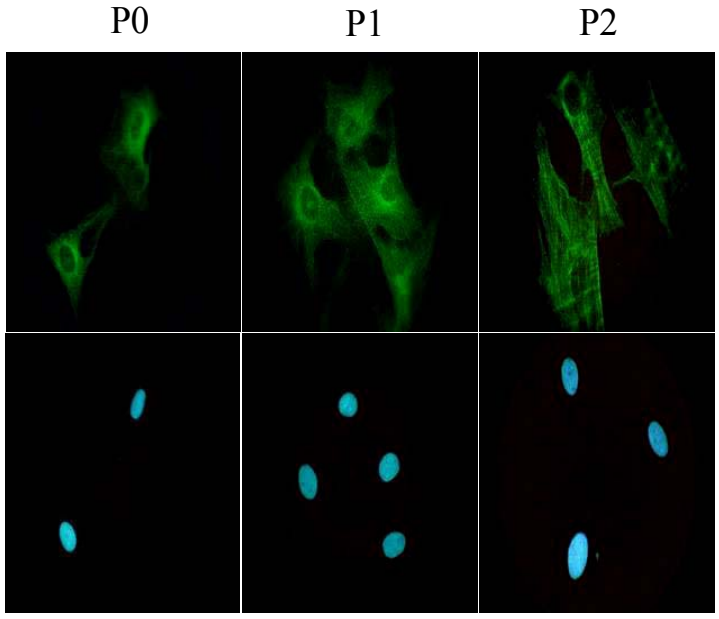

10 ng/ml TGFβ1 treatment

E.

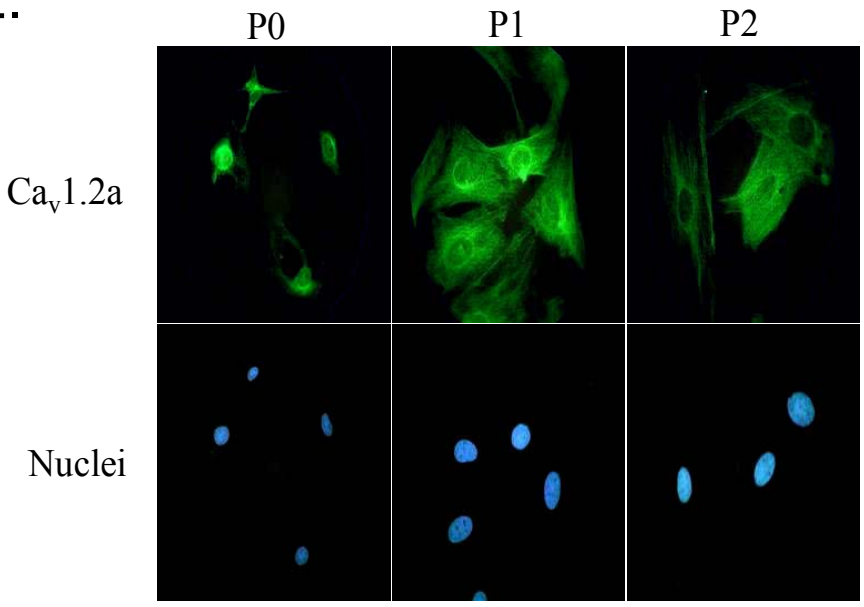

10 ng/ml CT-1 treatment

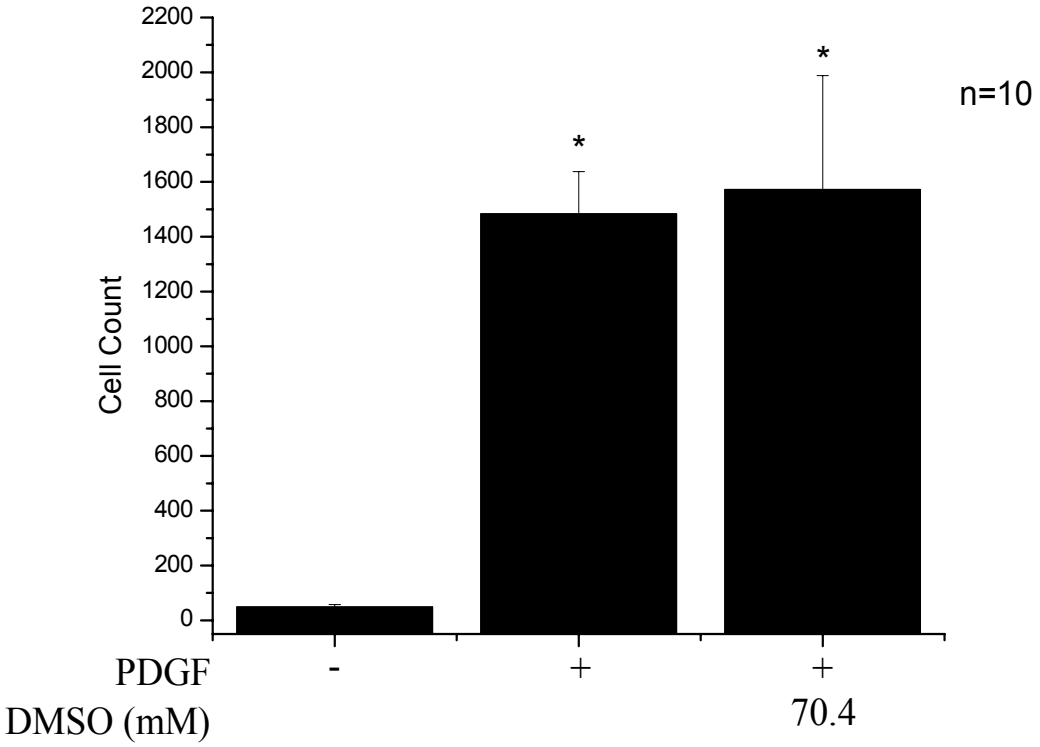

Figure 21. DMSO does not affect PDGF-induced motility. The effect of DMSO treatment on P1 cells was analyzed with Costar Transwell apparatuses. 50 ng/ml PDGF in serum free media was loaded into wells and 70.4 mM DMSO (0.5% v:v) and P1 myofibroblasts (2 x 10^5 cells/well) were loaded into inserts. Cell count is a measure of motility rate. *$p \leq 0.05$ vs. non-treated control; all data expressed as mean ± SEM.

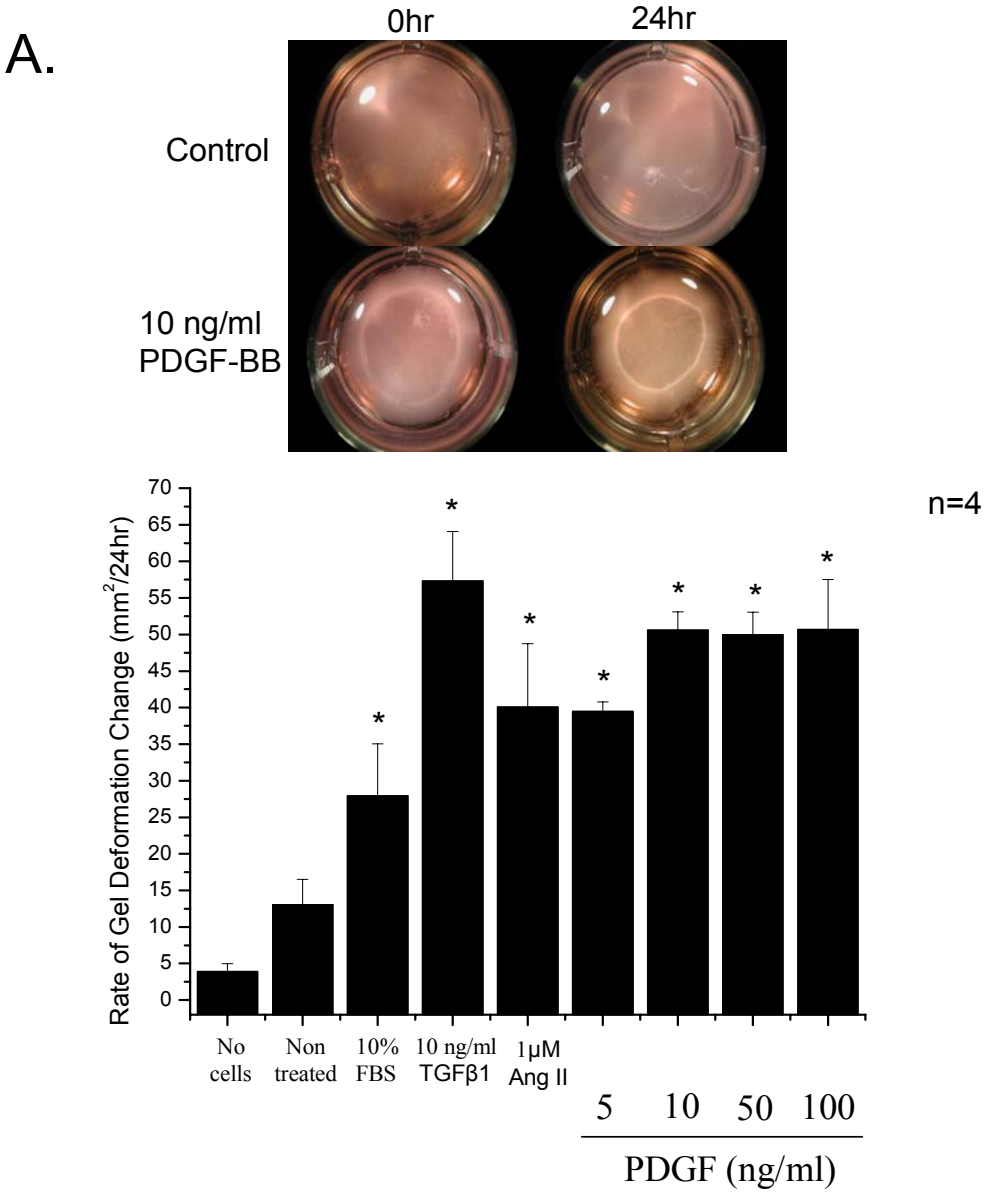

Figure 22. PDGF induced-contractile responses are dependent on transplasmalemmal Ca^{2+} flux. Collagen gel deformation assays were used to determine contractile responses in P1 myofibroblasts after 24 hour treatments. After rendered quiescent, cells (1 x 10^5 cells/well) were treated on pre-formed collagen type I gels with specified concentrations PDGF to determine optimal cell response (Panel A). Representative gel images show untreated control or PDGF (10 ng/ml) treated cells at 0 and 24 hr after stimulation. In a separate experiment, quiescent cells were treated with specified concentrations of EGTA, KB-R7943 (KBR), ML-7, and nifedipine (Panel B), and Gd^{3+} (Panel C). Digital images were measured with Measure Gel computer software. Contractile responses are expressed as gel deformation rate which refers to changes in gel surface area over the 24 hour treatment period. *p≤0.001 vs. non-treated control, #p≤0.001 vs. PDGF control; all data expressed as mean ± SEM.

B.

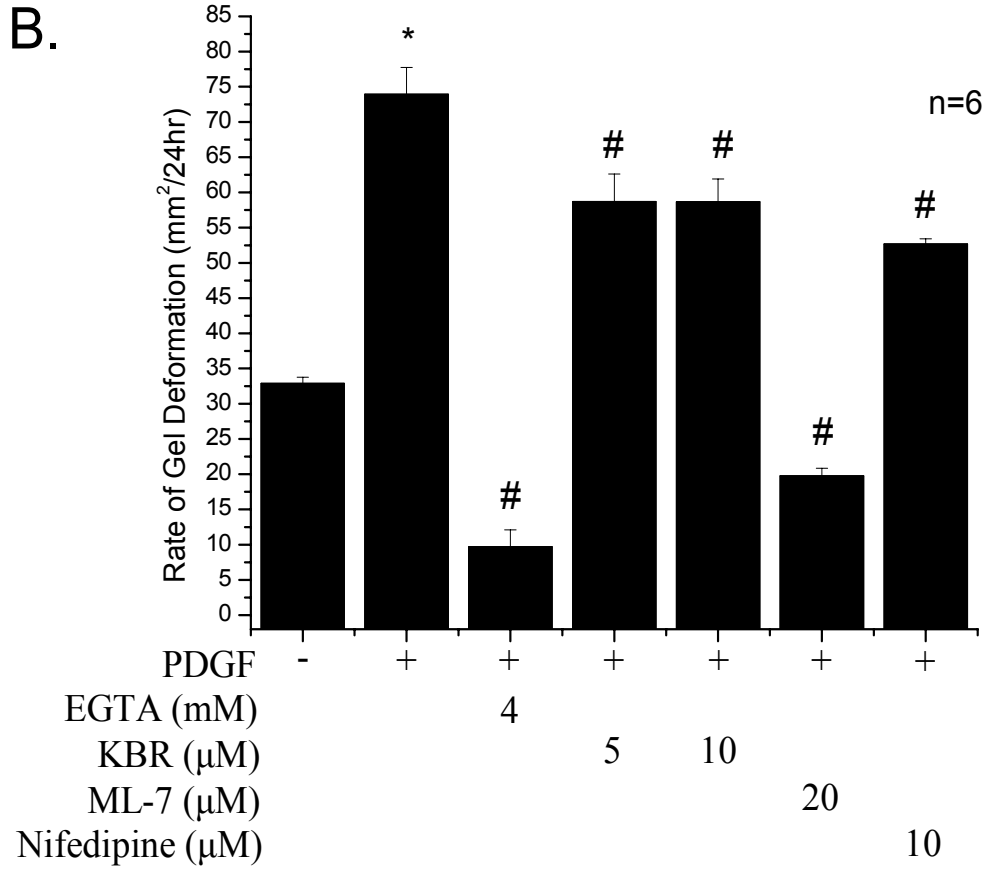
Rate of Gel Deformation (mm²/24hr)
n=6
*
#
#
#
#
PDGF - + + + + + +
EGTA (mM) 4
KBR (μM) 5 10
ML-7 (μM) 20
Nifedipine (μM) 10

C.

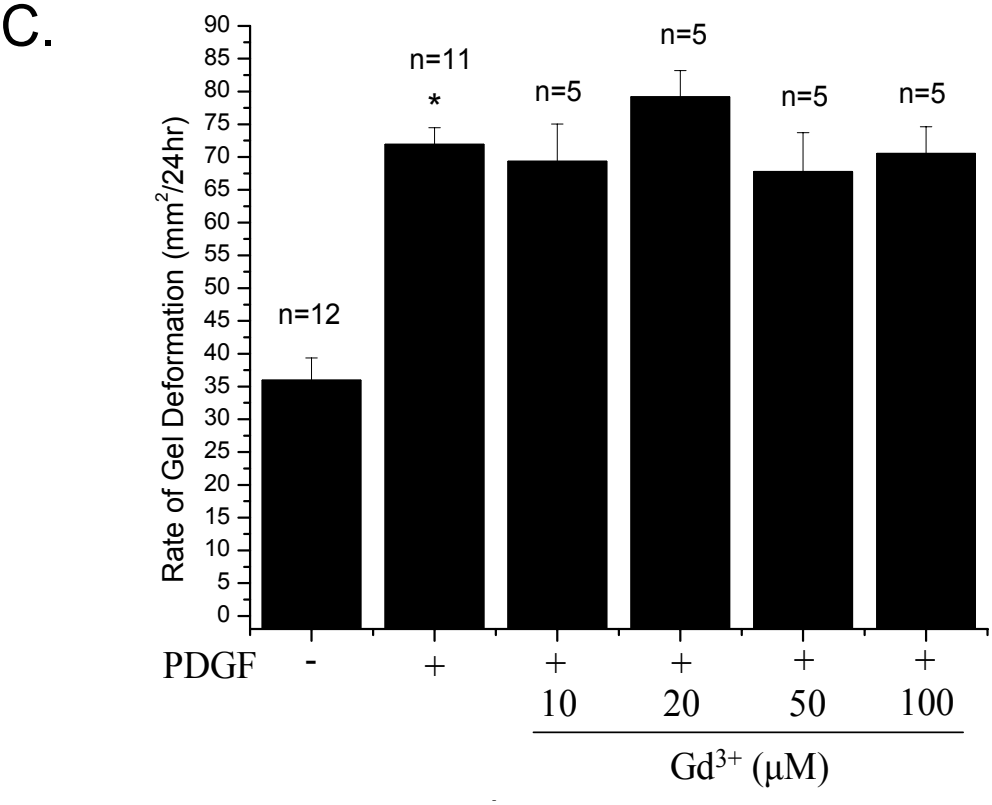
Rate of Gel Deformation (mm²/24hr)
n=12
n=11
*
n=5
n=5
n=5
n=5
PDGF - + + + + +
10 20 50 100
Gd3+ (μM)

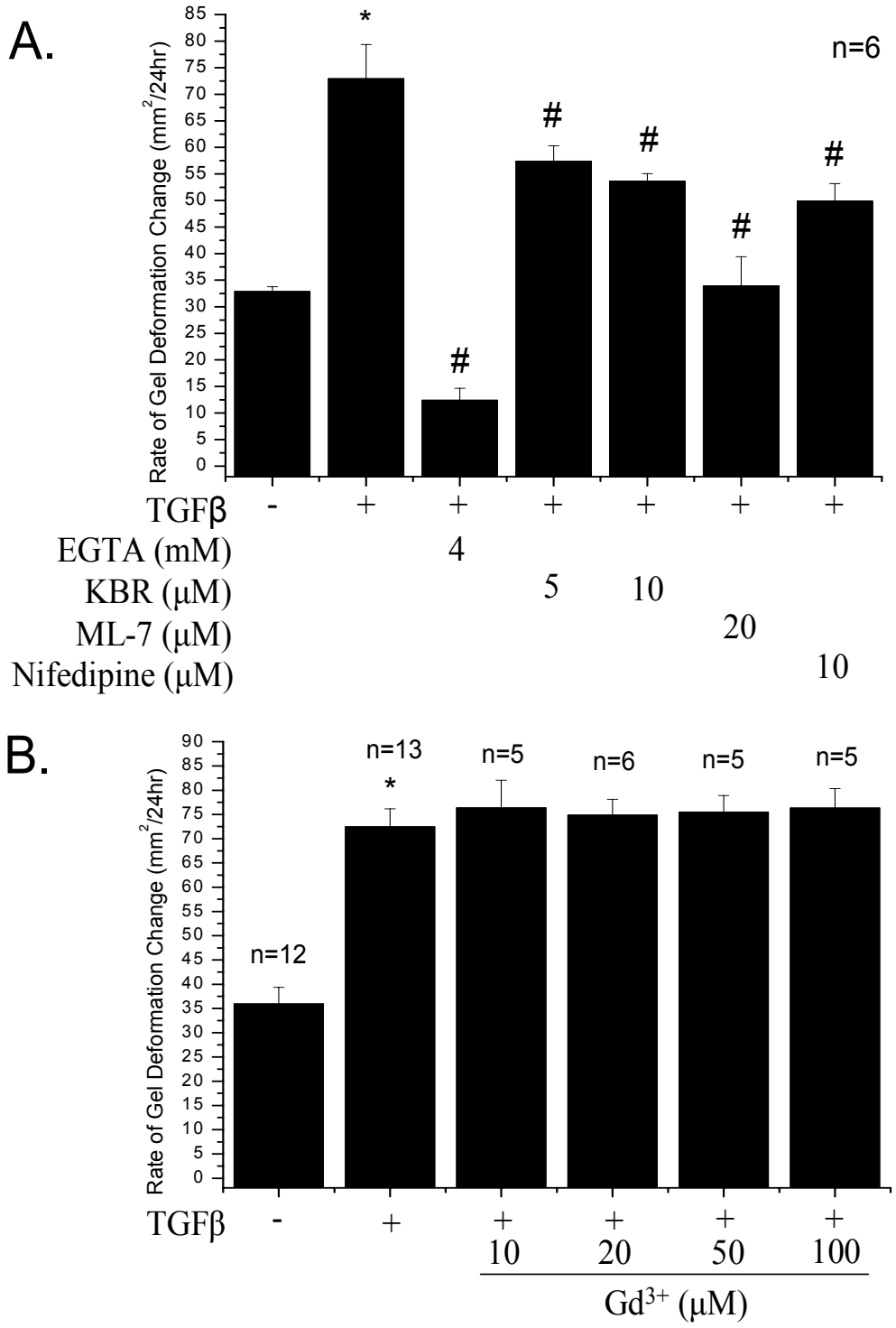

Figure 23. TGFβ1 induced-contractile responses are dependent on transplasmalemmal Ca^{2+} flux. Collagen gel deformation assays were used to determine contractile responses in P1 myofibroblasts. After being rendered quiescent, cells (1 x 10^5 cells/well) were treated on pre-formed collagen type I gels with 10 ng/ml TGFβ1 and EGTA, KB-R7943 (KBR), and nifedipine (Panel A) and Gd^{3+} (Panel B) at specified concentrations for 24 hours. Digital images were measured with Measure Gel computer IDL software. Contractile responses are expressed as gel deformation rate which refers to changes in gel surface area over the 24 hour treatment period; *p≤0.001 vs. non-treated control, #p≤0.001 vs. TGFβ1 control; all data expressed as mean ±

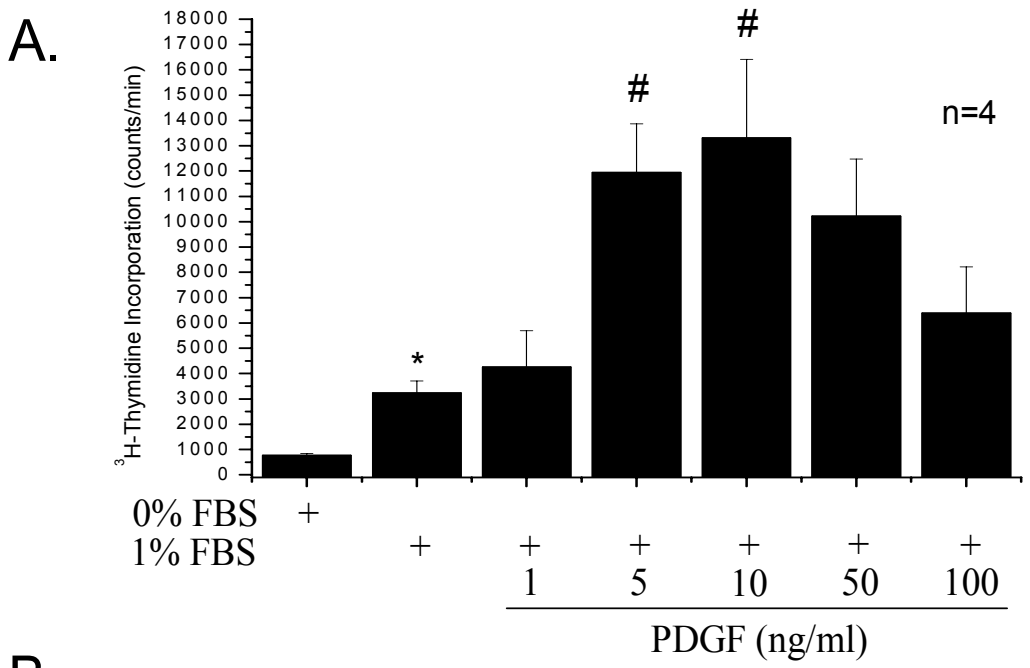

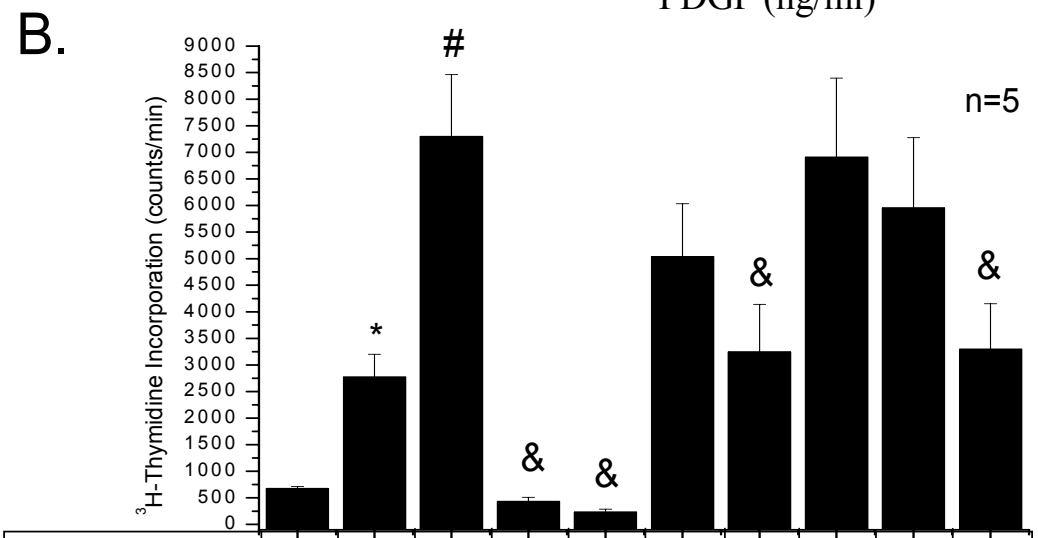

0% FBS	+									
1% FBS		+	+	+	+	+	+	+	+	+
PDGF			+	+	+	+	+	+	+	+
EGTA (mM)				3	4					
KBR (μM)						5	10			
Gd^{3+} (μM)								10	20	
Nifedipine (μM)										10

Figure 24. PDGF induced-proliferation is dependent on transplasmalemmal Ca^{2+} flux. Incorporation of ^{3}H-thymidine into P1 cardiac myofibroblast DNA was used to determine rate of cell proliferation. After being rendered quiescent, cells were treated in the presence of 1% FBS with specified concentrations of PDGF to determine optimal cell response (Panel A). In a separate experiment quiescent cells were treated with 10 ng/ml PDGF, EGTA, KB-R7943 (KBR), Gd^{3+} and nifedipine (Panel B) for 24 hours; *p≤0.05 vs. non-treated control, #p≤0.05 vs. 1% FBS control, &p≤0.05 vs. PDGF control; all data expressed as mean ± SEM.

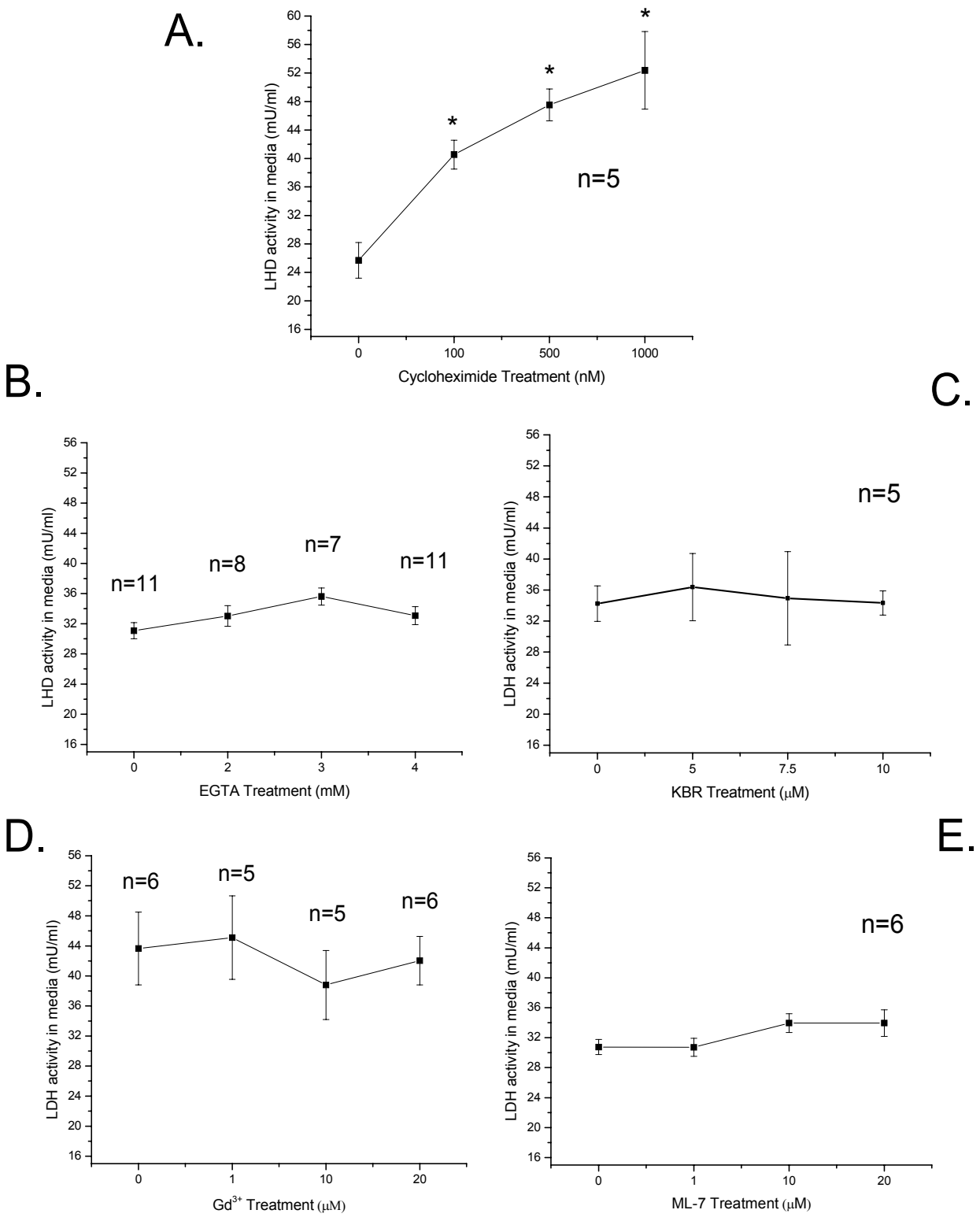

Figure 25. LDH as a measure of cytotoxicity. LDH activity was measured in cells (2 x 10^5) incubated with specified concentrations of cycloheximide (Panel A), EGTA (Panel B), KB-R7943 (Panel C), Gd^{3+} (Panel D), and ML-7 (Panel E) for 24 hours. *$p \leq 0.05$ vs. non-treated control; all data expressed as mean ± SEM.

V1 DISCUSSION

Ca^{2+} is an important intracellular second messenger and modulates a wide range of physiological processes including cell function in the myocardium. Cardiac fibroblasts and myofibroblasts are major players in cardiac wound healing and ventricular matrix remodeling, and are the principle cellular sources of collagen secretion. Fibroblast and myofibroblast motility e.g. a cyclical process involving coordinated cellular movement in response to increasing gradients of chemokines, contraction e.g. isometric force exerted by the cell on the extracellular environement resulting in matrix reorganization, and proliferation aid in healing the infarct site. Although the nature of Ca^{2+} regulation in other mesodermal derived cell types such as endothelial cells have been studied (415-417), Ca^{2+} handling in cardiac myofibroblast is unexplored. Furthermore, as hypersynthetic myofibroblast cells predominate in many conditions that lead to heart failure, we sought a better understanding of myofibroblast pathophysiology. Our hypothesis states that $[Ca^{2+}]_o$ modulates cardiac myofibroblast motility, and we investigated whether pharmacologic inhibition of NCX1.1 was effective in disrupting this process. As Ca^{2+} handling in cardiac myofibroblasts is poorly understood our first aim was to characterize proposed modes of Ca^{2+} flux. We compared the effects of PDGF-BB to other cytokines including CT-1 and FGF-2. These cytokines are recognized for participation in cardiac wound healing. We found that P0 fibroblasts exhibit relatively high motility when compared to αSMA and SMemb positive myofibroblasts. NCX1.1 has been well studied in cardiomyocytes but virtually no information is available for NCX function in myofibroblasts. For the first time we report that NCX1.1 function plays a role in cardiac myofibroblast motility, as well as in proliferative and contractile responses of these cells. Only one paper to date describes the effect of NCX blockade using KB-R7943 in Madin-Darby canine kidney cellular motility (56). Further we found that gadolinium (Gd^{3+}) blockade of NSCCs was associated only with attenuated cell motility, and that L-type Ca^{2+} channel blockade with nidedipine is involved in contraction and proliferation but not motility. We also demonstrate that activation of Ca^{2+}-dependent MLCK is linked to chemotaxis and cell contraction, and suggests a secondary role for $[Ca^{2+}]_i$ in activation of contractile machinery. We demonstrate that PDGF-BB dependent motility is associated with receptor activation and taken together with KB-R7943 and Gd^{3+}- sensitive motility in the presence of PDGF-BB, we provide evidence that NCX1.1 and NSCCs play key roles in these cellular processes.

The link between cytokines, cell motility, contraction and proliferation in the infarcted myocardium

Cardiac myofibroblast motility, contraction, and proliferation are activated at various stages during myocardial tissue injury and myocyte death (5). Fibroblast chemotaxis to the infarct site helps to restore *cellularity* to the infarct scar zone (10). However, over time fibroblast function is implicated in gross ventricular structural and humoral changes. The current results validate our previous work that cardiac myofibroblasts are motile, contractile, and proliferative (192, 196, 418). We determined that PDGF-BB, CT-1, and LoFGF-2 stimulate significant dose-dependent increases in cardiac myofibroblast motility, likely via cell surface receptor activation. We found incubation of myofibroblasts with AG1296, a PDGF-BB tyrosine receptor inhibitor, resulted in reduction in cell motility, suggesting that ligand binding of PDGF-BB activates downstream signals responsible for this process. Many cytokines and growth factors are pleiotrophic. We observed that while PDGF-BB is a potent chemokine, it also stimulates cardiac myofibroblast contraction as measured by collagen gel deformation. Past work from our lab demonstrated activation of PDGF-BB receptors in contractile responses of myofibroblasts (419). We also confirmed that PDGF-BB is a strong mitogen for myofibroblasts, as PDGF-BB induced significant incorporation of ^{3}H-thymidine into DNA. Though TGFβ1 is found to down-regulate proliferation in cardiac myofibroblasts (data not shown), it was also found to augment contractile responses.

Myofibroblast contraction is an important aspect of cardiac wound healing (22). During acute wound healing myofibroblast contraction aids in closure of the denuded edged of the wound, yet continual contraction contributes to hypertrophic scar formation in the chronic phase (106, 131). Collagen gel deformation assays resemble the an environment of the infarct scar *in vivo*, and therefore provide a reliable means to study myofibroblast contraction function *in vitro* (131, 295, 418). We used the anchored collagen type I method to resemble the latter stages of wound healing, which is most reflective of cardiac myofibroblast contraction (106). Tractional forces exerted by cells are isometric resulting in reorganization of collagen fibres (311). Following 24 hours of treatment, effects of mechanical tension exerted by myofibroblasts to the collagen matrix are clearly observed as the top layer of the lattice compressed inwards in a symmetrical fashion. As myofibroblasts are known to develop tension along lines of stress *in vitro* and *in vivo* (312), we suggest that myofibroblasts are synchronously contracting and

providing sufficient tractional forces to remodel the collagen lattice as is the case *in vivo*. We studied myofibroblast contraction in collagen gel deformation assays in previous investigations (418, 419) and have determined that cells remain situated on the surface of the gel rather than becoming imbedded in the collagen lattice (419). This finding may explain the fact that myofibroblast-seeded gels only partly compress inwards and that this compression is limited to the top half of the gel where the cells are originally seeded.

Data from our lab has shown (using a rat chronic MI model) that elevated expression of CT-1 in the infarct zone occurs as early as 24 hours and remains high up to 8 weeks post-MI (196). In separate *in vitro* work, CT-1 induced activation of the JAK/STAT pathway is linked to significant migration and proliferation in cultured cardiac myofibroblasts (10, 196). Using Costar Transwell apparatuses we confirmed the finding that 10 ng/ml CT-1 is a sufficient chemoattractant for rat cardiac myofibroblasts. As CT-1 stimulates myofibroblast migration and proliferation we speculate that expression in the infarct zone is beneficial in the acute stages of wound healing by providing signals necessary for repopulating and maintaining the cellularity of the infarct scar (10). Moreover, although CT-1 is a modest mitogen for cardiac fibroblasts (196), previous results from our lab demonstrated that CT-1 stimulation has no effect on myofibroblasts contraction (419). Mature collagen synthesis in media of cultured cardiac myofibroblasts is reduced in the presence of CT-1 (10), while CT-1 protects both cardiomyocytes (207), and the myocardium (205) from ischemia/reperfusion injury. Taken together these results support our hypothesis that CT-1 may oppose the pro-fibrotic effects of other cytokines such as TGFβ1 and PDGF-BB, thus supporting the role of CT-1 as a cardioprotectant by modulating excessive ECM remodelling and growth. However, its role in cardiac wound repair and as an anti-fibrotic agent still remains unclear and this necessitates further research.

PDGF-BB is well known for its potent chemotactic and mitogenic effects and its ability to induce contraction in fibroblasts. We demonstrated that in the presence of PDGF-BB, cardiac myofibroblasts are highly motile. This response is receptor dependent as treatment with AG1296, a selective PDGFRβ inhibitor, attenuated PDGF-BB induced cardiac myofibroblast migration. Previous findings show that PDGF-BB induced potent chemotactic responses in fetal skin fibroblasts (420) and vascular smooth muscle cells (421-423). We also demonstrate that PDGF-BB is a potent mitogen for cardiac myofibroblasts, and that PDGF-BB (along with TGFβ1) induces potent deformation of collagen gel assays. Our proliferation results are validated by

previous findings for PDGF-BB as a mitogen (27, 162, 424) in fibroblasts and vascular smooth muscle cells, and that PDGF-BB (425-427), TGFβ1 (425, 427, 428) and AngII (425, 429, 430) are all stimulators of fibroblast mediated contraction of collagen gels. Elevated levels of PDGF-BB are found in serum of post-MI and stable angina patients (28) while TGFβ1 is elevated in the chronic phase of myocardial infarct scar healing (93). PDGF-BB is implicated in the pathogenesis of atherosclerosis (26) where it is released from aggregating platelets and monocytes which gather around sites of arterial injury (86). Recently, microparticles containing molecules of PDGF-BB were reported to induce angiogenesis and stimulate post-ischemic revascularization both *in vitro* and *in vivo* (431). As PDGF-BB plays a role in regulating replication, survival and migration of myofibroblasts during the pathogenesis of fibrotic diseases (29) our result that PDGF-BB induces cardiac myofibroblast motility, contraction and proliferation confirms that elevated levels of PDGF-BB in the infarcted myocardium may contribute to repopulation of the infarct scar and aid in the healing process. TGFβ1 is critical in cardiac matrix remodelling, collagen synthesis by non-myocytes, tissue repair, and plays a role in cardiac myofibroblast phenotypic transdifferentiation. FGF-2 (432) and TNF-α (433) are also expressed during wound healing. FGF-2 plays a role in smooth muscle cell migration after arterial injury and induces chemotactic responses in these cells *in vitro* (253, 434). LoFGF-2 represents the 18kDa isoform with mRNA initiation occurring at the AUG start site (32). Although LoFGF-2 is widely recognized as a potent stimulator of cell migration in vascular endothelial cells and a major angiogenic factor for new capillary development (32, 435), no information is known about its chemotactic functions in cardiac myofibroblasts. Our results demonstrate that LoFGF-2 induces myofibroblast migration. In comparison, TNF-α weakly stimulated cardiac myofibroblast motility suggesting that this cytokine may also play a minor role in repopulation of the infarct scar.

Our results confirm previous findings that PDGF-BB induces a more potent chemotactic response compared to FGF-2 (436, 437). According to our results, PDGF-BB (50 ng/ml) induced over 60-fold greater number of migrating cells relative to non stimulated cells. LoFGF-2 (20 ng/ml) ranked second in chemotactic potency, CT-1 third (10 ng/ml) and TNF- α (20 ng/ml) stimulated the weakest response. The relative potency hierarchy between these cytokines and growth factors suggests that cardiac myofibroblasts respond differently to the type of signal present. As these signals are expressed at different stages during the wound healing process, the

combined net signalling cascade may significantly enhance cellularity in the scar. With respect to contraction, TGFβ1, AngII and PDGF-BB elicited similar individual responses: all cytokine treatments induced increases in contraction compared to stimulation with 10% serum. Our results indicate that net myofibroblast response and behaviour (migration, contraction or proliferation) may be dependent on the type of signal that is most abundant during the different phases of cardiac wound healing.

We also confirmed a biphasic dose-dependent motility curve common to PDGF-BB, LoFGF-2, CT-1, and TNF-α stimulated myofibroblasts. This biphasic dose-response relationship is characterized with a low-dose enhancement and a high dose inhibitory response. The number of motile cells increases with increasing chemokine and mitogen concentration, peaks at an optimal concentration then declines. These trends are previously described for a number of different cell types and chemokines (420, 422, 436-438) and mitogens (439). Inhibition of motility and proliferation at higher concentrations may reflect desensitisation of respective receptors due to receptor internalisation or degradation. Taken together, these results indicate that cardiac myofibroblasts respond differently to receptor signals, the magnitude of which is dependent on cytokine concentration and the type of end-point investigated. This might be of considerable interest in the wound healing process as fluctuations in cytokine levels may induce different cellular responses depending on not only the type of signal but also the level of exposure.

Extracellular Ca^{2+} and cellular responses

To directly address our hypothesis regarding Ca^{2+} as a modulator of cell motility, we treated cardiac myofibroblasts with a chelator agent, EGTA. By chelating endogenous Ca^{2+} in DMEM/F12 media from 1mM to 2.1, 0.1, or 0.0661 μM we observed a concomitant diminution in PDGF-BB stimulated cell motility, contraction and proliferation, as well TGFβ1 induced contraction. Thus, our results demonstrate that as culture medium Ca^{2+} is reduced, cell responses are also directly reduced. Although the effect of Ca^{2+} removal on all three endpoints is rapid and pronounced, we also found that it was just as reversible in motile cells. Exogenous addition of $CaCl_2$ back into chelated media enhanced PDGF-BB induced motility and suggests that the exogenous increase of $[Ca^{2+}]_o$ supersedes the chelating effects of EGTA. An earlier investigation of cultured fibroblast motility also suggested the importance of Ca^{2+} in cell migration, as

reduction of culture medium Ca^{2+} from 2 mM to 0.1 mM was sufficient in reducing motility in a wounded monolayer assay (440). As expected, drastic reduction in $[Ca^{2+}]_o$ is associated with cellular morphological changes such as retraction of cell extensions. Reintroduction of exogenous Ca^{2+} reversed these changes. Many actin-binding proteins, including myosins I and II, gelsolin, α-actinin, and fimbrin, are regulated by Ca^{2+}. Proteases such as calpain play an integral role in FA turnover and are modulated by $[Ca^{2+}]_i$ (441, 442). Moreover, during cell division these cell-substrate interactions provide anchoring support and regulate the G1 restriction point and M phase of the cell cycle (44). In cytokinesis, FA and associated cytoskeletal factors help to modulate momentary detachment from the substratum (443). Actin is necessary for lamellipodia extension and is dependent on $[Ca^{2+}]_i$ for its assembly and disassembly (444). Our data is consistent with the notion that cytosolic Ca^{2+} gradients regulate cellular processes in that functional changes (i.e. decreases in motility) accompany morphological changes (i.e. retraction of cellular extension) during removal of extracellular Ca^{2+} from the medium. Similar trends are documented. Schwartz demonstrated that addition of 20 μM EGTA to culture medium of endothelial cells resulted in decreases in cell spreading which was followed by a global decline in $[Ca^{2+}]_i$ as measured by fluo-2 dye (Ca^{2+} indicator) studies (278). Upon removal of Ca^{2+} from incubation medium of cultured rat cardiac fibroblasts, Azuma *et al.* demonstrated changes in cellular morphology such as formation of blebs, the ballooning of the cell membrane, and detachment from the culture dish (445). Unlike the latter finding of Azuma *et al.*, we did not observe any effects of cellular adherence as a result of EGTA treatment. In low Ca^{2+} conditions cells may still be able to maintain existing contacts with the substratum but may be unable to form new contacts. It may be argued that the loss of Ca^{2+} affects the formation of new contacts more than the maintenance of existing contacts, which would impact our EGTA motility experiment as cells may still migrate into the lower chamber but without being able to adhere well. Therefore, future studies must address whether decreased $[Ca^{2+}]_o$ inhibits motility by inhibiting cell mobility (i.e. crawling, due to actin/myosin interactions), or by inhibiting cell attachment (i.e. due to activation of FAK and formation of FA), or both.

In contrast to reduction of $[Ca^{2+}]_o$, we attempted to increase $[Ca^{2+}]_i$ by treatment with ionomycin, a Ca^{2+} ionophore. Consistent with other findings (446), ionomycin treatment in our current study resulted in no significant influence on motility rates of PDGF-BB or LoFGF-2 stimulated cardiac myofibroblasts but rather maintained the response. Moore *et al.* showed that

cultured cardiac fibroblast motility rates were increased in the presence of ionomycin in both control media and low Ca^{2+} media conditions. These results provide evidence that motility in these cells is dependent upon availability of Ca^{2+}, presumably for movement into the cell (440). Due to its selectivity for Ca^{2+} and its membrane soluble properties, ionomycin is a popular tool for studying activation of $[Ca^{2+}]_i$ dependent proteins, as demonstrated by increases in Ca^{2+} transients which occur concomitant to ionomycin treatment (444). Previous work from our lab showed that ionomycin mediated increases in cytosolic Ca^{2+} and that this was attended by increased expression of phospho-MLC2 (unpublished data), while other studies found that treatment of ionomycin in vascular smooth muscle cells and neutrophils results in expression of calmodulin kinase II (447, 448), and activation of Ca^{2+}-sensitive actin severing proteins such as gelsolin (444, 447). We also addressed whether influx of Ca^{2+} would affect cell phenotype as characterized by expression of αSMA and SMemb, and found no changes present between that of ionomycin treated and non-stimulated cells. Taken together, these results indicate that even though cytosolic Ca^{2+} may be involved in intracellular signaling of cardiac myofibroblasts, its cytosolic concentration is not the critical determinant or rate limiting factor of the migratory response. Continual influx of Ca^{2+} may overwhelm cellular Ca^{2+} extrusion mechanisms thereby giving rise to excessive increases in $[Ca^{2+}]_i$ thus preventing myosin/actin cross-bridge recycling as well as causing interference with FA assembly. As cell motility is a cyclical process, we speculate after 24 hour ionomycin treatment, cellular paralysis ensues, essentially locking contractile machinery and preventing FA turnover.

The role of NCX1.1 in cardiac myofibroblast motility, contraction, and proliferation

In this investigation we demonstrate that NCX1.1 provides a novel mechanism of transplasmalemmal Ca^{2+} movement for cell motility, contraction and proliferation. Our findings are based on previous electrophysiological findings that KB-R7943, a third generation isothiourea derivative, inhibits the reverse mode of NCX in cells expressing NCX1 (410). In human pulmonary artery smooth muscle cells which express NCX1 and NCX3, for instance, inhibition of NCX with KB-R7943 also attenuated increases in $[Ca^{2+}]_i$ via the reverse mode (390). Devela *et al.* found that KB-R7943 treatment of Madin-Darby canine kidney cells resulted in a marked diminution in cell migration in control situations (56). NCX1.1 is expressed in the heart, particularly in cardiomyocytes (376), and we confirm that NCX1.1 is also expressed in

fibroblasts and myofibroblasts. KB-R7943 is a popular tool to test the properties of the exchanger in cardiomyocytes and only one paper to date describes the application of KB-R7943 on myofibroblasts. Romero *et al.* showed that in human lung embryonic myofibroblasts, TGFβ stimulated expression of connective tissue growth factor (CTGF), a matrix signaling molecule found overexpressed in fibrotic disorders (57). These authors demonstrate that CTGF expression level was dependent on a KB-R7943-sensitive influx of Ca^{2+}. In addition to blocking influx of Ca^{2+}, NCX inhibition also interfered with collagen and αSMA expression, therefore suggesting that NCX function in lung myofibroblasts plays an important role in TGFβ mediated fibrogenesis. In this current study, we found a KB-R7943-sensitive decrease in cell motility when myofibroblasts were stimulated with CT-1 and PDGF-BB. KB-R7943 also partly blocked PDGF-BB and TGFβ1 induced contraction, as well as PDGF-BB induced proliferation. NCX1.1 protein levels are equally expressed in fibroblast sand myofibroblasts. Immunostaining confirms that NCX1.1 is present in plasma membranes of fibroblast and myofibroblasts but indicates that expression of this protein is reduced in P2 cells. The reduction in NCX1.1 expression may reflect the termainally differentiated state of myofibroblasts at high passage number. Combined with cytokine mediated reduction in P2 myofibroblast motility, loss of NCX1.1 protein expression may provide evidence that these cells also loose their functional properties *in vitro*, suggesting that NCX1.1 plays an important role in modulating cardiac myofibroblast physiology during wound healing conditions. Furthermore, based on these results we suggest that NCX1.1 may play an important role in myofibroblasts function during both the acute and chronic phase of wound healing after infarction.

Compared to SEA0400, KB-R7943 is not as efficacious in inhibiting the reverse mode. SEA0400, a fourth generation isothiourea derivative, is many fold more potent and selective for the reverse mode (449). To that end, KB-R7943 may not provide sufficient specificity to inhibit the reverse mode raising the uncertainty as to whether cell function is dependent on Ca^{2+} entry mode (reverse mode) or Ca^{2+} exit mode (forward mode). Our next step was to develop a pharmacological system for our motility assays that would account for a specific NCX1.1 mode. The Na^{+}- K^{+} ATPase pump is well studied in the heart and its pharmacology well characterized and ouabain is known to inhibit its ATP function (450, 451). In situations of ischemic heart disease, inhibition of Na^{+}-K^{+} ATPase by ouabain or digitalis (or cardiac glycosides) have proven clinically relevant for enhancing $[Ca^{2+}]_i$ in cardiomyocytes by induction of reverse mode NCX,

which in turn, increases contraction and improves myocardial function. Inhibition of the pump reduces the Na^+ gradient across the membrane thereby favoring the NCX Ca^{2+} entry mode (451). As intracellular Na^+ concentrations increase, or the gradient between extracellular and intracellular Na^+ weakens, NCX operates in reverse mode to extrude Na^+ in exchange for Ca^{2+} influx. An example of this Na^+ dependency, in smooth muscle cells removal of extracellular Na^+ switched NCX mode from forward to reverse, and was subsequently accompanied by an increase in $[Ca^{2+}]_i$ (390). We tested whether inhibition of Na^+K^+ ATPase in cardiac myofibroblasts would enhance PDGF-BB induce motility based on the notion that inhibition of the pump would result in increases in intracellular Na^+, therefore inducing reverse mode NCX and, in turn, increase $[Ca^{2+}]_i$ thereby augmenting the motility response. Contrary to this hypothesis, we found that ouabain treatment has no effect on cell motility compared to PDGF-BB control values. We deduce two possible explanations for lack of enhanced motility: 1) inhibition of Na^+-K^+ ATPase did not induce high enough intracellular Na^+ concentrations due to either drug efficacy or the nature of the Na^+ gradient in cardiac myofibroblasts, and therefore we were unable to pharmacologically induce the Ca^{2+} entry mode, or 2) Forward mode plays an important role in motility. Concerning the latter explanation, during migration and contraction $[Ca^{2+}]_i$ fluctuates in order to permit actin/myosin cross bridge formation and movement (173, 452-454). $[Ca^{2+}]_i$ must drop periodically to reset cross-bridges and NCX may be involved in this process. Blocking NCX1.1 in cardiac myofibroblasts would therefore block migration and contraction not by preventing Ca^{2+} entry but by interfering with Ca^{2+} exit, thereby locking the actin/myosin machinery into one state. These conjectures are supported by obsvervations of Drevel *et al.* that cell motility is sensitive to NCX blockade with KB-R7943 and that this blockade is accompanied by a dose-dependent increase in $[Ca^{2+}]_i$ (56). In cardiomyocytes, downregulation of NCX resulted in increases in cytosolic and SR Ca^{2+}, leading to Ca^{2+} overload and loss of mitochondrial membrane potential (455). Iwamoto *et al.* showed that over expression of NCX1 impairs Ca^{2+} signaling in fibroblast resulting in a delay of integrin-mediated adhesion (392). Retardation of cell adhesion was evident even when cells were treated in combination with ionomycin and KB-R7943 suggesting that a failure to eliminate $[Ca^{2+}]_i$ is the primary cause of the decline in cell function (392). Proliferation involves cell cycle progression, chromosome disjunction (456), translocation of specific transcription factors to the nucleus (457), and the participation of cell adhesion complexes. As $[Ca^{2+}]_i$ is a prerequisite for many of these processes, our result that

NCX1.1 blockade reduced PDGF-BB induced proliferation further demonstrates the role of NCX1.1 in myofibroblast function. Thus, cytosolic Ca^{2+} may be important for regulation of myofibroblast cellular responses and that NCX1.1 may function to regulate these cytosolic Ca^{2+} gradients.

The role of NSCC in cardiac myofibroblast motility, contraction, and proliferation

NSCCs represent another mode of Ca^{2+} flux in cardiac myofibroblasts as motility is sensitive to Gd^{3+} treatment in the presence of CT-1, PDGF-BB, and LoFGF-2. In contrast, Gd^{3+} treatment has no major affect on contractile responses or proliferation in these cells. Gd^{3+}-sensitive rates in motility are found in other cell types with dose responses falling within the range of 10-20 μM used in this study (56, 458-461). Upon stretch, fibroblasts transmit MIP, which can be blocked by Gd^{3+} (53, 462), suggesting that cardiac fibroblasts contribute to the mechanical and electrical syncytium during cardiac contraction. Arrhythmogenesis occurs in response to altered electrical continuity between cardiomyocytes. Recent evidence suggests that under ischemic reperfusion conditions, cardiac fibroblast membrane potential also changes in response to mechanical stress, indicating that these cells may contribute to the pathogenesis of arrhythmias (53).

The idea that mechanically induced Ca^{2+} flux through SAC or NSCC in cardiac fibroblasts (363) supports our hypothesis that Ca^{2+} is required for myofibroblast motility and contraction. In one study, keratinocytes subjected to mechanical stretch displayed MIPs and were accompanied by increases in $[Ca^{2+}]_i$, therefore augmenting locomotion by detachment of FA complexes at the cell rear (461). Similarly, we propose that stretching of the cell membrane in response to motility may trigger activation of NSCC, thus allowing influx of Ca^{2+} which in turn, augments the migratory response. Kamkin *et al.* showed that F-actin and tubulin fiber formation is associated with activation of MIPs (54). In another study, vinculin and phosphotyrosine expression found in FA complexes are regulated in part by Gd^{3+}-sensitive Ca^{2+} influx through SAC (458). In addition, the latter study found that local application of Gd^{3+} to the leading edge of migrating cells causes global inhibition of tractional forces thus impairing cell migration. In the current investigation the result that NSCC may not be involved in contraction was surprising, as collagen gel deformation would invariably transduce membrane stretch leading to activation of these channels. Although the exact mechanisms of NSCC associated increases in $[Ca^{2+}]_i$ is

unclear, stretching of the plasma membrane causes membrane hyperpolarization through activation of voltage activated potassium channel (Kv) activation, thereby driving inward Ca^{2+} currents through non-selective cation conductance (359). In excitable cells, such as cardiomyocytes, L-type Ca^{2+} channels mediate membrane depolarization to drive sufficient influx of Ca^{2+} to activate contractile machinery. Although we found that cardiac fibroblasts and myofibroblasts express $Ca_v1.2a$, an L-type Ca^{2+} channel isotype, L-type Ca^{2+} channels are not involved in the migratory response, as nifedipine did not block PDGF-BB induced cell motility. In addition, we found that $Ca_v1.2a$ staining is present in the cytosol indicating newly synthesiszed proteins in the ER which are being folded and transported to the plasma membrane. Our motility results are consistent with previous findings in our lab which show that motility is not dependent on nifedipine treatment in the presence of CT-1 (unpublished observations). On the other hand, we show that nifedipine treatment abrogated both the contraction and proliferation response, suggesting that L-type Ca^{2+} channels play a role in these cellular responses. SOCE is proposed to be the primary mechanism of Ca^{2+} entry in fibroblasts (463) and endothelial cells (416). In contrast and despite PDGF-BB-activated NSCC in fibroblast cell division being documented in the literature (463), our results indicate that these mechanisms are not involved in the contractile and proliferation response. L-type Ca^{2+} channels are generally known to not be expressed in non-excitable cell types like endothelial cells and fibroblasts as expression of these channels would indicate that these cells are able to become excitable (i.e. able to achieve an action potential) (51, 52). However, in a recent study, Kizana *et al.* questioned this claim by demonstrating that cardiac fibroblasts can be genetically modified into cells capable of electrical coupling (464). Others have reported that based on activation of L-type Ca^{2+} channel induced depolarization, fibroblasts are able to generate and propagate action potentials by forming an excitable syncytium with cardiomyocytes (465, 466). Based on our finding that L-type Ca^{2+} channels play a role in myofibroblast function it is likely that NSCC may not be the sole mechanism of Ca^{2+} movement in these cells. This result supports the notion that cardiac myofibroblasts may possess an excitable phenotype and/or that a pharmacomechanical mechanism may act to increase cytosolic free Ca^{2+} in these cells. Cardiac myofibroblast electrical excitability has important implications in treating arrhythmogenesis as a result of poor electrical coupling between fibroblasts and myocytes during fibrotic diseases.

Our lab has demonstrated that CT-1 induces hyperpolarization across plasma membranes of cardiac myofibroblasts (unpublished results), that these cells express mRNA specific for Kv 2.1, and that inwardly rectifying K^+ currents are sensitive to Gd^{2+} treatment (418). Unlike cultured neonatal fibroblasts (467), adult rat cardiac fibroblasts and myofibroblasts are more excitable and exhibit relatively depolarized membrane potentials (359). In the latter experiment, membrane potential of cardiac fibroblasts hyperpolarized during atrial relaxation and depolarized during atrial contraction, which is consistent with expression of $Ca_v1.2a$ found in the current study. The finding that activation of K^+ channels leads to increases in migration of differentiated intestinal epithelial cells (352) suggests that that the activity of Kv in cardiac myofibroblasts may control membrane potential which may further control cytosolic free Ca^{2+} concentration by governing the driving force for Ca^{2+} influx. Curry also found that hyperpolarization of endothelial cell membrane enhanced Ca^{2+} influx into these cells while depolarization reduced Ca^{2+} influx and thus overall cell permeability (317, 468). We suggest that cytoplasmic Ca^{2+} is controlled by both Ca^{2+} influx and Ca^{2+} release from intracellular stores in myofibroblasts just as it is in myocytes or endothelial cells. Subsequently NCX1.1 forward mode function may provide a novel mechanism for Ca^{2+} removal from the cytosol restoring $[Ca^{2+}]_i$ to basal levels.

The interaction between receptor stimulation and activation of NSCC Ca^{2+} influx remain unidentified. One mechanism proposed for agonist induced rises in $[Ca^{2+}]_i$ in fibroblasts is a capacitative model through SOCs. The Ca^{2+} signal evoked by agonists of G protein-coupled Ca^{2+} mobilization receptors involves activation of IP_3-mediated mobilization from intracellular stores within the ER eg. pharmacomechanical coupling, which is followed by activation of a plasma membrane-located-Ca^{2+}-influx pathway to maintain increases in $[Ca^{2+}]_i$ and replenish ER stores. The notion of SOCE is similar to excitation-contraction coupling in cardiomyocytes, in that small levels of Ca^{2+} invokes a greater magnitude of influx from larger stores in the extracellular environment through NSCCs. SOCs are encoded by a gene homologous to *trp*. Halaszovich *et al.* demonstrated, for instance, that in a cell line over expressing TRPC3, Gd^{3+} treatment blocked electrical currents generated by these channels (469). In human valvular myofibroblasts, histamine induced activation of a Ca^{2+}-signaling pathway involving SOCs and IP_3 mediated mobilization from ER stores (55). As control of TRPC and store-operated channels occurs by PKC activation (325) and as CT-1, PDGF-BB, and LoFGF-2 are all known to activate PKC via PLC generated IP_3 and DAG, it is possible that cardiac myofibroblast motility may partly depend

on both membrane hyperpolarization and a SOCC entry pathway. Activation of IP_3 sensitive stores in the ER may therefore result in an influx of Ca^{2+} through NSCC. Recently, Rosker *et al.* addressed the link between TRPC and NCX in a stable cell line (470). These authors demonstrated that influx of Na^+ through TRPC leads to membrane depolarization, activating reverse mode NCX and enhancing Ca^{2+} influx. These results suggest functional and physical interactions between nonselective TRPC cation channels with NCX proteins as a novel Ca^{2+} signaling mechanism.

Role of myosin motors in motility and contraction

Cell motility is a highly coordinated and cyclical process involving integration of numerous cell components including actin polymerization for lamellipodia extension, assembly and disassembly of integrin and its cytoskeletal associated structures that comprise FA complexes, and activation of contractile machinery in the cell cortex. These processes require the strict regulation of $[Ca^{2+}]_i$. To our knowledge little information is known about $[Ca^{2+}]_i$ signaling in primary cultures of cardiac myofibroblasts. In one study, fluorescent imaging microscopy assessed histamine-induced Ca^{2+} signaling in fura-2-loaded human valvular myofibroblasts (55), but Ca^{2+} signaling in the context of myofibroblast motility and contraction remains poorly understood.

Myosin motor function is a prerequisite for cell motility and contraction (39) and we have observed that inhibition of MLCK blocks PDGF-BB and LoFGF-2 induced migration, as well as PDGF-BB and TGFβ1 induced contraction. Phosphorylation of MLC is inhibited by ML-7 (a MLCK inhibitor) and as activation of MLC is required for actin-myosin cross-bridge cycling and contractile activity, our results indicates that migration is partially dependent on a phospho-MLCK mechanism. Maximal inhibitory effects are observed at 20 μM ML-7, which is in the range used to inhibit rMLC phosphorylation *in vitro* (412, 471). In smooth muscle cells, cross-bridge cycling and contractile activity is regulated by the activity of myosin motors, which is further regulated by phosphorylation of rMLC, and in turn, by MLCK and phosphatases (45). Myosin II-based contraction in migrating cells functions in the breaking of adhesive interactions by direct application of physical stress to the substratum, aids in directional movement by preventing unwanted lateral lamellipodia extension, and generates the forces necessary to pull the cell body forward over recently formed FA at the leading edge of the cell. Activation of

myosin motors in myofibroblasts employ non-muscle embryonic myosin type IIa, otherwise known as SMemb (15), as well as αSMA (472). The properties of SMemb are well-suited to confer rapid contraction as seen during contraction of the cell cortex during motility (45). Although, MLCK is also activated by Src kinases (46, 47) and ROCK-mediated inhibition of constitutively active MLC phosphatase (45, 308), increases in Ca^{2+} are also classically known to activate these contractile proteins. Ca^{2+} binds to calmodulin, in turn, binding to and activating MLCK (45, 49). By inhibiting MLCK activation during myofibroblast migration and contraction in the presence of PDGF-BB, LoFGF-2, and TGFβ1, we show that these cytokines and growth factors activate intracellular pathways that induce MLC phosphorylation, which leads to increased actin-myosin cross-bridge cycling and activation of contractile activity within the cell. These results are supported by previous findings in our lab. We found that CT-1 induces phospho-MLC expression and that migration is dependent on calmodulin and MLCK activation, as shown by immunoblotting and Boyden chamber techniques, respectively (unpublished data). Eddy *et al.* demonstrated that activation of Ca^{2+} transients in migrating neutrophils is accompanied by increases in myosin II motor activation, and that this migratory response is blunted with ML-7 (473). Other studies have demonstrated a connection between either FGF-2 or PDGF-BB, and activation of Ca^{2+}/calmodulin-dependent protein kinases in vascular smooth muscle (447, 448), and endothelial cell migration (446). Furthermore, our contraction results parallel other findings which show that fibroblast mediated gel deformation is abrogated in the presence of ML-7 (474, 475). Although we did not specifically demonstrate elevated $[Ca^{2+}]_i$ in cells treated with cytokines or growth factors, the participation of Ca^{2+} in migration and contractile responses are implied with the observation that increased MLC phosphorylation is associated with activation of these cellular functions. Furthermore, a great deal of evidence indicates that ligand binding of PDGF-BB accompany a rise in $[Ca^{2+}]_i$ (117, 341, 413, 452).

Fibroblasts vs. myofibroblasts

Masur *et al.* demonstrated that the absence of cell-cell contacts is one of the primary causes of myofibroblast differentiation in culture situations, and therefore resembles a model for which to examine mechanisms of wound healing (13). These authors confirm past work from our lab which show that myofibroblasts express increased levels of αSMA compared to fibroblast (ie. fibroblasts have basal levels of this protein). They found that if fibroblasts are passaged at

low density a large yield of myofibroblasts is produced after 5-7 days. Using similar cell culture guidelines, we demonstrate that unlike freshly isolated cardiac fibroblasts, myofibroblasts stain more heavily for αSMA, and expression is enhanced with increasing passage number (e.g. P1 and P2). As cell-cell contacts are lost at each passage, it is likely that cardiac myofibroblasts in culture acquire a more pronounced wound healing phenotype. SMemb, a non specific marker for dedifferentiated smooth muscle cells, is unique to highly contractile myofibroblasts (15). For the first time, we show that compared to cardiac fibroblasts (P0), cardiac myofibroblasts (P1 and P2) exhibit increased expression for SMemb. These results provide evidence that when passaged and plated at low density, freshly isolated quiescent cardiac fibroblasts (P0) transdifferentiate into a contractile, muscular myofibroblast phenotype. Our results are supported by *in vivo* findings that αSMA positive cells are found in healing human myocardial scars 4-6 days after infarction (18), and that cardiac myofibroblasts express αSMA during right ventricular pressure overload (17). Masur *et al.* also found that induction of the myofibroblast phenotype could be achieved with exogenous application of TGFβ to freshly isolated fibroblasts (13). TGFβ1 is considered to play an important role in controlling myofibroblast differentiation, and therefore has implications during wound healing and fibrosis. TGFβ1 type I and II receptors are expressed in granulation tissue of hypertrophic dermal scars of which expression remained elevated up to 20 months after injury (135). Many studies demonstrate both *in vitro* and *in vivo* that TGFβ1 induces αSMA protein and mRNA expression in growing and quiescent cultured fibroblasts as well as in granulation tissue myofibroblasts (12, 19, 300). Increased αSMA expression upregulated fibroblast contractile activity (129) which is consistent with the notion that mechanical tension is crucial for control of myofibroblast function and for maintenance of their contractile activity *in vivo* (140, 472). Consistent with these findings, the current results indicate that in the presence of 24 hour TGFβ1 treatment, P0 fibroblasts and P1 and P2 myofibroblasts express enhanced αSMA and SMemb. Expression of αSMA and SMemb in P0 fibroblasts is not as elevated compared to myofibroblasts, but when expression in TGFβ1 treated cells is compared to non-treated controls, small increases in αSMA and SMemb expression are observed. In prior studies, a fully differentiated myofibroblast phenotype is characterized by relatively increased expression of αSMA when fibroblasts are incubated with TGFβ1 for 48 hours (12). Furthermore, Tomasek *et al.* (106) described the appearance of a partly-differentiated myofibroblast, the proto-myofibroblast, as playing an important role in the wound healing process. It is possible that 24

hours of TGFβ1 treatment does not provide sufficient time to induce fully differentiated myofibroblasts but may instead exhibit a proto-myofibroblastic phenotype. Here we report that in the presence of PDGF-BB and for comparison, LoFGF-2, no change in αSMA and SMemb expression resulted in P0, P1, and P2 cells, indicating that these cytokines do not interfere with cell phenotype, but rather maintained in culture.

Myofibroblast phenotype is partly regulated by the degree of FA maturation, which, in turn, determines the degree of mechanical force conveyed to the ECM (142). Immature FAs are small (1 μm^2) and thought to evolve from initial integrin-ECM linkages upon application of intracellular and or extracellular force (142). They transmit sufficient force to promote cell migration (144) and are characteristic of early stage differentiated myofibroblasts (i.e. proto-myofibroblasts). Immature FA are situated in the cell periphery, are associated with β and γ cytoplasmic actins, and contain αv integrin, vinculin, paxillin, α-actinin, talin, small levels of FAK and tyrosine-phosphorylated proteins (106, 142). Cell contraction induces assembly of immature FA into larger (2-6 μm^2) mature FA (classical FAs). In fully differentiated myofibroblasts, mature FAs develop into supermature FA (>6 μm^2), a process that depends on high αSMA-mediated contractile activity of stress fibers (106). Supermature FAs are composed of a dense array of FA interactions and always contain FAK, αSMA and tensin (106, 142). Supermature FA transmit higher forces then immature and mature FA because they are larger and extend further into the cell cortex (106). This high transmission of force may also reflect a steadfast FAK-mediated phosphorylation state, whereas immature and mature FA display weaker force transmission due to dephosphorylation (142). It may be suggested that proto-myofibroblasts display higher rates of cell motility as immature and mature FA undergo increased rates of FAK turnover. The current results indicate that P0 fibroblasts, which stain weakly for αSMA and SMemb, have greater CT-1 induced motility rates compared to P1 and P2 cells. Similarly, P1 cells have increased migratory rates compared to that of P2 cells in the presence of CT-1. The same trend is observed for PDGF-BB induced motility, with P1 cells having increased migratory rates compared to P2s. Our results provide new evidence supporting the connections between contractile protein expression (αSMA and SMemb), and motility. Based on the study of Dugina *et al.* (142), we hypothesize that immature FA complexes are unique to P0 fibroblasts, and as FAs modulate cell adhesion to the substrata, increased FA turnover may be of more importance in regulating the motility response than contractile proteins found in the

cortex of the cell body. Differentiation of fibroblasts into myofibroblasts is associated with diminution of chemotaxis and this phenomenon may reflect maturation of FA complexes. Enhanced expression of αSMA and SMemb is found in P2 myofibroblasts and when compared to non-treated cells of the same passage and those treatment groups of P0 or P1 cells, in the presence of CT-1 and PDGF-BB these cells have relatively very weak motile responses. We speculate the possibility that P2 myofibroblasts express supermature FA complexes, thus further supporting the concept that supermature FA display lower rates of turnover. In the context of myocardial wound healing we believe that in response to elevated levels of cytokines and growth factors quiescent fibroblasts may infiltrate the infarct zone from the non-infarcted myocardium, but as they approach the border zone differentiation ensues concomitant with elevated levels of TGFβ1 in the infarcted region as well as enhanced mechanical tension in the scar. We speculate that differentiation of fibroblasts into myofibroblasts at the site of the infarct scar is marked by inhibition of motility, which may be an adaptive response in the infarct zone for diversion of cellular energy toward localized collagen production and deposition as well as proliferation in order to continue enhancing cellularity at the site of the infarct. Nonetheless, the origin of myofibroblasts in the infarcted myocardium is controversial. It is thought that myofibroblasts arise from either interstitial fibroblasts normally residing in the non-infarcted myocardium and once activated by chemotactic factors infiltrate the infarcted zone where they proliferate (127, 131); and/or circulating monocytes or bone-marrow-derived progenitor cells that transdifferentiate at the site of infarction in response to humoral activation (476-478). Recent *in vivo* evidence suggests that in rats to which the bone marrow of green fluorescent protein (GFP)-transgenic mice has been transplanted, the 7 day infarct scar stained prominently for αSMA positive myofibroblasts and not for GFP (11). Although this study provides convincing evidence that interstitial fibroblasts may be the origin of myofibroblasts in myocardial infarct repair *in vivo,* it still remains unresolved whether migratory fibroblasts or myofibroblasts are the predominant cell type responsible for sequestration to the site of tissue injury.

VI CONCLUSION

The findings from this study support our hypothesis that in the presence of PDGF-BB cardiac myofibroblast cellular motility, contraction, and proliferation are modulated by transplasmalemmal Ca^{2+} movement. NCX1.1 is present in cardiac myofibroblast plasma membrane and may contribute to altered $[Ca^{2+}]_i$ changes in responses to activation of PDGF-BB receptors, as determined by inhibition of PDGFRβ with AG1296. We show that NCX inhibition with KB-R7943 is linked to PDGF-BB mediated myofibroblast function including cellular motility, proliferation as well as contraction as assessed by collagen I gel deformation assays. In addition to NCX1.1, we show that in the presence of PDGF-BB Gd^{3+} but not nifedipine treatment was attended by reduction in motility, suggesting that NSCCs play a role in modulating this cellular function. Our results confirm that cultures of P1 and P2 cardiac myofibroblasts express elevated levels of αSMA and SMemb compared to P0 fibroblasts and that converstion of fibroblasts to myofibroblasts is associated with abrogations of chemotaxis in these cells (i.e. freshly isolated fibroblasts are more motile compared to cultures of myofibroblasts of increasing passage). In addition, we demonstrate that PDGF-BB induced myofibroblast chemotaxis and contraction are dependent on intracellular Ca^{2+} mediated phosphorylation of MLC, as determined by inhibition of MLCK by ML-7. Thus, this study provides novel insights into the mechanisms of cardiac myofibroblast cell function, *in vitro*, particularly with respect to NCX1.1 and NSCC involvement in these processes.

The results from this study deals with currently unknown and unreported aspects of myofibroblast physiology with respect to activation of specific Ca^{2+} transport proteins during cellular function. Myofibroblast physiology is an area of great importance in the responses of the infarcted myocardium, which in turn, determines how well the myocardium combats the serious cellular, physiological, and structural changes as a result of infarction.

VIII FUTURE DIRECTIONS

To gain a better understanding of myofibroblast function and its Ca^{2+} handling properties, we propose three main ideas to extend this current study. As this study is focused on modes of transplasmalemmal Ca^{2+} flux the next logical step would be to directly measure cytosolic free Ca^{2+} concentrations in fibroblast and myofibroblasts. Ca^{2+} imaging dyes such as fura-2 and fluo-3 are powerful tools in quantifying intracellular Ca^{2+} concentrations. In the current study, we have elucidated putative mechanisms of Ca^{2+} flux. By extending our pharmacological approach used in functional assays to that of Ca^{2+} measurements, Ca^{2+} as a point of control in myofibroblast function will be resolved. Our lab has previously used Ca^{2+} imaging in the presence of CT-1. A connection between a rise in cytoplasmic Ca^{2+} in fura2- or fluo3-loaded myofibroblasts in the presence of PDGF or FGF-2 needs to be established. The second aim would be to address the role of NCX1.1 (KB-R7943), NSCCs (Gd^{3+}), and L-type Ca^{2+} channels (nifedipine) in cytokine or growth factor mediated increases in cytoplasmic Ca^{2+} along with hyperpolarization and depolarization events initiated by PDGF-BB or CT-1 ligand binding. Although this current study provides direct support evidence that NCX1.1 plays a role in myofibroblast function, the exact mode of NCX operation i.e. Ca^{2+} entry or exit mode, remains unknown. Reducing the sodium gradient across myofibroblast plasma membrane in fura-2 or fluo-3 loaded cells is another means to extend the current study to gain a better understanding on the mode of NCX operation. Past results from our lab in combination with results from this current study provide evidence that capacitative mechanisms may play a role in Ca^{2+} influx in myofibroblasts. Since SOCE pathways require the emptying of intracellular stores for NSCC mediated Ca^{2+} influx, it would be worthwhile to target the ER (i.e. using thapsigargin and caffeine) in both functional assays and cytoplasmic Ca^{2+} imaging experiments. SOC flux also involves PLC mediated mechanisms. Using drugs to block this pathway would prove advantageous in identifying the molecular pathways involved.

Hurtado *et al.* recently developed a novel genetic tool, RNA interference (RNAi) adenovirus, in which to down-regulate the expression of NCX in neonatal cardiomyocytes (479). Silencing of genes is more unambiguous in identifying cellular processes than using pharmacological techniques. Thus, the second extension of this current study would be to characterize NCX ablation in cardiac myofibroblasts with the intention of assaying transfected

cells for motility, contraction and proliferation. This approach can also be applied in Ca^{2+} imaging experiments.

The last major addition to the current investigation would be to characterize the properties of P0 cardiac fibroblasts with respect to motility, contraction, and proliferation. Our findings that P0 cells have increased migratory rates than those of P1s and P2s, and that P1s have increased rates compared to P2s are novel. These results are consistent with previous findings that the degree of FA turnover is associated with both myofibroblast phenotype and rate of contraction (142). Using similar approaches, future work must address P0 fibroblast contractile responses (gel deformation assays) and proliferation (^{3}H-thymidine incorporation). Furthermore, characterization of FA expression in P0 fibroblasts using antibodies specific for phospho-FA, total FA, and FAK, would provide novel insights into the relationship between the degree of FA maturation and cell function. It is likely, that P0 cardiac fibroblasts express immature FA and thus may provide an explanation as to why these cells have elevated migratory rates. Contractile responses and proliferation will likely be diminished in immature FA expressing P0 cells.

IX LIST OF REFERENCES

1. Lee DS, Johansen H, Gong Y, Hall RE, Tu JV and Cox JL. Regional outcomes of heart failure in Canada. *Can J Cardiol* 20: 599-607, 2004.
2. Boersma E, Mercado N, Poldermans D, Gardien M, Vos J and Simoons ML. Acute myocardial infarction. *Lancet* 361: 847-858, 2003.
3. Weber KT and Brilla CG. Factors associated with reactive and reparative fibrosis of the myocardium. *Basic Res Cardiol* 87 Suppl 1: 291-301, 1992.
4. Sun Y and Weber KT. Cardiac remodelling by fibrous tissue: role of local factors and circulating hormones. *Ann Med* 30 Suppl 1: 3-8, 1998.
5. Cleutjens JP, Blankesteijn WM, Daemen MJ and Smits JF. The infarcted myocardium: simply dead tissue, or a lively target for therapeutic interventions. *Cardiovasc Res* 44: 232-241, 1999.
6. Sun Y, Kiani MF, Postlethwaite AE and Weber KT. Infarct scar as living tissue. *Basic Res Cardiol* 97: 343-347, 2002.
7. Burlew BS and Weber KT. Cardiac fibrosis as a cause of diastolic dysfunction. *Herz* 27: 92-98, 2002.
8. Desmouliere A, Redard M, Darby I and Gabbiani G. Apoptosis mediates the decrease in cellularity during the transition between granulation tissue and scar. *Am J Pathol* 146: 56-66, 1995.
9. Brown RD, Ambler SK, Mitchell MD and Long CS. The cardiac fibroblast: therapeutic target in myocardial remodeling and failure. *Annu Rev Pharmacol Toxicol* 45: 657-687, 2005.
10. Freed DH, Cunnington RH, Dangerfield AL, Sutton JS and Dixon IM. Emerging evidence for the role of cardiotrophin-1 in cardiac repair in the infarcted heart. *Cardiovasc Res* 65: 782-792, 2005.
11. Yano T, Miura T, Ikeda Y, Matsuda E, Saito K, Miki T, Kobayashi H, Nishino Y, Ohtani S and Shimamoto K. Intracardiac fibroblasts, but not bone marrow derived cells, are the origin of myofibroblasts in myocardial infarct repair. *Cardiovasc Pathol* 14: 241-246, 2005.
12. Malmstrom J, Lindberg H, Lindberg C, Bratt C, Wieslander E, Delander EL, Sarnstrand B, Burns JS, Mose-Larsen P, Fey S and Marko-Varga G. Transforming growth factor-beta 1 specifically induce proteins involved in the myofibroblast contractile apparatus. *Mol Cell Proteomics* 3: 466-477, 2004.
13. Masur SK, Dewal HS, Dinh TT, Erenburg I and Petridou S. Myofibroblasts differentiate from fibroblasts when plated at low density. *Proc Natl Acad Sci U S A* 93: 4219-4223, 1996.
14. Frangogiannis NG, Smith CW and Entman ML. The inflammatory response in myocardial infarction. *Cardiovasc Res* 53: 31-47, 2002.
15. Frangogiannis NG, Michael LH and Entman ML. Myofibroblasts in reperfused myocardial infarcts express the embryonic form of smooth muscle myosin heavy chain (SMemb). *Cardiovasc Res* 48: 89-100, 2000.
16. Bishop JE and Laurent GJ. Collagen turnover and its regulation in the normal and hypertrophying heart. *Eur Heart J* 16 Suppl C: 38-44, 1995.

17. Leslie KO, Taatjes DJ, Schwarz J, vonTurkovich M and Low RB. Cardiac myofibroblasts express alpha smooth muscle actin during right ventricular pressure overload in the rabbit. *Am J Pathol* 139: 207-216, 1991.
18. Willems IE, Havenith MG, De Mey JG and Daemen MJ. The alpha-smooth muscle actin-positive cells in healing human myocardial scars. *Am J Pathol* 145: 868-875, 1994.
19. Desmouliere A, Geinoz A, Gabbiani F and Gabbiani G. Transforming growth factor-beta 1 induces alpha-smooth muscle actin expression in granulation tissue myofibroblasts and in quiescent and growing cultured fibroblasts. *J Cell Biol* 122: 103-111, 1993.
20. Desmouliere A and Gabbiani G. Myofibroblast differentiation during fibrosis. *Exp Nephrol* 3: 134-139, 1995.
21. Cleutjens JP, Verluyten MJ, Smiths JF and Daemen MJ. Collagen remodeling after myocardial infarction in the rat heart. *Am J Pathol* 147: 325-338, 1995.
22. Gabbiani G. The myofibroblast in wound healing and fibrocontractive diseases. *J Pathol* 200: 500-503, 2003.
23. Talwar S, Squire IB, Downie PF, O'Brien RJ, Davies JE and Ng LL. Elevated circulating cardiotrophin-1 in heart failure: relationship with parameters of left ventricular systolic dysfunction. *Clin Sci (Lond)* 99: 83-88, 2000.
24. Talwar S, Downie PF, Squire IB, Davies JE, Barnett DB and Ng LL. Plasma N-terminal pro BNP and cardiotrophin-1 are elevated in aortic stenosis. *Eur J Heart Fail* 3: 15-19, 2001.
25. Sheng Z, Knowlton K, Chen J, Hoshijima M, Brown JH and Chien KR. Cardiotrophin 1 (CT-1) inhibition of cardiac myocyte apoptosis via a mitogen-activated protein kinase-dependent pathway. Divergence from downstream CT-1 signals for myocardial cell hypertrophy. *J Biol Chem* 272: 5783-5791, 1997.
26. Bouzegrhane F and Thibault G. Is angiotensin II a proliferative factor of cardiac fibroblasts? *Cardiovasc Res* 53: 304-312, 2002.
27. Battegay EJ, Rupp J, Iruela-Arispe L, Sage EH and Pech M. PDGF-BB modulates endothelial proliferation and angiogenesis in vitro via PDGF beta-receptors. *J Cell Biol* 125: 917-928, 1994.
28. Wallace JM, Freeburn JC, Gilmore WS, Sinnamon DG, Craig BM, McNally RJ and Strain JJ. The assessment of platelet derived growth factor concentration in post myocardial infarction and stable angina patients. *Ann Clin Biochem* 35 (Pt 2): 236-241, 1998.
29. Bonner JC. Regulation of PDGF and its receptors in fibrotic diseases. *Cytokine Growth Factor Rev* 15: 255-273, 2004.
30. Heldin CH and Westermark B. Mechanism of action and in vivo role of platelet-derived growth factor. *Physiol Rev* 79: 1283-1316, 1999.
31. Kardami E, Jiang ZS, Jimenez SK, Hirst CJ, Sheikh F, Zahradka P and Cattini PA. Fibroblast growth factor 2 isoforms and cardiac hypertrophy. *Cardiovasc Res* 63: 458-466, 2004.
32. Detillieux KA, Sheikh F, Kardami E and Cattini PA. Biological activities of fibroblast growth factor-2 in the adult myocardium. *Cardiovasc Res* 57: 8-19, 2003.
33. Fujii T, Yau TM, Weisel RD, Ohno N, Mickle DA, Shiono N, Ozawa T, Matsubayashi K and Li RK. Cell transplantation to prevent heart failure: a comparison of cell types. *Ann Thorac Surg* 76: 2062-2070, 2003.

34. Reffelmann T and Kloner RA. Cellular cardiomyoplasty--cardiomyocytes, skeletal myoblasts, or stem cells for regenerating myocardium and treatment of heart failure? *Cardiovasc Res* 58: 358-368, 2003.
35. Clark RA. Wound repair. *Curr Opin Cell Biol* 1: 1000-1008, 1989.
36. Lauffenburger DA and Horwitz AF. Cell migration: a physically integrated molecular process. *Cell* 84: 359-369, 1996.
37. Mitchison TJ and Cramer LP. Actin-based cell motility and cell locomotion. *Cell* 84: 371-379, 1996.
38. Mitra SK, Hanson DA and Schlaepfer DD. Focal adhesion kinase: in command and control of cell motility. *Nat Rev Mol Cell Biol* 6: 56-68, 2005.
39. Krendel M and Mooseker MS. Myosins: tails (and heads) of functional diversity. *Physiology (Bethesda)* 20: 239-251, 2005.
40. Pollard TD and Weihing RR. Actin and myosin and cell movement. *CRC Crit Rev Biochem* 2: 1-65, 1974.
41. Parsons JT, Martin KH, Slack JK, Taylor JM and Weed SA. Focal adhesion kinase: a regulator of focal adhesion dynamics and cell movement. *Oncogene* 19: 5606-5613, 2000.
42. Petit V and Thiery JP. Focal adhesions: structure and dynamics. *Biol Cell* 92: 477-494, 2000.
43. Hartwell LH and Weinert TA. Checkpoints: controls that ensure the order of cell cycle events. *Science* 246: 629-634, 1989.
44. Fresu M, Bianchi M, Parsons JT and Villa-Moruzzi E. Cell-cycle-dependent association of protein phosphatase 1 and focal adhesion kinase. *Biochem J* 358: 407-414, 2001.
45. Pfitzer G. Invited review: regulation of myosin phosphorylation in smooth muscle. *J Appl Physiol* 91: 497-503, 2001.
46. Birukov KG, Csortos C, Marzilli L, Dudek S, Ma SF, Bresnick AR, Verin AD, Cotter RJ and Garcia JG. Differential regulation of alternatively spliced endothelial cell myosin light chain kinase isoforms by p60(Src). *J Biol Chem* 276: 8567-8573, 2001.
47. Wu H, Reynolds AB, Kanner SB, Vines RR and Parsons JT. Identification and characterization of a novel cytoskeleton-associated pp60src substrate. *Mol Cell Biol* 11: 5113-5124, 1991.
48. Parizi M, Howard EW and Tomasek JJ. Regulation of LPA-promoted myofibroblast contraction: role of Rho, myosin light chain kinase, and myosin light chain phosphatase. *Exp Cell Res* 254: 210-220, 2000.
49. Ganitkevich V, Hasse V and Pfitzer G. Ca2+-dependent and Ca2+-independent regulation of smooth muscle contraction. *J Muscle Res Cell Motil* 23: 47-52, 2002.
50. Carafoli E. Calcium signaling: a tale for all seasons. *Proc Natl Acad Sci U S A* 99: 1115-1122, 2002.
51. Gray LS, Gnarra JR, Russell JH and Engelhard VH. The role of K+ in the regulation of the increase in intracellular Ca2+ mediated by the T lymphocyte antigen receptor. *Cell* 50: 119-127, 1987.
52. Nilius B, Viana F and Droogmans G. Ion channels in vascular endothelium. *Annu Rev Physiol* 59: 145-170, 1997.
53. Kamkin A, Kiseleva I, Wagner KD, Lozinsky I, Gunther J and Scholz H. Mechanically induced potentials in atrial fibroblasts from rat hearts are sensitive to hypoxia/reoxygenation. *Pflugers Arch* 446: 169-174, 2003.

54. Kamkin A, Kiseleva I, Wagner KD, Scholz H, Theres H, Kazanski V, Lozinsky I, Gunther J and Isenberg G. Mechanically induced potentials in rat atrial fibroblasts depend on actin and tubulin polymerisation. *Pflugers Arch* 442: 487-497, 2001.
55. Liang W, McDonald P, McManus B, van BC and Wang X. Histamine-induced Ca(2+) signaling in human valvular myofibroblasts. *J Mol Cell Cardiol* 35: 379-388, 2003.
56. Dreval V, Dieterich P, Stock C and Schwab A. The role of Ca2+ transport across the plasma membrane for cell migration. *Cell Physiol Biochem* 16: 119-126, 2005.
57. Romero JR, Rivera A, Lanca V, Bicho MD, Conlin PR and Ricupero DA. Na+/Ca2+ exchanger activity modulates connective tissue growth factor mRNA expression in transforming growth factor beta1- and Des-Arg10-kallidin-stimulated myofibroblasts. *J Biol Chem* 280: 14378-14384, 2005.
58. Mackay JMG.2004 The Atlas of Heart Disease and Stroke, Online resource, http://www.who.int/cardiovascular_diseases/resources/atlas/en/index.html. 2004.
59. Canadian Institute of Health Research (CIHR), Online resource, http://www.cihrirsc.gc.ca/e/documents/heart_disease_mpkit_2005_e.pdf. 2005.
60. Heart and Stroke Foundation of Canada in collaboration with Health Canada and Canadian Carviovascular Society.2003 The Growing Burden of Heart Disease and Stroke, Online resource, http://www.cvdinfobase.ca/cvdbook/CVD_En03.pdf. 2003.
61. Colucci WS and Braunwald E. Pathophysiology of Heart Failure. In: Heart Disease, edited by Braunwald E. Saunders Company, 1997, p. 394-420.
62. Bennett MR. Apoptosis in the cardiovascular system. *Heart* 87: 480-487, 2002.
63. Francis GS. Pathophysiology of chronic heart failure. *Am J Med* 110 Suppl 7A: 37S-46S, 2001.
64. Tu JV, Austin PC, Filate WA, Johansen HL, Brien SE, Pilote L and Alter DA. Outcomes of acute myocardial infarction in Canada. *Can J Cardiol* 19: 893-901, 2003.
65. LaRosa JC. Future cardiovascular end point studies: where will the research take us? *Am J Cardiol* 84: 454-458, 1999.
66. Rauch U, Osende JI, Fuster V, Badimon JJ, Fayad Z and Chesebro JH. Thrombus formation on atherosclerotic plaques: pathogenesis and clinical consequences. *Ann Intern Med* 134: 224-238, 2001.
67. Braunwald E. Unstable angina: an etiologic approach to management. *Circulation* 98: 2219-2222, 1998.
68. Ruwhof C and van der LA. Mechanical stress-induced cardiac hypertrophy: mechanisms and signal transduction pathways. *Cardiovasc Res* 47: 23-37, 2000.
69. Greenberg B. Treatment of heart failure: state of the art and prospectives. *J Cardiovasc Pharmacol* 38 Suppl 2: S59-S63, 2001.
70. Towbin JA and Bowles NE. The failing heart. *Nature* 415: 227-233, 2002.
71. Mogensen J, Klausen IC, Pedersen AK, Egeblad H, Bross P, Kruse TA, Gregersen N, Hansen PS, Baandrup U and Borglum AD. Alpha-cardiac actin is a novel disease gene in familial hypertrophic cardiomyopathy. *J Clin Invest* 103: R39-R43, 1999.
72. Francis GS. Diabetic cardiomyopathy: fact or fiction? *Heart* 85: 247-248, 2001.
73. Marwick TH. Diabetic heart disease. *Heart* 2005.
74. Bekeredjian R and Grayburn PA. Valvular heart disease: aortic regurgitation. *Circulation* 112: 125-134, 2005.

75. Spies CD, Sander M, Stangl K, Fernandez-Sola J, Preedy VR, Rubin E, Andreasson S, Hanna EZ and Kox WJ. Effects of alcohol on the heart. *Curr Opin Crit Care* 7: 337-343, 2001.
76. Calabrese F and Thiene G. Myocarditis and inflammatory cardiomyopathy: microbiological and molecular biological aspects. *Cardiovasc Res* 60: 11-25, 2003.
77. Levine SA. Coronary thrombosis:its various clinical features. *Medicine* 8: 245-418, 1929.
78. Lodge-Patch I. The ageing of cardiac infarcts, and its influence on cardiac rupture. *Br Heart J* 13: 37-42, 1951.
79. Mallory GK, White PD and Salcedo-Salgar J. The speed of healing of myocardial infarction. A study of the pathologic anatomy in seventy-two cases. *Am Heart J* 18: 647-671, 1939.
80. Dhalla NS, Temsah RM and Netticadan T. Role of oxidative stress in cardiovascular diseases. *J Hypertens* 18: 655-673, 2000.
81. Dhalla NS, Temsah RM, Netticadan T and Sandhu MS. Calcium Overload in Ischemia/Reperfusion Injury. In: Heart Physiology and Pathophysiology, edited by Sperelakis N, Kurachi Y, Terzic A and Cohen M. Academic Press, 2001, p. 949-964.
82. Bolli R. Oxygen-derived free radicals and postischemic myocardial dysfunction ("stunned myocardium"). *J Am Coll Cardiol* 12: 239-249, 1988.
83. Olivetti G, Abbi R, Quaini F, Kajstura J, Cheng W, Nitahara JA, Quaini E, Di LC, Beltrami CA, Krajewski S, Reed JC and Anversa P. Apoptosis in the failing human heart. *N Engl J Med* 336: 1131-1141, 1997.
84. Haunstetter A and Izumo S. Apoptosis: basic mechanisms and implications for cardiovascular disease. *Circ Res* 82: 1111-1129, 1998.
85. Giordano FJ. Oxygen, oxidative stress, hypoxia, and heart failure. *J Clin Invest* 115: 500-508, 2005.
86. Raines EW. PDGF and cardiovascular disease. *Cytokine Growth Factor Rev* 15: 237-254, 2004.
87. Zhang M, Xu YJ, Saini HK, Turan B, Liu PP and Dhalla NS. TNF-alpha as a potential mediator of cardiac dysfunction due to intracellular Ca2+-overload. *Biochem Biophys Res Commun* 327: 57-63, 2005.
88. Peng J, Gurantz D, Tran V, Cowling RT and Greenberg BH. Tumor necrosis factor-alpha-induced AT1 receptor upregulation enhances angiotensin II-mediated cardiac fibroblast responses that favor fibrosis. *Circ Res* 91: 1119-1126, 2002.
89. Sun M, Dawood F, Wen WH, Chen M, Dixon I, Kirshenbaum LA and Liu PP. Excessive tumor necrosis factor activation after infarction contributes to susceptibility of myocardial rupture and left ventricular dysfunction. *Circulation* 110: 3221-3228, 2004.
90. Sturk A, Hack CE, Aarden LA, Brouwer M, Koster RR and Sanders GT. Interleukin-6 release and the acute-phase reaction in patients with acute myocardial infarction: a pilot study. *J Lab Clin Med* 119: 574-579, 1992.
91. Matsumori A, Furukawa Y, Hashimoto T, Yoshida A, Ono K, Shioi T, Okada M, Iwasaki A, Nishio R, Matsushima K and Sasayama S. Plasma levels of the monocyte chemotactic and activating factor/monocyte chemoattractant protein-1 are elevated in patients with acute myocardial infarction. *J Mol Cell Cardiol* 29: 419-423, 1997.
92. Sakai S, Miyauchi T, Sakurai T, Kasuya Y, Ihara M, Yamaguchi I, Goto K and Sugishita Y. Endogenous endothelin-1 participates in the maintenance of cardiac function in rats

with congestive heart failure. Marked increase in endothelin-1 production in the failing heart. *Circulation* 93: 1214-1222, 1996.
93. Hao J, Ju H, Zhao S, Junaid A, Scammell-La FT and Dixon IM. Elevation of expression of Smads 2, 3, and 4, decorin and TGF-beta in the chronic phase of myocardial infarct scar healing. *J Mol Cell Cardiol* 31: 667-678, 1999.
94. Sun Y and Weber KT. Infarct scar: a dynamic tissue. *Cardiovasc Res* 46: 250-256, 2000.
95. Spinale FG. Matrix metalloproteinases: regulation and dysregulation in the failing heart. *Circ Res* 90: 520-530, 2002.
96. Cleutjens JP, Kandala JC, Guarda E, Guntaka RV and Weber KT. Regulation of collagen degradation in the rat myocardium after infarction. *J Mol Cell Cardiol* 27: 1281-1292, 1995.
97. Blankesteijn WM, Essers-Janssen YP, Verluyten MJ, Daemen MJ and Smits JF. A homologue of Drosophila tissue polarity gene frizzled is expressed in migrating myofibroblasts in the infarcted rat heart. *Nat Med* 3: 541-544, 1997.
98. Chen L, Wu Q, Guo F, Xia B and Zuo J. Expression of Dishevelled-1 in wound healing after acute myocardial infarction: possible involvement in myofibroblast proliferation and migration. *J Cell Mol Med* 8: 257-264, 2004.
99. Chareonthaitawee P, Christian TF, Hirose K, Gibbons RJ and Rumberger JA. Relation of initial infarct size to extent of left ventricular remodeling in the year after acute myocardial infarction. *J Am Coll Cardiol* 25: 567-573, 1995.
100. Jugdutt BI. Remodeling of the myocardium and potential targets in the collagen degradation and synthesis pathways. *Curr Drug Targets Cardiovasc Haematol Disord* 3: 1-30, 2003.
101. Bartosova D, Chvapil M, Korecky B, Poupa O, Rakusan K, Turek Z and Vizek M. The growth of the muscular and collagenous parts of the rat heart in various forms of cardiomegaly. *J Physiol* 200: 285-295, 1969.
102. Jugdutt BI. Ventricular remodeling after infarction and the extracellular collagen matrix: when is enough enough? *Circulation* 108: 1395-1403, 2003.
103. Lijnen PJ, Petrov VV and Fagard RH. Induction of cardiac fibrosis by transforming growth factor-beta(1). *Mol Genet Metab* 71: 418-435, 2000.
104. Weber KT. Fibrosis, a common pathway to organ failure: angiotensin II and tissue repair. *Semin Nephrol* 17: 467-491, 1997.
105. Weber KT, Sun Y and Katwa LC. Wound healing following myocardial infarction. *Clin Cardiol* 19: 447-455, 1996.
106. Tomasek JJ, Gabbiani G, Hinz B, Chaponnier C and Brown RA. Myofibroblasts and mechano-regulation of connective tissue remodelling. *Nat Rev Mol Cell Biol* 3: 349-363, 2002.
107. Lindsey ML, Mann DL, Entman ML and Spinale FG. Extracellular matrix remodeling following myocardial injury. *Ann Med* 35: 316-326, 2003.
108. Caulfield JB and Borg TK. The collagen network of the heart. *Lab Invest* 40: 364-372, 1979.
109. Ju H and Dixon IM. Extracellular matrix and cardiovascular diseases. *Can J Cardiol* 12: 1259-1267, 1996.
110. Leask A and Abraham DJ. TGF-beta signaling and the fibrotic response. *FASEB J* 18: 816-827, 2004.

111. Derynck R and Zhang YE. Smad-dependent and Smad-independent pathways in TGF-beta family signalling. *Nature* 425: 577-584, 2003.
112. Shi Y and Massague J. Mechanisms of TGF-beta signaling from cell membrane to the nucleus. *Cell* 113: 685-700, 2003.
113. Volders PG, Willems IE, Cleutjens JP, Arends JW, Havenith MG and Daemen MJ. Interstitial collagen is increased in the non-infarcted human myocardium after myocardial infarction. *J Mol Cell Cardiol* 25: 1317-1323, 1993.
114. Brilla CG, Janicki JS and Weber KT. Impaired diastolic function and coronary reserve in genetic hypertension. Role of interstitial fibrosis and medial thickening of intramyocardial coronary arteries. *Circ Res* 69: 107-115, 1991.
115. Weber KT. Targeting pathological remodeling: concepts of cardioprotection and reparation. *Circulation* 102: 1342-1345, 2000.
116. Dixon IM, Ju H, Reid NL, Scammell-La FT, Werner JP and Jasmin G. Cardiac collagen remodeling in the cardiomyopathic Syrian hamster and the effect of losartan. *J Mol Cell Cardiol* 29: 1837-1850, 1997.
117. Dixon IM, Hao J, Reid NL and Roth JC. Effect of chronic AT(1) receptor blockade on cardiac Smad overexpression in hereditary cardiomyopathic hamsters. *Cardiovasc Res* 46: 286-297, 2000.
118. Gough KM, Zelinski D, Wiens R, Rak M and Dixon IM. Fourier transform infrared evaluation of microscopic scarring in the cardiomyopathic heart: effect of chronic AT1 suppression. *Anal Biochem* 316: 232-242, 2003.
119. Hao J, Wang B, Jones SC, Jassal DS and Dixon IM. Interaction between angiotensin II and Smad proteins in fibroblasts in failing heart and in vitro. *Am J Physiol Heart Circ Physiol* 279: H3020-H3030, 2000.
120. Makino N, Hata T, Sugano M, Dixon IM and Yanaga T. Regression of hypertrophy after myocardial infarction is produced by the chronic blockade of angiotensin type 1 receptor in rats. *J Mol Cell Cardiol* 28: 507-517, 1996.
121. Maisch B. Extracellular matrix and cardiac interstitium: restriction is not a restricted phenomenon. *Herz* 20: 75-80, 1995.
122. Manabe I, Shindo T and Nagai R. Gene expression in fibroblasts and fibrosis: involvement in cardiac hypertrophy. *Circ Res* 91: 1103-1113, 2002.
123. Gabbiani G and Rungger-Brandle E. The Fibroblast. In: Handbook of Inflammation: Tissue Repair and Regeneration, edited by Glynn LE. 1981, p. 1-50.
124. Camelliti P, Green CR, LeGrice I and Kohl P. Fibroblast network in rabbit sinoatrial node: structural and functional identification of homogeneous and heterogeneous cell coupling. *Circ Res* 94: 828-835, 2004.
125. Gaudesius G, Miragoli M, Thomas SP and Rohr S. Coupling of cardiac electrical activity over extended distances by fibroblasts of cardiac origin. *Circ Res* 93: 421-428, 2003.
126. Goldsmith EC, Hoffman A, Morales MO, Potts JD, Price RL, McFadden A, Rice M and Borg TK. Organization of fibroblasts in the heart. *Dev Dyn* 230: 787-794, 2004.
127. Powell DW, Mifflin RC, Valentich JD, Crowe SE, Saada JI and West AB. Myofibroblasts. I. Paracrine cells important in health and disease. *Am J Physiol* 277: C1-C9, 1999.
128. Eyden B. The myofibroblast: an assessment of controversial issues and a definition useful in diagnosis and research. *Ultrastruct Pathol* 25: 39-50, 2001.

129. Hinz B, Celetta G, Tomasek JJ, Gabbiani G and Chaponnier C. Alpha-smooth muscle actin expression upregulates fibroblast contractile activity. *Mol Biol Cell* 12: 2730-2741, 2001.
130. Shin D and Minn KW. The effect of myofibroblast on contracture of hypertrophic scar. *Plast Reconstr Surg* 113: 633-640, 2004.
131. Desmouliere A. Factors influencing myofibroblast differentiation during wound healing and fibrosis. *Cell Biol Int* 19: 471-476, 1995.
132. Serini G and Gabbiani G. Mechanisms of myofibroblast activity and phenotypic modulation. *Exp Cell Res* 250: 273-283, 1999.
133. Booz GW and Baker KM. Molecular signalling mechanisms controlling growth and function of cardiac fibroblasts. *Cardiovasc Res* 30: 537-543, 1995.
134. Gabbiani G. Evolution and clinical implications of the myofibroblast concept. *Cardiovasc Res* 38: 545-548, 1998.
135. Schmid P, Itin P, Cherry G, Bi C and Cox DA. Enhanced expression of transforming growth factor-beta type I and type II receptors in wound granulation tissue and hypertrophic scar. *Am J Pathol* 152: 485-493, 1998.
136. Leicht M, Briest W, Holzl A and Zimmer HG. Serum depletion induces cell loss of rat cardiac fibroblasts and increased expression of extracellular matrix proteins in surviving cells. *Cardiovasc Res* 52: 429-437, 2001.
137. Gabbiani G, Ryan GB and Majne G. Presence of modified fibroblasts in granulation tissue and their possible role in wound contraction. *Experientia* 27: 549-550, 1971.
138. MacKenna D, Summerour SR and Villarreal FJ. Role of mechanical factors in modulating cardiac fibroblast function and extracellular matrix synthesis. *Cardiovasc Res* 46: 257-263, 2000.
139. Chiquet M. Regulation of extracellular matrix gene expression by mechanical stress. *Matrix Biol* 18: 417-426, 1999.
140. Hinz B, Mastrangelo D, Iselin CE, Chaponnier C and Gabbiani G. Mechanical tension controls granulation tissue contractile activity and myofibroblast differentiation. *Am J Pathol* 159: 1009-1020, 2001.
141. Wang HB, Dembo M, Hanks SK and Wang Y. Focal adhesion kinase is involved in mechanosensing during fibroblast migration. *Proc Natl Acad Sci U S A* 98: 11295-11300, 2001.
142. Dugina V, Fontao L, Chaponnier C, Vasiliev J and Gabbiani G. Focal adhesion features during myofibroblastic differentiation are controlled by intracellular and extracellular factors. *J Cell Sci* 114: 3285-3296, 2001.
143. Lygoe KA, Norman JT, Marshall JF and Lewis MP. AlphaV integrins play an important role in myofibroblast differentiation. *Wound Repair Regen* 12: 461-470, 2004.
144. Hinz B and Gabbiani G. Mechanisms of force generation and transmission by myofibroblasts. *Curr Opin Biotechnol* 14: 538-546, 2003.
145. Kapanci Y, Ribaux C, Chaponnier C and Gabbiani G. Cytoskeletal features of alveolar myofibroblasts and pericytes in normal human and rat lung. *J Histochem Cytochem* 40: 1955-1963, 1992.
146. Tomasek JJ, Haaksma CJ, Eddy RJ and Vaughan MB. Fibroblast contraction occurs on release of tension in attached collagen lattices: dependency on an organized actin cytoskeleton and serum. *Anat Rec* 232: 359-368, 1992.

147. Lorena D, Uchio K, Costa AM and Desmouliere A. Normal scarring: importance of myofibroblasts. *Wound Repair Regen* 10: 86-92, 2002.
148. Hinz B, Dugina V, Ballestrem C, Wehrle-Haller B and Chaponnier C. Alpha-smooth muscle actin is crucial for focal adhesion maturation in myofibroblasts. *Mol Biol Cell* 14: 2508-2519, 2003.
149. Ross R, Glomset J, Kariya B and Harker L. A platelet-dependent serum factor that stimulates the proliferation of arterial smooth muscle cells in vitro. *Proc Natl Acad Sci U S A* 71: 1207-1210, 1974.
150. Heldin CH, Eriksson U and Ostman A. New members of the platelet-derived growth factor family of mitogens. *Arch Biochem Biophys* 398: 284-290, 2002.
151. Ronnstrand L and Heldin CH. Mechanisms of platelet-derived growth factor-induced chemotaxis. *Int J Cancer* 91: 757-762, 2001.
152. Hoch RV and Soriano P. Roles of PDGF in animal development. *Development* 130: 4769-4784, 2003.
153. Heldin CH. Simultaneous induction of stimulatory and inhibitory signals by PDGF. *FEBS Lett* 410: 17-21, 1997.
154. Heldin CH, Westermark B and Wasteson A. Platelet-derived growth factor. Isolation by a large-scale procedure and analysis of subunit composition. *Biochem J* 193: 907-913, 1981.
155. Dirks RP and Bloemers HP. Signals controlling the expression of PDGF. *Mol Biol Rep* 22: 1-24, 1995.
156. LaMarre J, Hayes MA, Wollenberg GK, Hussaini I, Hall SW and Gonias SL. An alpha 2-macroglobulin receptor-dependent mechanism for the plasma clearance of transforming growth factor-beta 1 in mice. *J Clin Invest* 87: 39-44, 1991.
157. Fischer WH and Schubert D. Characterization of a novel platelet-derived growth factor-associated protein. *J Neurochem* 66: 2213-2216, 1996.
158. Price RL, Chintanowonges C, Shiraishi I, Borg TK and Terracio L. Local and regional variations in myofibrillar patterns in looping rat hearts. *Anat Rec* 245: 83-93, 1996.
159. Schonherr E, Jarvelainen HT, Sandell LJ and Wight TN. Effects of platelet-derived growth factor and transforming growth factor-beta 1 on the synthesis of a large versican-like chondroitin sulfate proteoglycan by arterial smooth muscle cells. *J Biol Chem* 266: 17640-17647, 1991.
160. Blatti SP, Foster DN, Ranganathan G, Moses HL and Getz MJ. Induction of fibronectin gene transcription and mRNA is a primary response to growth-factor stimulation of AKR-2B cells. *Proc Natl Acad Sci U S A* 85: 1119-1123, 1988.
161. Heldin P, Laurent TC and Heldin CH. Effect of growth factors on hyaluronan synthesis in cultured human fibroblasts. *Biochem J* 258: 919-922, 1989.
162. Diez C, Nestler M, Friedrich U, Vieth M, Stolte M, Hu K, Hoppe J and Simm A. Down-regulation of Akt/PKB in senescent cardiac fibroblasts impairs PDGF-induced cell proliferation. *Cardiovasc Res* 49: 731-740, 2001.
163. Simm A and Diez C. Density dependent expression of PDGF-A modulates the angiotensin II dependent proliferation of rat cardiac fibroblasts. *Basic Res Cardiol* 94: 464-471, 1999.
164. Schollmann C, Grugel R, Tatje D, Hoppe J, Folkman J, Marme D and Weich HA. Basic fibroblast growth factor modulates the mitogenic potency of the platelet-derived growth

factor (PDGF) isoforms by specific upregulation of the PDGF alpha receptor in vascular smooth muscle cells. *J Biol Chem* 267: 18032-18039, 1992.
165. Desmouliere A, Rubbia-Brandt L, Grau G and Gabbiani G. Heparin induces alpha-smooth muscle actin expression in cultured fibroblasts and in granulation tissue myofibroblasts. *Lab Invest* 67: 716-726, 1992.
166. Rubbia-Brandt L, Sappino AP and Gabbiani G. Locally applied GM-CSF induces the accumulation of alpha-smooth muscle actin containing myofibroblasts. *Virchows Arch B Cell Pathol Incl Mol Pathol* 60: 73-82, 1991.
167. Kazlauskas A and Cooper JA. Autophosphorylation of the PDGF receptor in the kinase insert region regulates interactions with cell proteins. *Cell* 58: 1121-1133, 1989.
168. Centrella M, McCarthy TL, Kusmik WF and Canalis E. Isoform-specific regulation of platelet-derived growth factor activity and binding in osteoblast-enriched cultures from fetal rat bone. *J Clin Invest* 89: 1076-1084, 1992.
169. Bonner JC, Badgett A, Lindroos PM and Coin PG. Basic fibroblast growth factor induces expression of the PDGF receptor-alpha on human bronchial smooth muscle cells. *Am J Physiol* 271: L880-L888, 1996.
170. Paulsson Y, Karlsson C, Heldin CH and Westermark B. Density-dependent inhibitory effect of transforming growth factor-beta 1 on human fibroblasts involves the down-regulation of platelet-derived growth factor alpha-receptors. *J Cell Physiol* 157: 97-103, 1993.
171. Siegbahn A, Hammacher A, Westermark B and Heldin CH. Differential effects of the various isoforms of platelet-derived growth factor on chemotaxis of fibroblasts, monocytes, and granulocytes. *J Clin Invest* 85: 916-920, 1990.
172. Lindqvist A, Nilsson BO, Ekblad E and Hellstrand P. Platelet-derived growth factor receptors expressed in response to injury of differentiated vascular smooth muscle in vitro: effects on Ca2+ and growth signals. *Acta Physiol Scand* 173: 175-184, 2001.
173. Hollenbeck ST, Nelson PR, Yamamura S, Faries PL, Liu B and Kent KC. Intracellular calcium transients are necessary for platelet-derived growth factor but not extracellular matrix protein-induced vascular smooth muscle cell migration. *J Vasc Surg* 40: 351-358, 2004.
174. Pierce GF, Tarpley JE, Tseng J, Bready J, Chang D, Kenney WC, Rudolph R, Robson MC, Vande BJ, Berg, J, and Reid, P. Detection of platelet-derived growth factor (PDGF)-AA in actively healing human wounds treated with recombinant PDGF-BB and absence of PDGF in chronic nonhealing wounds. *J Clin Invest* 96: 1336-1350, 1995.
175. Langerak AW, De Laat PA, Van der Linden-Van Beurden CA, Delahaye M, Van Der Kwast TH, Hoogsteden HC, Benner R and Versnel MA. Expression of platelet-derived growth factor (PDGF) and PDGF receptors in human malignant mesothelioma in vitro and in vivo. *J Pathol* 178: 151-160, 1996.
176. Levitzki A. PDGF receptor kinase inhibitors for the treatment of restenosis. *Cardiovasc Res* 65: 581-586, 2005.
177. Pennica D, King KL, Shaw KJ, Luis E, Rullamas J, Luoh SM, Darbonne WC, Knutzon DS, Yen R, and Chien, KR. Expression cloning of cardiotrophin 1, a cytokine that induces cardiac myocyte hypertrophy. *Proc Natl Acad Sci U S A* 92: 1142-1146, 1995.
178. Wollert KC and Chien KR. Cardiotrophin-1 and the role of gp130-dependent signaling pathways in cardiac growth and development. *J Mol Med* 75: 492-501, 1997.

179. Heinrich PC, Behrmann I, Muller-Newen G, Schaper F and Graeve L. Interleukin-6-type cytokine signalling through the gp130/Jak/STAT pathway. *Biochem J* 334 (Pt 2): 297-314, 1998.
180. Yin T, Taga T, Tsang ML, Yasukawa K, Kishimoto T and Yang YC. Involvement of IL-6 signal transducer gp130 in IL-11-mediated signal transduction. *J Immunol* 151: 2555-2561, 1993.
181. Guschin D, Rogers N, Briscoe J, Witthuhn B, Watling D, Horn F, Pellegrini S, Yasukawa K, Heinrich P, and Stark, GR. A major role for the protein tyrosine kinase JAK1 in the JAK/STAT signal transduction pathway in response to interleukin-6. *EMBO J* 14: 1421-1429, 1995.
182. Narazaki M, Witthuhn BA, Yoshida K, Silvennoinen O, Yasukawa K, Ihle JN, Kishimoto T and Taga T. Activation of JAK2 kinase mediated by the interleukin 6 signal transducer gp130. *Proc Natl Acad Sci U S A* 91: 2285-2289, 1994.
183. Zhong Z, Wen Z and Darnell JE, Jr. Stat3: a STAT family member activated by tyrosine phosphorylation in response to epidermal growth factor and interleukin-6. *Science* 264: 95-98, 1994.
184. Fujimoto M and Naka T. Regulation of cytokine signaling by SOCS family molecules. *Trends Immunol* 24: 659-666, 2003.
185. Luo C and Laaja P. Inhibitors of JAKs/STATs and the kinases: a possible new cluster of drugs. *Drug Discov Today* 9: 268-275, 2004.
186. Yasukawa H, Hoshijima M, Gu Y, Nakamura T, Pradervand S, Hanada T, Hanakawa Y, Yoshimura A, Ross J, Jr. and Chien KR. Suppressor of cytokine signaling-3 is a biomechanical stress-inducible gene that suppresses gp130-mediated cardiac myocyte hypertrophy and survival pathways. *J Clin Invest* 108: 1459-1467, 2001.
187. Calegari VC, Bezerra RM, Torsoni MA, Torsoni AS, Franchini KG, Saad MJ and Velloso LA. Suppressor of cytokine signaling 3 is induced by angiotensin II in heart and isolated cardiomyocytes, and participates in desensitization. *Endocrinology* 144: 4586-4596, 2003.
188. Heymann D and Rousselle AV. gp130 Cytokine family and bone cells. *Cytokine* 12: 1455-1468, 2000.
189. Richards CD, Langdon C, Deschamps P, Pennica D and Shaughnessy SG. Stimulation of osteoclast differentiation in vitro by mouse oncostatin M, leukaemia inhibitory factor, cardiotrophin-1 and interleukin 6: synergy with dexamethasone. *Cytokine* 12: 613-621, 2000.
190. Kuwahara K, Saito Y, Harada M, Ishikawa M, Ogawa E, Miyamoto Y, Hamanaka I, Kamitani S, Kajiyama N, Takahashi N, Nakagawa O, Masuda I and Nakao K. Involvement of cardiotrophin-1 in cardiac myocyte-nonmyocyte interactions during hypertrophy of rat cardiac myocytes in vitro. *Circulation* 100: 1116-1124, 1999.
191. Funamoto M, Hishinuma S, Fujio Y, Matsuda Y, Kunisada K, Oh H, Negoro S, Tone E, Kishimoto T and Yamauchi-Takihara K. Isolation and characterization of the murine cardiotrophin-1 gene: expression and norepinephrine-induced transcriptional activation. *J Mol Cell Cardiol* 32: 1275-1284, 2000.
192. Freed DH, Borowiec AM, Angelovska T and Dixon IM. Induction of protein synthesis in cardiac fibroblasts by cardiotrophin-1: integration of multiple signaling pathways. *Cardiovasc Res* 60: 365-375, 2003.

193. Tsuruda T, Jougasaki M, Boerrigter G, Huntley BK, Chen HH, D'Assoro AB, Lee SC, Larsen AM, Cataliotti A and Burnett JC, Jr. Cardiotrophin-1 stimulation of cardiac fibroblast growth: roles for glycoprotein 130/leukemia inhibitory factor receptor and the endothelin type A receptor. *Circ Res* 90: 128-134, 2002.
194. Ishikawa M, Saito Y, Miyamoto Y, Harada M, Kuwahara K, Ogawa E, Nakagawa O, Hamanaka I, Kajiyama N, Takahashi N, Masuda I, Hashimoto T, Sakai O, Hosoya T and Nakao K. A heart-specific increase in cardiotrophin-1 gene expression precedes the establishment of ventricular hypertrophy in genetically hypertensive rats. *J Hypertens* 17: 807-816, 1999.
195. Aoyama T, Takimoto Y, Pennica D, Inoue R, Shinoda E, Hattori R, Yui Y and Sasayama S. Augmented expression of cardiotrophin-1 and its receptor component, gp130, in both left and right ventricles after myocardial infarction in the rat. *J Mol Cell Cardiol* 32: 1821-1830, 2000.
196. Freed DH, Moon MC, Borowiec AM, Jones SC, Zahradka P and Dixon IM. Cardiotrophin-1: expression in experimental myocardial infarction and potential role in post-MI wound healing. *Mol Cell Biochem* 254: 247-256, 2003.
197. Jin H, Yang R, Keller GA, Ryan A, Ko A, Finkle D, Swanson TA, Li W, Pennica D, Wood WI and Paoni NF. In vivo effects of cardiotrophin-1. *Cytokine* 8: 920-926, 1996.
198. Wollert KC, Taga T, Saito M, Narazaki M, Kishimoto T, Glembotski CC, Vernallis AB, Heath JK, Pennica D, Wood WI and Chien KR. Cardiotrophin-1 activates a distinct form of cardiac muscle cell hypertrophy. Assembly of sarcomeric units in series VIA gp130/leukemia inhibitory factor receptor-dependent pathways. *J Biol Chem* 271: 9535-9545, 1996.
199. Bristow MR and Long CS. Cardiotrophin-1 in heart failure. *Circulation* 106: 1430-1432, 2002.
200. Hishinuma S, Funamoto M, Fujio Y, Kunisada K and Yamauchi-Takihara K. Hypoxic stress induces cardiotrophin-1 expression in cardiac myocytes. *Biochem Biophys Res Commun* 264: 436-440, 1999.
201. Pan J, Fukuda K, Saito M, Matsuzaki J, Kodama H, Sano M, Takahashi T, Kato T and Ogawa S. Mechanical stretch activates the JAK/STAT pathway in rat cardiomyocytes. *Circ Res* 84: 1127-1136, 1999.
202. Sano M, Fukuda K, Kodama H, Pan J, Saito M, Matsuzaki J, Takahashi T, Makino S, Kato T and Ogawa S. Interleukin-6 family of cytokines mediate angiotensin II-induced cardiac hypertrophy in rodent cardiomyocytes. *J Biol Chem* 275: 29717-29723, 2000.
203. Bordet T, Lesbordes JC, Rouhani S, Castelnau-Ptakhine L, Schmalbruch H, Haase G and Kahn A. Protective effects of cardiotrophin-1 adenoviral gene transfer on neuromuscular degeneration in transgenic ALS mice. *Hum Mol Genet* 10: 1925-1933, 2001.
204. Kuwahara K, Saito Y, Kishimoto I, Miyamoto Y, Harada M, Ogawa E, Hamanaka I, Kajiyama N, Takahashi N, Izumi T, Kawakami R and Nakao K. Cardiotrophin-1 phosphorylates akt and BAD, and prolongs cell survival via a PI3K-dependent pathway in cardiac myocytes. *J Mol Cell Cardiol* 32: 1385-1394, 2000.
205. Liao Z, Brar BK, Cai Q, Stephanou A, O'Leary RM, Pennica D, Yellon DM and Latchman DS. Cardiotrophin-1 (CT-1) can protect the adult heart from injury when added both prior to ischaemia and at reperfusion. *Cardiovasc Res* 53: 902-910, 2002.

206. Brar BK, Stephanou A, Pennica D and Latchman DS. CT-1 mediated cardioprotection against ischaemic re-oxygenation injury is mediated by PI3 kinase, Akt and MEK1/2 pathways. *Cytokine* 16: 93-96, 2001.
207. Brar BK, Stephanou A, Liao Z, O'Leary RM, Pennica D, Yellon DM and Latchman DS. Cardiotrophin-1 can protect cardiac myocytes from injury when added both prior to simulated ischaemia and at reoxygenation. *Cardiovasc Res* 51: 265-274, 2001.
208. Zou Y, Takano H, Mizukami M, Akazawa H, Qin Y, Toko H, Sakamoto M, Minamino T, Nagai T and Komuro I. Leukemia inhibitory factor enhances survival of cardiomyocytes and induces regeneration of myocardium after myocardial infarction. *Circulation* 108: 748-753, 2003.
209. Hamanaka I, Saito Y, Nishikimi T, Magaribuchi T, Kamitani S, Kuwahara K, Ishikawa M, Miyamoto Y, Harada M, Ogawa E, Kajiyama N, Takahashi N, Izumi T, Shirakami G, Mori K, Inobe Y, Kishimoto I, Masuda I, Fukuda K and Nakao K. Effects of cardiotrophin-1 on hemodynamics and endocrine function of the heart. *Am J Physiol Heart Circ Physiol* 279: H388-H396, 2000.
210. Gospodarowicz D. Localisation of a fibroblast growth factor and its effect alone and with hydrocortisone on 3T3 cell growth. *Nature* 249: 123-127, 1974.
211. Chen CH, Poucher SM, Lu J and Henry PD. Fibroblast growth factor 2: from laboratory evidence to clinical application. *Curr Vasc Pharmacol* 2: 33-43, 2004.
212. Gospodarowicz D, Weseman J, Moran JS and Lindstrom J. Effect of fibroblast growth factor on the division and fusion of bovine myoblasts. *J Cell Biol* 70: 395-405, 1976.
213. Szebenyi G and Fallon JF. Fibroblast growth factors as multifunctional signaling factors. *Int Rev Cytol* 185: 45-106, 1999.
214. The fibroblast growth factor family. Nomenclature meeting report and recommendations. January 17, 1991. *Ann N Y Acad Sci* 638: xiii-xxvi, 1991.
215. Wiedlocha A and Sorensen V. Signaling, internalization, and intracellular activity of fibroblast growth factor. *Curr Top Microbiol Immunol* 286: 45-79, 2004.
216. Cordon-Cardo C, Vlodavsky I, Haimovitz-Friedman A, Hicklin D and Fuks Z. Expression of basic fibroblast growth factor in normal human tissues. *Lab Invest* 63: 832-840, 1990.
217. Galzie Z, Kinsella AR and Smith JA. Fibroblast growth factors and their receptors. *Biochem Cell Biol* 75: 669-685, 1997.
218. Vagner S, Gensac MC, Maret A, Bayard F, Amalric F, Prats H and Prats AC. Alternative translation of human fibroblast growth factor 2 mRNA occurs by internal entry of ribosomes. *Mol Cell Biol* 15: 35-44, 1995.
219. Patry V, Bugler B, Amalric F, Prome JC and Prats H. Purification and characterization of the 210-amino acid recombinant basic fibroblast growth factor form (FGF-2). *FEBS Lett* 349: 23-28, 1994.
220. Bugler B, Amalric F and Prats H. Alternative initiation of translation determines cytoplasmic or nuclear localization of basic fibroblast growth factor. *Mol Cell Biol* 11: 573-577, 1991.
221. Florkiewicz RZ and Sommer A. Human basic fibroblast growth factor gene encodes four polypeptides: three initiate translation from non-AUG codons. *Proc Natl Acad Sci U S A* 86: 3978-3981, 1989.
222. Renko M, Quarto N, Morimoto T and Rifkin DB. Nuclear and cytoplasmic localization of different basic fibroblast growth factor species. *J Cell Physiol* 144: 108-114, 1990.

223. Foletti A, Vuadens F and Beermann F. Nuclear localization of mouse fibroblast growth factor 2 requires N-terminal and C-terminal sequences. *Cell Mol Life Sci* 60: 2254-2265, 2003.
224. Quarto N, Finger FP and Rifkin DB. The NH2-terminal extension of high molecular weight bFGF is a nuclear targeting signal. *J Cell Physiol* 147: 311-318, 1991.
225. Vlodavsky I, Folkman J, Sullivan R, Fridman R, Ishai-Michaeli R, Sasse J and Klagsbrun M. Endothelial cell-derived basic fibroblast growth factor: synthesis and deposition into subendothelial extracellular matrix. *Proc Natl Acad Sci U S A* 84: 2292-2296, 1987.
226. Bikfalvi A, Klein S, Pintucci G, Quarto N, Mignatti P and Rifkin DB. Differential modulation of cell phenotype by different molecular weight forms of basic fibroblast growth factor: possible intracellular signaling by the high molecular weight forms. *J Cell Biol* 129: 233-243, 1995.
227. Mignatti P, Morimoto T and Rifkin DB. Basic fibroblast growth factor, a protein devoid of secretory signal sequence, is released by cells via a pathway independent of the endoplasmic reticulum-Golgi complex. *J Cell Physiol* 151: 81-93, 1992.
228. Florkiewicz RZ, Majack RA, Buechler RD and Florkiewicz E. Quantitative export of FGF-2 occurs through an alternative, energy-dependent, non-ER/Golgi pathway. *J Cell Physiol* 162: 388-399, 1995.
229. Bikfalvi A, Klein S, Pintucci G and Rifkin DB. Biological roles of fibroblast growth factor-2. *Endocr Rev* 18: 26-45, 1997.
230. Moscatelli D. High and low affinity binding sites for basic fibroblast growth factor on cultured cells: absence of a role for low affinity binding in the stimulation of plasminogen activator production by bovine capillary endothelial cells. *J Cell Physiol* 131: 123-130, 1987.
231. Yayon A, Klagsbrun M, Esko JD, Leder P and Ornitz DM. Cell surface, heparin-like molecules are required for binding of basic fibroblast growth factor to its high affinity receptor. *Cell* 64: 841-848, 1991.
232. Kesavan K, Lobel-Rice K, Sun W, Lapadat R, Webb S, Johnson GL and Garrington TP. MEKK2 regulates the coordinate activation of ERK5 and JNK in response to FGF-2 in fibroblasts. *J Cell Physiol* 199: 140-148, 2004.
233. Bossard C, Laurell H, Van den BL, Meunier S, Zanibellato C and Prats H. Translokin is an intracellular mediator of FGF-2 trafficking. *Nat Cell Biol* 5: 433-439, 2003.
234. Bonnet H, Filhol O, Truchet I, Brethenou P, Cochet C, Amalric F and Bouche G. Fibroblast growth factor-2 binds to the regulatory beta subunit of CK2 and directly stimulates CK2 activity toward nucleolin. *J Biol Chem* 271: 24781-24787, 1996.
235. Gospodarowicz D, Ferrara N, Schweigerer L and Neufeld G. Structural characterization and biological functions of fibroblast growth factor. *Endocr Rev* 8: 95-114, 1987.
236. Kardami E, Liu L and Doble BW. Basic fibroblast growth factor in cultured cardiac myocytes. *Ann N Y Acad Sci* 638: 244-255, 1991.
237. Akimoto S, Ishikawa O, Iijima C and Miyachi Y. Expression of basic fibroblast growth factor and its receptor by fibroblast, macrophages and mast cells in hypertrophic scar. *Eur J Dermatol* 9: 357-362, 1999.
238. Liu L, Pasumarthi KB, Padua RR, Massaeli H, Fandrich RR, Pierce GN, Cattini PA and Kardami E. Adult cardiomyocytes express functional high-affinity receptors for basic fibroblast growth factor. *Am J Physiol* 268: H1927-H1938, 1995.

239. Kaye DM, Kelly RA and Smith TW. Cytokines and cardiac hypertrophy: roles of angiotensin II and basic fibroblast growth factor. *Clin Exp Pharmacol Physiol Suppl* 3: S136-S141, 1996.
240. Abramov D, Erez E, Dagan O, Abramov Y, Pearl E, Veena G, Katz J, Vidne BA and Barak V. Increased levels of basic fibroblast growth factor are found in the cross-clamped heart during cardiopulmonary bypass. *Can J Cardiol* 16: 313-318, 2000.
241. Weihrauch D, Tessmer J, Warltier DC and Chilian WM. Repetitive coronary artery occlusions induce release of growth factors into the myocardial interstitium. *Am J Physiol* 275: H969-H976, 1998.
242. Jiang ZS, Srisakuldee W, Soulet F, Bouche G and Kardami E. Non-angiogenic FGF-2 protects the ischemic heart from injury, in the presence or absence of reperfusion. *Cardiovasc Res* 62: 154-166, 2004.
243. Yajima S, Ishikawa M, Kubota T, Moroi M, Sugi K and Namiki A. Intramyocardial injection of fibroblast growth factor-2 plus heparin suppresses cardiac failure progression in rats with hypertensive heart disease. *Int Heart J* 46: 289-301, 2005.
244. Horrigan MC, MacIsaac AI, Nicolini FA, Vince DG, Lee P, Ellis SG and Topol EJ. Reduction in myocardial infarct size by basic fibroblast growth factor after temporary coronary occlusion in a canine model. *Circulation* 94: 1927-1933, 1996.
245. Nishida S, Nagamine H, Tanaka Y and Watanabe G. Protective effect of basic fibroblast growth factor against myocyte death and arrhythmias in acute myocardial infarction in rats. *Circ J* 67: 334-339, 2003.
246. Doble BW and Kardami E. Basic fibroblast growth factor stimulates connexin-43 expression and intercellular communication of cardiac fibroblasts. *Mol Cell Biochem* 143: 81-87, 1995.
247. Jiang ZS, Padua RR, Ju H, Doble BW, Jin Y, Hao J, Cattini PA, Dixon IM and Kardami E. Acute protection of ischemic heart by FGF-2: involvement of FGF-2 receptors and protein kinase C. *Am J Physiol Heart Circ Physiol* 282: H1071-H1080, 2002.
248. Sheikh F, Sontag DP, Fandrich RR, Kardami E and Cattini PA. Overexpression of FGF-2 increases cardiac myocyte viability after injury in isolated mouse hearts. *Am J Physiol Heart Circ Physiol* 280: H1039-H1050, 2001.
249. Pellieux C, Foletti A, Peduto G, Aubert JF, Nussberger J, Beermann F, Brunner HR and Pedrazzini T. Dilated cardiomyopathy and impaired cardiac hypertrophic response to angiotensin II in mice lacking FGF-2. *J Clin Invest* 108: 1843-1851, 2001.
250. Lazarous DF, Scheinowitz M, Shou M, Hodge E, Rajanayagam S, Hunsberger S, Robison WG, Jr., Stiber JA, Correa R, Epstein SE and . Effects of chronic systemic administration of basic fibroblast growth factor on collateral development in the canine heart. *Circulation* 91: 145-153, 1995.
251. Schultz JE, Witt SA, Nieman ML, Reiser PJ, Engle SJ, Zhou M, Pawlowski SA, Lorenz JN, Kimball TR and Doetschman T. Fibroblast growth factor-2 mediates pressure-induced hypertrophic response. *J Clin Invest* 104: 709-719, 1999.
252. Hoerstrup SP, Zund G, Schnell AM, Kolb SA, Visjager JF, Schoeberlein A and Turina M. Optimized growth conditions for tissue engineering of human cardiovascular structures. *Int J Artif Organs* 23: 817-823, 2000.
253. Pickering JG, Ford CM, Tang B and Chow LH. Coordinated effects of fibroblast growth factor-2 on expression of fibrillar collagens, matrix metalloproteinases, and tissue inhibitors of matrix metalloproteinases by human vascular smooth muscle cells. Evidence

for repressed collagen production and activated degradative capacity. *Arterioscler Thromb Vasc Biol* 17: 475-482, 1997.
254. Spyrou GE and Naylor IL. The effect of basic fibroblast growth factor on scarring. *Br J Plast Surg* 55: 275-282, 2002.
255. Van Haastert PJ and Devreotes PN. Chemotaxis: signalling the way forward. *Nat Rev Mol Cell Biol* 5: 626-634, 2004.
256. Ridley AJ, Schwartz MA, Burridge K, Firtel RA, Ginsberg MH, Borisy G, Parsons JT and Horwitz AR. Cell migration: integrating signals from front to back. *Science* 302: 1704-1709, 2003.
257. Chicurel M. Cell biology. Cell migration research is on the move. *Science* 295: 606-609, 2002.
258. Cameron VA, Rademaker MT, Ellmers LJ, Espiner EA, Nicholls MG and Richards AM. Atrial (ANP) and brain natriuretic peptide (BNP) expression after myocardial infarction in sheep: ANP is synthesized by fibroblasts infiltrating the infarct. *Endocrinology* 141: 4690-4697, 2000.
259. Dunn GA and Jones GE. Cell motility under the microscope: Vorsprung durch Technik. *Nat Rev Mol Cell Biol* 5: 667-672, 2004.
260. Wells A, Gupta K, Chang P, Swindle S, Glading A and Shiraha H. Epidermal growth factor receptor-mediated motility in fibroblasts. *Microsc Res Tech* 43: 395-411, 1998.
261. Wong MM and Fish EN. Chemokines: attractive mediators of the immune response. *Semin Immunol* 15: 5-14, 2003.
262. Kole TP, Tseng Y, Huang L, Katz JL and Wirtz D. Rho kinase regulates the intracellular micromechanical response of adherent cells to rho activation. *Mol Biol Cell* 15: 3475-3484, 2004.
263. Kole TP, Tseng Y, Jiang I, Katz JL and Wirtz D. Intracellular mechanics of migrating fibroblasts. *Mol Biol Cell* 16: 328-338, 2005.
264. Brundage RA, Fogarty KE, Tuft RA and Fay FS. Calcium gradients underlying polarization and chemotaxis of eosinophils. *Science* 254: 703-706, 1991.
265. Cramer LP, Siebert M and Mitchison TJ. Identification of novel graded polarity actin filament bundles in locomoting heart fibroblasts: implications for the generation of motile force. *J Cell Biol* 136: 1287-1305, 1997.
266. Huang C, Liu J, Haudenschild CC and Zhan X. The role of tyrosine phosphorylation of cortactin in the locomotion of endothelial cells. *J Biol Chem* 273: 25770-25776, 1998.
267. Kaksonen M, Peng HB and Rauvala H. Association of cortactin with dynamic actin in lamellipodia and on endosomal vesicles. *J Cell Sci* 113 Pt 24: 4421-4426, 2000.
268. Lua BL and Low BC. Cortactin phosphorylation as a switch for actin cytoskeletal network and cell dynamics control. *FEBS Lett* 579: 577-585, 2005.
269. Patel AS, Schechter GL, Wasilenko WJ and Somers KD. Overexpression of EMS1/cortactin in NIH3T3 fibroblasts causes increased cell motility and invasion in vitro. *Oncogene* 16: 3227-3232, 1998.
270. Weed SA and Parsons JT. Cortactin: coupling membrane dynamics to cortical actin assembly. *Oncogene* 20: 6418-6434, 2001.
271. Takenawa T and Miki H. WASP and WAVE family proteins: key molecules for rapid rearrangement of cortical actin filaments and cell movement. *J Cell Sci* 114: 1801-1809, 2001.

272. Welch MD. The world according to Arp: regulation of actin nucleation by the Arp2/3 complex. *Trends Cell Biol* 9: 423-427, 1999.
273. Sheetz MP, Felsenfeld D, Galbraith CG and Choquet D. Cell migration as a five-step cycle. *Biochem Soc Symp* 65: 233-243, 1999.
274. Burridge K, Fath K, Kelly T, Nuckolls G and Turner C. Focal adhesions: transmembrane junctions between the extracellular matrix and the cytoskeleton. *Annu Rev Cell Biol* 4: 487-525, 1988.
275. Rodriguez-Fernandez JL. Why do so many stimuli induce tyrosine phosphorylation of FAK? *Bioessays* 21: 1069-1075, 1999.
276. Gu J and Taniguchi N. Regulation of integrin functions by N-glycans. *Glycoconj J* 21: 9-15, 2004.
277. Schwartz MA, Both G and Lechene C. Effect of cell spreading on cytoplasmic pH in normal and transformed fibroblasts. *Proc Natl Acad Sci U S A* 86: 4525-4529, 1989.
278. Schwartz MA. Spreading of human endothelial cells on fibronectin or vitronectin triggers elevation of intracellular free calcium. *J Cell Biol* 120: 1003-1010, 1993.
279. Shen Y and Schaller MD. Focal adhesion targeting: the critical determinant of FAK regulation and substrate phosphorylation. *Mol Biol Cell* 10: 2507-2518, 1999.
280. Pelham RJ, Jr. and Wang Y. Cell locomotion and focal adhesions are regulated by substrate flexibility. *Proc Natl Acad Sci U S A* 94: 13661-13665, 1997.
281. Tilghman RW, Slack-Davis JK, Sergina N, Martin KH, Iwanicki M, Hershey ED, Beggs HE, Reichardt LF and Parsons JT. Focal adhesion kinase is required for the spatial organization of the leading edge in migrating cells. *J Cell Sci* 118: 2613-2623, 2005.
282. Calalb MB, Polte TR and Hanks SK. Tyrosine phosphorylation of focal adhesion kinase at sites in the catalytic domain regulates kinase activity: a role for Src family kinases. *Mol Cell Biol* 15: 954-963, 1995.
283. Hauck CR, Hsia DA and Schlaepfer DD. The focal adhesion kinase--a regulator of cell migration and invasion. *IUBMB Life* 53: 115-119, 2002.
284. Galbraith CG and Sheetz MP. A micromachined device provides a new bend on fibroblast traction forces. *Proc Natl Acad Sci U S A* 94: 9114-9118, 1997.
285. Evans E, Leung A and Zhelev D. Synchrony of cell spreading and contraction force as phagocytes engulf large pathogens. *J Cell Biol* 122: 1295-1300, 1993.
286. Babu GJ, Warshaw DM and Periasamy M. Smooth muscle myosin heavy chain isoforms and their role in muscle physiology. *Microsc Res Tech* 50: 532-540, 2000.
287. Chin ER. Role of Ca2+/calmodulin-dependent kinases in skeletal muscle plasticity. *J Appl Physiol* 99: 414-423, 2005.
288. Besson A, Gurian-West M, Schmidt A, Hall A and Roberts JM. p27Kip1 modulates cell migration through the regulation of RhoA activation. *Genes Dev* 18: 862-876, 2004.
289. Palecek SP, Schmidt CE, Lauffenburger DA and Horwitz AF. Integrin dynamics on the tail region of migrating fibroblasts. *J Cell Sci* 109 (Pt 5): 941-952, 1996.
290. Regen CM and Horwitz AF. Dynamics of beta 1 integrin-mediated adhesive contacts in motile fibroblasts. *J Cell Biol* 119: 1347-1359, 1992.
291. Cox EA and Huttenlocher A. Regulation of integrin-mediated adhesion during cell migration. *Microsc Res Tech* 43: 412-419, 1998.
292. Schlaepfer DD, Mitra SK and Ilic D. Control of motile and invasive cell phenotypes by focal adhesion kinase. *Biochim Biophys Acta* 1692: 77-102, 2004.

293. Tejero-Trujeque R. Understanding the final stages of wound contraction. *J Wound Care* 10: 259-264, 2001.
294. Tejero-Trujeque R. How do fibroblasts interact with the extracellular matrix in wound contraction? *J Wound Care* 10: 237-242, 2001.
295. Ehrlich HP and Rajaratnam JB. Cell locomotion forces versus cell contraction forces for collagen lattice contraction: an in vitro model of wound contraction. *Tissue Cell* 22: 407-417, 1990.
296. Norman D. An exploration of two opposing theories of wound contraction. *J Wound Care* 13: 138-140, 2004.
297. Gabbiani G, Hirschel BJ, Ryan GB, Statkov PR and Majno G. Granulation tissue as a contractile organ. A study of structure and function. *J Exp Med* 135: 719-734, 1972.
298. Darby I, Skalli O and Gabbiani G. Alpha-smooth muscle actin is transiently expressed by myofibroblasts during experimental wound healing. *Lab Invest* 63: 21-29, 1990.
299. Skalli O, Ropraz P, Trzeciak A, Benzonana G, Gillessen D and Gabbiani G. A monoclonal antibody against alpha-smooth muscle actin: a new probe for smooth muscle differentiation. *J Cell Biol* 103: 2787-2796, 1986.
300. Ronnov-Jessen L and Petersen OW. Induction of alpha-smooth muscle actin by transforming growth factor-beta 1 in quiescent human breast gland fibroblasts. Implications for myofibroblast generation in breast neoplasia. *Lab Invest* 68: 696-707, 1993.
301. Golias CH, Charalabopoulos A and Charalabopoulos K. Cell proliferation and cell cycle control: a mini review. *Int J Clin Pract* 58: 1134-1141, 2004.
302. Heichman KA and Roberts JM. Rules to replicate by. *Cell* 79: 557-562, 1994.
303. Pardee AB. G1 events and regulation of cell proliferation. *Science* 246: 603-608, 1989.
304. Stevens C and La Thangue NB. E2F and cell cycle control: a double-edged sword. *Arch Biochem Biophys* 412: 157-169, 2003.
305. Tyson JJ, Csikasz-Nagy A and Novak B. The dynamics of cell cycle regulation. *Bioessays* 24: 1095-1109, 2002.
306. Stopak D and Harris AK. Connective tissue morphogenesis by fibroblast traction. I. Tissue culture observations. *Dev Biol* 90: 383-398, 1982.
307. Burridge K. Are stress fibres contractile? *Nature* 294: 691-692, 1981.
308. Parizi M, Howard EW and Tomasek JJ. Regulation of LPA-promoted myofibroblast contraction: role of Rho, myosin light chain kinase, and myosin light chain phosphatase. *Exp Cell Res* 254: 210-220, 2000.
309. Katoh K, Kano Y, Amano M, Onishi H, Kaibuchi K and Fujiwara K. Rho-kinase--mediated contraction of isolated stress fibers. *J Cell Biol* 153: 569-584, 2001.
310. Cukierman E, Pankov R, Stevens DR and Yamada KM. Taking cell-matrix adhesions to the third dimension. *Science* 294: 1708-1712, 2001.
311. Grinnell F. Fibroblasts, myofibroblasts, and wound contraction. *J Cell Biol* 124: 401-404, 1994.
312. Grinnell F. Fibroblast-collagen-matrix contraction: growth-factor signalling and mechanical loading. *Trends Cell Biol* 10: 362-365, 2000.
313. Rosenfeldt H and Grinnell F. Fibroblast quiescence and the disruption of ERK signaling in mechanically unloaded collagen matrices. *J Biol Chem* 275: 3088-3092, 2000.

314. Arora PD, Narani N and McCulloch CA. The compliance of collagen gels regulates transforming growth factor-beta induction of alpha-smooth muscle actin in fibroblasts. *Am J Pathol* 154: 871-882, 1999.
315. Mochitate K, Pawelek P and Grinnell F. Stress relaxation of contracted collagen gels: disruption of actin filament bundles, release of cell surface fibronectin, and down-regulation of DNA and protein synthesis. *Exp Cell Res* 193: 198-207, 1991.
316. Cole K and Kohn E. Calcium-mediated signal transduction: biology, biochemistry, and therapy. *Cancer Metastasis Rev* 13: 31-44, 1994.
317. Curry FE. Modulation of venular microvessel permeability by calcium influx into endothelial cells. *FASEB J* 6: 2456-2466, 1992.
318. Luckhoff A and Busse R. Calcium influx into endothelial cells and formation of endothelium-derived relaxing factor is controlled by the membrane potential. *Pflugers Arch* 416: 305-311, 1990.
319. Van Den Brink GR, Bloemers SM, Van Den BB, Tertoolen LG, Van Deventer SJ and Peppelenbosch MP. Study of calcium signaling in non-excitable cells. *Microsc Res Tech* 46: 418-433, 1999.
320. Bers DM. Cardiac excitation-contraction coupling. *Nature* 415: 198-205, 2002.
321. Ringer S. A further contribution regarding the influence of the different constituents of the blood on the contraction of the heart. *The Journal of Physiology* 2: 251-272, 1883.
322. Berridge MJ, Bootman MD and Lipp P. Calcium--a life and death signal. *Nature* 395: 645-648, 1998.
323. McCarron JG, Bradley KN, MacMillan D, Chalmers S and Muir TC. The sarcoplasmic reticulum, Ca2+ trapping, and wave mechanisms in smooth muscle. *News Physiol Sci* 19: 138-147, 2004.
324. Clapham DE. Calcium signaling. *Cell* 80: 259-268, 1995.
325. Venkatachalam K, Zheng F and Gill DL. Control of TRPC and store-operated channels by protein kinase C. *Novartis Found Symp* 258: 172-185, 2004.
326. Huber PA. Caldesmon. *Int J Biochem Cell Biol* 29: 1047-1051, 1997.
327. Kamm KE and Stull JT. Dedicated myosin light chain kinases with diverse cellular functions. *J Biol Chem* 276: 4527-4530, 2001.
328. Carragher NO and Frame MC. Calpain: a role in cell transformation and migration. *Int J Biochem Cell Biol* 34: 1539-1543, 2002.
329. Glading A, Lauffenburger DA and Wells A. Cutting to the chase: calpain proteases in cell motility. *Trends Cell Biol* 12: 46-54, 2002.
330. Sun HQ, Yamamoto M, Mejillano M and Yin HL. Gelsolin, a multifunctional actin regulatory protein. *J Biol Chem* 274: 33179-33182, 1999.
331. Zitt C, Halaszovich CR and Luckhoff A. The TRP family of cation channels: probing and advancing the concepts on receptor-activated calcium entry. *Prog Neurobiol* 66: 243-264, 2002.
332. Cosens DJ and Manning A. Abnormal electroretinogram from a Drosophila mutant. *Nature* 224: 285-287, 1969.
333. Montell C and Rubin GM. Molecular characterization of the Drosophila trp locus: a putative integral membrane protein required for phototransduction. *Neuron* 2: 1313-1323, 1989.
334. Hardie RC and Minke B. The trp gene is essential for a light-activated Ca2+ channel in Drosophila photoreceptors. *Neuron* 8: 643-651, 1992.

335. Phillips AM, Bull A and Kelly LE. Identification of a Drosophila gene encoding a calmodulin-binding protein with homology to the trp phototransduction gene. *Neuron* 8: 631-642, 1992.
336. Huang CL. The transient receptor potential superfamily of ion channels. *J Am Soc Nephrol* 15: 1690-1699, 2004.
337. Tominaga M, Caterina MJ, Malmberg AB, Rosen TA, Gilbert H, Skinner K, Raumann BE, Basbaum AI and Julius D. The cloned capsaicin receptor integrates multiple pain-producing stimuli. *Neuron* 21: 531-543, 1998.
338. Liu D and Liman ER. Intracellular Ca2+ and the phospholipid PIP2 regulate the taste transduction ion channel TRPM5. *Proc Natl Acad Sci U S A* 100: 15160-15165, 2003.
339. Parekh AB and Penner R. Store depletion and calcium influx. *Physiol Rev* 77: 901-930, 1997.
340. Inoue R, Okada T, Onoue H, Hara Y, Shimizu S, Naitoh S, Ito Y and Mori Y. The transient receptor potential protein homologue TRP6 is the essential component of vascular alpha(1)-adrenoceptor-activated Ca(2+)-permeable cation channel. *Circ Res* 88: 325-332, 2001.
341. Tiruppathi C, Freichel M, Vogel SM, Paria BC, Mehta D, Flockerzi V and Malik AB. Impairment of store-operated Ca2+ entry in TRPC4(-/-) mice interferes with increase in lung microvascular permeability. *Circ Res* 91: 70-76, 2002.
342. Pulver RA, Rose-Curtis P, Roe MW, Wellman GC and Lounsbury KM. Store-operated Ca2+ entry activates the CREB transcription factor in vascular smooth muscle. *Circ Res* 94: 1351-1358, 2004.
343. Putney JW, Jr. A model for receptor-regulated calcium entry. *Cell Calcium* 7: 1-12, 1986.
344. Casteels R and Droogmans G. Exchange characteristics of the noradrenaline-sensitive calcium store in vascular smooth muscle cells or rabbit ear artery. *J Physiol* 317: 263-279, 1981.
345. Thastrup O, Dawson AP, Scharff O, Foder B, Cullen PJ, Drobak BK, Bjerrum PJ, Christensen SB and Hanley MR. Thapsigargin, a novel molecular probe for studying intracellular calcium release and storage. *Agents Actions* 27: 17-23, 1989.
346. Takemura H, Hughes AR, Thastrup O and Putney JW, Jr. Activation of calcium entry by the tumor promoter thapsigargin in parotid acinar cells. Evidence that an intracellular calcium pool and not an inositol phosphate regulates calcium fluxes at the plasma membrane. *J Biol Chem* 264: 12266-12271, 1989.
347. Parekh AB, Terlau H and Stuhmer W. Depletion of InsP3 stores activates a Ca2+ and K+ current by means of a phosphatase and a diffusible messenger. *Nature* 364: 814-818, 1993.
348. Randriamampita C and Tsien RY. Emptying of intracellular Ca2+ stores releases a novel small messenger that stimulates Ca2+ influx. *Nature* 364: 809-814, 1993.
349. Irvine RF. 'Quantal' Ca2+ release and the control of Ca2+ entry by inositol phosphates--a possible mechanism. *FEBS Lett* 263: 5-9, 1990.
350. Patterson RL, van Rossum DB and Gill DL. Store-operated Ca2+ entry: evidence for a secretion-like coupling model. *Cell* 98: 487-499, 1999.
351. Jin M, Defoe DM and Wondergem R. Hepatocyte growth factor/scatter factor stimulates Ca2+-activated membrane K+ current and migration of MDCK II cells. *J Membr Biol* 191: 77-86, 2003.

352. Rao JN, Platoshyn O, Li L, Guo X, Golovina VA, Yuan JX and Wang JY. Activation of K(+) channels and increased migration of differentiated intestinal epithelial cells after wounding. *Am J Physiol Cell Physiol* 282: C885-C898, 2002.
353. Reinhardt J, Golenhofen N, Pongs O, Oberleithner H and Schwab A. Migrating transformed MDCK cells are able to structurally polarize a voltage-activated K+ channel. *Proc Natl Acad Sci U S A* 95: 5378-5382, 1998.
354. Wang JY, Wang J, Golovina VA, Li L, Platoshyn O and Yuan JX. Role of K(+) channel expression in polyamine-dependent intestinal epithelial cell migration. *Am J Physiol Cell Physiol* 278: C303-C314, 2000.
355. Cook KK and Fadool DA. Two adaptor proteins differentially modulate the phosphorylation and biophysics of Kv1.3 ion channel by SRC kinase. *J Biol Chem* 277: 13268-13280, 2002.
356. Cayabyab FS and Schlichter LC. Regulation of an ERG K+ current by Src tyrosine kinase. *J Biol Chem* 277: 13673-13681, 2002.
357. Sachs F and Morris CE. Mechanosensitive ion channels in nonspecialized cells. *Rev Physiol Biochem Pharmacol* 132: 1-77, 1998.
358. Yang XC and Sachs F. Mechanically sensitive, nonselective cation channels. *EXS* 66: 79-92, 1993.
359. Kamkin A, Kiseleva I and Isenberg G. Activation and inactivation of a non-selective cation conductance by local mechanical deformation of acutely isolated cardiac fibroblasts. *Cardiovasc Res* 57: 793-803, 2003.
360. Kohl P, Kamkin AG, Kiseleva IS and Noble D. Mechanosensitive fibroblasts in the sino-atrial node region of rat heart: interaction with cardiomyocytes and possible role. *Exp Physiol* 79: 943-956, 1994.
361. Hu H and Sachs F. Stretch-activated ion channels in the heart. *J Mol Cell Cardiol* 29: 1511-1523, 1997.
362. Naruse K, Yamada T and Sokabe M. Involvement of SA channels in orienting response of cultured endothelial cells to cyclic stretch. *Am J Physiol* 274: H1532-H1538, 1998.
363. Kiseleva I, Kamkin A, Kohl P and Lab MJ. Calcium and mechanically induced potentials in fibroblasts of rat atrium. *Cardiovasc Res* 32: 98-111, 1996.
364. Gannier F, White E, Garnier and Le Guennec JY. A possible mechanism for large stretch-induced increase in [Ca2+]i in isolated guinea-pig ventricular myocytes. *Cardiovasc Res* 32: 158-167, 1996.
365. Yang XC and Sachs F. Block of stretch-activated ion channels in Xenopus oocytes by gadolinium and calcium ions. *Science* 243: 1068-1071, 1989.
366. Philipson KD, Longoni S and Ward R. Purification of the cardiac Na+-Ca2+ exchange protein. *Biochim Biophys Acta* 945: 298-306, 1988.
367. Nicoll DA, Longoni S and Philipson KD. Molecular cloning and functional expression of the cardiac sarcolemmal Na(+)-Ca2+ exchanger. *Science* 250: 562-565, 1990.
368. Blaustein MP and Lederer WJ. Sodium/calcium exchange: its physiological implications. *Physiol Rev* 79: 763-854, 1999.
369. Fujioka Y, Komeda M and Matsuoka S. Stoichiometry of Na+-Ca2+ exchange in inside-out patches excised from guinea-pig ventricular myocytes. *J Physiol* 523 Pt 2: 339-351, 2000.
370. Kang TM and Hilgemann DW. Multiple transport modes of the cardiac Na+/Ca2+ exchanger. *Nature* 427: 544-548, 2004.

371. Nicoll DA, Hryshko LV, Matsuoka S, Frank JS and Philipson KD. Mutation of amino acid residues in the putative transmembrane segments of the cardiac sarcolemmal Na+-Ca2+ exchanger. *J Biol Chem* 271: 13385-13391, 1996.
372. Schwarz EM and Benzer S. Calx, a Na-Ca exchanger gene of Drosophila melanogaster. *Proc Natl Acad Sci U S A* 94: 10249-10254, 1997.
373. Philipson KD and Nicoll DA. Sodium-calcium exchange: a molecular perspective. *Annu Rev Physiol* 62: 111-133, 2000.
374. Matsuoka S, Nicoll DA, Hryshko LV, Levitsky DO, Weiss JN and Philipson KD. Regulation of the cardiac Na(+)-Ca2+ exchanger by Ca2+. Mutational analysis of the Ca(2+)-binding domain. *J Gen Physiol* 105: 403-420, 1995.
375. Li Z, Matsuoka S, Hryshko LV, Nicoll DA, Bersohn MM, Burke EP, Lifton RP and Philipson KD. Cloning of the NCX2 isoform of the plasma membrane Na(+)-Ca2+ exchanger. *J Biol Chem* 269: 17434-17439, 1994.
376. Quednau BD, Nicoll DA and Philipson KD. Tissue specificity and alternative splicing of the Na+/Ca2+ exchanger isoforms NCX1, NCX2, and NCX3 in rat. *Am J Physiol* 272: C1250-C1261, 1997.
377. Lee SL, Yu AS and Lytton J. Tissue-specific expression of Na(+)-Ca2+ exchanger isoforms. *J Biol Chem* 269: 14849-14852, 1994.
378. White KE, Gesek FA and Friedman PA. Structural and functional analysis of Na+/Ca2+ exchange in distal convoluted tubule cells. *Am J Physiol* 271: F560-F570, 1996.
379. Schnetkamp PP, Basu DK and Szerencsei RT. Na+-Ca2+ exchange in bovine rod outer segments requires and transports K+. *Am J Physiol* 257: C153-C157, 1989.
380. Levesque PC, Leblanc N and Hume JR. Release of calcium from guinea pig cardiac sarcoplasmic reticulum induced by sodium-calcium exchange. *Cardiovasc Res* 28: 370-378, 1994.
381. Makino N, Dhruvarajan R, Elimban V, Beamish RE and Dhalla NS. Alterations of sarcolemmal Na+-Ca2+ exchange in catecholamine-induced cardiomyopathy. *Can J Cardiol* 1: 225-232, 1985.
382. Litwin SE and Bridge JH. Enhanced Na(+)-Ca2+ exchange in the infarcted heart. Implications for excitation-contraction coupling. *Circ Res* 81: 1083-1093, 1997.
383. Flesch M, Schwinger RH, Schiffer F, Frank K, Sudkamp M, Kuhn-Regnier F, Arnold G and Bohm M. Evidence for functional relevance of an enhanced expression of the Na(+)-Ca2+ exchanger in failing human myocardium. *Circulation* 94: 992-1002, 1996.
384. Gomez AM, Schwaller B, Porzig H, Vassort G, Niggli E and Egger M. Increased exchange current but normal Ca2+ transport via Na+-Ca2+ exchange during cardiac hypertrophy after myocardial infarction. *Circ Res* 91: 323-330, 2002.
385. Hurtado C and Pierce GN. Inhibition of Na(+)/H(+) exchange at the beginning of reperfusion is cardioprotective in isolated, beating adult cardiomyocytes. *J Mol Cell Cardiol* 32: 1897-1907, 2000.
386. Pierce GN and Czubryt MP. The contribution of ionic imbalance to ischemia/reperfusion-induced injury. *J Mol Cell Cardiol* 27: 53-63, 1995.
387. Arnon A, Hamlyn JM and Blaustein MP. Na(+) entry via store-operated channels modulates Ca(2+) signaling in arterial myocytes. *Am J Physiol Cell Physiol* 278: C163-C173, 2000.

388. Juhaszova M, Ambesi A, Lindenmayer GE, Bloch RJ and Blaustein MP. Na(+)-Ca2+ exchanger in arteries: identification by immunoblotting and immunofluorescence microscopy. *Am J Physiol* 266: C234-C242, 1994.
389. Moccia F, Berra-Romani R, Baruffi S, Spaggiari S, Signorelli S, Castelli L, Magistretti J, Taglietti V and Tanzi F. Ca2+ uptake by the endoplasmic reticulum Ca2+-ATPase in rat microvascular endothelial cells. *Biochem J* 364: 235-244, 2002.
390. Zhang S, Yuan JX, Barrett KE and Dong H. Role of Na+/Ca2+ exchange in regulating cytosolic Ca2+ in cultured human pulmonary artery smooth muscle cells. *Am J Physiol Cell Physiol* 288: C245-C252, 2005.
391. Schulze DH, Muqhal M, Lederer WJ and Ruknudin AM. Sodium/calcium exchanger (NCX1) macromolecular complex. *J Biol Chem* 278: 28849-28855, 2003.
392. Iwamoto T, Wakabayashi S, Imagawa T and Shigekawa M. Na+/Ca2+ exchanger overexpression impairs calcium signaling in fibroblasts: inhibition of the [Ca2+] increase at the cell periphery and retardation of cell adhesion. *Eur J Cell Biol* 76: 228-236, 1998.
393. Iwamoto T and Shigekawa M. Differential inhibition of Na+/Ca2+ exchanger isoforms by divalent cations and isothiourea derivative. *Am J Physiol* 275: C423-C430, 1998.
394. Karwatowska-Prokopczuk E, Nordberg JA, Li HL, Engler RL and Gottlieb RA. Effect of vacuolar proton ATPase on pHi, Ca2+, and apoptosis in neonatal cardiomyocytes during metabolic inhibition/recovery. *Circ Res* 82: 1139-1144, 1998.
395. Siegl PK, Cragoe EJ, Jr., Trumble MJ and Kaczorowski GJ. Inhibition of Na+/Ca2+ exchange in membrane vesicle and papillary muscle preparations from guinea pig heart by analogs of amiloride. *Proc Natl Acad Sci U S A* 81: 3238-3242, 1984.
396. Iwamoto T. Forefront of Na+/Ca2+ exchanger studies: molecular pharmacology of Na+/Ca2+ exchange inhibitors. *J Pharmacol Sci* 96: 27-32, 2004.
397. Iwamoto T and Kita S. Development and application of Na+/Ca2+ exchange inhibitors. *Mol Cell Biochem* 259: 157-161, 2004.
398. Amran MS, Homma N and Hashimoto K. Pharmacology of KB-R7943: a Na+-Ca2+ exchange inhibitor. *Cardiovasc Drug Rev* 21: 255-276, 2003.
399. Padua RR, Merle PL, Doble BW, Yu CH, Zahradka P, Pierce GN, Panagia V and Kardami E. FGF-2-induced negative inotropism and cardioprotection are inhibited by chelerythrine: involvement of sarcolemmal calcium-independent protein kinase C. *J Mol Cell Cardiol* 30: 2695-2709, 1998.
400. Brilla CG, Zhou G, Matsubara L and Weber KT. Collagen metabolism in cultured adult rat cardiac fibroblasts: response to angiotensin II and aldosterone. *J Mol Cell Cardiol* 26: 809-820, 1994.
401. Ju H, Hao J, Zhao S and Dixon IM. Antiproliferative and antifibrotic effects of mimosine on adult cardiac fibroblasts. *Biochim Biophys Acta* 1448: 51-60, 1998.
402. Rodriguez LG, Wu X and Guan J. Cell Migration: Developmental Methods and Protocols. In: Methods in Molecular Biology, edited by Guan J. Humana Press Inc, 2004, p. 23-29.
403. Richards KL and McCullough J. A modified microchamber method for chemotaxis and chemokinesis. *Immunol Commun* 13: 49-62, 1984.
404. Kim CH, Pelus LM, White JR and Broxmeyer HE. Differential chemotactic behavior of developing T cells in response to thymic chemokines. *Blood* 91: 4434-4443, 1998.
405. Jo DY, Rafii S, Hamada T and Moore MA. Chemotaxis of primitive hematopoietic cells in response to stromal cell-derived factor-1. *J Clin Invest* 105: 101-111, 2000.

406. Smith PK, Krohn RI, Hermanson GT, Mallia AK, Gartner FH, Provenzano MD, Fujimoto EK, Goeke NM, Olson BJ and Klenk DC. Measurement of protein using bicinchoninic acid. *Anal Biochem* 150: 76-85, 1985.
407. Collares-Buzato CB, McEwan GT, Jepson MA, Simmons NL and Hirst BH. Paracellular barrier and junctional protein distribution depend on basolateral extracellular Ca2+ in cultured epithelia. *Biochim Biophys Acta* 1222: 147-158, 1994.
408. Beeler TJ, Jona I and Martonosi A. The effect of ionomycin on calcium fluxes in sarcoplasmic reticulum vesicles and liposomes. *J Biol Chem* 254: 6229-6231, 1979.
409. Lui M, Chakraburtty K and Mehler AH. Partial reactions of aminoacyl-tRNA synthetases as functions of pH. *J Biol Chem* 253: 8061-8064, 1978.
410. Iwamoto T, Watano T and Shigekawa M. A novel isothiourea derivative selectively inhibits the reverse mode of Na+/Ca2+ exchange in cells expressing NCX1. *J Biol Chem* 271: 22391-22397, 1996.
411. Watano T, Kimura J, Morita T and Nakanishi H. A novel antagonist, No. 7943, of the Na+/Ca2+ exchange current in guinea-pig cardiac ventricular cells. *Br J Pharmacol* 119: 555-563, 1996.
412. Saitoh M, Ishikawa T, Matsushima S, Naka M and Hidaka H. Selective inhibition of catalytic activity of smooth muscle myosin light chain kinase. *J Biol Chem* 262: 7796-7801, 1987.
413. Cirillo M, Quinn SJ, Romero JR and Canessa ML. Regulation of Ca2+ transport by platelet-derived growth factor-BB in rat vascular smooth muscle cells. *Circ Res* 72: 847-856, 1993.
414. McDonald TF, Pelzer S, Trautwein W and Pelzer DJ. Regulation and modulation of calcium channels in cardiac, skeletal, and smooth muscle cells. *Physiol Rev* 74: 365-507, 1994.
415. He P and Curry FE. Albumin modulation of capillary permeability: role of endothelial cell [Ca2+]i. *Am J Physiol* 265: H74-H82, 1993.
416. He P, Zhang X and Curry FE. Ca2+ entry through conductive pathway modulates receptor-mediated increase in microvessel permeability. *Am J Physiol* 271: H2377-H2387, 1996.
417. Pagakis SN and Curry FE. Imaging of Ca2+ transients in endothelial cells of single perfused capillaries: correlation of peak [Ca2+]i with sites of macromolecule leakage. *Microcirculation* 1: 213-230, 1994.
418. Chilton L, Ohya S, Freed D, George E, Drobic V, Shibukawa Y, Maccannell KA, Imaizumi Y, Clark RB, Dixon IM and Giles WR. K+ currents regulate the resting membrane potential, proliferation, and contractile responses in ventricular fibroblasts and myofibroblasts. *Am J Physiol Heart Circ Physiol* 288: H2931-H2939, 2005.
419. Drobic V. *Effects of CT-1, TGF-Beta1, and PDGF on the proliferation of primary cardiac myofibroblasts and wound contraction in cell culture* (Dissertation). Winnipeg, Manitoba, Canada: Department of Physiology, Faculty of Medicine, University of Manitoba, 2005.
420. Seppa H, Grotendorst G, Seppa S, Schiffmann E and Martin GR. Platelet-derived growth factor in chemotactic for fibroblasts. *J Cell Biol* 92: 584-588, 1982.
421. Cospedal R, Abedi H and Zachary I. Platelet-derived growth factor-BB (PDGF-BB) regulation of migration and focal adhesion kinase phosphorylation in rabbit aortic

vascular smooth muscle cells: roles of phosphatidylinositol 3-kinase and mitogen-activated protein kinases. *Cardiovasc Res* 41: 708-721, 1999.
422. Grotendorst GR, Chang T, Seppa HE, Kleinman HK and Martin GR. Platelet-derived growth factor is a chemoattractant for vascular smooth muscle cells. *J Cell Physiol* 113: 261-266, 1982.
423. Nelson PR, Yamamura S and Kent KC. Platelet-derived growth factor and extracellular matrix proteins provide a synergistic stimulus for human vascular smooth muscle cell migration. *J Vasc Surg* 26: 104-112, 1997.
424. Dahlfors G, Chen Y, Wasteson M and Arnqvist HJ. PDGF-BB-induced DNA synthesis is delayed by angiotensin II in vascular smooth muscle cells. *Am J Physiol* 274: H1742-H1748, 1998.
425. Carver W, Molano I, Reaves TA, Borg TK and Terracio L. Role of the alpha 1 beta 1 integrin complex in collagen gel contraction in vitro by fibroblasts. *J Cell Physiol* 165: 425-437, 1995.
426. Gullberg D, Tingstrom A, Thuresson AC, Olsson L, Terracio L, Borg TK and Rubin K. Beta 1 integrin-mediated collagen gel contraction is stimulated by PDGF. *Exp Cell Res* 186: 264-272, 1990.
427. Zagai U, Fredriksson K, Rennard SI, Lundahl J and Skold CM. Platelets stimulate fibroblast-mediated contraction of collagen gels. *Respir Res* 4: 13, 2003.
428. Lijnen P, Petrov V and Fagard R. Transforming growth factor-beta 1-mediated collagen gel contraction by cardiac fibroblasts. *J Renin Angiotensin Aldosterone Syst* 4: 113-118, 2003.
429. Burgess ML, Carver WE, Terracio L, Wilson SP, Wilson MA and Borg TK. Integrin-mediated collagen gel contraction by cardiac fibroblasts. Effects of angiotensin II. *Circ Res* 74: 291-298, 1994.
430. Graf K, Neuss M, Stawowy P, Hsueh WA, Fleck E and Law RE. Angiotensin II and alpha(v)beta(3) integrin expression in rat neonatal cardiac fibroblasts. *Hypertension* 35: 978-984, 2000.
431. Brill A, Dashevsky O, Rivo J, Gozal Y and Varon D. Platelet-derived microparticles induce angiogenesis and stimulate post-ischemic revascularization. *Cardiovasc Res* 67: 30-38, 2005.
432. Iwabu A, Murakami T, Kusachi S, Nakamura K, Takemoto S, Komatsubara I, Sezaki S, Hayashi J, Ninomiya Y and Tsuji T. Concomitant expression of heparin-binding epidermal growth factor-like growth factor mRNA and basic fibroblast growth factor mRNA in myocardial infarction in rats. *Basic Res Cardiol* 97: 214-222, 2002.
433. Frangogiannis NG, Lindsey ML, Michael LH, Youker KA, Bressler RB, Mendoza LH, Spengler RN, Smith CW and Entman ML. Resident cardiac mast cells degranulate and release preformed TNF-alpha, initiating the cytokine cascade in experimental canine myocardial ischemia/reperfusion. *Circulation* 98: 699-710, 1998.
434. Jackson CL and Reidy MA. Basic fibroblast growth factor: its role in the control of smooth muscle cell migration. *Am J Pathol* 143: 1024-1031, 1993.
435. Staton CA, Stribbling SM, Tazzyman S, Hughes R, Brown NJ and Lewis CE. Current methods for assaying angiogenesis in vitro and in vivo. *Int J Exp Pathol* 85: 233-248, 2004.
436. Andresen JL and Ehlers N. Chemotaxis of human keratocytes is increased by platelet-derived growth factor-BB, epidermal growth factor, transforming growth factor-alpha,

acidic fibroblast growth factor, insulin-like growth factor-I, and transforming growth factor-beta. *Curr Eye Res* 17: 79-87, 1998.
437. Liu G, Eskin SG and Mikos AG. Integrin alpha(v)beta(3) is involved in stimulated migration of vascular adventitial fibroblasts by basic fibroblast growth factor but not platelet-derived growth factor. *J Cell Biochem* 83: 129-135, 2001.
438. Calabrese EJ. Cell migration/chemotaxis: biphasic dose responses. *Crit Rev Toxicol* 31: 615-624, 2001.
439. Senior RM, Huang JS, Griffin GL and Deuel TF. Dissociation of the chemotactic and mitogenic activities of platelet-derived growth factor by human neutrophil elastase. *J Cell Biol* 100: 351-356, 1985.
440. Moore L and Pastan I. A calcium requirement for movement of cultured cells. *J Cell Physiol* 101: 101-108, 1979.
441. Bhatt A, Kaverina I, Otey C and Huttenlocher A. Regulation of focal complex composition and disassembly by the calcium-dependent protease calpain. *J Cell Sci* 115: 3415-3425, 2002.
442. Lawson MA and Maxfield FR. Ca(2+)- and calcineurin-dependent recycling of an integrin to the front of migrating neutrophils. *Nature* 377: 75-79, 1995.
443. Tsubakimoto K, Matsumoto K, Abe H, Ishii J, Amano M, Kaibuchi K and Endo T. Small GTPase RhoD suppresses cell migration and cytokinesis. *Oncogene* 18: 2431-2440, 1999.
444. Downey GP, Chan CK, Trudel S and Grinstein S. Actin assembly in electropermeabilized neutrophils: role of intracellular calcium. *J Cell Biol* 110: 1975-1982, 1990.
445. Azuma M, Takahashi K, Kimura A, Matsuda T, Schaffer SW and Azuma J. Protective effect of taurine on the detachment of cultured cardiac fibroblasts from the substratum induced by calcium depletion. *Amino Acids* 26: 159-162, 2004.
446. Ranta-Knuuttila T, Kiviluoto T, Mustonen H, Puolakkainen P, Watanabe S, Sato N and Kivilaakso E. Migration of primary cultured rabbit gastric epithelial cells requires intact protein kinase C and Ca2+/calmodulin activity. *Dig Dis Sci* 47: 1008-1014, 2002.
447. Bilato C, Pauly RR, Melillo G, Monticone R, Gorelick-Feldman D, Gluzband YA, Sollott SJ, Ziman B, Lakatta EG and Crow MT. Intracellular signaling pathways required for rat vascular smooth muscle cell migration. Interactions between basic fibroblast growth factor and platelet-derived growth factor. *J Clin Invest* 96: 1905-1915, 1995.
448. Pauly RR, Bilato C, Sollott SJ, Monticone R, Kelly PT, Lakatta EG and Crow MT. Role of calcium/calmodulin-dependent protein kinase II in the regulation of vascular smooth muscle cell migration. *Circulation* 91: 1107-1115, 1995.
449. Magee WP, Deshmukh G, Deninno MP, Sutt JC, Chapman JG and Tracey WR. Differing cardioprotective efficacy of the Na+/Ca2+ exchanger inhibitors SEA0400 and KB-R7943. *Am J Physiol Heart Circ Physiol* 284: H903-H910, 2003.
450. Muller-Ehmsen J, McDonough AA, Farley RA and Schwinger RH. Sodium pump isoform expression in heart failure: implication for treatment. *Basic Res Cardiol* 97 Suppl 1: I25-I30, 2002.
451. McDonough AA, Velotta JB, Schwinger RH, Philipson KD and Farley RA. The cardiac sodium pump: structure and function. *Basic Res Cardiol* 97 Suppl 1: I19-I24, 2002.
452. Scherberich A, Campos-Toimil M, Ronde P, Takeda K and Beretz A. Migration of human vascular smooth muscle cells involves serum-dependent repeated cytosolic calcium transients. *J Cell Sci* 113 (Pt 4): 653-662, 2000.

453. Fay FS, Gilbert SH and Brundage RA. Calcium signalling during chemotaxis. *Ciba Found Symp* 188: 121-135, 1995.
454. Schwab A, Finsterwalder F, Kersting U, Danker T and Oberleithner H. Intracellular Ca2+ distribution in migrating transformed epithelial cells. *Pflugers Arch* 434: 70-76, 1997.
455. Miyamoto S, Howes AL, Adams JW, Dorn GW and Brown JH. Ca2+ dysregulation induces mitochondrial depolarization and apoptosis: role of Na+/Ca2+ exchanger and AKT. *J Biol Chem* 280: 38505-38512, 2005.
456. Groigno L and Whitaker M. An anaphase calcium signal controls chromosome disjunction in early sea urchin embryos. *Cell* 92: 193-204, 1998.
457. Deisseroth K, Heist EK and Tsien RW. Translocation of calmodulin to the nucleus supports CREB phosphorylation in hippocampal neurons. *Nature* 392: 198-202, 1998.
458. Munevar S, Wang YL and Dembo M. Regulation of mechanical interactions between fibroblasts and the substratum by stretch-activated Ca2+ entry. *J Cell Sci* 117: 85-92, 2004.
459. Cox JL, Lancaster T and Carlson CG. Changes in the motility of B16F10 melanoma cells induced by alterations in resting calcium influx. *Melanoma Res* 12: 211-219, 2002.
460. Verrall J, Fraser SP and Djamgoz MB. Effects of gadolinium ions upon rat prostatic cancer cell lines of markedly different metastatic potential. *Cancer Lett* 145: 79-83, 1999.
461. Lee J, Ishihara A, Oxford G, Johnson B and Jacobson K. Regulation of cell movement is mediated by stretch-activated calcium channels. *Nature* 400: 382-386, 1999.
462. Kamkin A, Kiseleva I, Wagner KD, Pylaev A, Leiterer KP, Theres H, Scholz H, Gunther J and Isenberg G. A possible role for atrial fibroblasts in postinfarction bradycardia. *Am J Physiol Heart Circ Physiol* 282: H842-H849, 2002.
463. Munaron L. Calcium signalling and control of cell proliferation by tyrosine kinase receptors (review). *Int J Mol Med* 10: 671-676, 2002.
464. Kizana E, Ginn SL, Allen DG, Ross DL and Alexander IE. Fibroblasts can be genetically modified to produce excitable cells capable of electrical coupling. *Circulation* 111: 394-398, 2005.
465. De RA, Willems PH, van Zoelen EJ and Theuvenet AP. Synchronized Ca2+ signaling by intercellular propagation of Ca2+ action potentials in NRK fibroblasts. *Am J Physiol* 273: C1900-C1907, 1997.
466. Harks EG, Torres JJ, Cornelisse LN, Ypey DL and Theuvenet AP. Ionic basis for excitability of normal rat kidney (NRK) fibroblasts. *J Cell Physiol* 196: 493-503, 2003.
467. Rook MB, van Ginneken AC, de JB, el AA, Gros D and Jongsma HJ. Differences in gap junction channels between cardiac myocytes, fibroblasts, and heterologous pairs. *Am J Physiol* 263: C959-C977, 1992.
468. He P and Curry FE. Endothelial cell hyperpolarization increases [Ca2+]i and venular microvessel permeability. *J Appl Physiol* 76: 2288-2297, 1994.
469. Halaszovich CR, Zitt C, Jungling E and Luckhoff A. Inhibition of TRP3 channels by lanthanides. Block from the cytosolic side of the plasma membrane. *J Biol Chem* 275: 37423-37428, 2000.
470. Rosker C, Graziani A, Lukas M, Eder P, Zhu MX, Romanin C and Groschner K. Ca(2+) signaling by TRPC3 involves Na(+) entry and local coupling to the Na(+)/Ca(2+) exchanger. *J Biol Chem* 279: 13696-13704, 2004.

471. Saitoh M, Naka M and Hidaka H. The modulatory role of myosin light chain phosphorylation in human platelet activation. *Biochem Biophys Res Commun* 140: 280-287, 1986.
472. Wang J, Chen H, Seth A and McCulloch CA. Mechanical force regulation of myofibroblast differentiation in cardiac fibroblasts. *Am J Physiol Heart Circ Physiol* 285: H1871-H1881, 2003.
473. Eddy RJ, Pierini LM, Matsumura F and Maxfield FR. Ca2+-dependent myosin II activation is required for uropod retraction during neutrophil migration. *J Cell Sci* 113 (Pt 7): 1287-1298, 2000.
474. Levinson H, Moyer KE, Saggers GC and Ehrlich HP. Calmodulin-myosin light chain kinase inhibition changes fibroblast-populated collagen lattice contraction, cell migration, focal adhesion formation, and wound contraction. *Wound Repair Regen* 12: 505-511, 2004.
475. Takayama Y and Mizumachi K. Effects of lactoferrin on collagen gel contractile activity and myosin light chain phosphorylation in human fibroblasts. *FEBS Lett* 508: 111-116, 2001.
476. Brittan M, Hunt T, Jeffery R, Poulsom R, Forbes SJ, Hodivala-Dilke K, Goldman J, Alison MR and Wright NA. Bone marrow derivation of pericryptal myofibroblasts in the mouse and human small intestine and colon. *Gut* 50: 752-757, 2002.
477. Epperly MW, Guo H, Gretton JE and Greenberger JS. Bone marrow origin of myofibroblasts in irradiation pulmonary fibrosis. *Am J Respir Cell Mol Biol* 29: 213-224, 2003.
478. Forbes SJ, Russo FP, Rey V, Burra P, Rugge M, Wright NA and Alison MR. A significant proportion of myofibroblasts are of bone marrow origin in human liver fibrosis. *Gastroenterology* 126: 955-963, 2004.
479. Hurtado C, Ander BP, Maddaford TG, Lukas A, Hryshko LV and Pierce GN. Adenovirally delivered shRNA strongly inhibits Na+-Ca2+ exchanger expression but does not prevent contraction of neonatal cardiomyocytes. *J Mol Cell Cardiol* 38: 647-654, 2005.